

# The Light company

Houston Lighting & Power

P.O. Box 1700 Houston, Texas 77001 (713) 228-9211

June 15, 1988  
ST-HL-AE-2683  
File No.: G9.1, R5  
10CFR50

U. S. Nuclear Regulatory Commission  
Attention: Document Control Desk  
Washington, DC 20555

South Texas Project Electric Generating Station  
Unit 2  
Docket Nos. STN 50-499  
Annotated FSAR Revisions Regarding  
the Revised Unit 2 Cycle 1  
Core Design/Energy Requirements

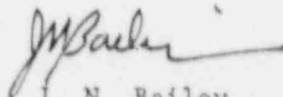
Attached for your information and review are annotated revisions to the South Texas Project (STP) FSAR regarding the redesign of the Unit 2 initial core. The Unit 2 initial core has been redesigned to accommodate a revised cycle length of approximately 400 effective full power days (EFPD). Included are revisions to FSAR Chapter 4 describing the Unit 2 core design change and FSAR Chapter 15 which provides the results of the evaluations/analyses that are impacted by the proposed change. Westinghouse (W) has evaluated the effects of this change on the existing Loss-of-Coolant-Accident (LOCA) analyses documented in the FSAR and has concluded that the LOCA analysis is unaffected by this change and remains bounding for both Units 1 & 2.

It should also be noted that the highest enrichment being used has not changed from that currently identified in the FSAR.

This change has already been implemented on STP Unit 2 and will be incorporated in a future FSAR amendment. HL&P requests that the NRC review this change on a schedule consistent with the licensing of STP Unit 2.

If you should have any questions on this matter, please contact Mr. M. E. Powell at (713) 993-1226 or (512) 972-7062.

8806210245 880615  
PDR ADDCK 05000499  
A PDR



J. N. Bailey  
Manager, Engineering and Licensing

MEP/yd

Attachment: Annotated Revisions to FSAR Chapters 1, 4 & 15  
and affected NRC Question Responses

L1/NRC/b

A Subsidiary of Houston Industries Incorporated

Boo/11

Houston Lighting & Power Company

ST-HL-AE-2683  
File No.: G9.1, R5  
Page 2

cc:

Regional Administrator, Region IV  
Nuclear Regulatory Commission  
611 Ryan Plaza Drive, Suite 1C00  
Arlington, TX 76011

George Dick, Project Manager  
U.S. Nuclear Regulatory Commission  
Washington, DC 20555

Jack E. Bess  
Resident Inspector/Operations  
c/o U.S. Nuclear Regulatory  
Commission  
P. O. Box 910  
Bay City, TX 77414

Don L. Garrison  
Resident Inspector/Construction  
c/o U.S. Nuclear Regulatory  
Commission  
P. O. Box 910  
Bay City, TX 77414

J. R. Newman, Esquire  
Newman & Holtzinger, P.C.  
1615 L Street, N.W.  
Washington, DC 20036

R. L. Range/R. P. Verret  
Central Power & Light Company  
P. O. Box 2121  
Corpus Christi, TX 78403

R. John Miner (2 copies)  
Chief Operating Officer  
City of Austin Electric Utility  
721 Barton Springs Road  
Austin, TX 78704

R. J. Costello/M. T. Hardt  
City Public Service Board  
P. O. Box 1771  
San Antonio, TX 78296

Rufus S. Scott  
Associate General Counsel  
Houston Lighting & Power Company  
P. O. Box 1700  
Houston, TX 77001

INPO  
Records Center  
1100 Circle 75 Parkway  
Atlanta, GA 30339-3064

Dr. Joseph M. Hendrie  
50 Bellport Lane  
Bellport, NY 11713

Revised 06/07/88

L1/NRC/b



TABLE 1.6-2 (SHEET 20 OF 20)

WESTINGHOUSE TOPICAL REPORTS INCORPORATED BY REFERENCE

Westinghouse Topical Report No. (a)	Title Number	WRC Submittal Date	Revision Number	FSAR Section Reference	Review (b) Status
WCAP-10865 (P) WCAP-10866	South Texas Plant (TGX) Reactor Internals Flow- Induced Vibration Assessment	6/85		1.5	U
WCAP-11340 (P) WCAP-11341	Noise, Fault, Surge, and Radio Frequency Interference Test Report: Westinghouse Eagle-21 Digital Family as Used in GDPS, PSMS, RVLIS, and ICCM	12/86		7.1	U
WCAP-10559 (P) WCAP-10560	Technical Bases for Eliminating Large Primary Loop Pipe Rupture as the Structural Design Basis for South Texas Projects Units 1 & 2	7/84		3.6	B

58

57

59

STP FSAR

a. (P) - Proprietary

b. Legend for the review status code letters:

- A - WRC review complete; WRC evaluation letter issued.
- AE - WRC accepted as part of the Westinghouse emergency core cooling system (ECCS) evaluation model only; does not constitute acceptance for any purpose other than for ECCS analyses.
- B - Submitted to WRC as background information; not undergoing formal WRC review.
- O - On file with WRC; older generation report with current validity; not actively under formal WRC review.
- U - Actively under formal WRC review.

1.6-23

INSERT  
B →

Amendment 59

INSERT B

W TOPICAL REPORT

TITLE NUMBER      NRL SUBM. DATE

REV NUMBER      FSM SECTION Reference

Review STATUS

WCAP-10965 (P)  
WCAP-10966

ANC: A Westinghouse 9/86  
ADVANCED NODAL  
CODE

4.3 A

4.0 REACTOR

## 4.1 SUMMARY DESCRIPTION

*For Unit 1 and 16 months for Unit 2.*

This chapter describes 1) the mechanical components of the reactor and reactor core including the fuel rods and fuel assemblies, 2) the nuclear design, and 3) the thermal-hydraulic design.

The reactor core is comprised of an array of fuel assemblies which are identical in mechanical design, but different in fuel enrichment. The reference three region first core design described herein results in a first cycle length of approximately one year. ~~However, cycles over eighteen months or less than one year may be accommodated by initial fuel loadings that contain from three to six enrichment loadings.~~

The core is cooled and moderated by light water at a pressure of 2250 psia in the Reactor Coolant System (RCS). The moderator coolant contains boron as a neutron poison. The concentration of boron in the coolant is varied as required to control relatively slow reactivity changes including the effects of fuel burnup. Additional boron, in the form of burnable poison rods, is employed in the first core to establish the desired initial reactivity.

Two hundred and sixty four fuel rods are mechanically joined in a square array to form a fuel assembly. The fuel rods are supported in intervals along their length by grid assemblies which maintain the lateral spacing between the rods throughout the design life of the assembly. The grid assembly consists of an "egg-crate" arrangement of interlocked straps. The straps contain spring fingers and dimples for fuel rod support as well as coolant mixing vanes. The fuel rods consist of slightly enriched uranium dioxide ceramic cylindrical pellets contained in slightly cold worked Zircaloy-4 tubing which is plugged and seal welded at the ends to encapsulate the fuel. All fuel rods are pressurized with helium during fabrication to reduce stresses, strains, and to increase fatigue life.

The center position in the assembly is reserved for the incore instrumentation, while the remaining 24 positions in the array are equipped with guide thimbles joined to the grids and the top and bottom nozzles. Depending upon the position of the assembly in the core, the guide thimbles are used as core locations for rod cluster control assemblies (RCCA's), neutron source assemblies, and burnable poison assemblies. Otherwise, the guide thimbles are fitted with thimble plug assemblies, which are plugging devices that limit bypass flow.

The bottom nozzle is a box-like structure which serves as a bottom structural element of the fuel assembly and directs the coolant flow distribution to the assembly.

The top nozzle assembly functions as the upper structural element of the fuel assembly in addition to providing a partial protective housing for the RCCA or other components.

TABLE 4.1-1 (Continued)

## REACTOR DESIGN COMPARISON TABLE

CORE MECHANICAL DESIGN PARAMETERS	W. B. McGuire UNITS 1 & 2	South Texas Project UNIT 1	South Texas Project UNIT 2
31. Fuel Weight (as UO <sub>2</sub> ), lb	222,739	261,000 (Nominal)	262,000 (Nominal)
32. Zircaloy Weight, lb	50,913	54,840	54,840
33. Number of Grids per Assembly	8 - Type R	10 - Type R	10 - Type R
34. Loading Technique	3 region non-uniform	3 region non-uniform	3 region non-uniform
FUEL RODS			
35. Number	50,952	50,952	50,952
36. Outside Diameter, in.	0.374	0.374	0.374
37. Diametral Gap, in.	0.0065	0.0065	0.0065
38. Clad Thickness, in.	0.0225	0.0225	0.0225
39. Clad Material	Zircaloy-4	Zircaloy-4	Zircaloy-4
FUEL PELLETS			
40. Material	UO <sub>2</sub> Sintered	UO <sub>2</sub> Sintered	UO <sub>2</sub> Sintered
41. Density (% of Theoretical)	95	95	95
42. Diameter, in.	0.3225	0.3225	0.3225
43. Length, in.	0.530	0.530	0.530 0.387 (for assemblies) 0.530 (for 40 - units)
ROD CLUSTER CONTROL ASSEMBLIES			
44. Neutron Absorber	Ag-In-Cd	Neptunium	Neptunium
45. Cladding Material	Type 304	Type 304	Type 304
	SS-Cold Worked	SS-Cold Worked	SS-Cold Worked

18

30

4.1-6

Amendment 54

STP PSAR

TABLE 4.1-1 (Continued)

REACTOR DESIGN COMPARISON TABLE

	<u>W. B. McGuire</u> <u>UNITS 1 &amp; 2</u>	<u>South Texas Project</u> <u>UNIT 1</u>	<u>South Texas Project</u> <u>UNIT 1      2</u>	
FEED ENRICHMENT, W/O				
57. Region 1	2.10	1.50	<del>1.90</del>	2.1
58. Region 2	2.60	2.20	<del>2.30</del>	2.6
59. Region 3	3.10	2.90	2.90	

NOTES:

- a. See Subsection 4.3.2.2.6
- b. This is the value of  $F_0$  for normal operation.

TABLE 4.1-2 (Continued)

ANALYTICAL TECHNIQUES IN CORE DESIGN

<u>Analysis</u>	<u>Technique</u>	<u>Computer Code</u>	<u>Section Referenced</u>
Nuclear Design (Continued)			
	Group constants for control rods with self-shielding	HAMMER-AIM	4.3.3.2
2. X-Y Power Distributions, Fuel Depletion, Critical Boron Concentrations, x-y Xenon Distributions, Reactivity Coefficients	2-D, 2-Group Diffusion Theory 2-D and 3-D Diffusion Theory - based Model Method	TURTLE TORTISE PALADIN ANC	4.3.3.3 4.3.3.3
3. Axial Power Distributions, Control Rod Worths, and Axial Xenon Distribution	1-D, 2-Group Diffusion Theory	PANDA APOLLO	4.3.3.3
4. Fuel Rod Power	Integral Transport Theory	LASER	4.3.3.1
Effective Resonance Temperature	Monte Carlo Weighting Function	REPAD	

53

4.1-11

Amendment 53

STP PSAR



The core is designed so that diametral and azimuthal oscillations due to spatial xenon effects are self-damping and no operator action or control action is required to suppress them. The stability to diametral oscillations is so great that this excitation is highly improbable. Convergent azimuthal oscillations can be excited by prohibited motion of individual control rods. Such oscillations are readily observable and alarmed, using the excore long ion chambers. Indications are also continuously available from incore thermocouples and loop temperature measurements. Moveable incore detectors can be activated to provide more detailed information. In all proposed cores these horizontal plane oscillations are self-damping by virtue of reactivity feedback effects designed into the core.

However, axial xenon spatial power oscillations may occur <sup>during</sup> ~~late in~~ core life. The control banks, and excore detectors are provided for control and monitoring of axial power distributions. Assurance that fuel design limits are not exceeded is provided by reactor overpower  $\Delta T$  and overtemperature  $\Delta T$  trip functions which use the measured axial power imbalance as an input.

4.3.1.7 Anticipated Transients Without Trip (ATWT). The effects of anticipated transients with failure to trip are not considered in the design bases of the plant. Analysis has shown that the likelihood of such a hypothetical event is negligibly small. [4.3-1] Furthermore, analysis of the consequences of a hypothetical failure to trip following anticipated transients has shown that no significant core damage would result, system peak pressures would be limited to acceptable values and no failure of the Reactor Coolant System (RCS) would result. These analyses were documented [Ref. 4.3-2] in November, 1974 in accordance with the AEC policy outlined in WASH-1270 "Technical Report on Anticipated Transients Without Scram for Water-Cooled Power Reactors," September, 1973.

#### 4.3.2 Description

4.3.2.1 Nuclear Design Description. The reactor core consists of a specified number of fuel rods which are held in bundles by spacer grids and top and bottom fittings. The fuel rods are constructed of Zircaloy cylindrical tubes containing uranium dioxide fuel pellets. The bundles, known as fuel assemblies, are arranged in a pattern which approximates a right circular cylinder.

Each fuel assembly contains a 17 x 17 rod array composed of 264 fuel rods, 24 rod cluster control thimbles and an incore instrumentation thimble. Figure 4.2-1 shows a cross sectional view of a 17 x 17 fuel assembly and the related rod cluster control locations. Further details of the fuel assembly are given in Section 4.2.

The fuel rods within a given assembly have the same uranium enrichment in both the radial and axial planes. Fuel assemblies of three different enrichments are used in the initial core loading to establish a favorable radial power distribution. Figure 4.3-1 shows the fuel loading pattern to be used in the first core. Two regions consisting of the two lower enrichments are interspersed so as to form a checkerboard pattern in the central portion of the core. The third region is arranged around the periphery of the core and contains the highest enrichment. The enrichments for the first core are shown in Table 4.3-1.

The reference reloading pattern is typically similar to Figure 4.3-1 with depleted fuel interspersed checkerboard style in the center and new fuel mixed with depleted fuel on the periphery. The core will normally operate ~~approximately~~ <sup>on a</sup> ~~twelve month~~ <sup>cycle</sup> ~~between reloadings~~, accumulating approximately ~~12,000~~ <sup>10,000</sup> Mwd/MTU ~~per cycle~~. The exact reloading pattern, initial and final positions of assemblies, number of fresh assemblies and their placement are dependent on the energy requirement for the next cycle and burnup and power histories of the previous cycles.

The core average enrichment is determined by the amount of fissionable material required to provide the desired core lifetime and energy requirements, namely a region average discharge burnup of 33,000 Mwd/MTU. The physics of the burnup process is such that operation of the reactor depletes the amount of fuel available due to the absorption of neutrons by the uranium-235 atoms and their subsequent fission. The rate of uranium-235 depletion is directly proportional to the power level at which the reactor is operated. In addition, the fission process results in the formation of fission products, some of which readily absorb neutrons. These effects, depletion and the buildup of fission products, are partially offset by the buildup of plutonium shown on Figure 4.3-2 for the 17 x 17 fuel assembly, which occurs due to the non-fission absorption of neutrons in uranium-238. Therefore, at the beginning of any cycle a reactivity reserve equal to the depletion of the fissionable fuel and the buildup of fission product poisons over the specified cycle life must be "built" into the reactor. This excess reactivity is controlled by removable neutron absorbing material in the form of boron dissolved in the primary coolant and in the case of the first cycle, by burnable poison rods.

The concentration of boric acid in the primary coolant is varied to provide control and to compensate for long-term reactivity requirements. The concentration of the soluble neutron absorber is varied to compensate for reactivity changes due to fuel burnup, fission product poisoning including xenon and samarium, burnable poison depletion, and the cold-to-operating moderator temperature change. Using its normal makeup path, the Chemical and Volume Control System (CVCS) is capable of inserting negative reactivity at a rate of approximately 60 pcm/min when the reactor coolant boron concentration is 1000 ppm and approximately 70 pcm/min when the reactor coolant boron concentration is 100 ppm. The peak burnout rate for xenon is 25 pcm/min (Section 9.3.4.3.1 | 30 discusses the capability of the CVCS to counteract xenon decay). Rapid transient reactivity requirements and safety shutdown requirements are met with control rods.

As the boron concentration is increased, the moderator temperature coefficient becomes less negative. The use of a soluble poison alone would result in a positive moderator coefficient at beginning-of-life (BOL) for the first cycle. Therefore, burnable poison rods are used in the first core to reduce the soluble boron concentration sufficiently to ensure that the moderator temperature coefficient is negative for power operating conditions. During operation the poison content in these rods is depleted thus adding positive reactivity to offset some of the negative reactivity from fuel depletion and fission product buildup. The depletion rate of the burnable poison rods is not critical since chemical

they require control of the axial offset (flux difference divided by fractional power) at all power levels within a permissible operating band of a target value corresponding to the equilibrium full power value. In the first cycle, the target value changes from about -15 to ~~X~~ percent linearly through the life of the cycle. This minimizes xenon transient effects on the axial power distribution, since the procedures essentially keep the xenon distribution in phase with the power distribution.

Calculations are performed for normal operation of the reactor including load following maneuvers. Beginning, middle and end of cycle conditions are included in the calculations. Different histories of operation are assumed prior to calculating the effect of load follow transients on the axial power distribution. These different histories assume base loaded operation and extensive load following. For a given plant and fuel cycle a finite number of maneuvers are studied to determine the general behavior of the local power density as a function of core elevation.

These cases represent many possible reactor states in the life of one fuel cycle and they have been chosen as sufficiently definitive of the cycle by comparison with much more exhaustive studies performed on some 20 or 30 different, but typical, plant and fuel cycle combinations. The cases are described in detail in Reference 4.3-9 and are considered to be necessary and sufficient to generate a local power density limit which, when increased by 5 percent for conservatism, will not be exceeded with a 95 percent confidence level. Many of the points do not approach the limiting envelope, however they are part of the time histories which lead to the hundreds of shapes which do define the envelope. They also serve as a check that the reactor studied is typical of those studied more exhaustively.

Thus it is not possible to single out any transient or steady state condition which defines the most limiting case. It is not even possible to separate out a small number which form an adequate analysis. The process of generating a myriad of shapes is essential to the philosophy that leads to the required level of confidence. A maneuver which provides a limiting case for one reactor fuel cycle, defined as approaching the line of Figure 4.3-21, is not necessarily a limiting case for another reactor or fuel cycle with different control bank worths, enrichments, burnup, coefficients, etc. Each shape depends on the detailed history of operation up to that time and on the manner in which the operator conditioned xenon in the days immediately prior to the time at which the power distribution is calculated.

The calculated points are synthesized from axial calculations combined with radial factors appropriate for rodded and unrodded planes in the first cycle. In these calculations the effects on the unrodded radial peak of xenon redistribution that occurs following the withdrawal of a control bank (or banks) from a rodded region is obtained from two-dimensional XY calculations. A 1.03 factor to be applied on the unrodded radial peak was obtained from calculations in which xenon distribution was preconditioned by the presence of control rods



Limits for alarms, reactor trip, etc. will be given in the Technical Specifications. Descriptions of the systems provided are given in Section 7.7. |27

4.3.2.3 Reactivity Coefficients. The kinetic characteristics of the reactor core determine the response of the core to changing plant conditions or to operator adjustments made during normal operation, as well as the core response during abnormal or accidental transients. These kinetic characteristics are quantified in reactivity coefficients. The reactivity coefficients reflect the changes in the neutron multiplication due to varying plant conditions such as power, moderator or fuel temperatures, or less significantly due to a change in pressure or void conditions. Since reactivity coefficients change during the life of the core, ranges of coefficients are employed in transient analysis to determine the response of the plant throughout life. The results of such simulations and the reactivity coefficients used are presented in Chapter 15. The reactivity coefficients are calculated on a corewise basis by radial and axial diffusion theory methods. The effect of radial and axial power distribution on core average reactivity coefficients is implicit in those calculations and is not significant under normal operating conditions. For example, a skewed xenon distribution which results in changing axial offset by 5 percent changes the moderator and Doppler temperature coefficients by less than 0.01 pcm/°F and 0.03 pcm/°F respectively. An artificially skewed xenon distribution which results in changing the radial  $F_{\Delta H}^N$  by 3 percent changes the moderator and Doppler temperature coefficients by less than 0.03 pcm/°F and 0.001 pcm/°F respectively. The spatial effects are accentuated in some transient conditions such as the postulated rupture of the main steamline break and rupture of RCCA mechanism housing described in Sections 15.1.5 and 15.4.8, and are included in these analyses. |53

The analytical methods and calculational models used in calculating the reactivity coefficients are given in Section 4.3.3. These models have been confirmed through extensive testing of more than thirty cores similar to the plant described herein; results of these tests are discussed in Section 4.3.3.

Quantitative information for calculated reactivity coefficients, including fuel Doppler coefficient, moderator coefficients (density, temperature, pressure, void) and power coefficient is given in the following sections.

4.3.2.3.1 Fuel Temperature (Doppler) Coefficient: The fuel temperature (Doppler) coefficient is defined as the change in reactivity per degree change in effective fuel temperature and is primarily a measure of Doppler broadening of uranium-238 and plutonium-240 resonance absorption peaks. Doppler broadening of other isotopes such as uranium-236, neptunium-237, etc. are also considered but their contributions to the Doppler effect are small. An increase in fuel temperature increases the effective resonance absorption cross sections of the fuel and produces a corresponding reduction in reactivity. |53

The fuel temperature coefficient is calculated by performing two-group X-Y calculations using an updated version of the TURTLE [4.3-12] Code. Moderator temperature is held constant and the power level is varied. Spatial variation of fuel temperature is taken into account by calculating the effective fuel temperature as a function of power density as discussed in Section 4.3.3.1.

change in boron concentration is required to compensate for additional reactivity changes. Since the insertion limit is set by a rod travel limit, a conservatively high calculation of the inserted worth is made which exceeds the normally inserted reactivity.

4.3.2.4.6 Burnup: Excess reactivity of <sup>approximately</sup> 10 percent  $\Delta\rho$  (hot) is installed at the beginning of each cycle to provide sufficient reactivity to compensate for fuel depletion and fission products throughout the cycle. This reactivity is controlled by the addition of soluble boron to the coolant and by burnable poisons. The soluble boron concentration for several core configurations, the unit boron worth, and burnable poison worth are given in Tables 4.3-1 and 4.3-2. Since the excess reactivity for burnup is controlled by soluble boron and/or burnable poisons it is not included in control rod requirements. | 53

4.3.2.4.7 Xenon and Samarium Poisoning and pH Effects: Changes in xenon and samarium concentrations in the core occur at a sufficiently slow rate, even following rapid power level changes, that the resulting reactivity change is controlled by changing the soluble boron concentration. Changes in reactivity due to a change in coolant pH, if any, are sufficiently small in magnitude and occur slowly enough to be controlled by the boron system. Further details are provided in Reference 4.3-13. | 53

4.3.2.4.8 Combined Control Requirements: The reactivity requirements at EOL of a typical cycle for a 168 in and a 144 in 17 x 17 four loop core are listed on a comparable basis in Table 4.3-4. The Doppler defect is slightly less for the 168 in core due to the lower average linear power density (5.20 vs. 5.44 Kw/ft). The moderator defect is higher due to the slightly more negative moderator temperature coefficient at the higher temperature of the 168 in core. The redistribution requirement is greater for the longer core (1.20 percent  $\Delta\rho$  vs. 0.85 percent  $\Delta\rho$ ). More excess margin is available to the 168 in core than the 12 ft core due to the use of 57 rather than 53 control rods in this example. Both cores operate in the same range of expected reactivity parameters as shown in Table 4.3-5. | 53

4.3.2.4.9 Experimental Confirmation: Following a normal shutdown, the total core reactivity change during cooldown with a stuck rod has been measured on a 121 assembly, 10 ft high core and 121 assembly, 12 ft high core. In each case, the core was allowed to cool down until it reached criticality simulating the steam line break accident. For the 10 ft core, the total reactivity change associated with the cooldown is overpredicted by about 0.3 percent  $\Delta\rho$  with respect to the measured result. This represents an error of about 5 percent in the total reactivity change and is about half the uncertainty allowance for this quantity. For the 12 ft core, the difference between the measured and predicted reactivity change was an even smaller 0.2 percent  $\Delta\rho$ . These measurements and others demonstrate the capability of the methods described in Section 4.3.3. | 53

4.3.2.4.10 Control: Core reactivity is controlled by means of a chemical poison dissolved in the coolant, RCCAs and burnable poison rods as described below.

control unit located along the diagonal axis. Following the perturbation, the uncontrolled oscillation was monitored using the moveable detector and thermocouple system and the excore power range detectors. The quadrant tilt difference (QTD) is the quantity that properly represents the diametral oscillation in the X-Y plane of the reactor core in that the differences of the quadrant average powers over two symmetrically opposite quadrants essentially eliminates the contribution to the oscillation from the azimuthal mode. The QTD data were fitted in the form of equation (4.3-2) through a least-square method. A stability index of  $-0.076 \text{ hr}^{-1}$  with a period of 29.6 hours was obtained from the thermocouple data shown on Figure 4.3-41.

It was observed in the second X-Y xenon test that at the PWR core with 157 fuel assemblies had become more stable due to an increased fuel depletion and the stability index was not determined.

4.3.2.7.5 Comparison of Calculations with Measurements: The analysis of the axial xenon transient tests was performed in an axial slab geometry using a flux synthesis technique. The direct simulation of the axial offset data was carried out using the PANDA Code (Ref. 4.3-20). *For Unit 1 and using Apollo, an updated version of the PANDA code for Unit 2*  
 The analysis of the X-Y xenon transient tests was performed in an X-Y geometry using a modified TURTLE (Ref. 4.3-12) Code. Both the PANDA and TURTLE codes solve the two-group time-dependent neutron diffusion equation with time-dependent xenon and iodine concentrations. The fuel temperature and moderator density feedback is limited to a steady-state model. All the X-Y calculations were performed in an average enthalpy plane.

The basic nuclear cross-sections used in this study were generated from a unit cell depletion program which has evolved from the codes LEOPARD (Ref. 4.3-21) and CINDER (Ref. 4.3-22). The detailed experimental data during the tests including the reactor power level, enthalpy rise and the impulse motion of the control rod assembly, as well as the plant follow burnup data were closely simulated in the study.

The results of the stability calculation for the axial tests are compared with the experimental data in Table 4.3-7. The calculations show conservative results for both of the axial tests with a margin of approximately  $-0.01 \text{ hr}^{-1}$  in the stability index.

An analytical simulation of the first X-Y xenon oscillation test shows a calculated stability index of  $-0.081 \text{ hr}^{-1}$ , in good agreement with the measured value of  $-0.076 \text{ hr}^{-1}$ . As indicated earlier, the second X-Y xenon test showed that the core had become more stable compared to the first test and no evaluation of the stability index was attempted. This increase in the core stability in the X-Y plane due to increased fuel burnup is due mainly to the increased magnitude of the negative moderator temperature coefficient.

Previous studies of the physics of xenon oscillations, including three-dimensional analysis, are reported in the series of topical reports, Refs. 4.3-16, 4.3-17 and 4.3-18. A more detailed description of the experimental results and analysis of the axial and X-Y xenon transient tests is presented in Ref. 4.3-19 and Section 1 of Ref. 4.3-23.



4.3.2.7.6 Stability Control and Protection: The excore detector system is utilized to provide indications of xenon-induced spatial oscillations. The readings from the excore detectors are available to the operator and also form part of the protection system.

#### 1. Axial Power Distribution

For maintenance of proper axial power distributions, the operator is instructed to maintain an axial offset within a prescribed operating band, based on the excore detector readings. Should the axial offset be permitted to move far enough outside this band, the protection limit will be reached and power will be automatically reduced.

Both 12 and 14 ft PWR cores become less stable to axial xenon oscillations as fuel burnup progresses. However, free xenon oscillations are not allowed to occur except for special tests. The control rod banks are sufficient to dampen and control any axial xenon oscillations present. Should the axial offset be inadvertently permitted to move far enough outside the control band due to an axial xenon oscillation, or any other reason, the protection limit on axial offset will be reached and power will be automatically reduced. | 30

At BOL (150 MWD/MTU) stability indexes of about  $-0.047 \text{ hrs}^{-1}$  and  $-0.020 \text{ hrs}^{-1}$  were obtained, respectively, for 12 ft and 14 ft cores. The axial stability index is essentially zero in the 11,000 to 12,000 MWD/MTU range for 12 ft cores and in the 8000 to 9000 MWD/MTU range for 14 ft cores. At extended burnup (~15,000 MWD/MTU) both 12 and 14 ft cores have essentially the same stability index of about  $0.02 \text{ hrs}^{-1}$  or less. The axial oscillation period for both 12 and 14 ft cores increases with burnup. A period of 27 to 28 hours is obtained for both 12 ft and 14 ft cores at BOL. At EOL periods of about 32 and 34 hours are obtained, respectively, for the 12 and 14 ft cores. The long periods and vertical control rod systems make axial xenon transients easily controllable in modern PWRs at all times of life.

These values depend upon the core design as well as burnup, and the stability index can be positive throughout core life for both 12 and 14 ft cores. However,

#### 2. Radial Power Distribution

The core described herein is calculated to be stable against X-Y xenon induced oscillations at all times in life.

The X-Y stability of large PWRs has been further verified as part of the startup physics test program for cores with 193 fuel assemblies. The measured X-Y stability of the cores with 157 and 193 assemblies was in good agreement with the calculated stability as discussed in Subsections 4.3.2.7.4 and 4.3.2.7.5. In the unlikely event that X-Y oscillations occur, back-up actions are possible and would be implemented, if necessary, to increase the natural stability of the core. This is based on the fact that several actions could be taken to make the moderator temperature coefficient more negative,, which will increase the stability of the core in the X-Y plane.

4.3.3.2 Macroscopic Group Constants. Macroscopic few-group constants (analogous microscopic cross sections needed for feedback and microscopic depletion calculations) are generated for fuel cells by a recent version of the LEOPARD [4.3-21] and CINDER [4.3-22] codes, which are linked internally and provide burnup dependent cross sections. Normally a simplified approximation of the main fuel chains is used; however, where needed, a complete solution for all the significant isotopes in the fuel chains from thorium-232 to curium-244 is available [4.3-26]. Fast and thermal cross section library tapes contain microscopic cross sections taken for the most part from the ENDF/B [4.3-27] library, with a few exceptions where other data provided better agreement with critical experiments, isotopic measurements, and plant critical boron values. The effect on the unit fuel cell of non-lattice components in the fuel assembly is obtained by supplying an appropriate volume fraction of these materials in an extra region which is homogenized with the unit cell in the fast (MUFT) and thermal (SOFOCATE) flux calculations. In the thermal calculation, the fuel rod, clad, and moderator are homogenized by energy-dependent disadvantage factors derived from an analytical fit to integral transport theory results.

Group constants for burnable poison cells, guide thimbles, instrument thimbles and interassembly gaps are generated in a manner analogous to the fuel cell calculation. Reflector group constants are taken from infinite medium LEOPARD calculations. Baffle group constants are calculated from an average of core and radial reflector microscopic group constants for stainless steel.

Group constants for control rods are calculated in a linked version of the HAMMER [4.3-28] and AIM [4.3-29] codes which provide an improved treatment of self shielding in the broad resonance structure of these isotopes at epithermal energies than is available in LEOPARD. The Doppler broadened cross sections of the control rod materials are represented as smooth cross sections in the 54 group LEOPARD fast group structure and in 30 thermal groups. The four group constants in the rod cell and appropriate extra region are generated in the coupled space-energy transport HAMMER calculation. A corresponding AIM calculation of the homogenized rod cell with extra region is used to adjust the absorption cross sections of the rod cell to match the reaction rates in HAMMER. These transport-equivalent group constants are reduced to two-groups constants for use in space-dependent diffusion calculations. In discrete X-Y calculations only one mesh interval per cell is used, and the rod group constants are further adjusted for use in this standard mesh by reaction rate matching the standard mesh unit assembly to a fine-mesh unit assembly calculation.

Nodal group constants are obtained by a flux-volume homogenization of the fuel cells, burnable poison cells, guide thimbles, instrumentation thimbles, interassembly gaps, and control rod cells from one mesh interval per cell x-y unit fuel assembly diffusion calculations for Unit 1 and from one mesh interval per cell x-y diffusion calculations for Unit 2.

Validation of the cross section method is based on analysis of critical experiments as shown in Table 4.3-6, isotopic data as shown in Table 4.3-10, plant critical boron ( $C_B$ ) values at H2P, BOL, as shown in Table 4.3-11 and at HFP as a function of burnup as shown on Figures 4.3-43 through 4.3-45. Control rod worth measurements are shown in Table 4.3-12.

Confirmatory critical experiments on burnable poisons are described in Reference 4.3-30.

4.3.3.3 Spatial Few-Group Diffusion Calculations. <sup>FOR UNIT 1,</sup> A spatial few-group calculations consist primarily of two-group diffusion X-Y calculations using an updated version of the TURTLE Code, two-group x-y nodal calculation using the PALADON [4.3-33] code, and two-group axial calculations using an updated version of the PANDA Code.

Discrete X-Y calculations (1 mesh per cell) are carried out to determine critical boron concentrations and power distributions in the X-Y plane. An axial average in the X-Y plane is obtained by synthesis from unrodded and rodded planes. Axial effects in unrodded depletion calculations are accounted for by the axial buckling, which varies with burnup and is determined by radial depletion calculations which are matched in reactivity to the analogous R-Z depletion calculation. The moderator coefficient is evaluated by varying the inlet temperature in the same X-Y calculations used for power distribution and reactivity predictions.

Validation of TURTLE reactivity calculations is associated with the validation of the group constants themselves, as discussed in Section 4.3.3.2. Validation of the Doppler calculations is associated with the fuel temperature validation discussed in Section 4.3.3.1. Validation of the moderator coefficient calculations is obtained by comparison with plant measurements at hot zero power conditions as shown in Table 4.3-13.

PALADON is used in two dimensional and three dimensional calculations. PALADON can be used in safety analysis calculations, and to determine critical boron concentrations, control rod worths, and reactivity coefficients. | 53

Axial calculations are used to determine differential control rod worth curves (reactivity versus rod insertion) and axial power shapes during steady state and transient xenon conditions (flyspeck curve). Group constants and the radial buckling used in the axial calculation are obtained from the three dimensional TURTLE calculation from which group constants are homogenized by flux-volume weighting. | 53

*INSERT A* → Validation of the spatial codes for calculating power distributions involves the use of incore and excore detectors and is discussed in Section 4.3.2.2.7.

Based on comparison with measured data it is estimated that the accuracy of current analytical methods is:

- + 0.2 percent  $\Delta\rho$  for Doppler defect
- +  $2 \times 10^{-6}/^{\circ}\text{F}$  for moderator coefficient
- + 50 ppm for critical boron concentration with depletion
- + 3 percent for power distribution
- + 0.2 percent  $\Delta\rho$  for rod bank worth
- + 4 pcm/step for differential rod worth
- + 0.5 pcm/ppm for boron worth
- + 0.1 percent  $\Delta\rho$  for moderator defect

INSERT A

4.3.3.3 Spatial Few-Group Calculations. For Unit 2, spatial few-group calculations consist of two group diffusion x-y calculations using TORTISE, an updated version of the TURTLE code and nodal calculations using the PALADON (4.4-33) and ANC (4.4-34) codes. Two group axial calculations utilize APOLLO, an updated version of the PANDA code.

Two dimensional calculations are carried out to determine critical boron concentrations and power distributions in the X-Y plane. An axial average in the X-Y plane is obtained by synthesis from rodded and unrodded planes. Axial effects are accounted for by an input axial buckling, which varies with burnup and was determined by radial depletion calculations matched in reactivity to an analogous R-Z depletion calculation. The moderator coefficient is evaluated by varying the inlet temperature in the same X-Y calculations used for power distribution and reactivity predictions.

Validation of TORTISE reactivity calculations is associated with the validation of the group constants themselves, as discussed in Section 4.3.3.2. PALADON and ANC have been qualified with respect to TORTISE results. Validation of the Doppler calculations is associated with the fuel temperature validation discussed in Section 4.3.3.1. Validation of the moderator coefficient calculations is obtained by comparison with plant measurements at hot zero power conditions as shown in Table 4.3-13.

PALADON and ANC are used in both two and three dimensional calculations. They can be used in safety analysis calculations, and to determine critical boron concentrations, control rod worths, and reactivity coefficients.

Axial calculations are used to determine differential control rod worth curves (reactivity versus rod insertion) and axial power shapes during steady state and transient conditions (flyspeck curve). Group constants and the radial buckling used in the axial calculation are obtained from three dimensional calculations from which group constants are homogenized by flux-volume weighting.



- 4.3-28 Suich, J. E. and Honeck, H. C., "The HAMMER System, Heterogeneous Analysis by Multigroup Methods of Exponentials and Reactors," DP-1064, January, 1967.
- 4.3-29 Flatt, H. P. and Buller, D. C., "AIM-5, A Multigroup, One Dimensional Diffusion Equation Code," NAA-SR-4694, March, 1960.
- 4.3-30 Moore, J. S., "Nuclear Design of Westinghouse Pressurized Water Reactors with Burnable Poison Rods," WCAP-9000-L, Revision 1 (Proprietary), July, 1969 and WCAP-7806, December, 1971. | 53
- 4.3-31 Leamer, R.D., et al., "F<sub>2</sub>O<sub>2</sub>-UO<sub>2</sub> Fueled Critical Experiments," WCAP-3726-1, July, 1967.
- 4.3-32 Nodvik, R.J., "Saxton Core II Fuel Performance Evaluation," WCAP-3385-56, Part II, "Evaluation of Mass Spectrometric and Radiochemical Analyses of Irradiated Saxton Plutonium Fuel," July, 1970.
- 4.3-33 Camden, T.M., et al., "PALADON-Westinghouse Nodal Computer Code," WCAP-9485A (Proprietary) and WCAP 9486A (Non-Proprietary), December 1979, and Supplement 1, September, 1981. | 53
- 4.3-34 Liu, Y.S., et al., "ANC: A Westinghouse Advanced Nodal Code," ~~WCAP-10965-A, Sept 1986~~  
WCAP-10965-A (Proprietary) and  
WCAP-10966 A (Non Proprietary) September, 1986.

TABLE 4.3-1

REACTOR CORE DESCRIPTION

(First Cycle)

Active Core

Equivalent Diameter, in.	132.7
Active Fuel Height, First Core, in.	168
Height-to-Diameter Ratio	1.27
Total Cross-Section Area, ft <sup>2</sup>	96.06
H <sub>2</sub> O/U Molecular Ratio, lattice (Cold)	2.41

Reflector Thickness and Composition

Top - Water plus Steel, in.	~10
Bottom - Water plus Steel, in.	~10
Side - Water plus Steel, in.	~15

Fuel Assemblies

Number	193	
Rod Array	17 x 17	
Rods per assembly	264	
Rod Pitch, in.	0.496	
Overall Transverse Dimensions, in.	8.426 x 8.426	<u>UNIT 2</u>
Fuel Weight (as UO <sub>2</sub> ), lb	26000 <del>25986</del> (Nominal)	26000 (Nominal)
Zircalloy Weight, lbs (active core)	54840	
Number of Grids per Assembly	10 - Type R	18
Composition of Grids	Inconel 718	
Weight of Grids (Effective in Core), lb	2979	18
Number of Guide Thimbles per Assembly	24	
Composition of Guide Thimbles	Zircalloy 4	



STP FSAR

TABLE 4.3-1 (Continued)  
REACTOR CORE DESCRIPTION

(First Cycle)

Diameter of Guide Thimbles (upper part), in.	0.450 I.D.	
	0.482 O.D.	
Diameter of Guide Thimbles (lower part), in.	0.397 I.D.	
	0.429 O.D.	
Diameter of Instrument Guide Thimbles, in.	0.450 I.D.	
	0.482 O.D.	
<u>Fuel Rods</u>		
Number	50,952	
Outside Diameter, in.	0.374	
Diametral Gap, in.	0.0065	
Clad Thickness, in.	0.0225	
Clad Material	Zircaloy-4	
<u>Fuel Pellets</u>		
Material	UO <sub>2</sub> Sintered	
Density (percent of Theoretical)	95	
Fuel Enrichments, wt %		<u>UNIT 2</u>
Region 1	1.50	2.10
Region 2	2.20	2.60
Region 3	2.90	
Diameter, in.	0.3225	} 0.530 for 4 assemblies 0.387 for 189 assemblies
Length, in.	0.530	
Mass of UO <sub>2</sub> per Foot of Fuel Rod, lb/ft	0.366	0.364   54
<u>Rod Cluster Control Assemblies</u>		
Neutron Absorber	Hafnium	30   54
Composition	9.53% min	
Diameter, in.	0.366	

STP FSAR

TABLE 4.3-1 (Continued)

REACTOR CORE DESCRIPTION

(First Cycle)

Density, lb/in <sup>3</sup>	0.470 (min)	30	54
Cladding Material	Type 304, Cold Worked Stainless Steel		
Clad Thickness, in.	0.0185		30
Number of Clusters	57		
Number of Absorber Rods per Cluster	24		
<u>Burnable Poison Rods (First Core)</u>			
Number	946		18
Material	Borosilicate Glass		
Clad Outside Diameter, in.	0.381		54
Inner Tube, O.D., in.	0.1815		
Clad Material	Stainless Steel		
Inner Tube Material	Stainless Steel		
Boron Loading (w/o B <sub>2</sub> O <sub>3</sub> in glass rod)	12.5		
Weight of Boron-10 per foot of rod, lb/ft	.000419		30
Initial Reactivity Worth, $\beta \Delta\rho$	Unit 1 4.65 (HFP), 4.65 (H2P) 3.40 (cold)		
	Unit 2 7.23 (HFP), 7.23 (H2P) 5.28 (cold)		
<u>Excess Reactivity</u>			
Maximum Fuel Assembly k <sub>∞</sub> (Cold, Clean, Unborated Water)	1.39		
Maximum Core Reactivity (Cold, Zero Power, Beginning of Cycle)	1.22		

TABLE 4.3-2

## NUCLEAR DESIGN PARAMETERS

(First Cycle)

<u>Core Average Linear Power, kW/ft, including densification effects</u>	5.20			
<u>Total Heat Flux Hot Channel Factor, <math>F_Q</math></u>	2.50			
<u>Nuclear Enthalpy Rise Hot Channel Factor, <math>F_{\Delta R}^H</math></u>	1.52			
		<u>Best Estimate</u>		
<u>Reactivity Coefficients<sup>+</sup></u>	<u>Design Limits</u>	<u>Unit 1</u>	<u>Unit 2</u>	
Doppler-only Power, <u>Upper Curve</u> Coefficients, pcm/°F	-19.4 to 12.6	-15.5 to -11.5	-13.8 to -10.0	53
(See Figure 15.0-5), <u>Lower Curve</u>	-10.2 to -6.7	-12.5 to -9	-11.4 to -8.1	
Doppler Temperature Coefficient pcm/°F	-2.9 to -1.1	-2.5 to -1.8	-2.2 to -1.4	
Rodderator Temperature Coefficient, pcm/°F	0 to -40	-6. to -30.0	-6.4 to -35.4	
Boron Coefficient, pcm/ppm <sup>++</sup>	-16 to -7 <sup>5</sup>	-14 to -9 <sup>5</sup>	-14 to -8	
Rodded Moderator Density Coefficient, pcm/gw/cc <sup>++</sup>	$\leq 0.43 \times 10^5$	$\leq 0.34 \times 10^5$	$\leq 0.39 \times 10^5$	

4.3-47

Amendment 53

\*Uncertainties are given in Section 4.3.3.3.

TABLE 4.3-2 (Continued)

NUCLEAR DESIGN PARAMETERS

(First Cycle)

	<u>Unit 1</u>	<u>Unit 2</u>
<u>Delayed Neutron Fraction and Lifetime</u>		
$\beta_{eff}$ BOL, (EOL)	0.0075, (0.0044)	0.0075, (0.0047)
$t^*$ , BOL, (EOL) $\mu$ sec	25.0 (16.0)	25.0 (17.0)
<u>Control Rods</u>		
Rod Requirements	See Table 4.3-3	See Table 4.3-3
Maximum Bank Worth, pcm	< 2000	< 2000
Maximum Ejected Rod Worth	See Chapter 15	See curve 15
Bank Worth, pcm <sup>++</sup> (BOL)	BOL, Xe free	BOL, Xe free
Bank D	650	746
Bank C	1250	1308
Bank B	1200	1315
Bank Worth, pcm <sup>++</sup> (EOL)	EOL Eq. Xe	EOL Eq. Xe
Bank D	750	748
Bank C	1450	1308
Bank B	1400	1199

++Note: 1 pcm  $\equiv$  (percent millirho) =  $10^{-5} \Delta\rho$  where  $\Delta\rho$  is calculated from two statepoint values of  $k_{eff}$  by  $\ln(k_2/k_1)$ .

TABLE 4.3-2 (Continued)

## NUCLEAR DESIGN PARAMETERS

Reactor Factor (ROF, to ROL)	(First Cycle)	
	UNIT 1	UNIT 2
Unrodded	1.41 to 1.28	1.36 to 1.24
D bank	1.50 to 1.45	1.44 to 1.35
D + C	1.60 to 1.45	1.59 to 1.34
D + C + B	1.80 to 1.55	1.66 to 1.56

Boron Concentrations, B0L, ppm	UNIT 1	UNIT 2
	Zero Power, $K_{off} = 0.99$ , Cold, Rod Cluster Control Assemblies Out, clean	1080
Zero Power, $K_{off} = 0.99$ , Hot, Rod Cluster Control Assemblies Out, clean	1030	1325
Design Basis Refueling Boron Concentration	2500	2500
Zero Power, $K_{off} = 0.95$ , Cold, Rod Cluster Control Assemblies In, Clean	910	1205
Zero Power, $K_{off} = 1.00$ , Hot, Rod Cluster Control Assemblies Out, Clean	930	1222
Full Power, No Xenon, $k_{eff} = 1.0$ , Hot, Rod Cluster Control Assemblies out	835	1114
Zero Power, No Xenon $k_{eff} = .99$ , Cold, Rod Cluster Control Assemblies in less	730	1009
Most Reactive Rod Stuck in Full Out Position		

53

TABLE 4.3-2 (Continued)

NUCLEAR DESIGN PARAMETERS

(First Cycle)

<u>Boron Concentrations (Cont'd)</u>	<u>UNIT 1</u>	<u>UNIT 2</u>
Full Power, Equilibrium Xenon, $k_{eff} = 1.0$ , Hot, Rod Cluster Control Assemblies Out	590	807
Reduction with Fuel Burnup		
First Cycle ppm/GWD/MTU**	See Figure 4.3-3 A	see Figure 4.3-3 B
Reload Cycle, ppm/GWD/MTU	~ 100	~ 100

\*\* Gigawatt Day (GWD) = 1000 Megawatt Day (1000 MWD). During the first cycle, fixed burnable poison rod are present which significantly reduce the boron depletion rate compared to reload cycles.



STP PSAR

TABLE 4.3-3

REACTIVITY REQUIREMENTS FOR ROD CLUSTER CONTROL ASSEMBLIES

Reactivity Effects, percent	Beginning-of-Life (First Cycle)		End-of-Life (First Cycle)		End-of-Life (Equilibrium Cycle)
	UNIT 1	UNIT 2	UNIT 1	UNIT 2	UNITS 1 & 2
1. Control requirements					
Fuel temperature (Doppler), $\Delta\rho$	1.35	1.16	1.10	0.97	1.15
Moderator temperature*, $\Delta\rho$	0.20	0.30	1.15	1.05	1.20
Redistribution, $\Delta\rho$	0.50	0.50	1.20	1.20	1.20
Rod Insertion Allowance, $\Delta\rho$	.60	.60	0.60	0.60	0.60
2. Total Control, $\Delta\rho$	2.65	2.56	4.05	3.82	4.15
3. Estimated Rod Cluster Control Assembly Worth (57 Rods)					
a. All assemblies inserted, $\Delta\rho$	9.50	9.09	9.50	8.68	8.50
b. All but one (highest worth) assembly inserted, $\Delta\rho$	8.00	7.78	8.00	7.41	6.90
4. Estimated Rod Cluster Control Assembly credit with 10 percent adjustment to accommodate uncertainties (3b - 10 percent), $\Delta\rho$	7.20	7.00	7.20	6.67	6.20

4.3-51

Amendment 30

STP PSAR

130

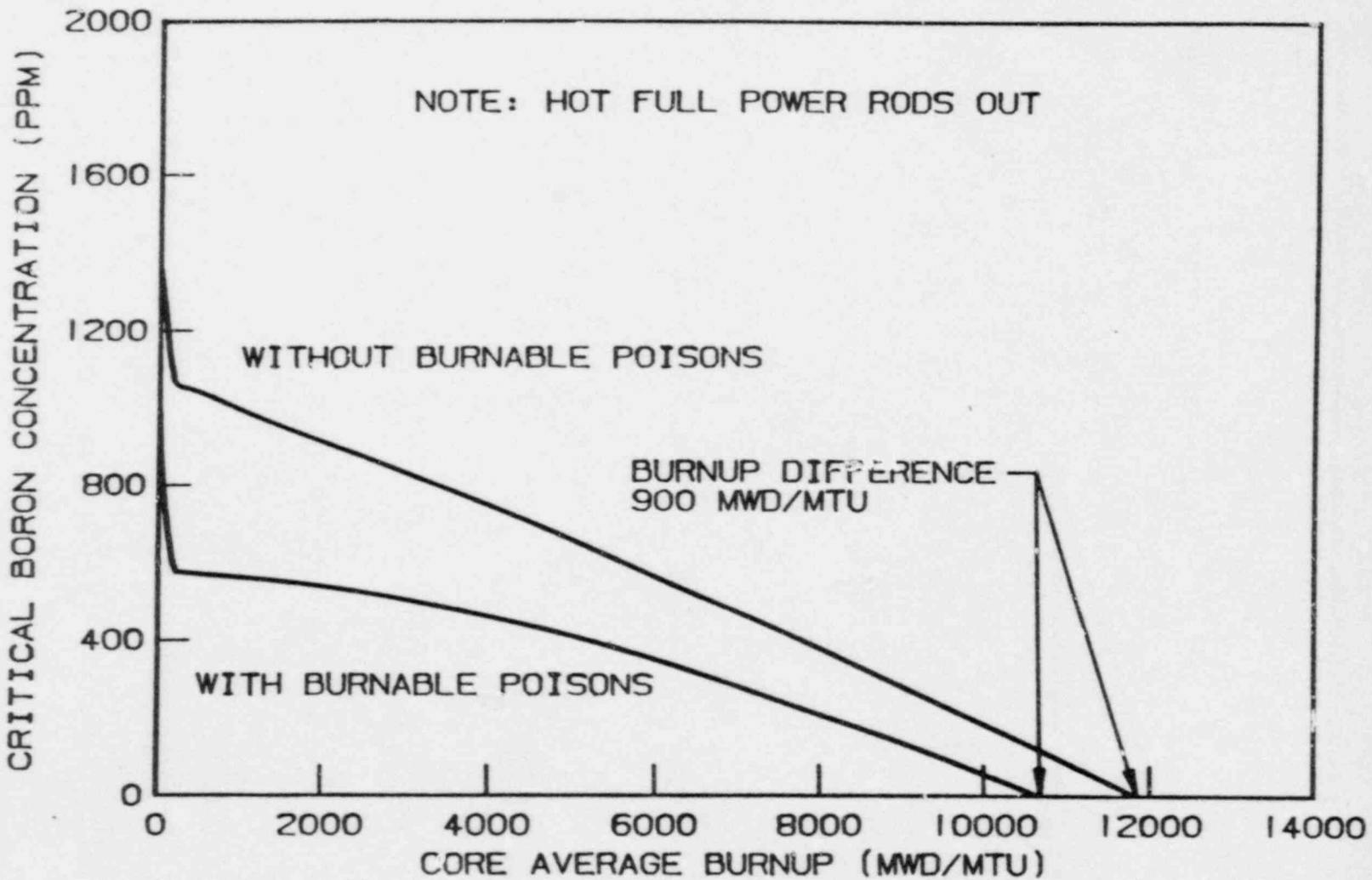
TABLE 4.3-3 (Continued)

REACTIVITY REQUIREMENTS FOR ROD CLUSTER CONTROL ASSEMBLIES

Reactivity Effects, <u>percent</u>	Beginning-of-Life		End-of-Life		End-of-Life
	(First Cycle)		(First Cycle)		(Equilibrium Cycle)
	<u>UNIT 1</u>	<u>UNIT 2</u>	<u>UNIT 1</u>	<u>UNIT 2</u>	<u>UNITS 1 &amp; 2</u>
5. Shutdown margin available (4-2), %Δρ	4.55	4.44	3.15	2.85	2.05**

\* Includes void effects

\*\* The design basis minimum shutdown is 1.75%Δρ

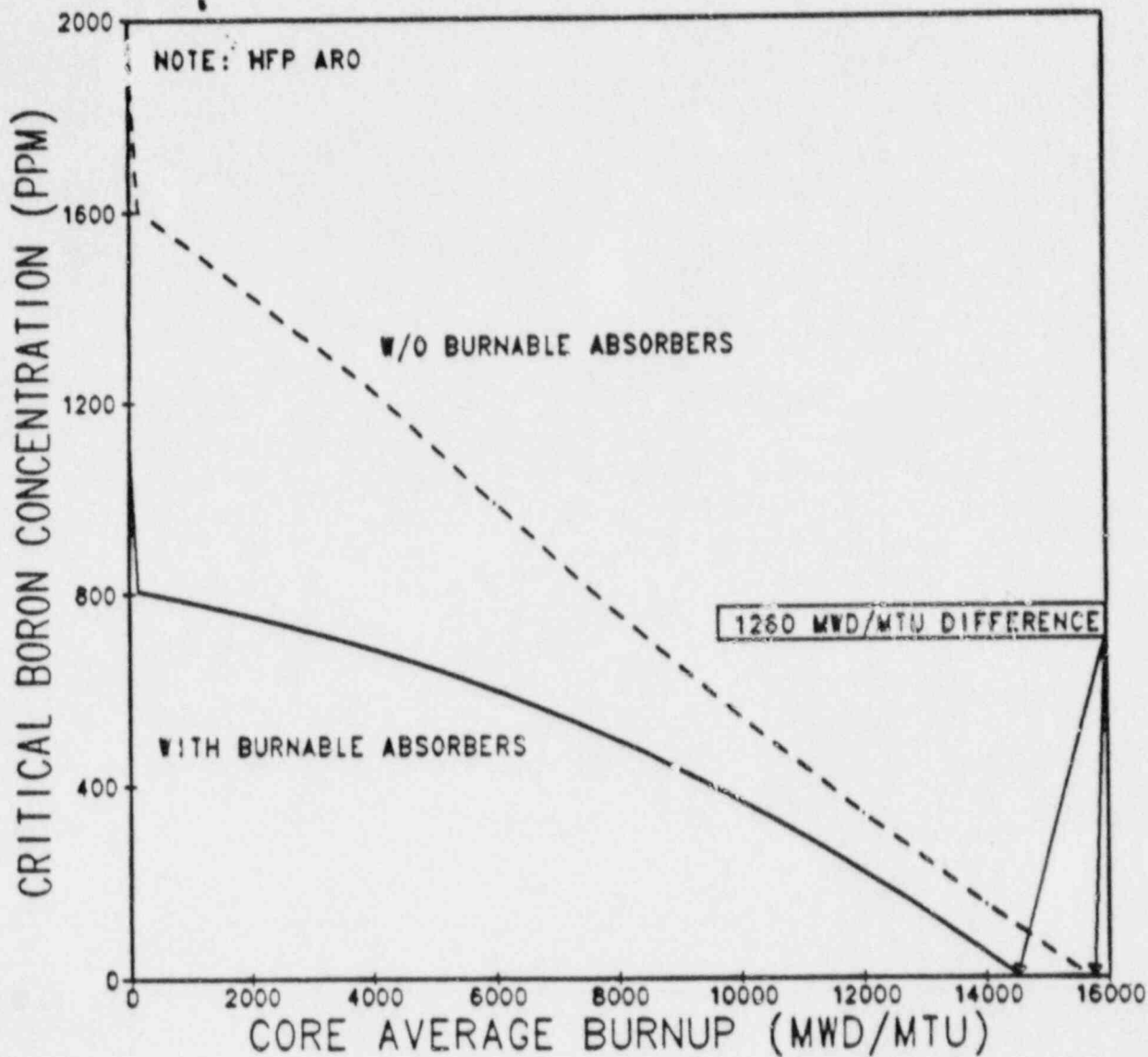


**SOUTH TEXAS PROJECT  
UNITS 1 & 2**

BORON CONCENTRATION VERSUS  
FIRST CYCLE BURN-UP WITH AND  
WITHOUT BURNABLE POISON RODS

Figure 4.3-34

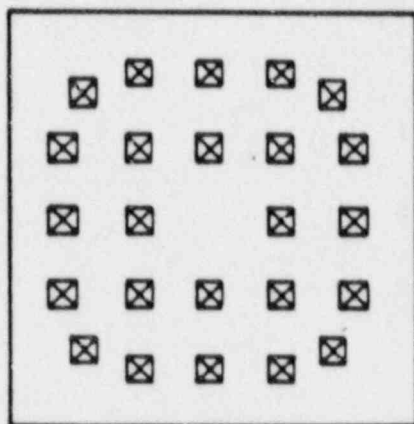
Amendment 53



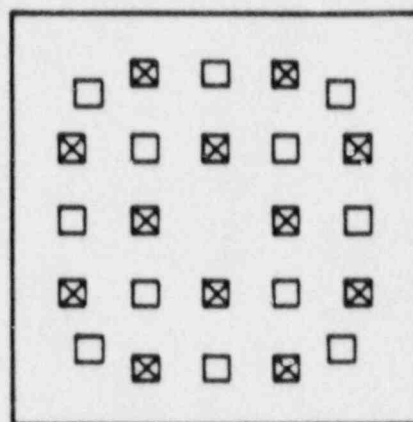
**SOUTH TEXAS PROJECT  
UNIT 2**

BORON CONCENTRATION VERSUS  
FIRST CYCLE BURN-UP WITH AND  
WITHOUT BURNABLE POISON RODS

Figure 4.3-3 B

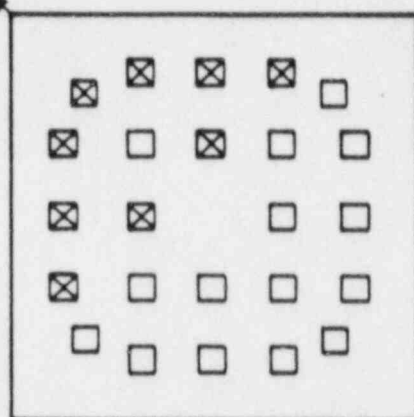


24 BP'S

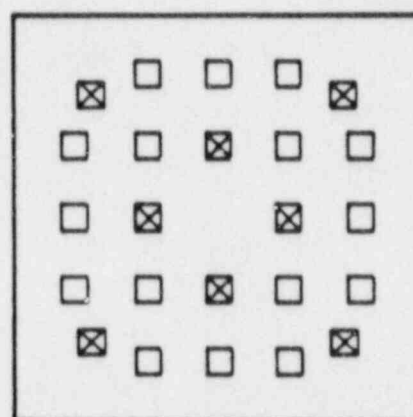


12 BP'S

CORE CENTER



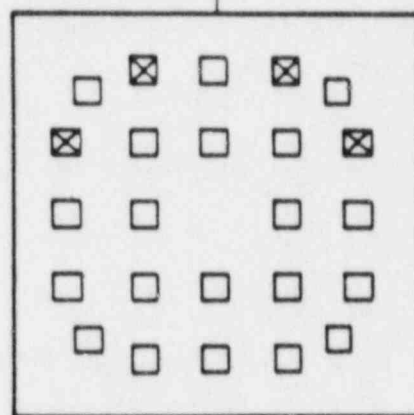
9 BP'S



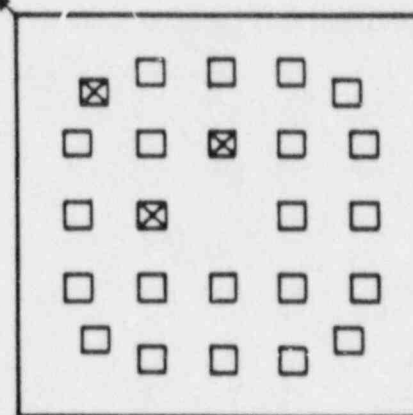
8 BP'S

CORE CENTER

CORE CENTER



4 BP'S

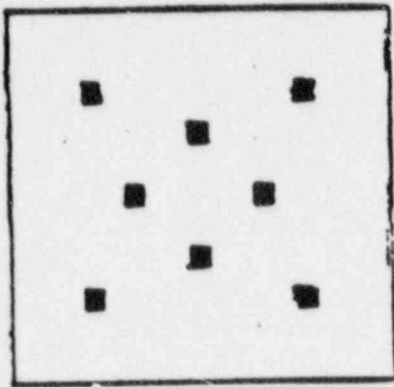


3 BP'S

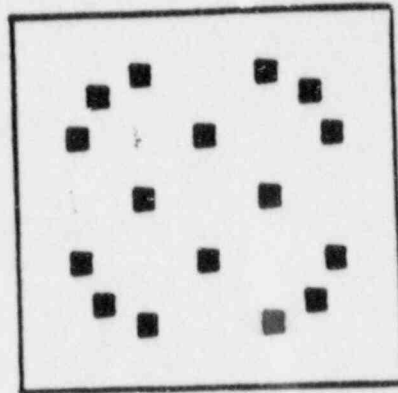
**SOUTH TEXAS PROJECT  
UNITS 1 & 2**

Burnable Poison Rod Arrangement Within  
an Assembly  
Figure 4.3-4<sup>A</sup>

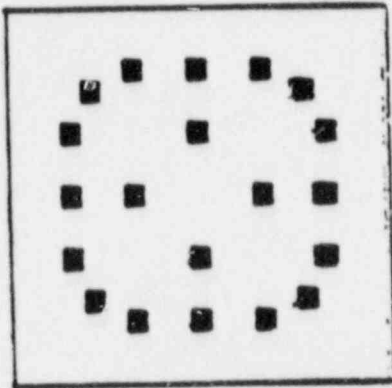




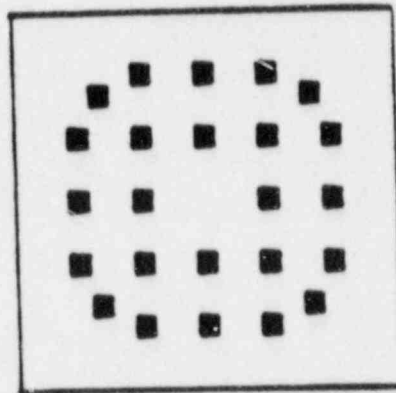
8 BA'S



16 BA'S



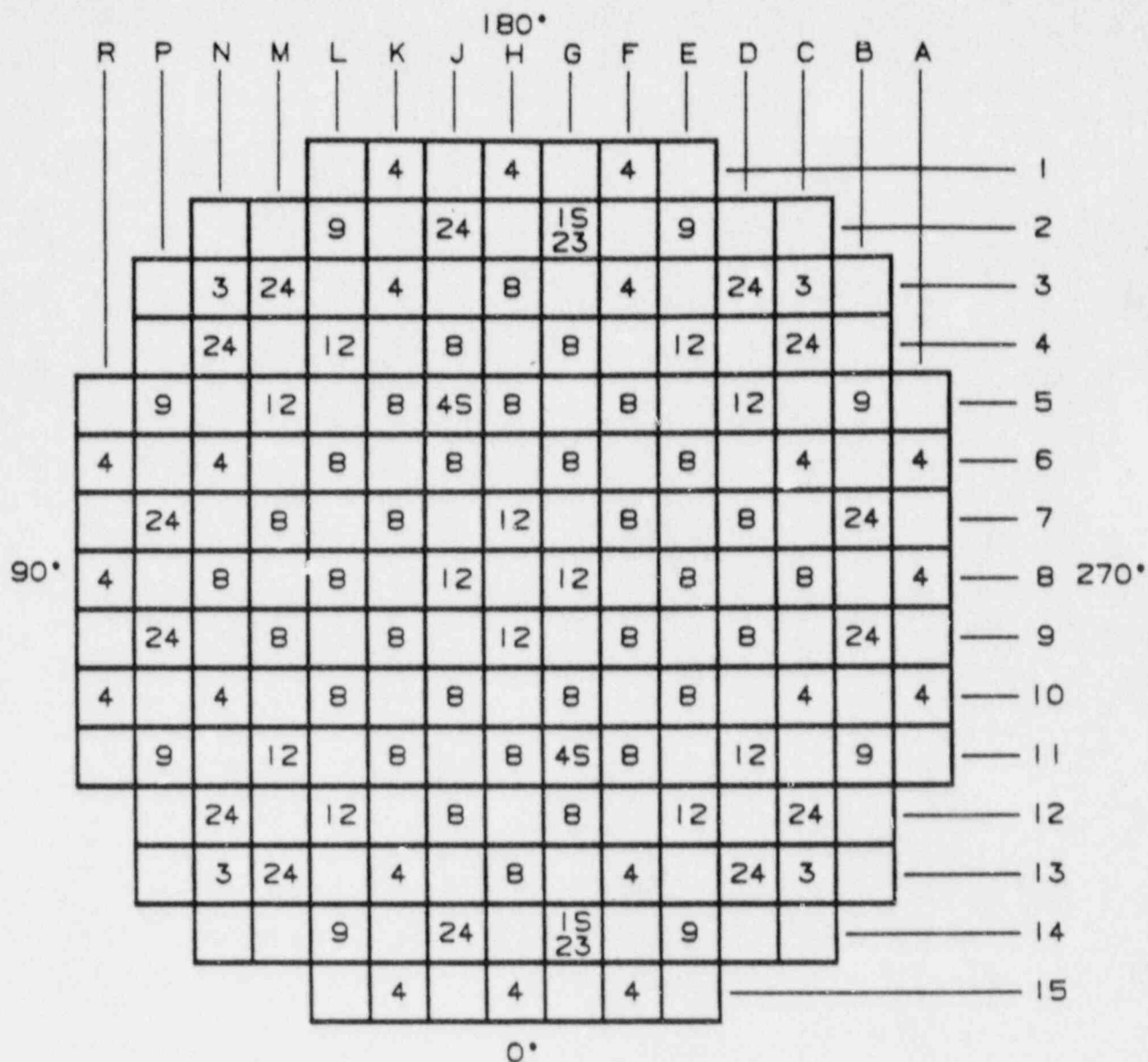
20 BA'S



24 BA'S

SOUTH TEXAS PROJECT  
UNIT 2

Burnable Poison Rod Arrangement Within  
an Assembly  
Figure 4.3-4. B



NUMBER INDICATES NUMBER OF  
BURNABLE POISON RODS

S-INDICATES SOURCE ROD

946 BP RODS

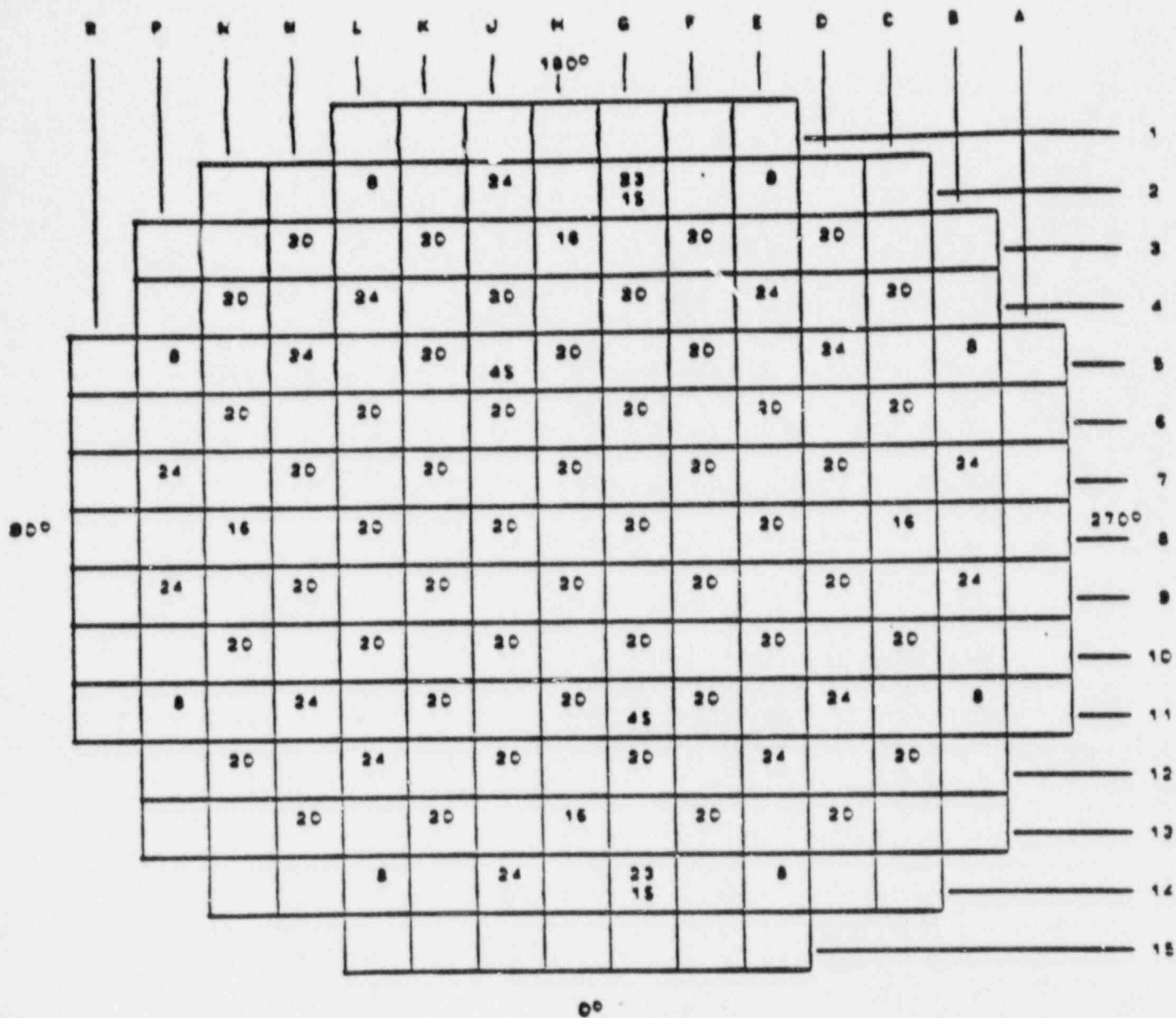
12.5 W/O B<sub>2</sub>O<sub>3</sub>

**SOUTH TEXAS PROJECT  
UNITS 1 & 2**

BURNABLE POISON LOADING  
PATTERN

Figure 4.3-5A

Amendment 53



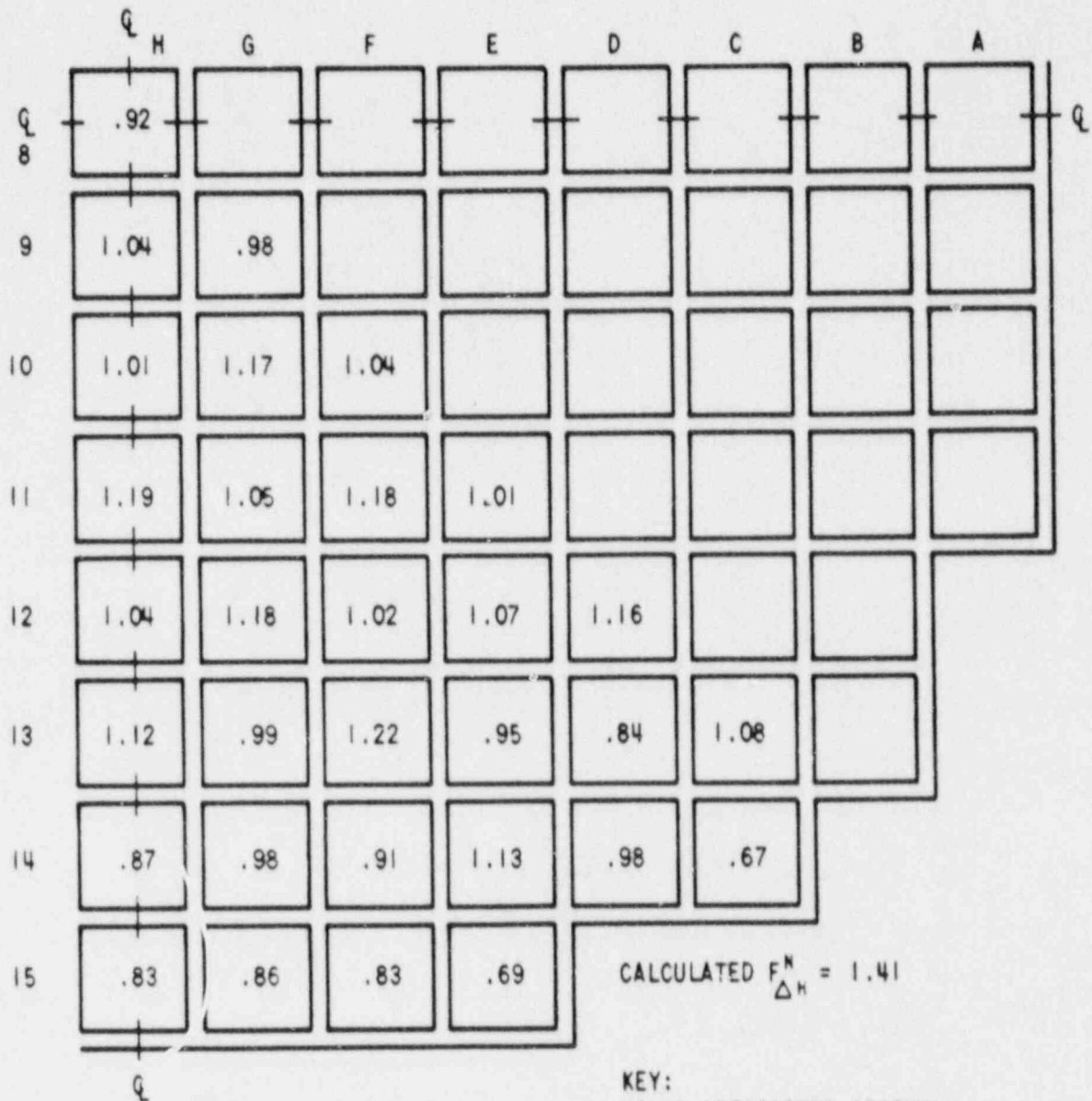
X - NUMBER OF BURNABLE ABSORBERS  
 S - SOURCE RODS

1470 BURNABLE ABSORBERS - 12.5 W/D BDRON

**SOUTH TEXAS PROJECT  
 UNIT 2**

**BURNABLE POISON LOADING  
 PATTERN**

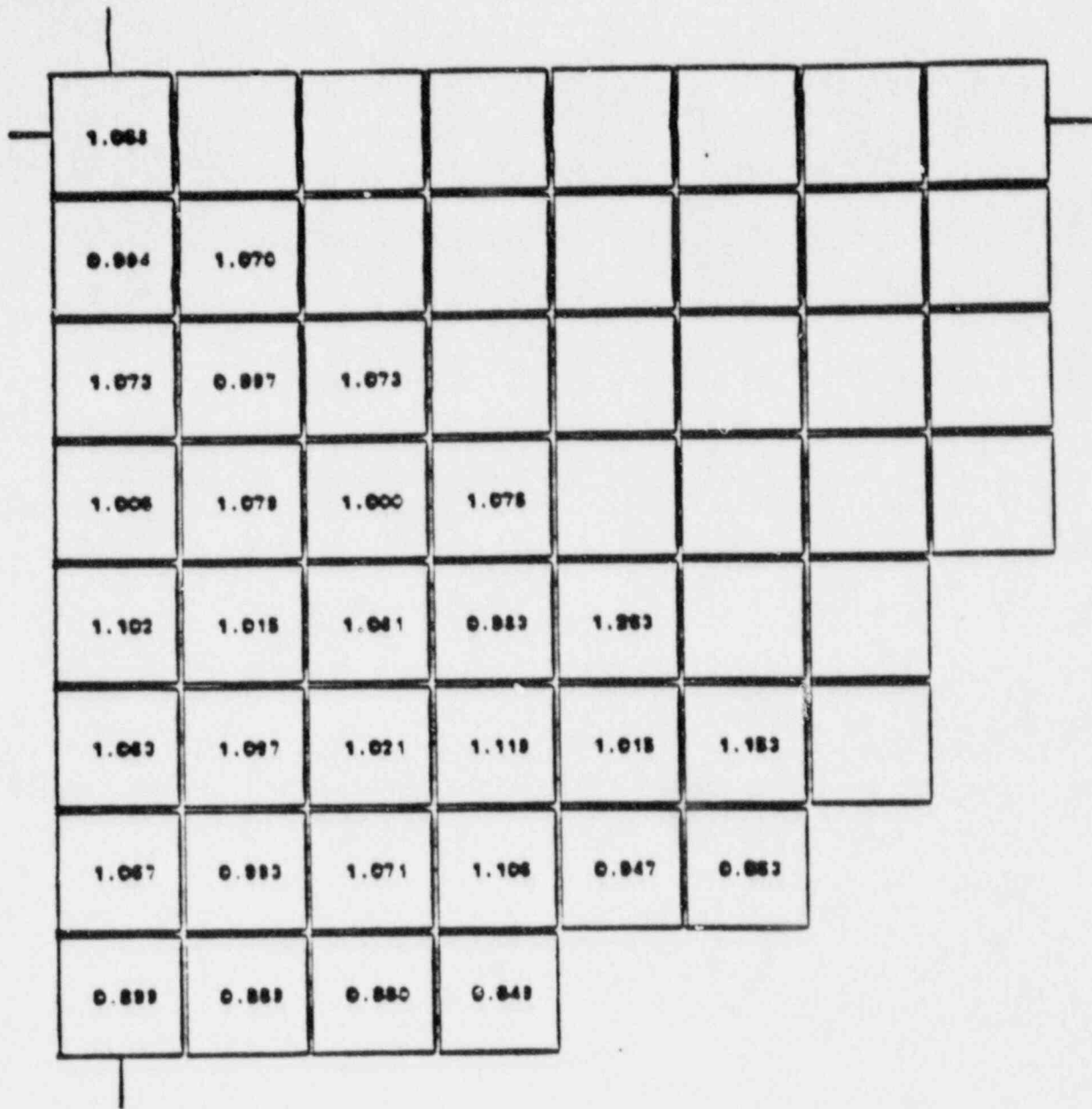
Figure 4.3.5 B



## SOUTH TEXAS PROJECT UNITS 1 & 2

Normalized Power Density Distribution Near Beginning  
of Life, Unrodded Core, Hot Full Power, No Xenon

Figure 4.3-6<sup>A</sup>



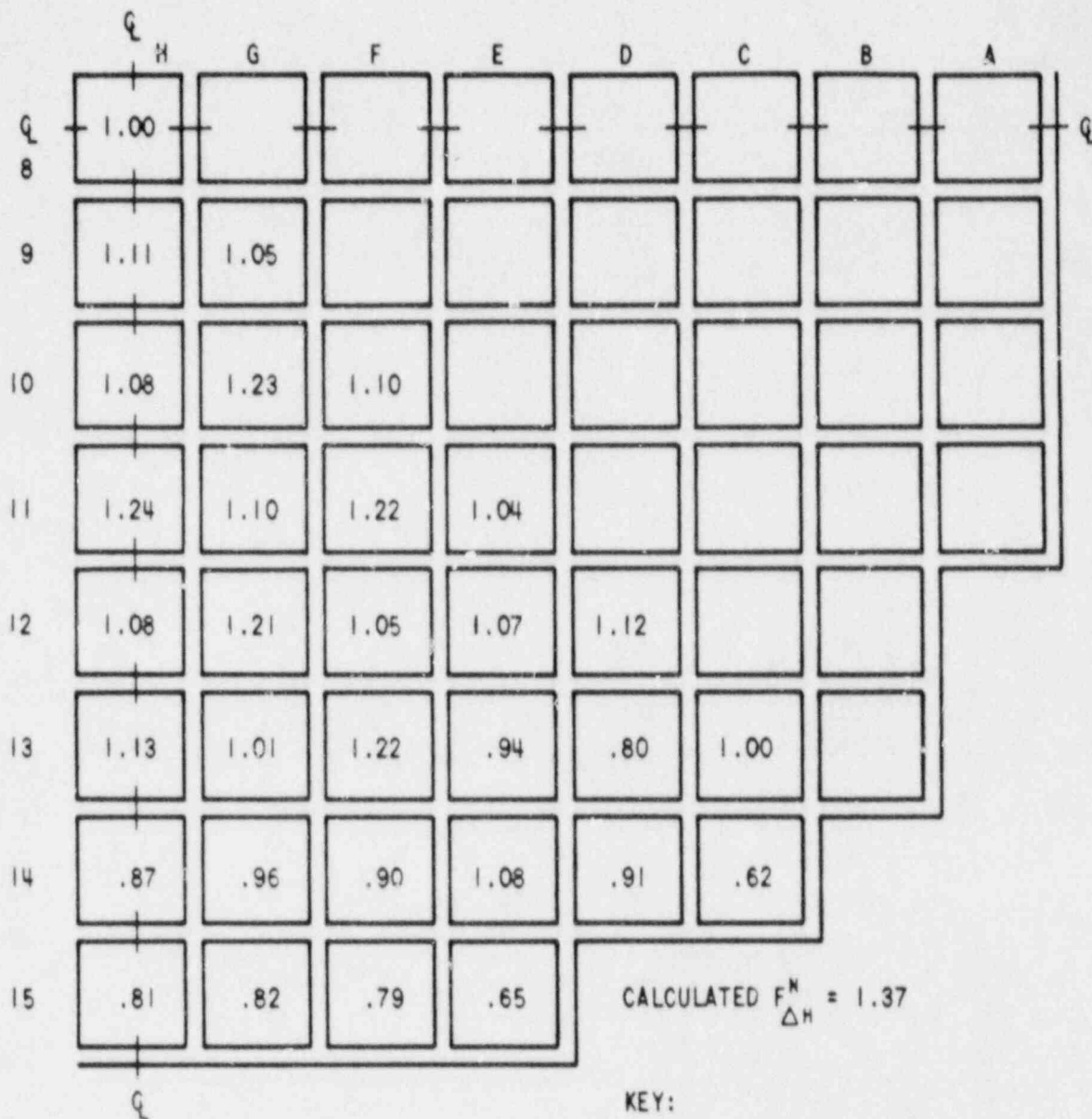
CALCULATED P&H = 1.288

## SOUTH TEXAS PROJECT UNIT 2

Normalized Power Density Distribution Near Beginning  
of Life, Unroaded Cars, Not Full Power, No Xenon

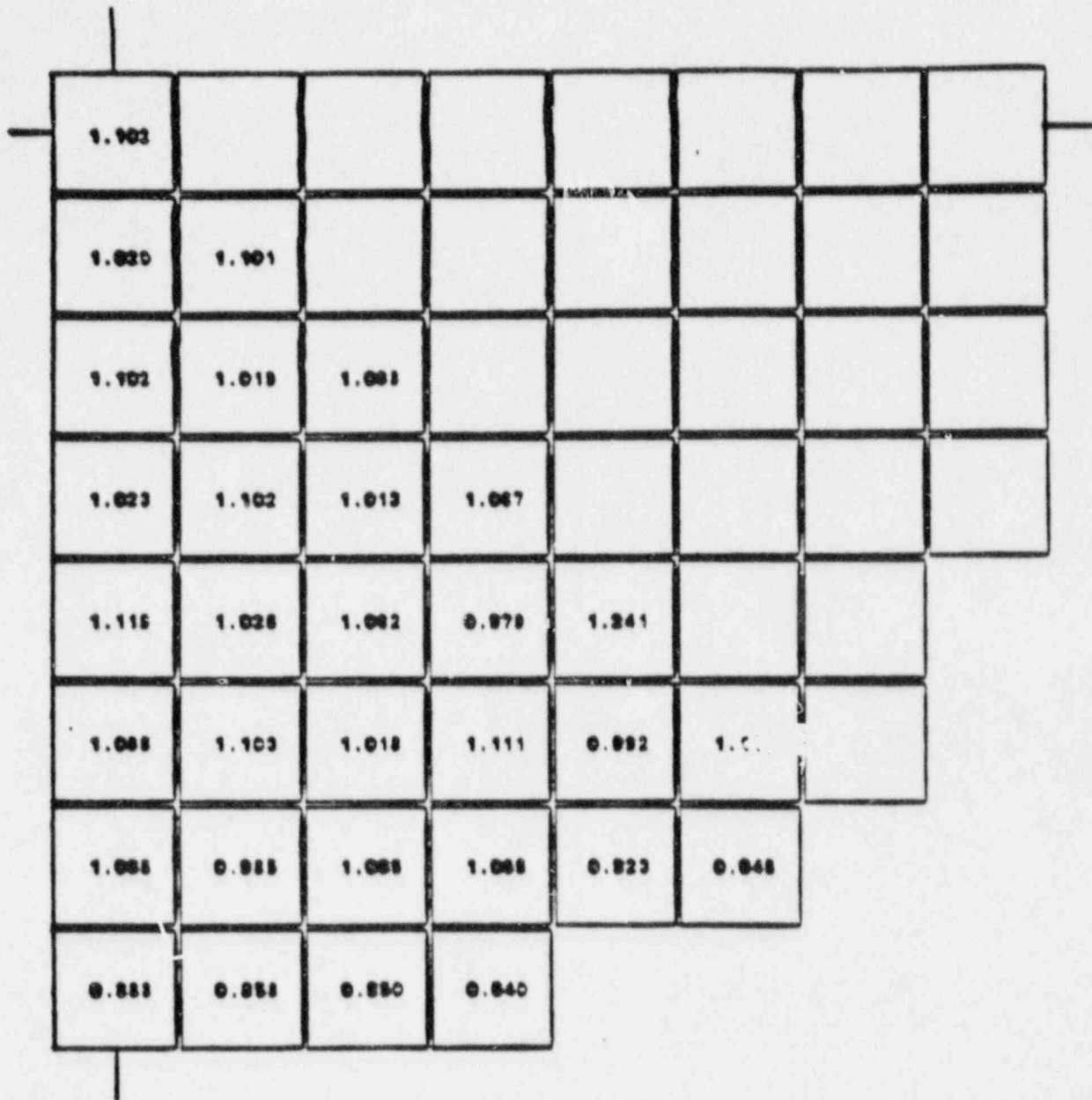
Figure 4.3-6. B





## SOUTH TEXAS PROJECT UNITS 1 & 2

Normalized Power Density Distribution Near Beginning  
of Life, Unrodded Core, Hot Full Power, Equilibrium  
Xenon  
Figure 4.3-4

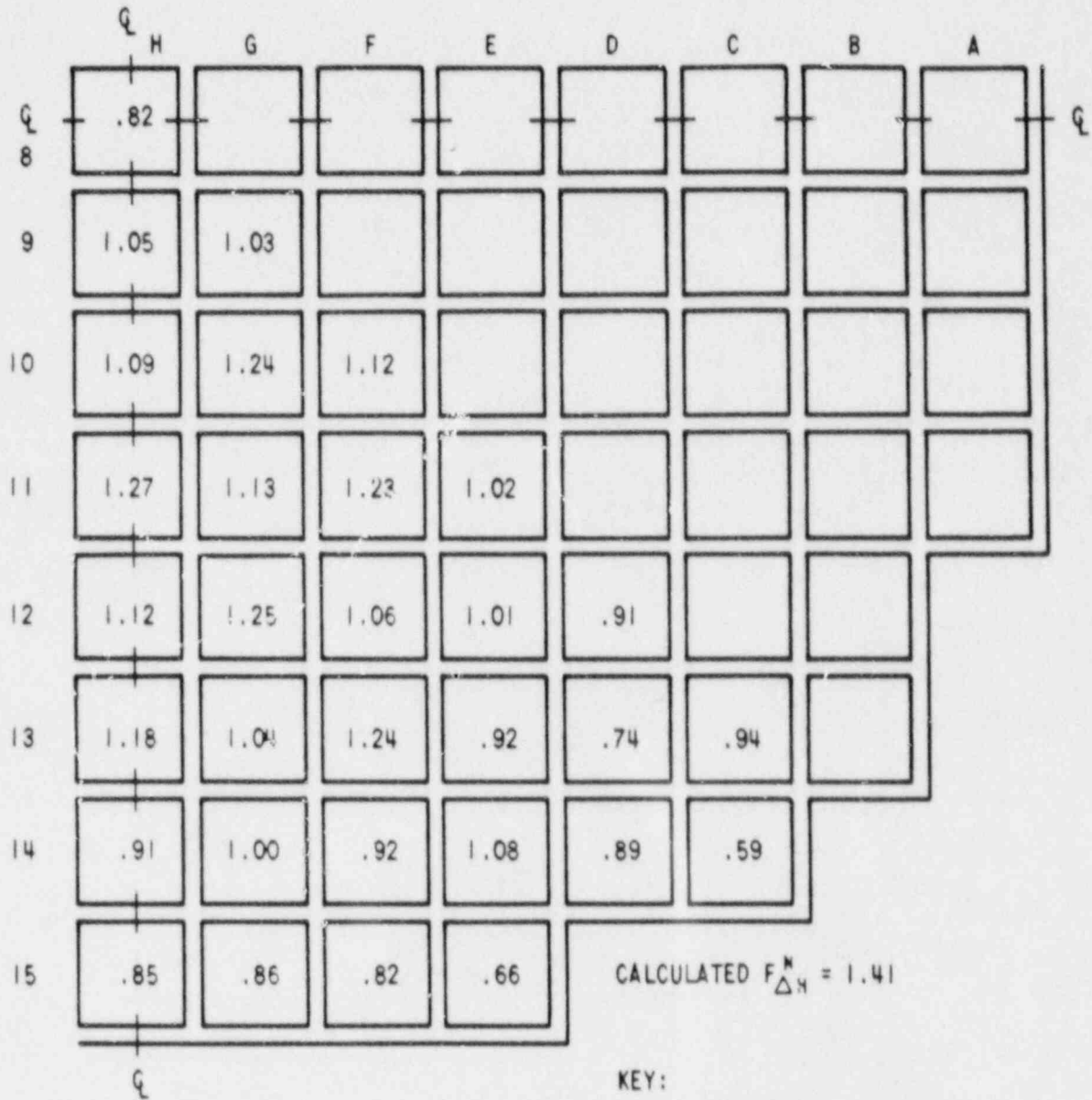


CALCULATED R<sub>0H</sub> = 1.844

**SOUTH TEXAS PROJECT  
UNIT 2**

Normalized Power Density Distribution Near Beginning  
of Life, Unrodded Core, Hot Full Power, Equilibrium  
Xe<sub>135</sub>

Figure 4.3-7 B



KEY:

VALUE REPRESENTS ASSEMBLY  
RELATIVE POWER

## SOUTH TEXAS PROJECT UNITS 1 & 2

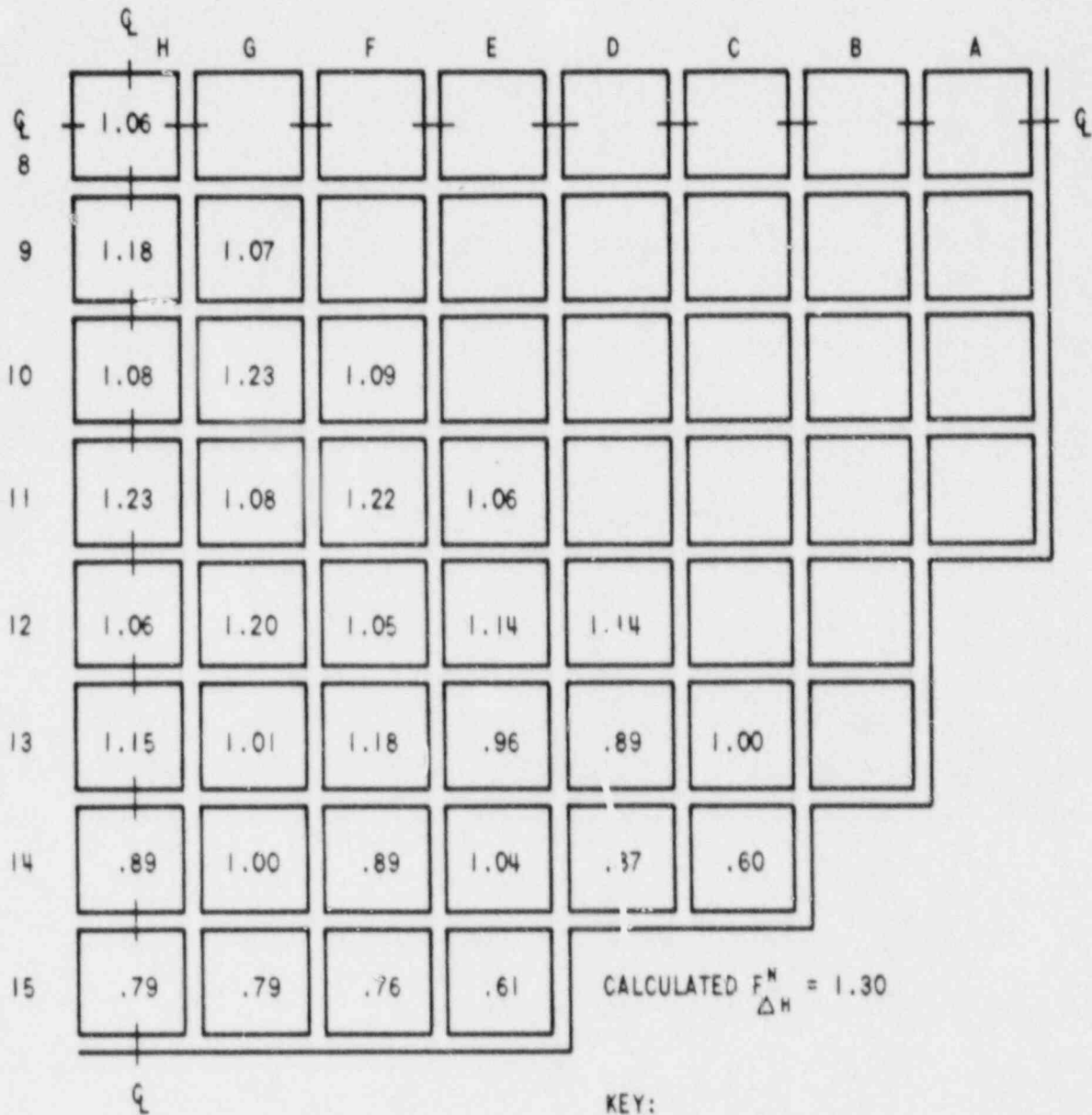
Normalized Power Density Distribution Near Beginning  
of Life, Group D 40% Inserted, Hot Full Power,  
Equilibrium Xenon  
Figure 4.3-8<sup>A</sup>

0.978							
0.990	1.001						
1.112	1.032	1.112					
1.049	1.125	1.023	1.071				
1.152	1.051	1.009	0.841	1.009			
1.122	1.194	1.029	1.088	0.831	1.084		
1.104	1.018	1.054	1.083	0.899	0.822		
0.821	0.886	0.889	0.847				

CALCULATED FWH = 1.843

## SOUTH TEXAS PROJECT UNIT 2

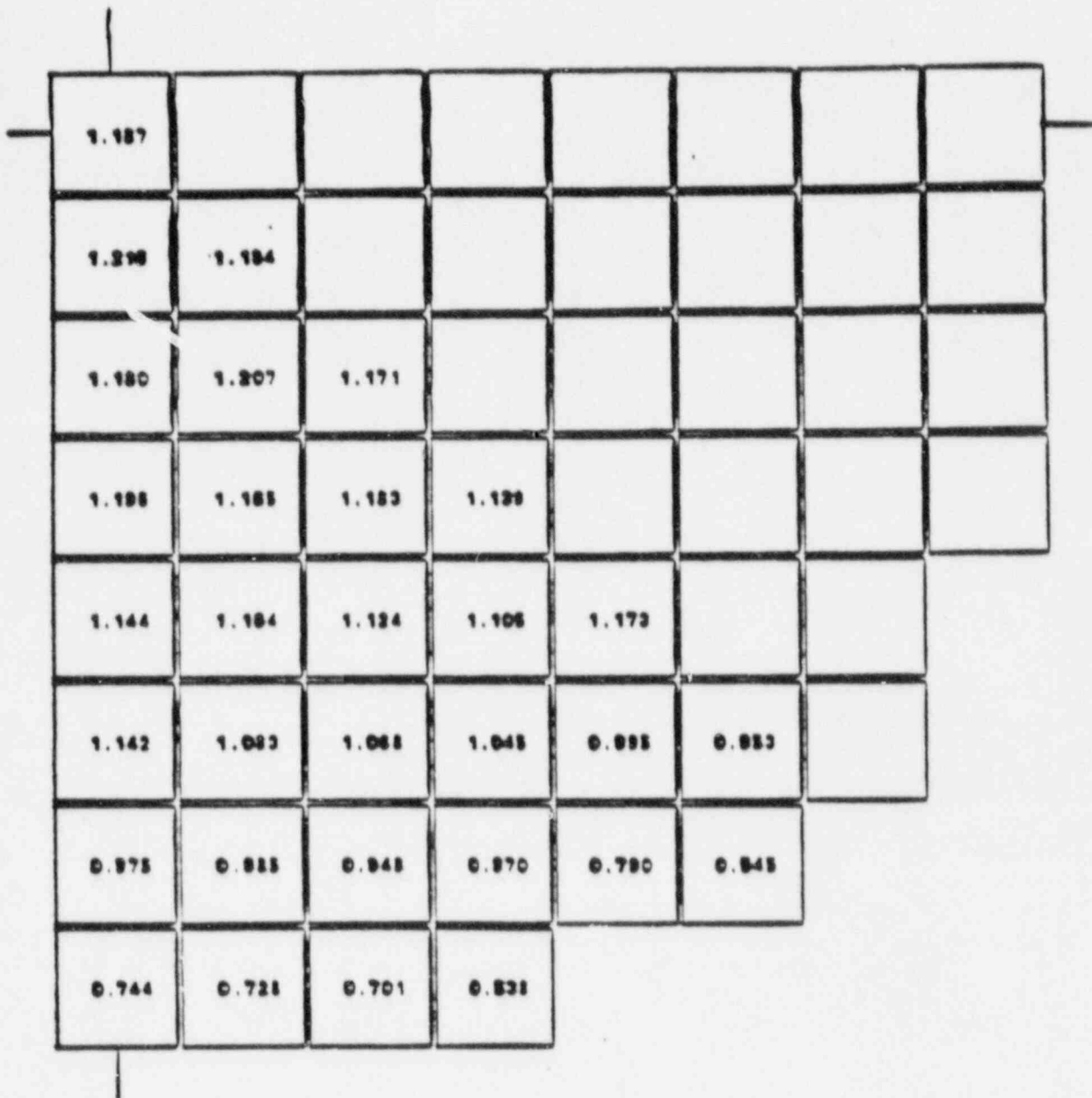
Normalized Power Density Distribution Near Beginning  
of LHe, Group D 80% Inserted, Hot Full Power,  
Equilibrium Xenon  
Figure 4.3-8 B



**SOUTH TEXAS PROJECT  
 UNITS 1 & 2**

Normalized Power Density Distribution Near Middle  
 of Life, Unrodded Core, Hot Full Power, Equilibrium  
 Xenon  
 Figure 4.3-9<sup>A</sup>

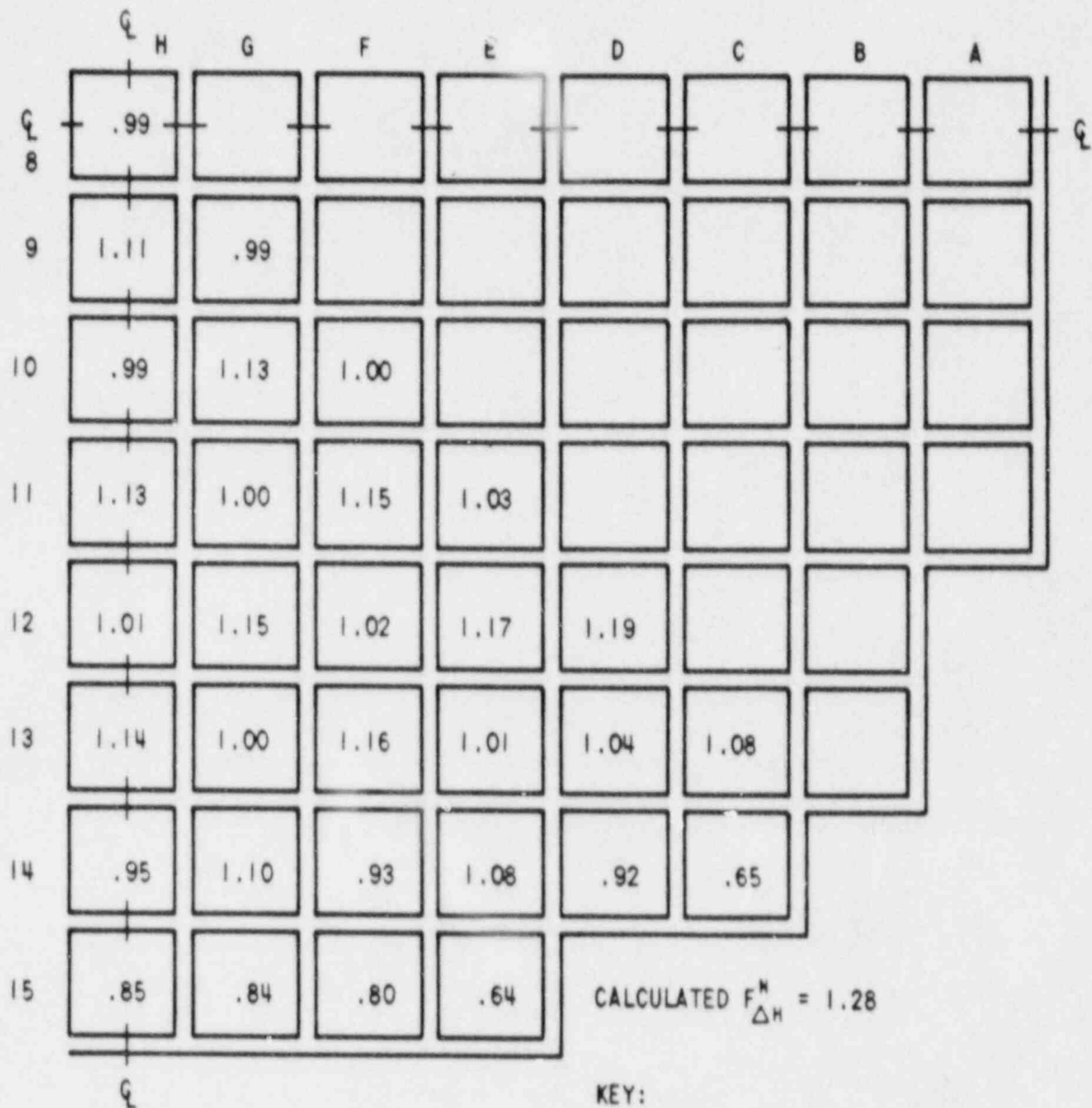




CALCULATED PAM = 1.801

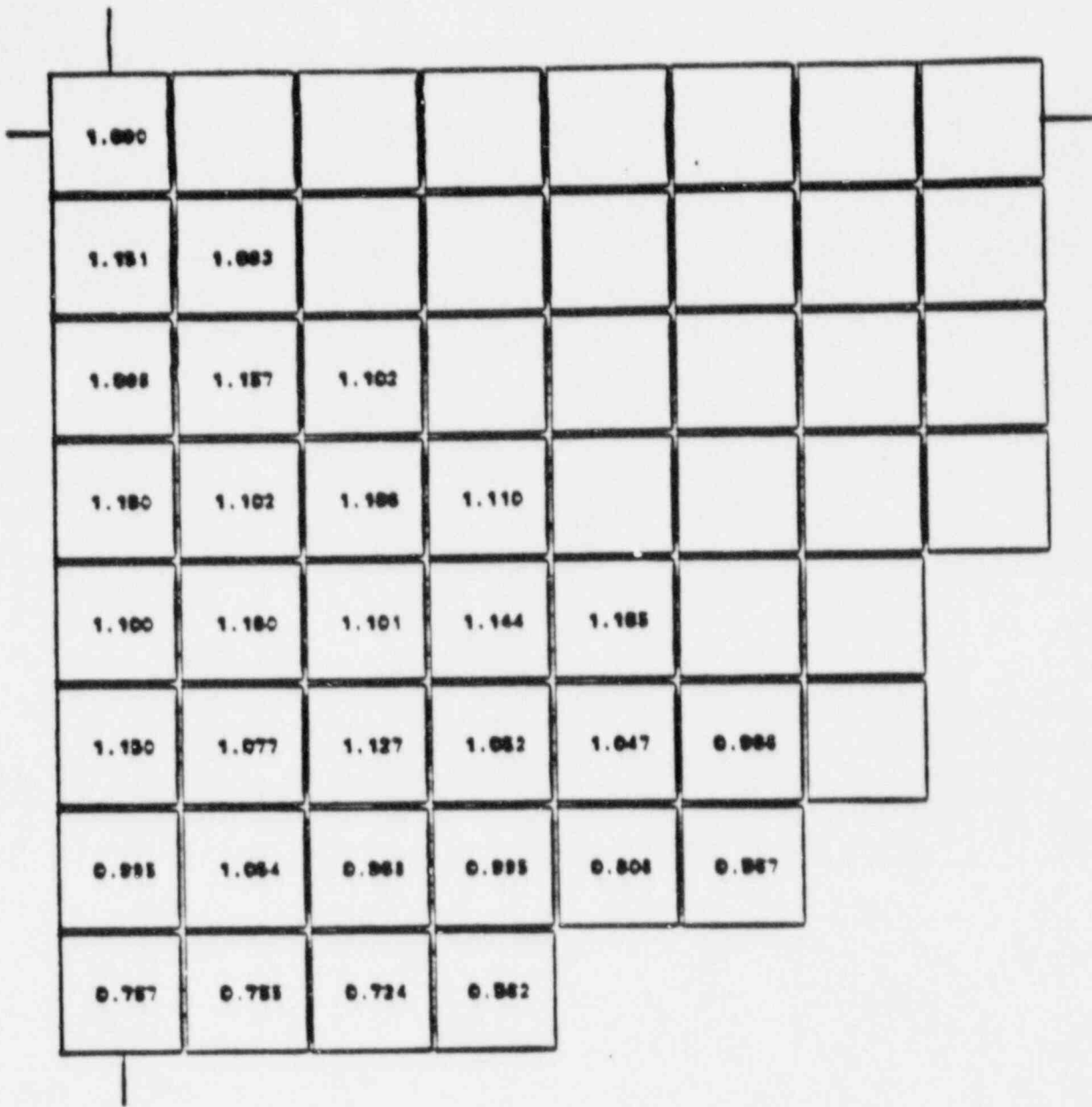
## SOUTH TEXAS PROJECT UNIT 2

Normalized Power Density Distribution Near Middle  
of LHe, Unrodded Core, Hot Full Power, Equilibrium  
Xenon  
Figure 4.3-8 B



## SOUTH TEXAS PROJECT UNITS 1 & 2

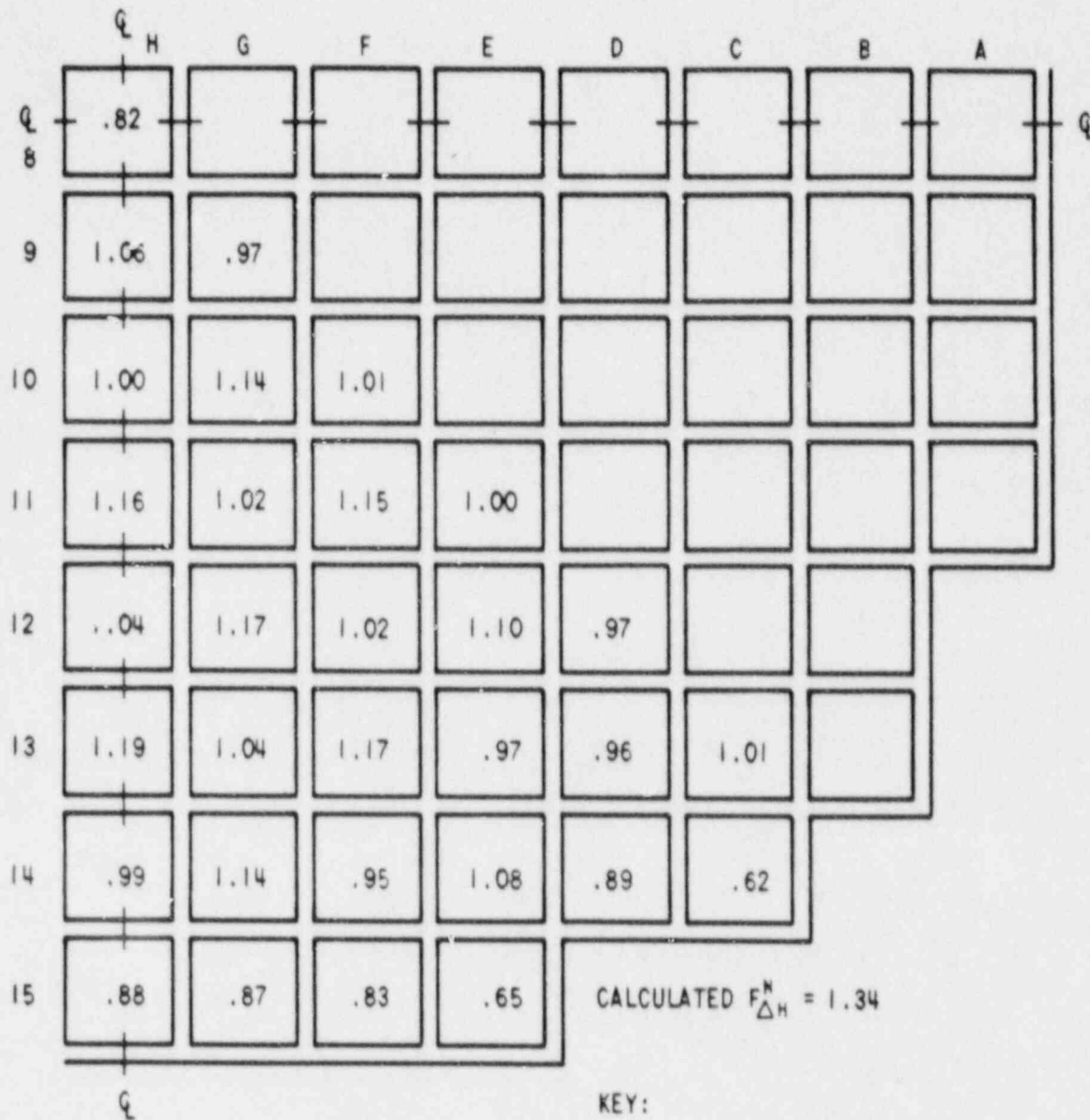
Normalized Power Density Distribution Near End of  
Life, Unrodded Core, Not Full Power, Equilibrium  
Xenon  
Figure 4.3-10<sup>A</sup>



CALCULATED P&H = 1.239

## SOUTH TEXAS PROJECT UNIT 2

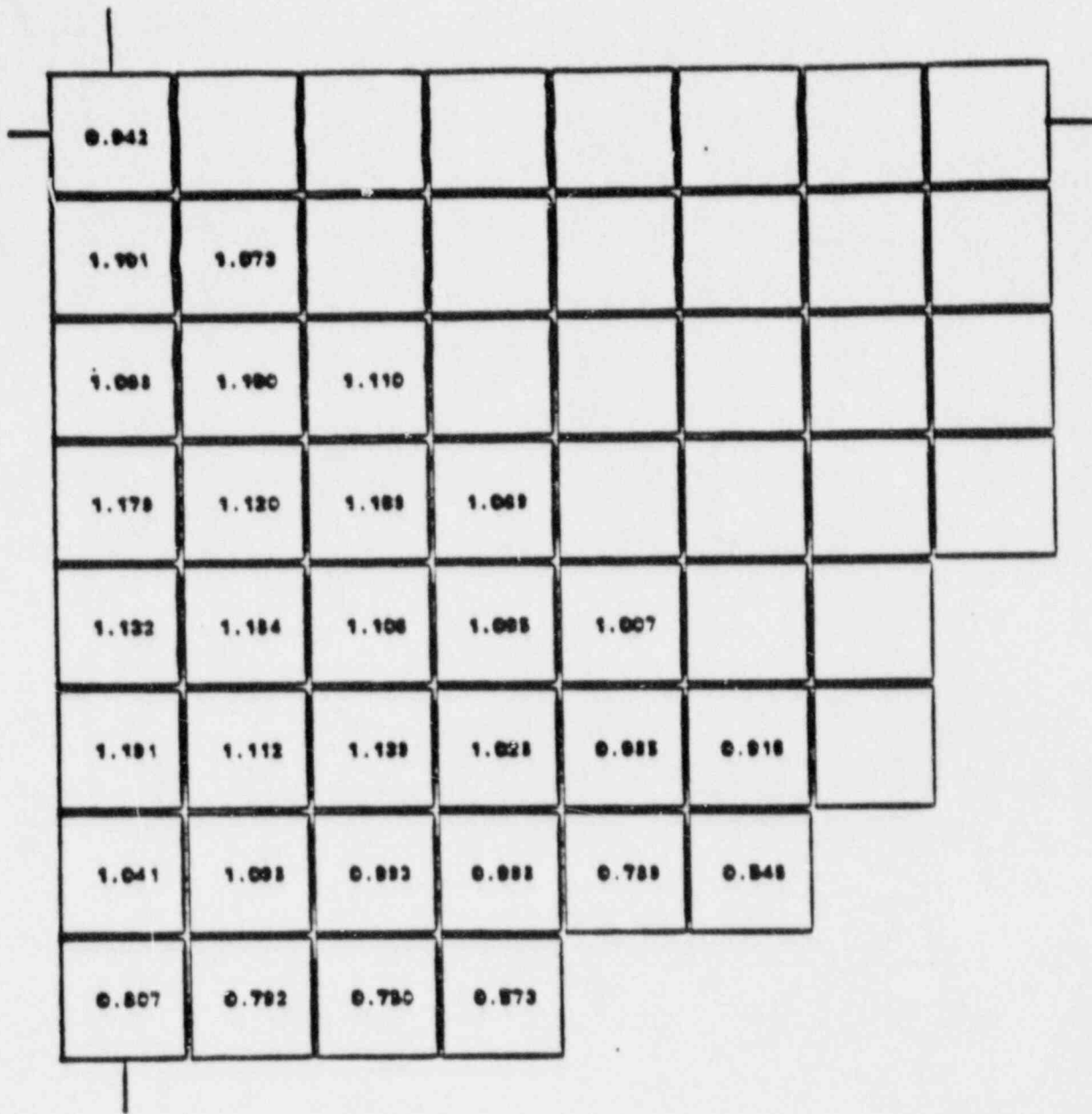
Normalized Power Density Distribution Near End of  
Life, Unroaded Cars, Hot Full Power, Equilibrium  
Xenon  
Figure 4.3-10 B



KEY:  
 VALUE REPRESENTS ASSEMBLY  
 RELATIVE POWER

## SOUTH TEXAS PROJECT UNITS 1 & 2

Normalized Power Density Distribution Near End of  
 Life, Hot Full Power, Equilibrium Xenon, Group D  
 40% Inserted  
 Figure 4.3-11

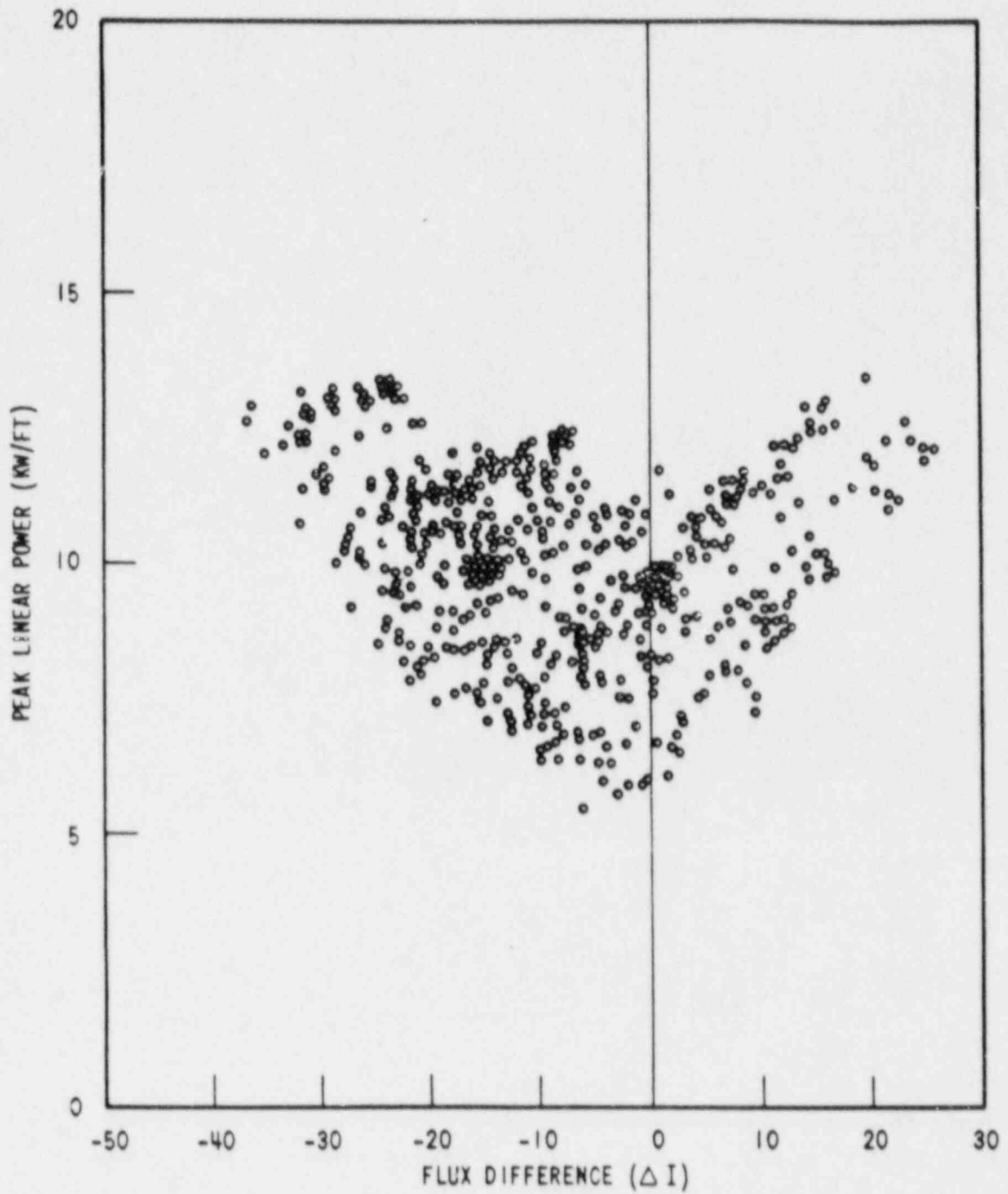


CALCULATED RHM = 1.848

## SOUTH TEXAS PROJECT UNIT 2

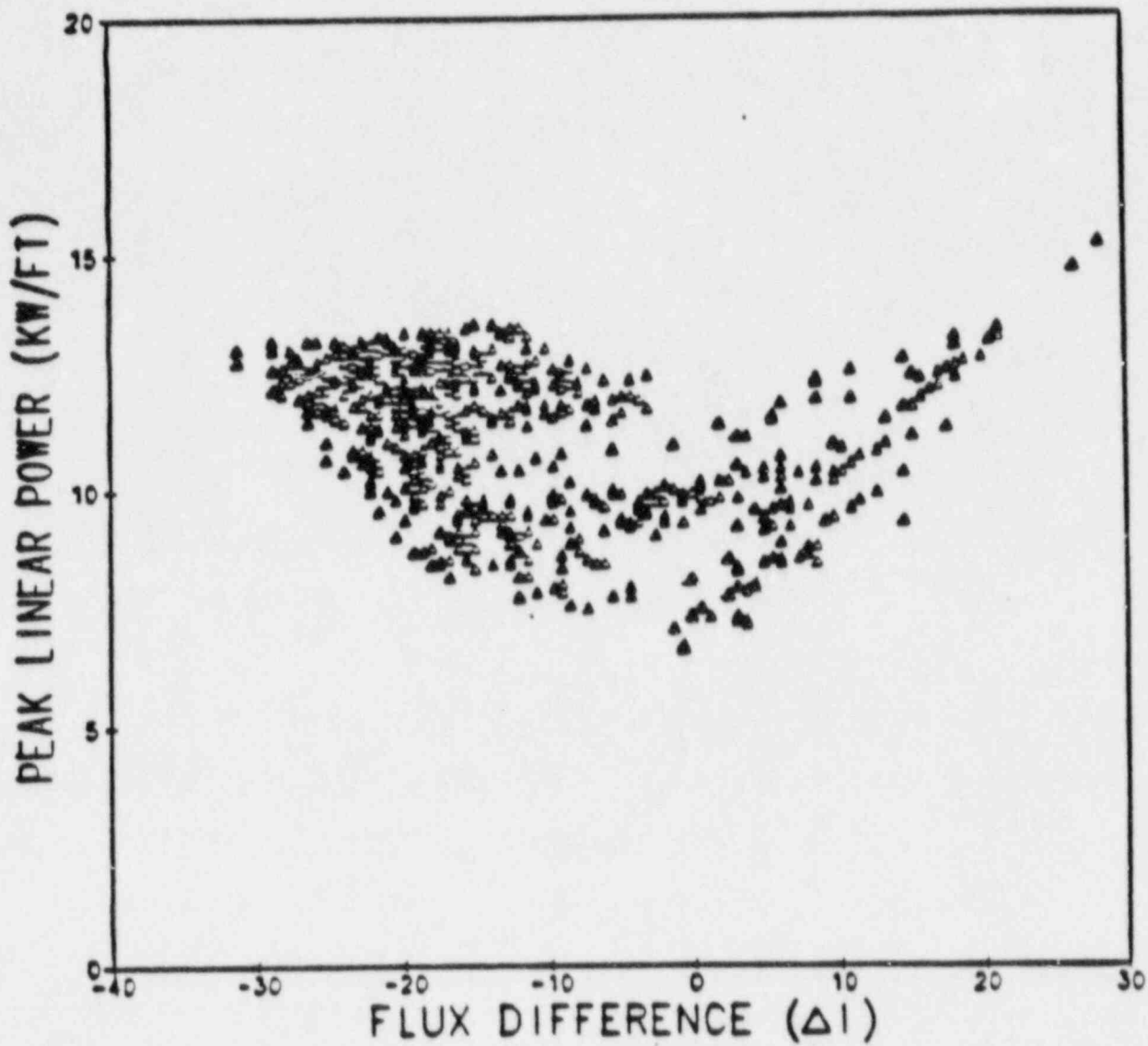
Normalized Power Density Distribution Near End of  
LHe, Hot Full Power, Equilibrium Xenon, Group D  
80% Inserted  
Figure 4.3-11 B





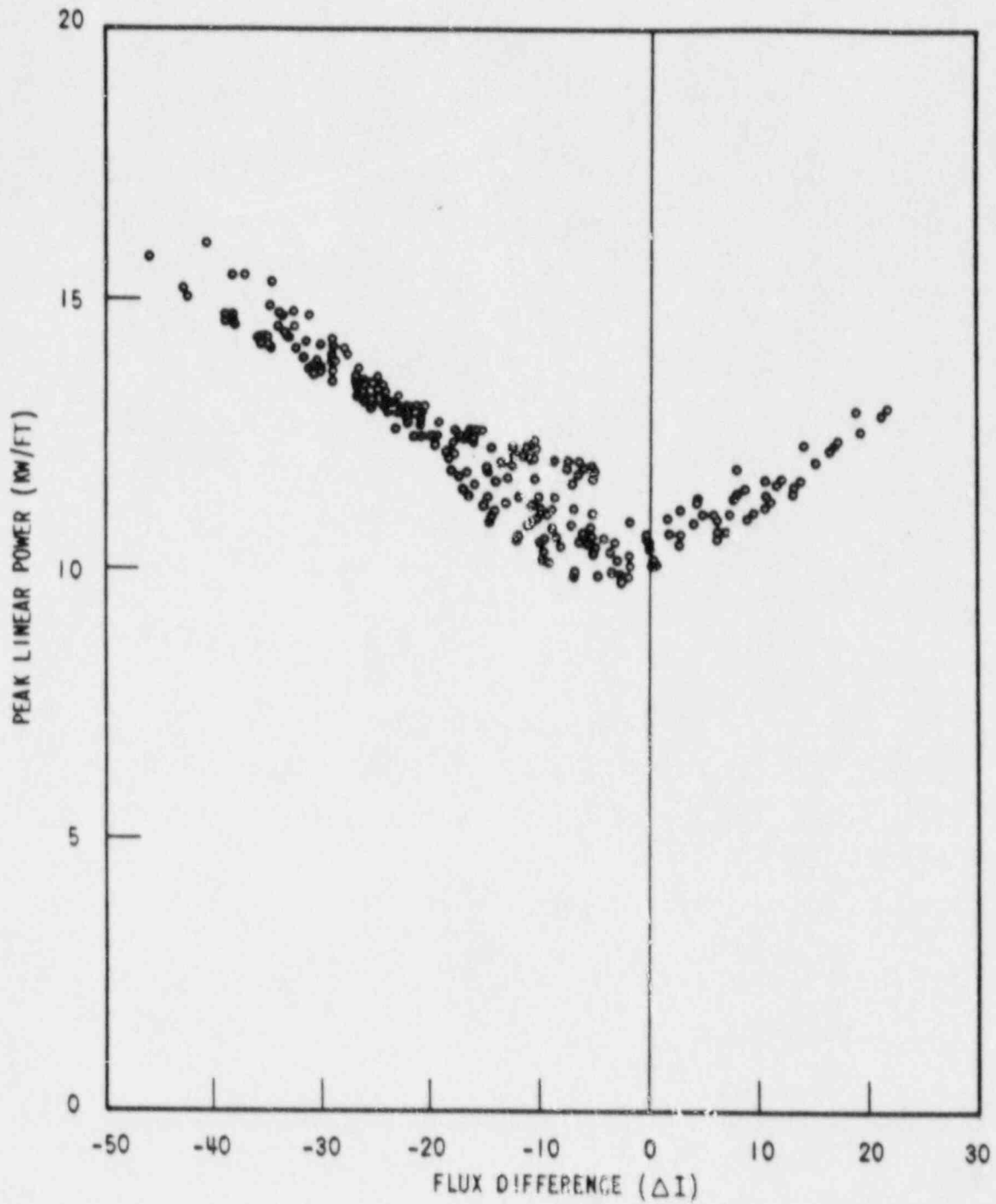
**SOUTH TEXAS PROJECT  
UNITS 1 & 2**

Peak Linear Power During Control Rod  
Malfunction Overpower Transients  
Figure 4.3-22<sup>A</sup>



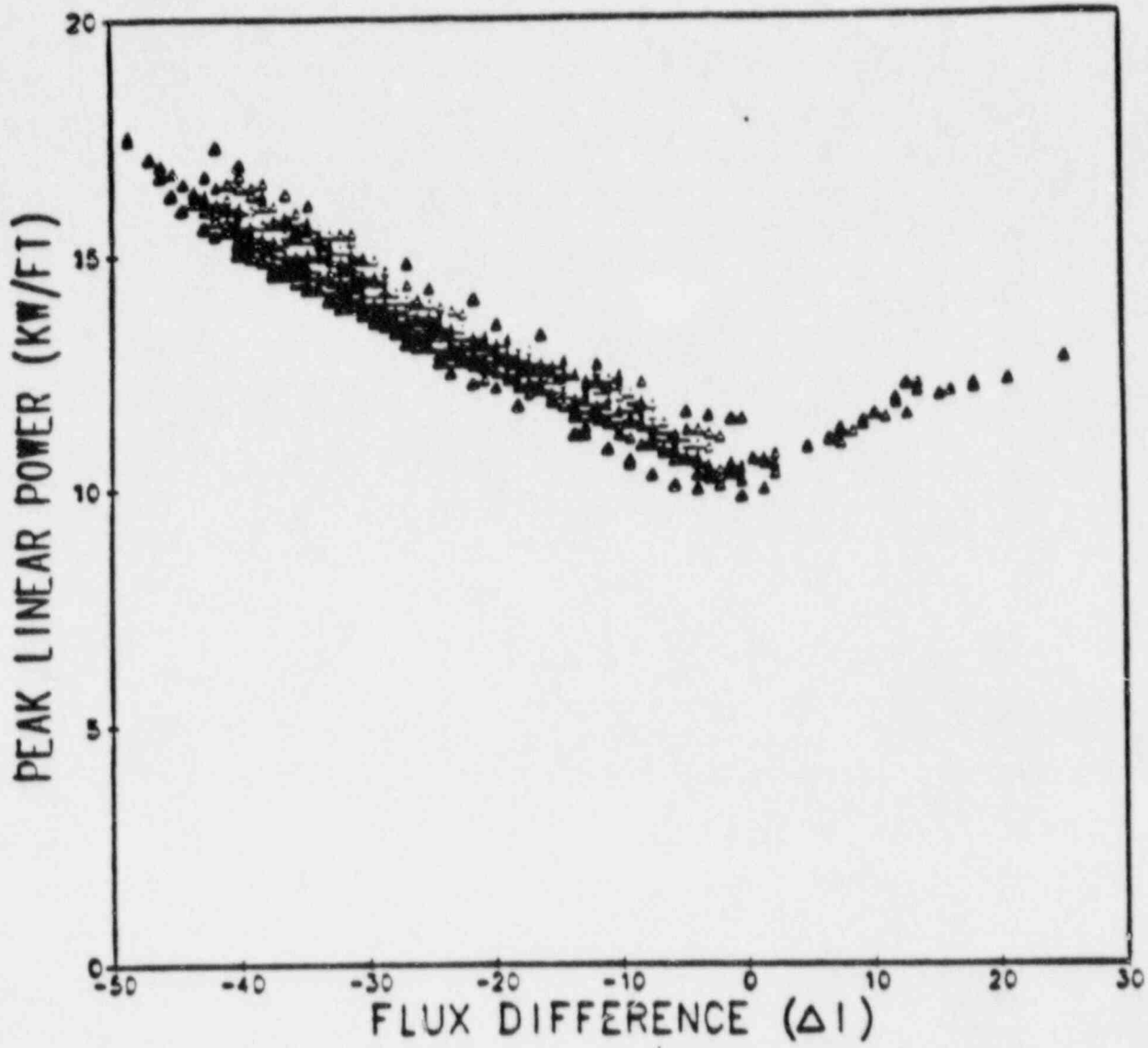
**SOUTH TEXAS PROJECT  
UNIT 2**

Peak Linear Power During Control Rod  
Malfunction Overpower Transients  
Figure 4.3-22 B

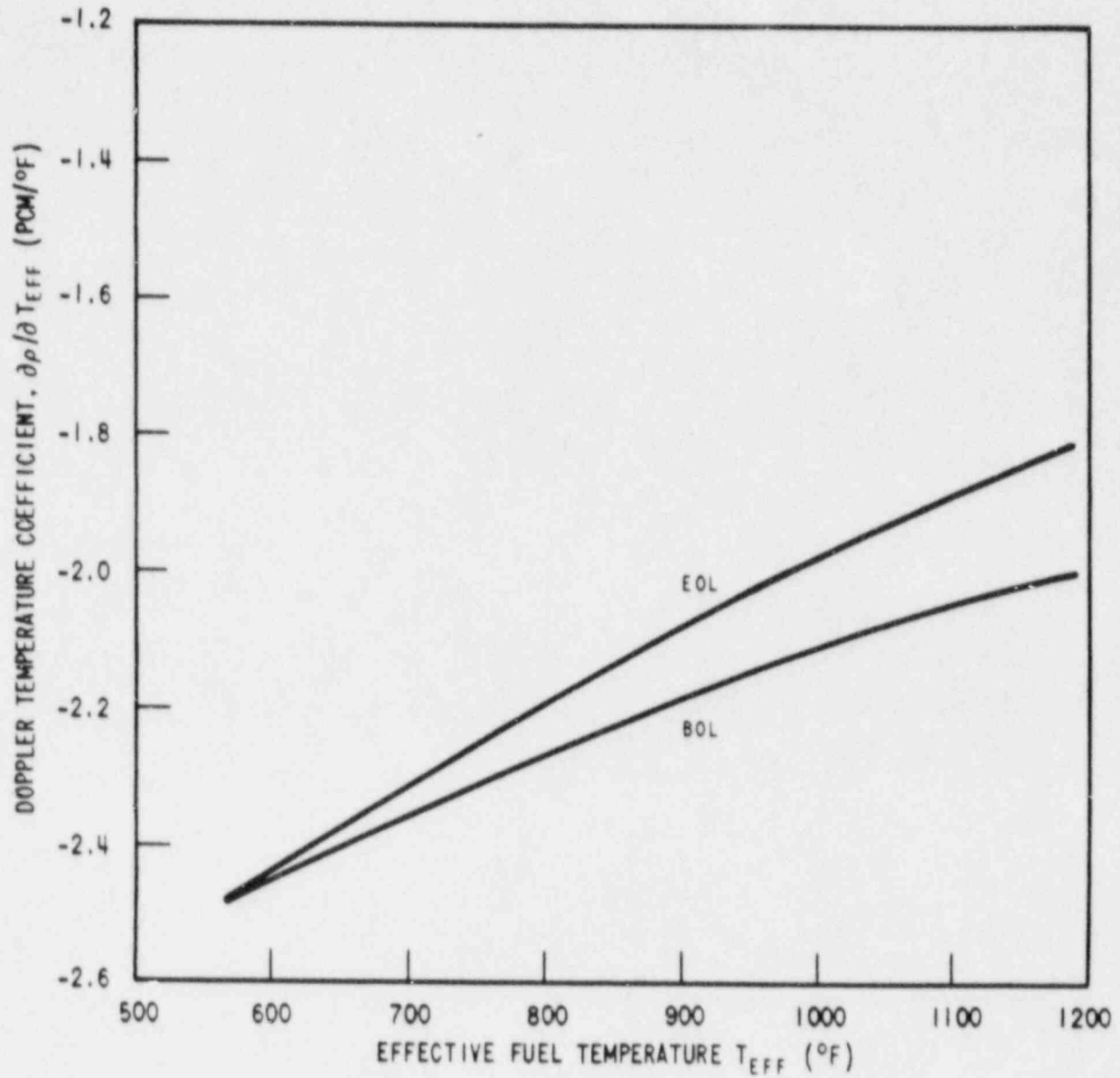


**SOUTH TEXAS PROJECT  
UNITS 1 & 2**

Peak Linear Power During Boration/  
Dilution Overpower Transients  
Figure 4.3-23<sup>A</sup>

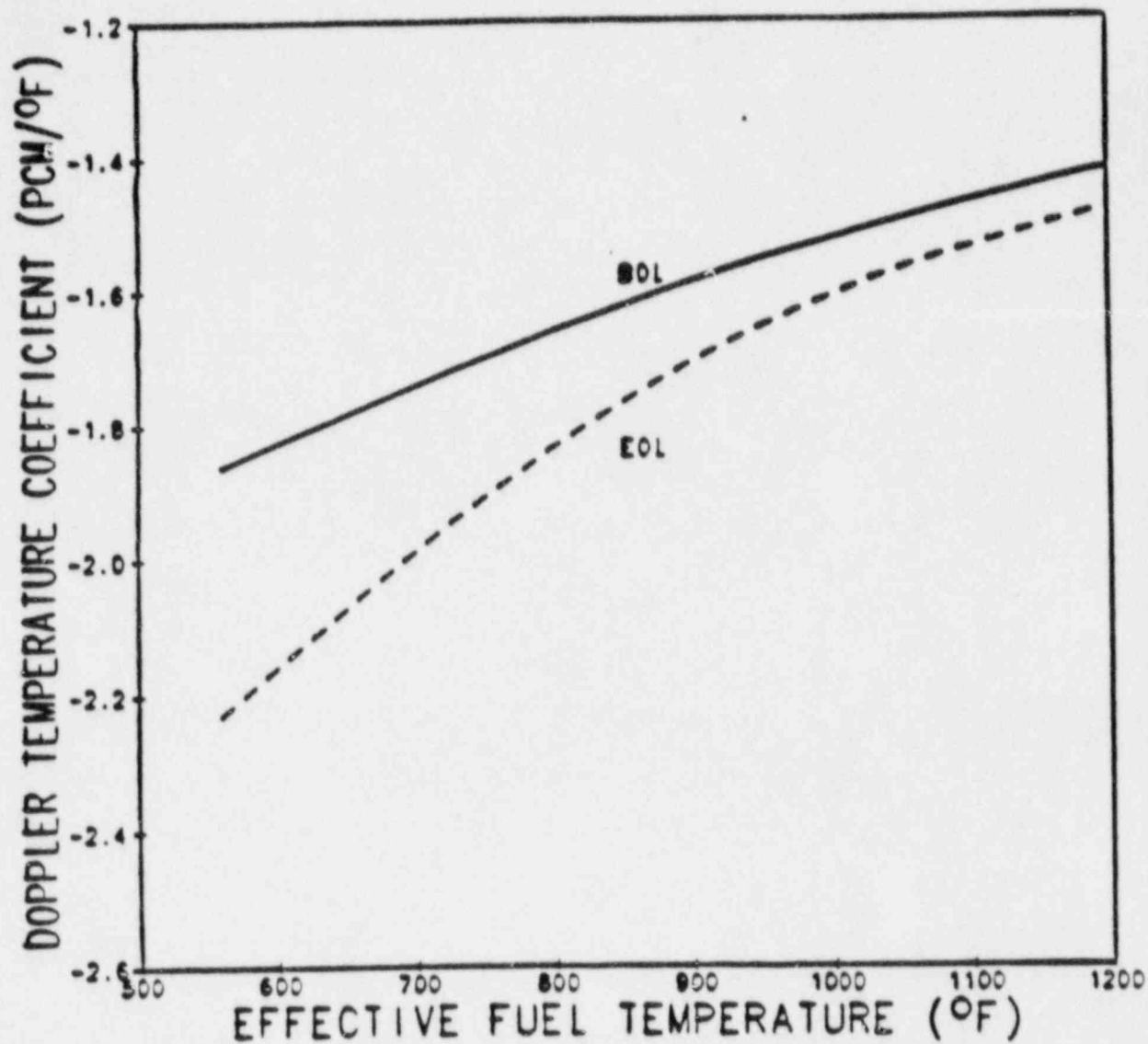


**SOUTH TEXAS PROJECT  
UNITS 1 & 2**  
Peak Linear Power During Boration/  
Dilution Overpower Transients  
Figure 4.3-23.B



**SOUTH TEXAS PROJECT**  
**UNITS 1 & 2**

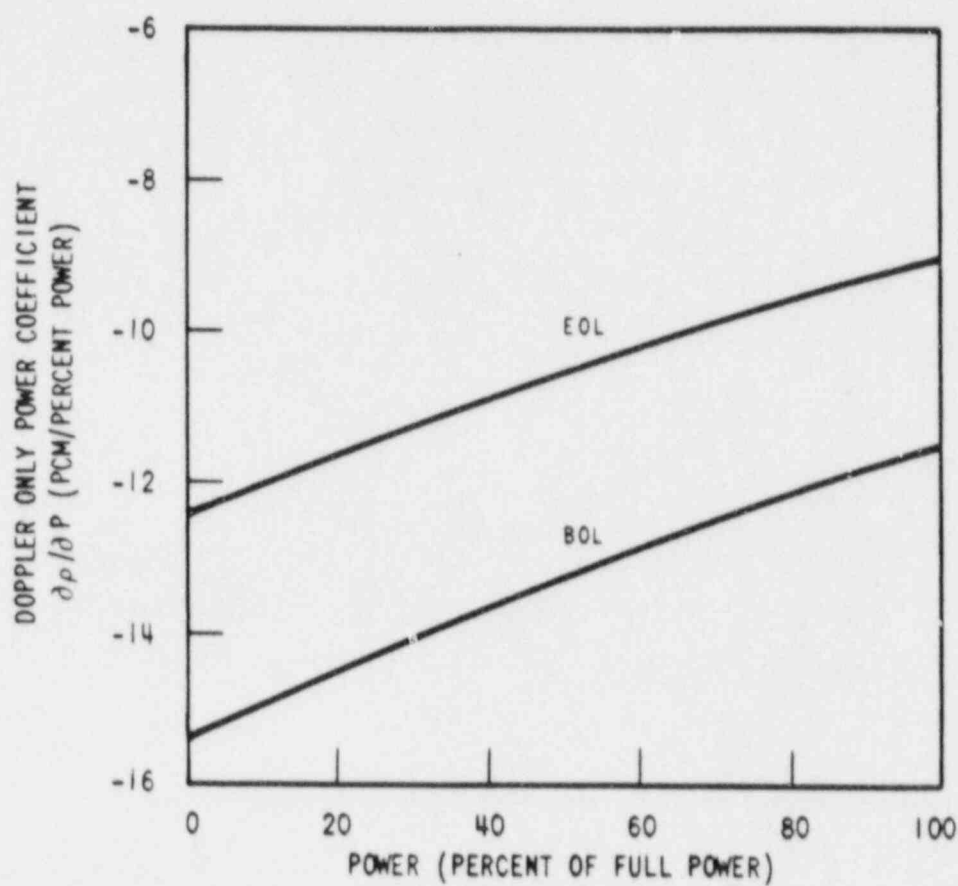
Doppler Temperature Coefficient at BOL and EOL Cycle 1  
Figure 4.3-27<sup>A</sup>



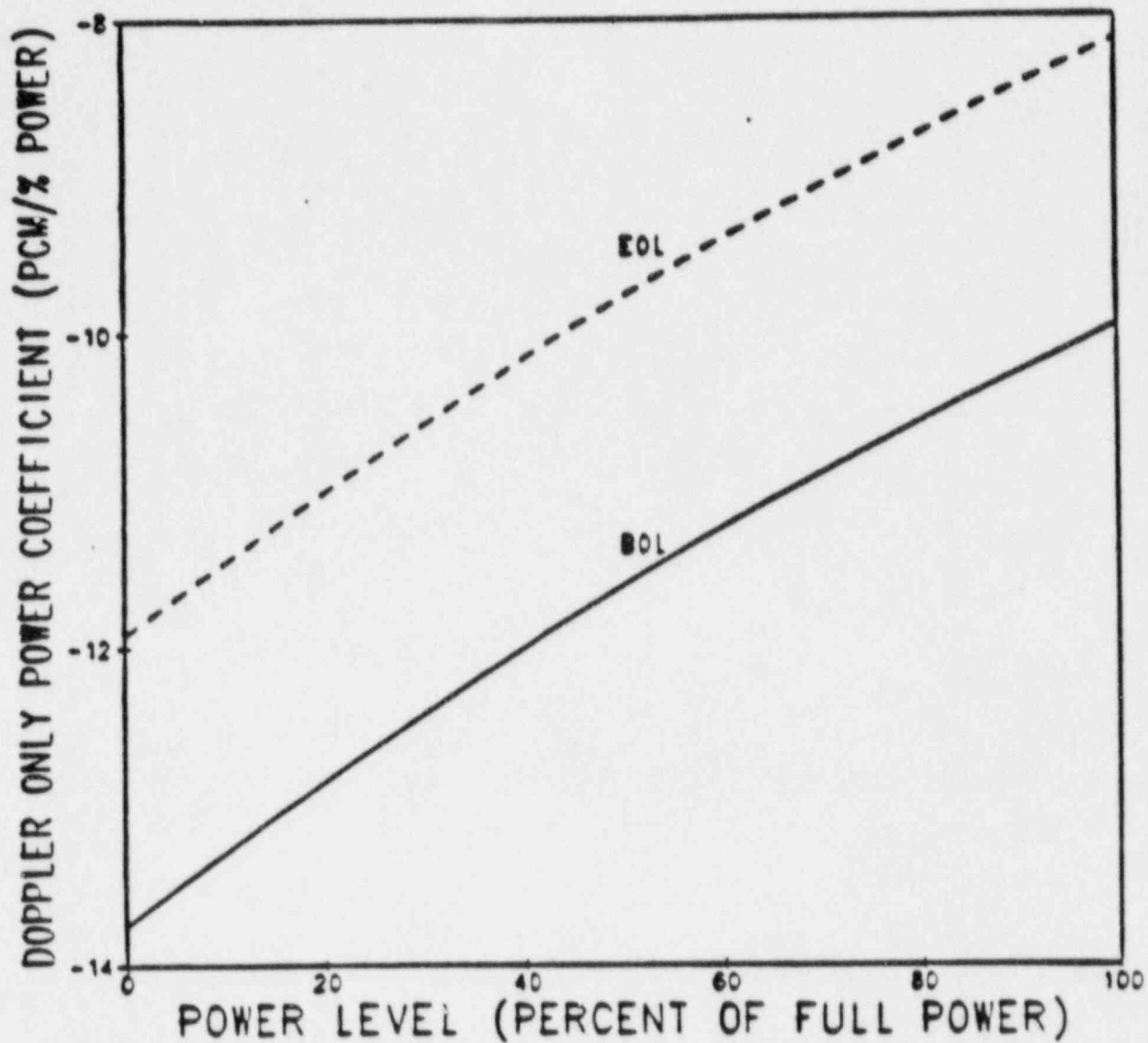
**SOUTH TEXAS PROJECT  
UNIT 2**

Doppler Temperature Coefficient at BOL  
and EOL Cycle 1  
Figure 4.3-27 B



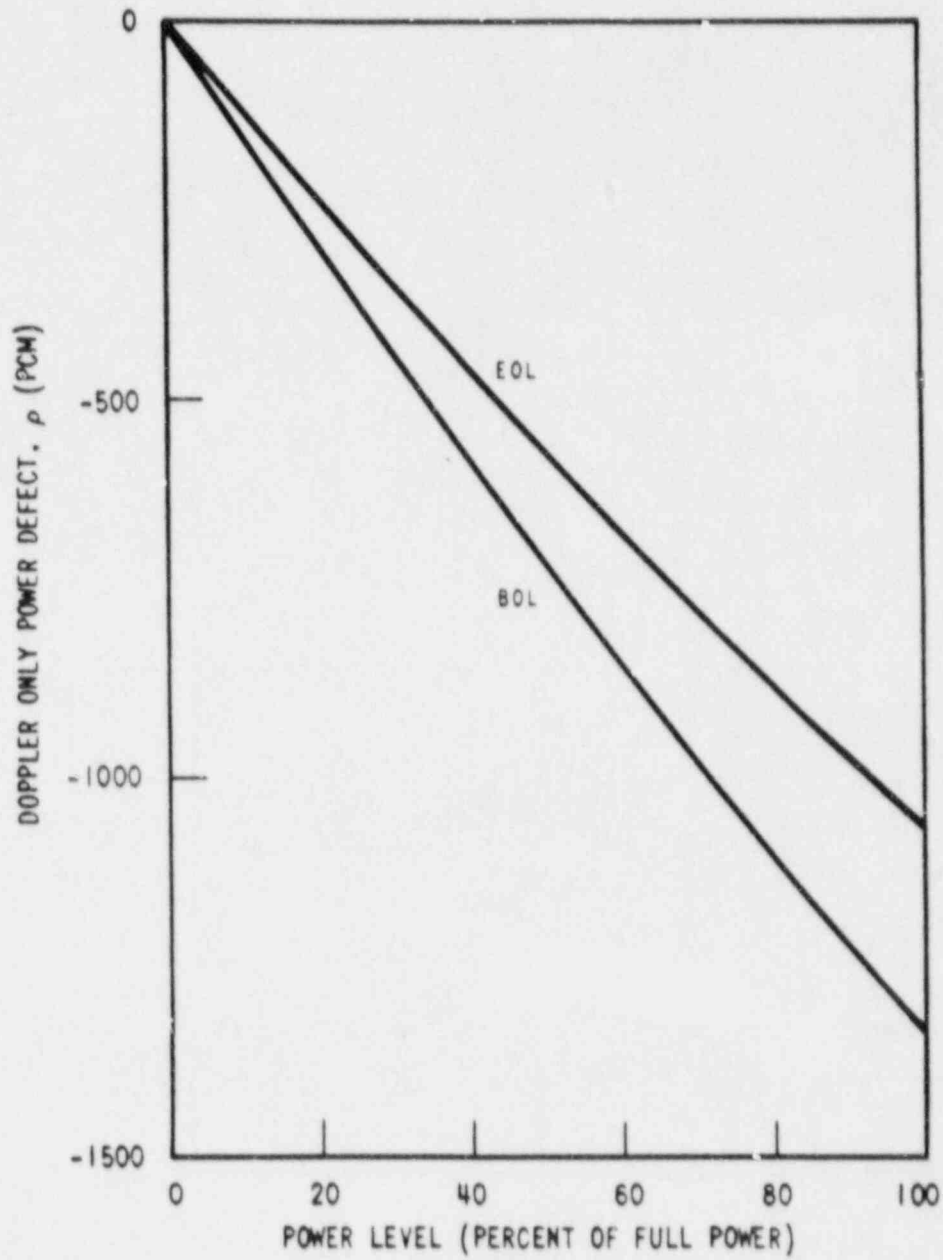
**SOUTH TEXAS PROJECT  
UNITS 1 & 2**

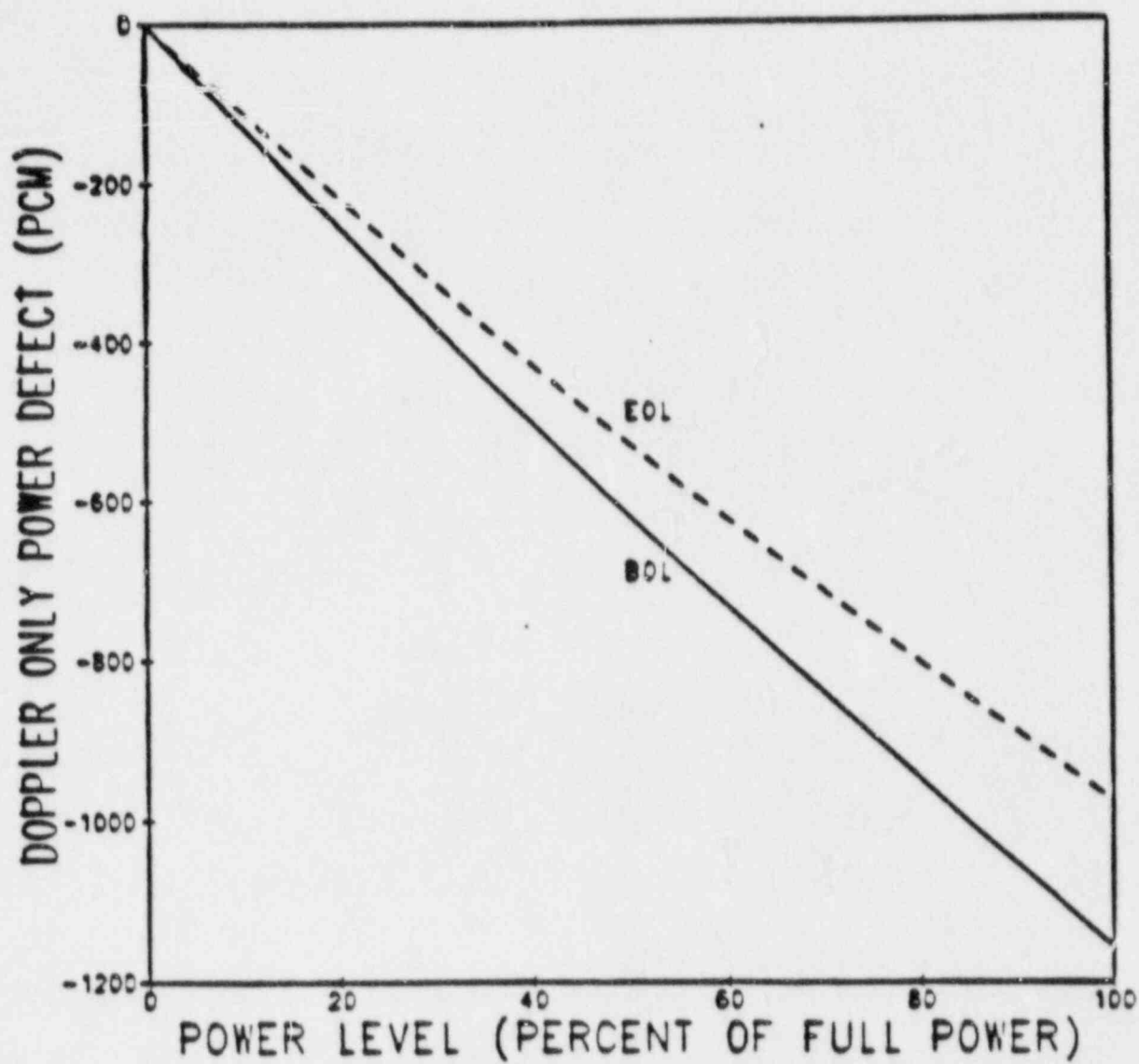
Doppler Only Power Coefficient -  
BOL, EOL Cycle 1  
Figure 4.3-28<sup>A</sup>



**SOUTH TEXAS PROJECT  
UNIT 2**

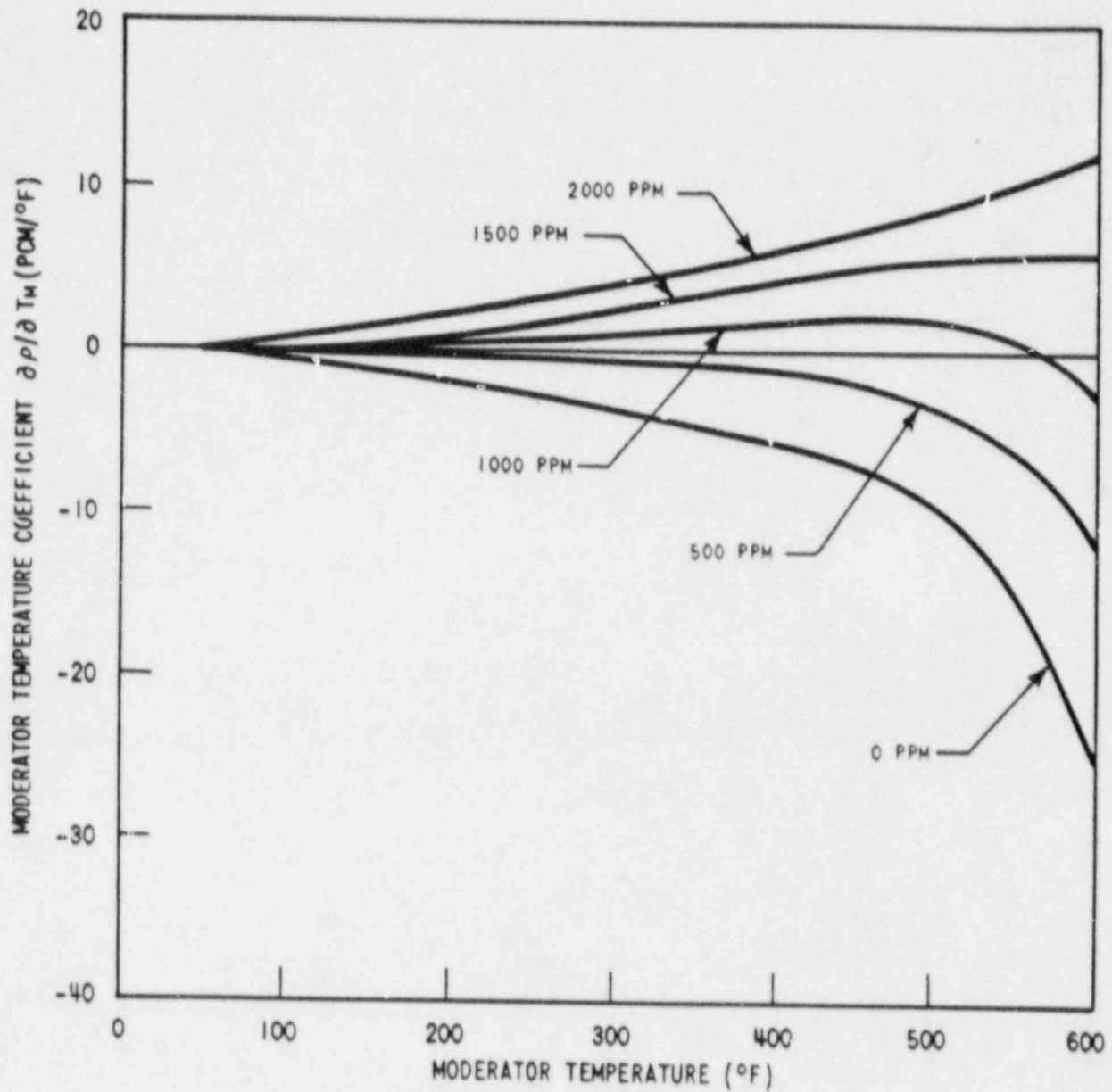
Doppler Only Power Coefficient -  
BOL, EOL Cycle 1  
Figure 4.3-29 B

**SOUTH TEXAS PROJECT  
UNITS 1 & 2**Doppler Only Power Defect BOL,  
EOL Cycle 1Figure 4.3-29<sup>A</sup>



**SOUTH TEXAS PROJECT  
UNIT 2**

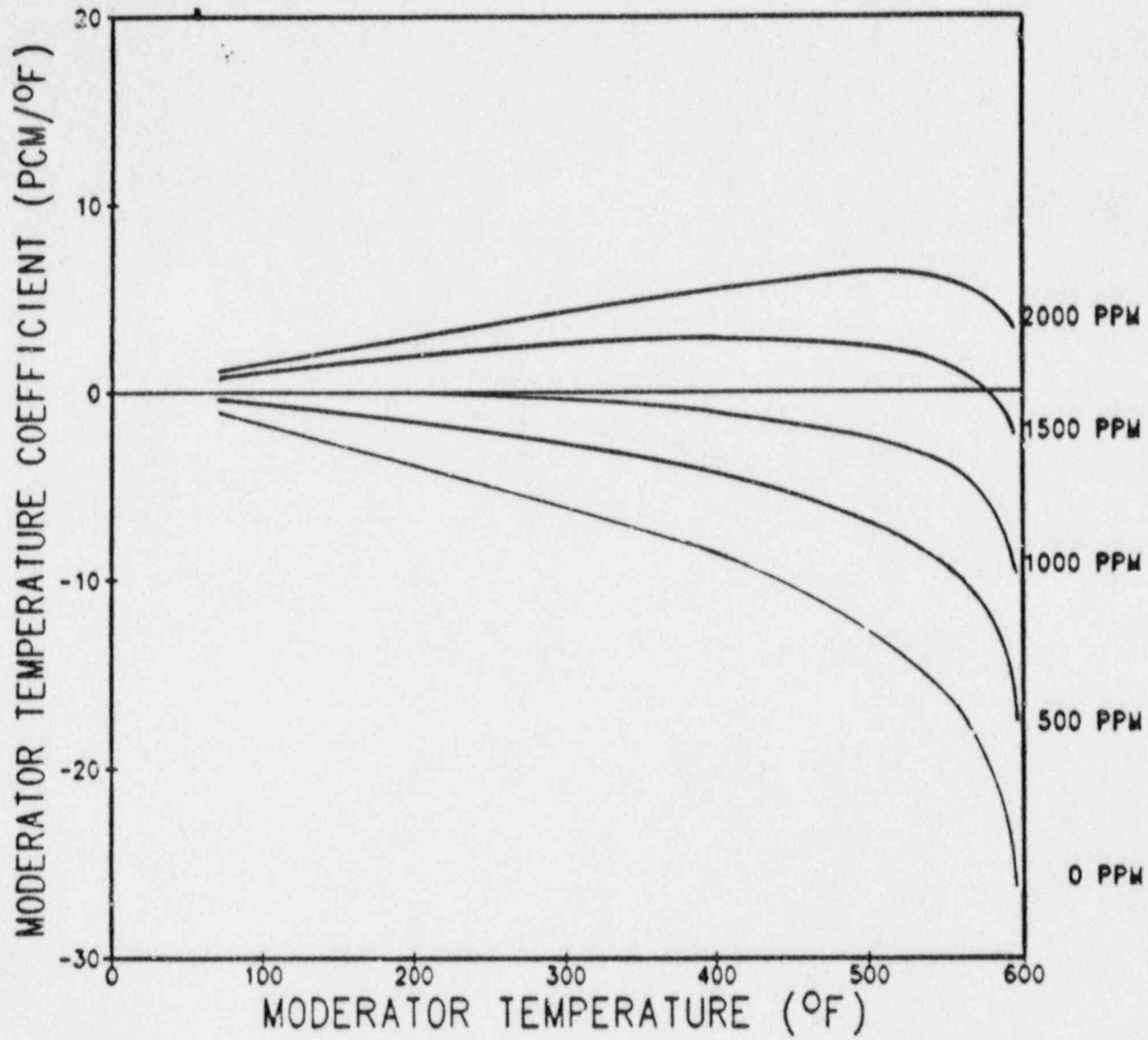
Doppler Only Power Defect BOL,  
EOL Cycle 1  
Figure 4.3-28 B



### SOUTH TEXAS PROJECT UNITS 1 & 2

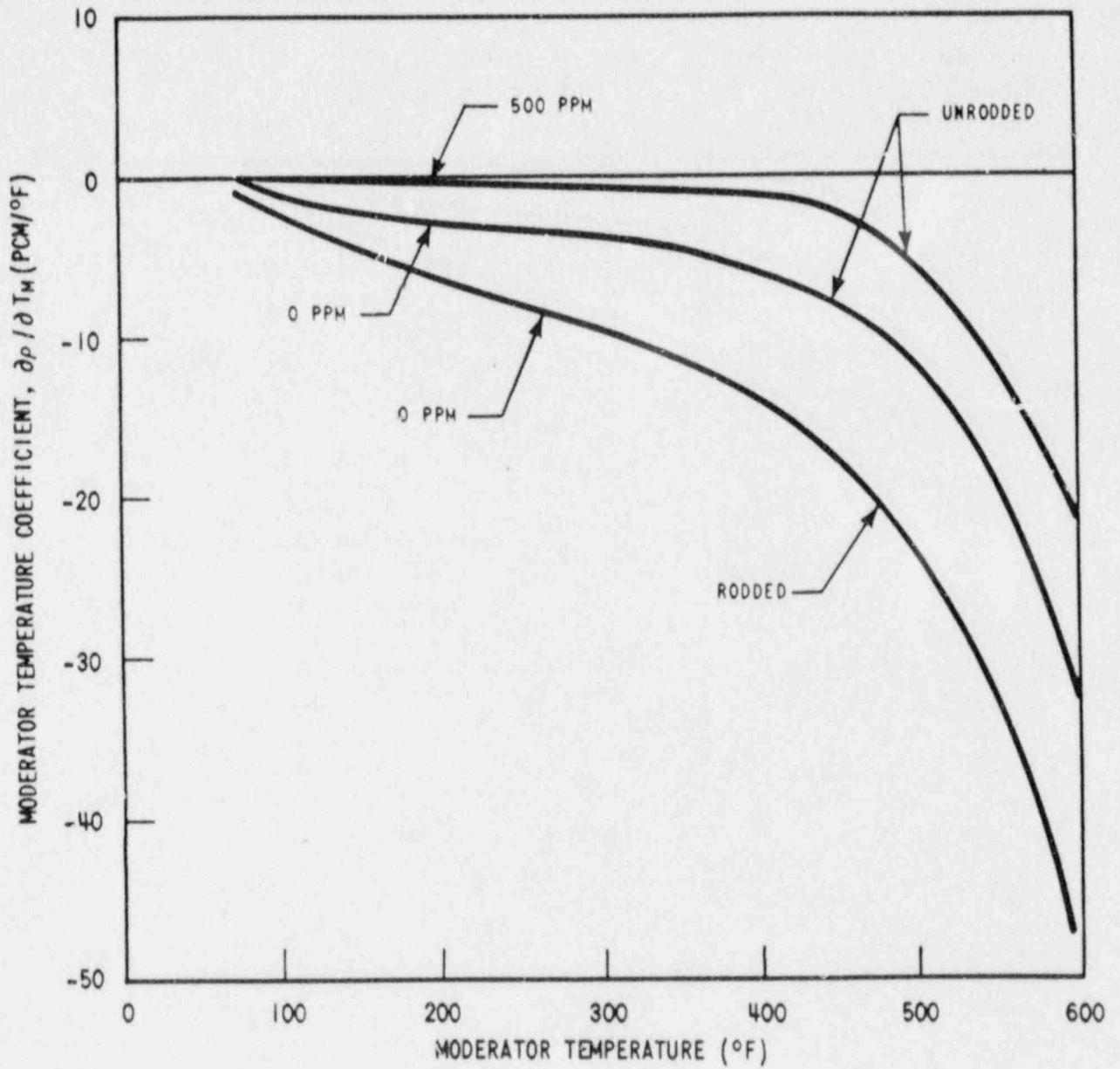
Moderator Temperature Coefficient --  
BOL, Cycle 1, No Rods

Figure 4.3-30<sup>A</sup>



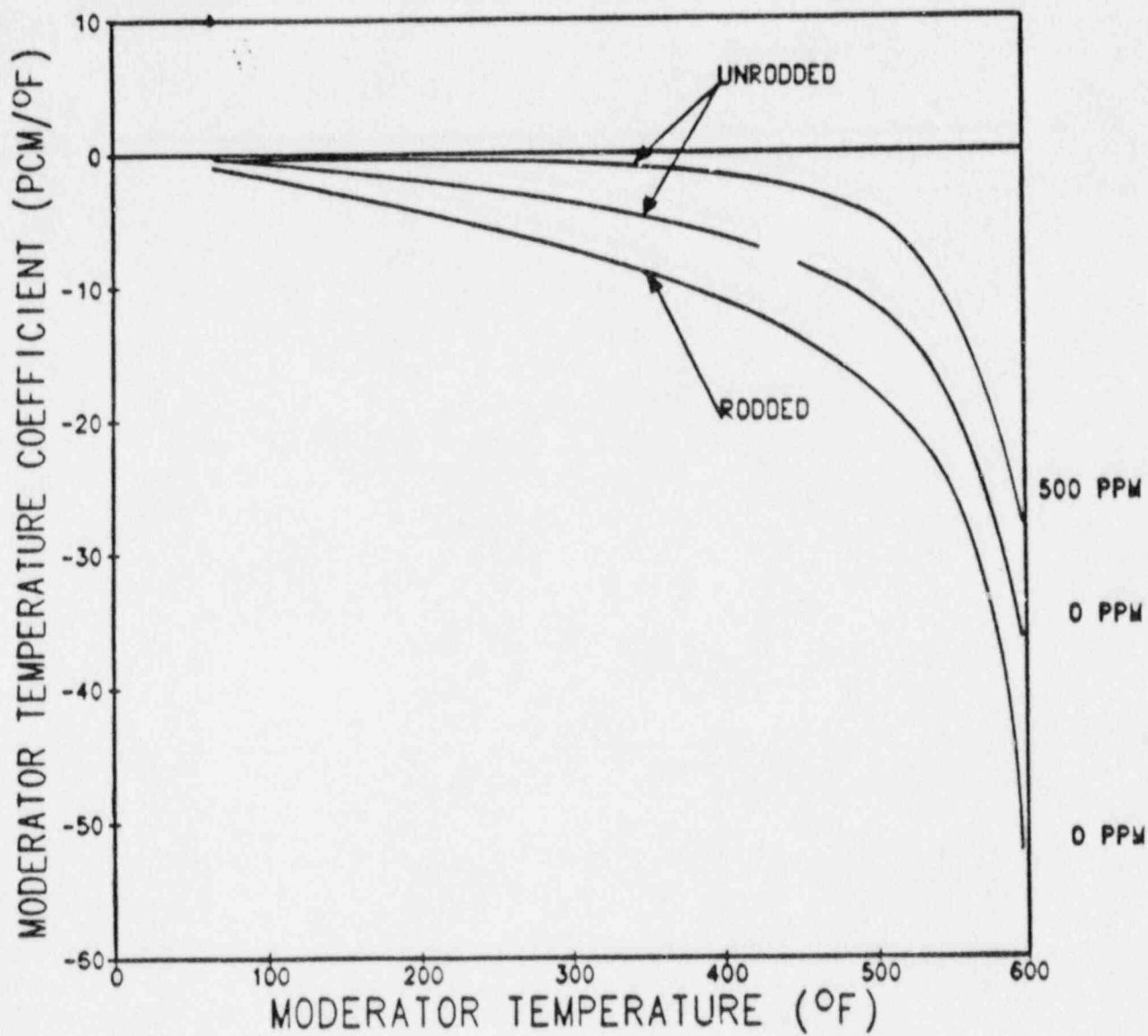
**SOUTH TEXAS PROJECT  
UNIT 2**  
Moderator Temperature Coefficient -  
BOL, Cycle 1, No Rods  
Figure 4.3-30 B





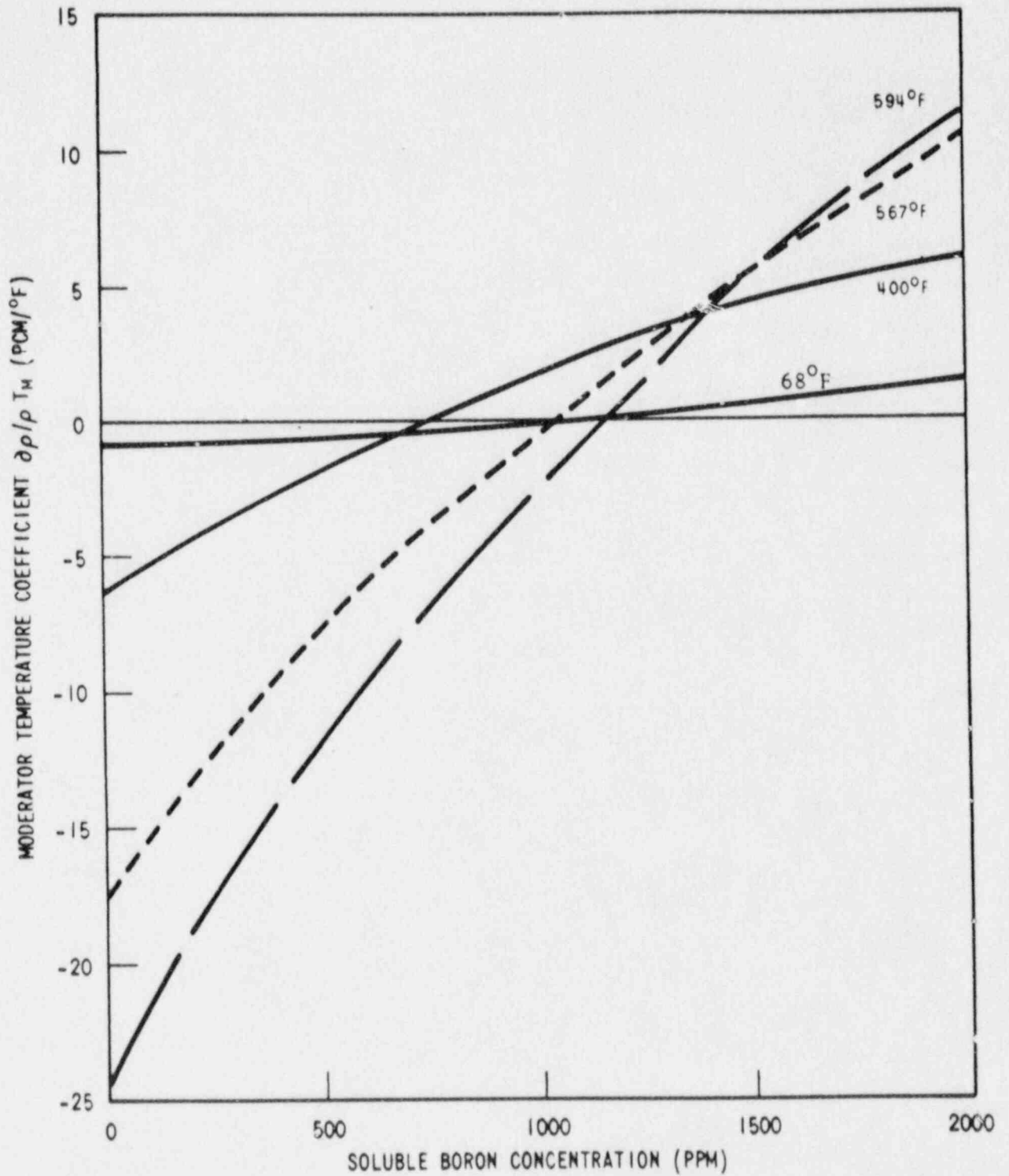
## SOUTH TEXAS PROJECT UNITS 1 & 2

Moderator Temperature Coefficient -  
EOL, Cycle 1  
Figure 4.3-31<sup>A</sup>



**SOUTH TEXAS PROJECT  
UNIT 2**

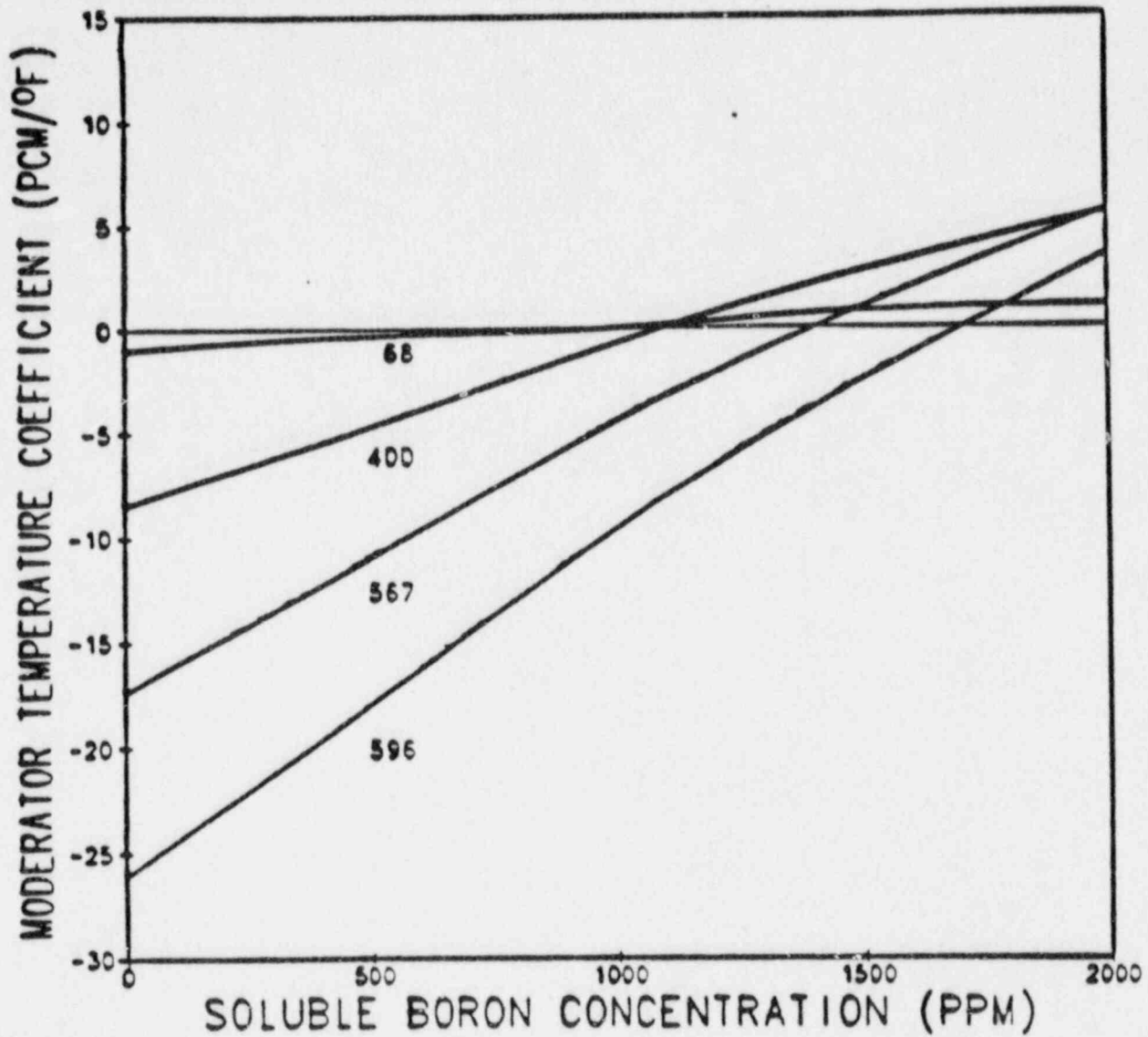
Moderator Temperature Coefficient -  
EOL, Cycle 1  
Figure 4.3-31. B



**SOUTH TEXAS PROJECT**  
**UNITS 1 & 2**

Moderator Temperature Coefficient as a Function of Boron Concentration - BOL, Cycle 1, No Rods

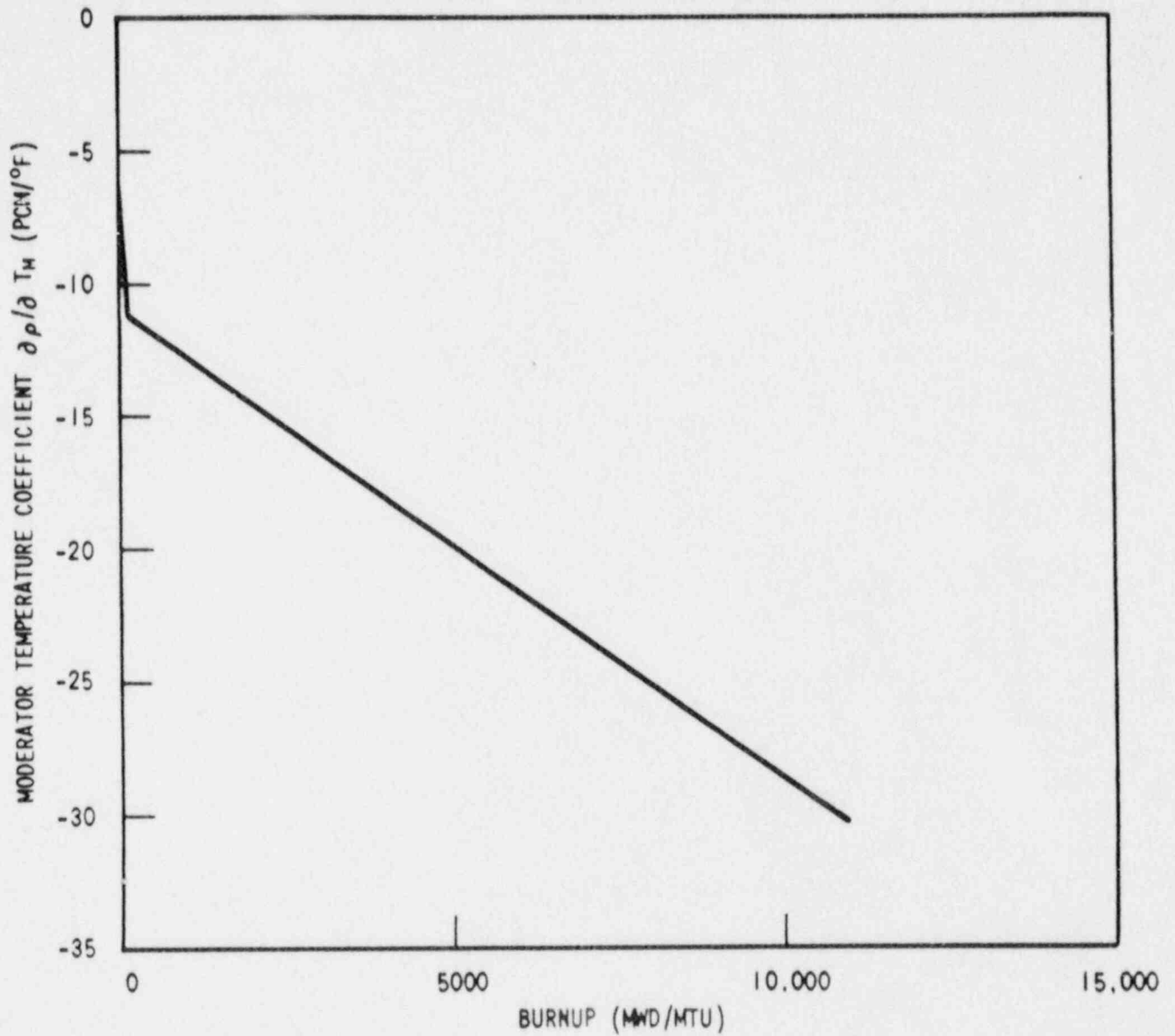
Figure 4.3-32<sup>A</sup>



**SOUTH TEXAS PROJECT  
UNIT 2**

Moderator Temperature Coefficient as a Function of  
Boron Concentration - BOL, Cycle 1, No Rods

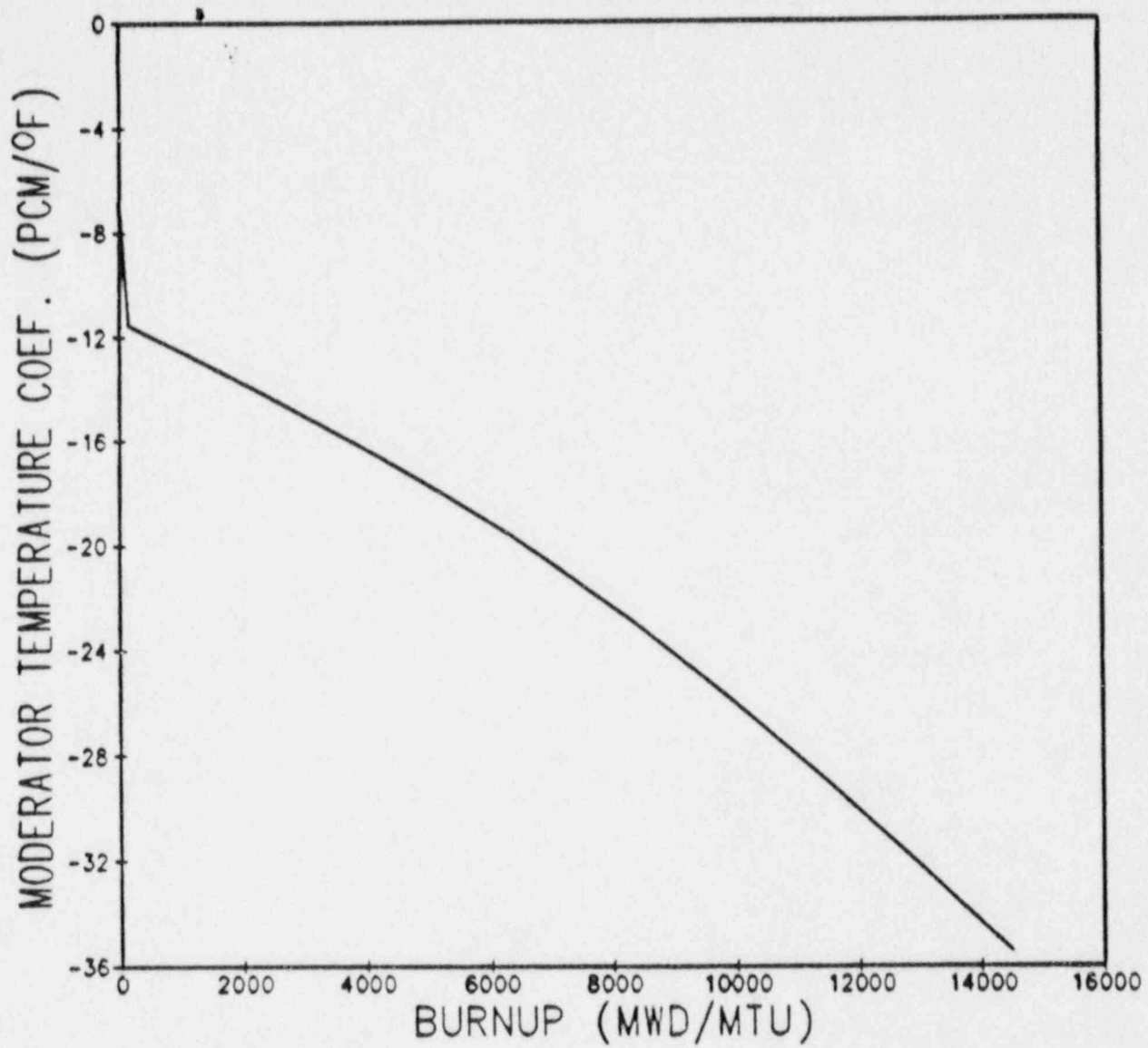
Figure 4.3-32 B



### SOUTH TEXAS PROJECT UNITS 1 & 2

Hot Full Power Moderator Temperature Coefficient  
During Cycle 1 for the Critical Boron Concentration

Figure 4.3-33<sup>A</sup>

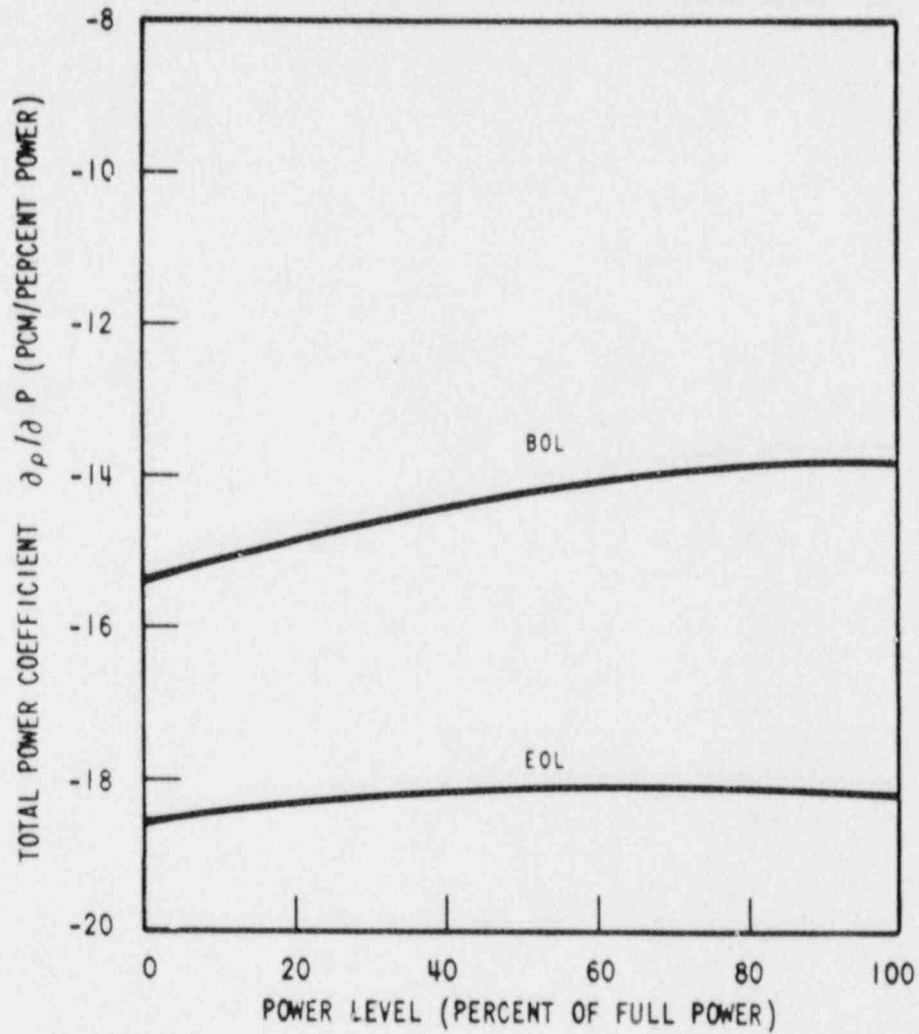


**SOUTH TEXAS PROJECT  
UNIT 2**

Net Full Power Moderator Temperature Coefficient  
During Cycle 1 for the Critical Boron Concentration

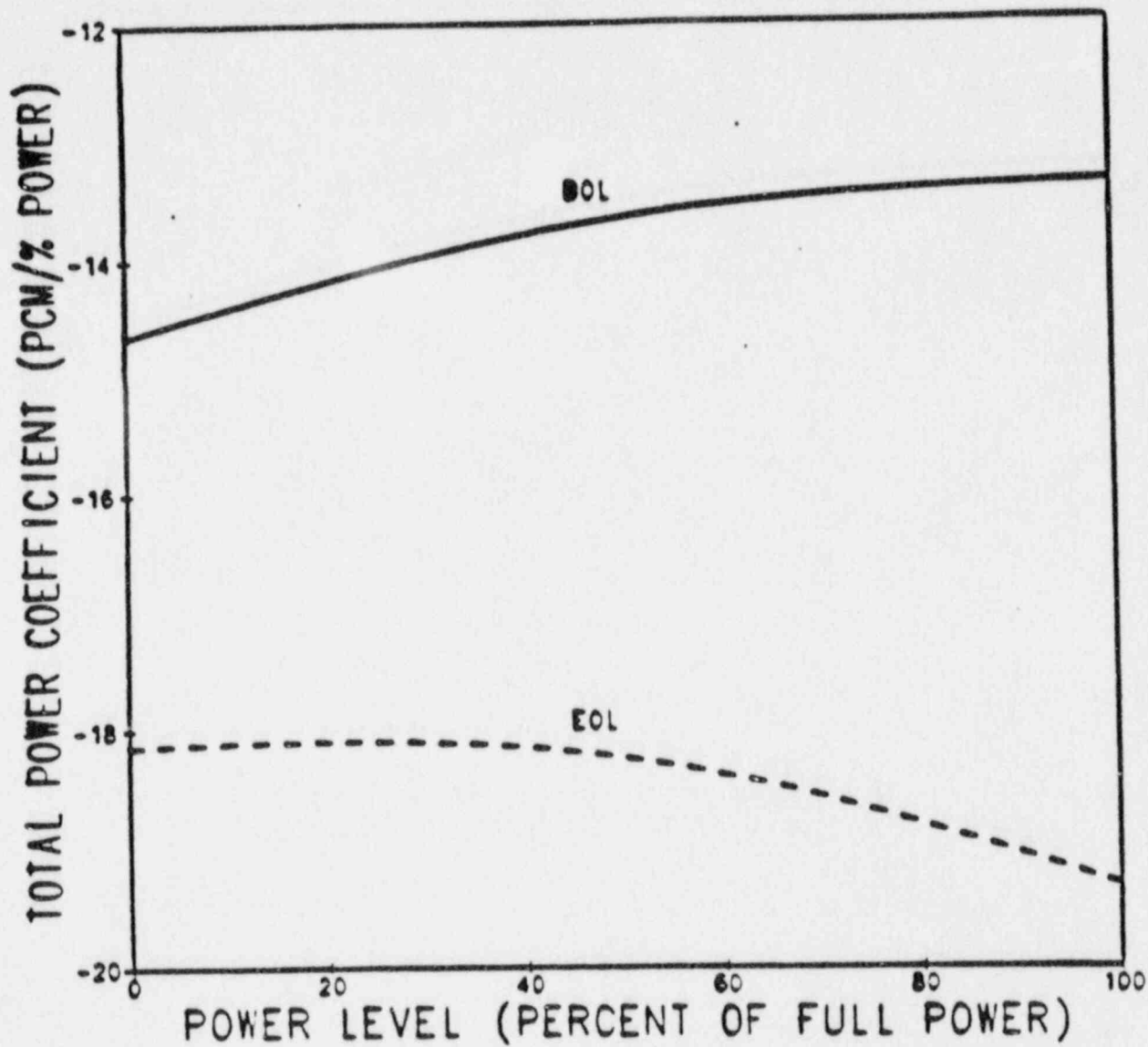
Figure 4.3-33 **B**





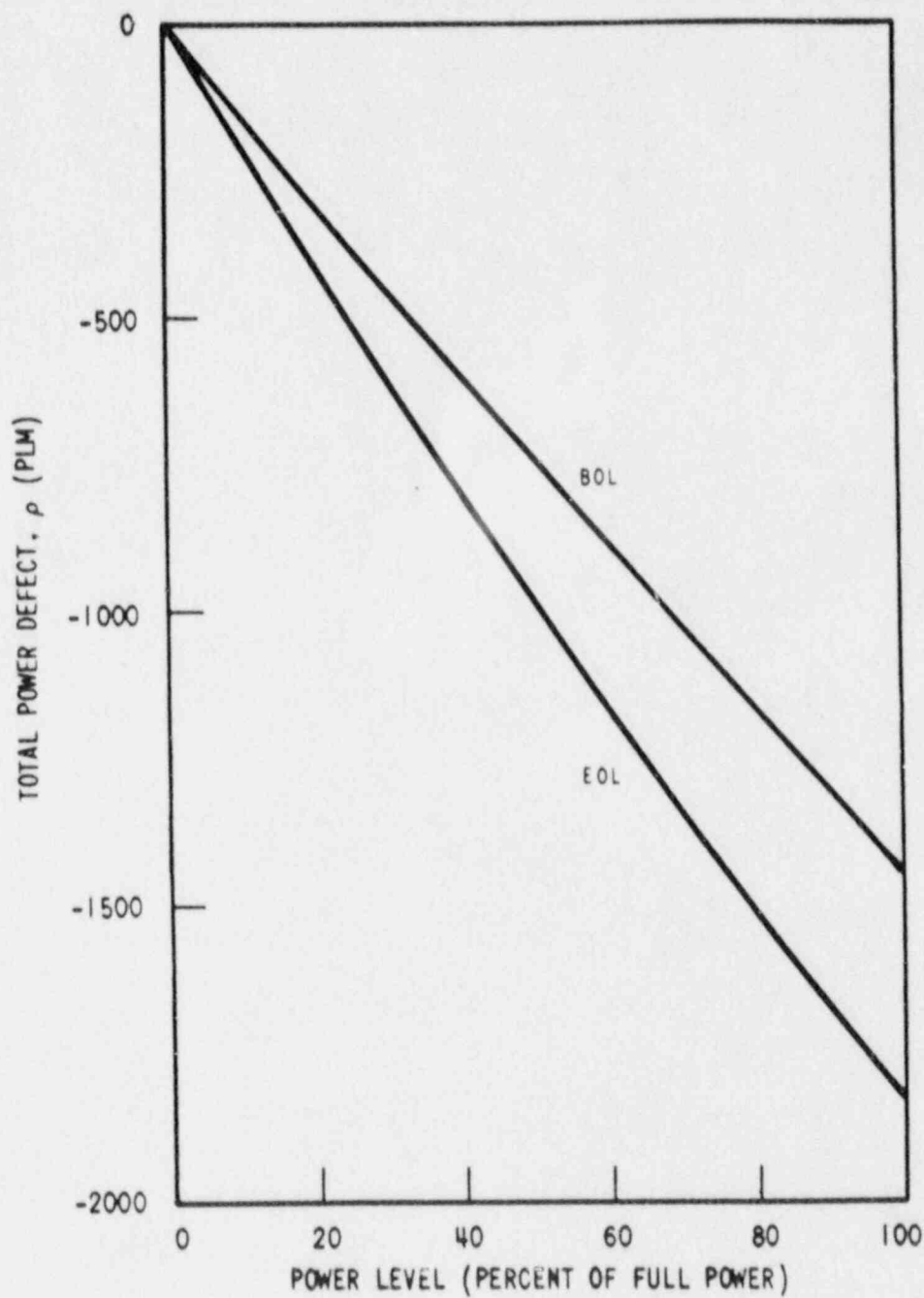
**SOUTH TEXAS PROJECT  
UNITS 1 & 2**

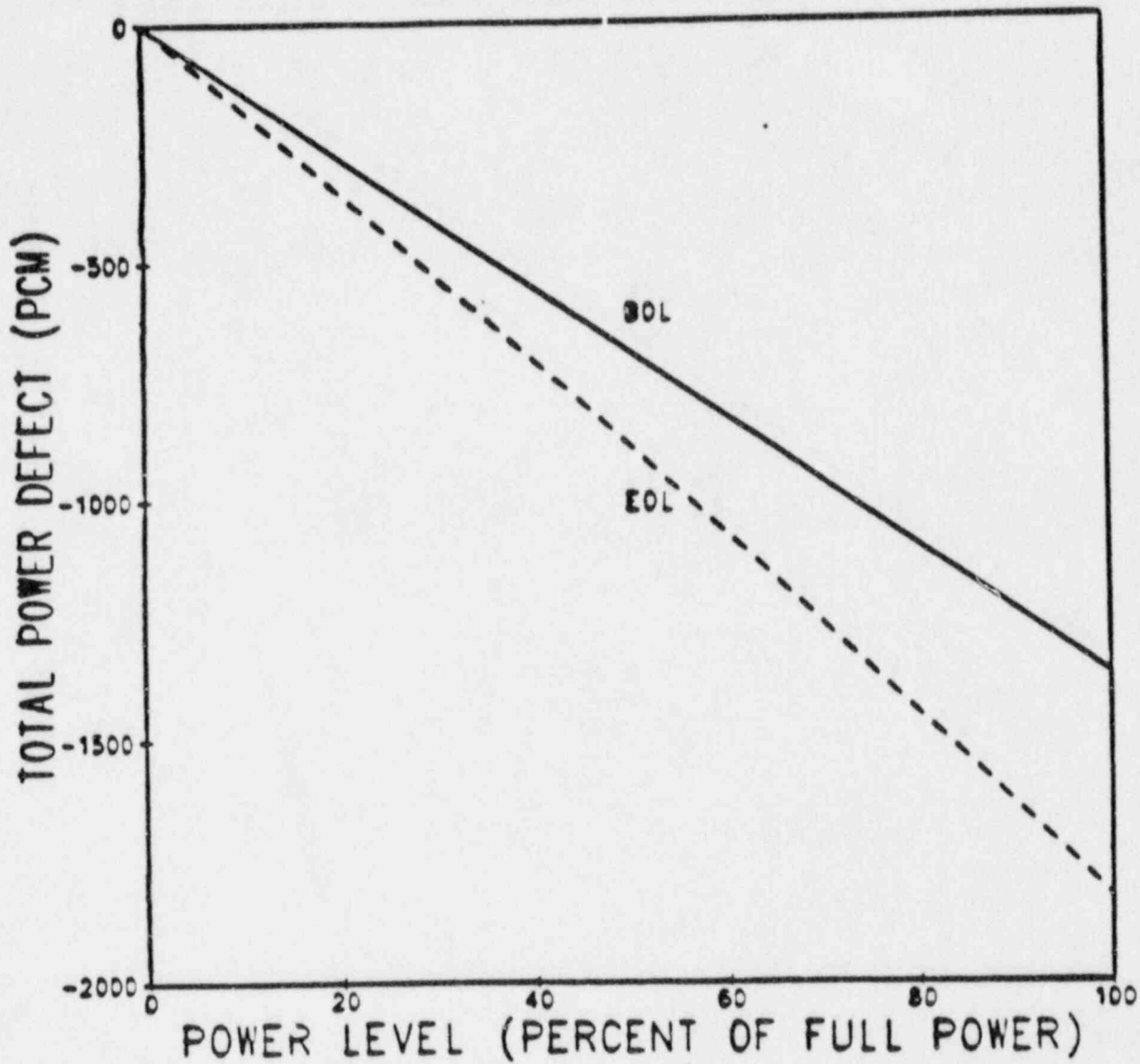
Total Power Coefficient BOL, EOL  
Cycle 1  
Figure 4.3-34<sup>A</sup>



**SOUTH TEXAS PROJECT  
UNIT 2**

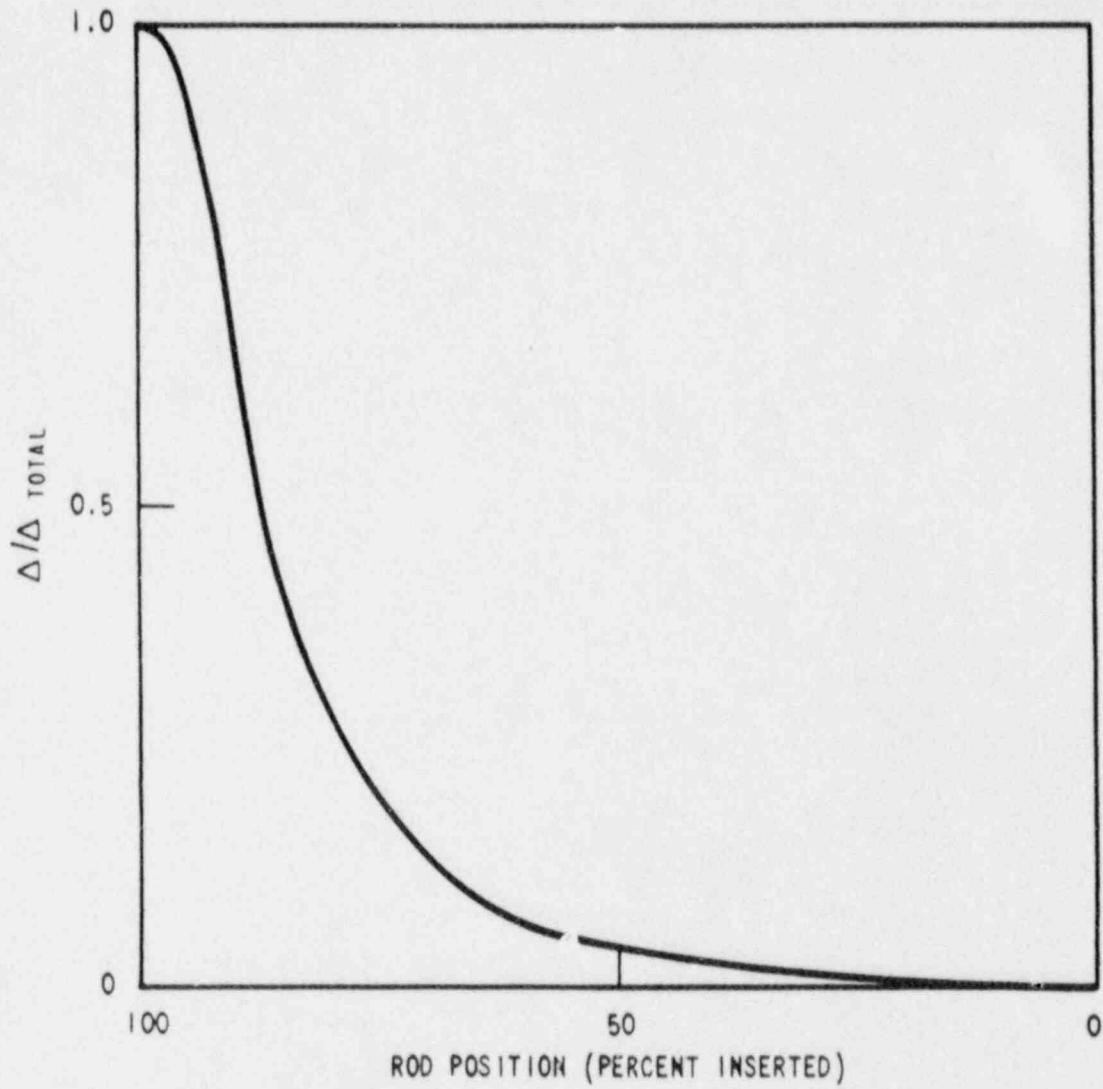
Total Power Coefficient BOL, EOL  
Cycle 1  
Figure 4.3-34 B

**SOUTH TEXAS PROJECT  
UNITS 1 & 2**Total Power Defect BOL, EOL  
Cycle 1Figure 4.3-35<sup>A</sup>



**SOUTH TEXAS PROJECT  
UNIT 2**

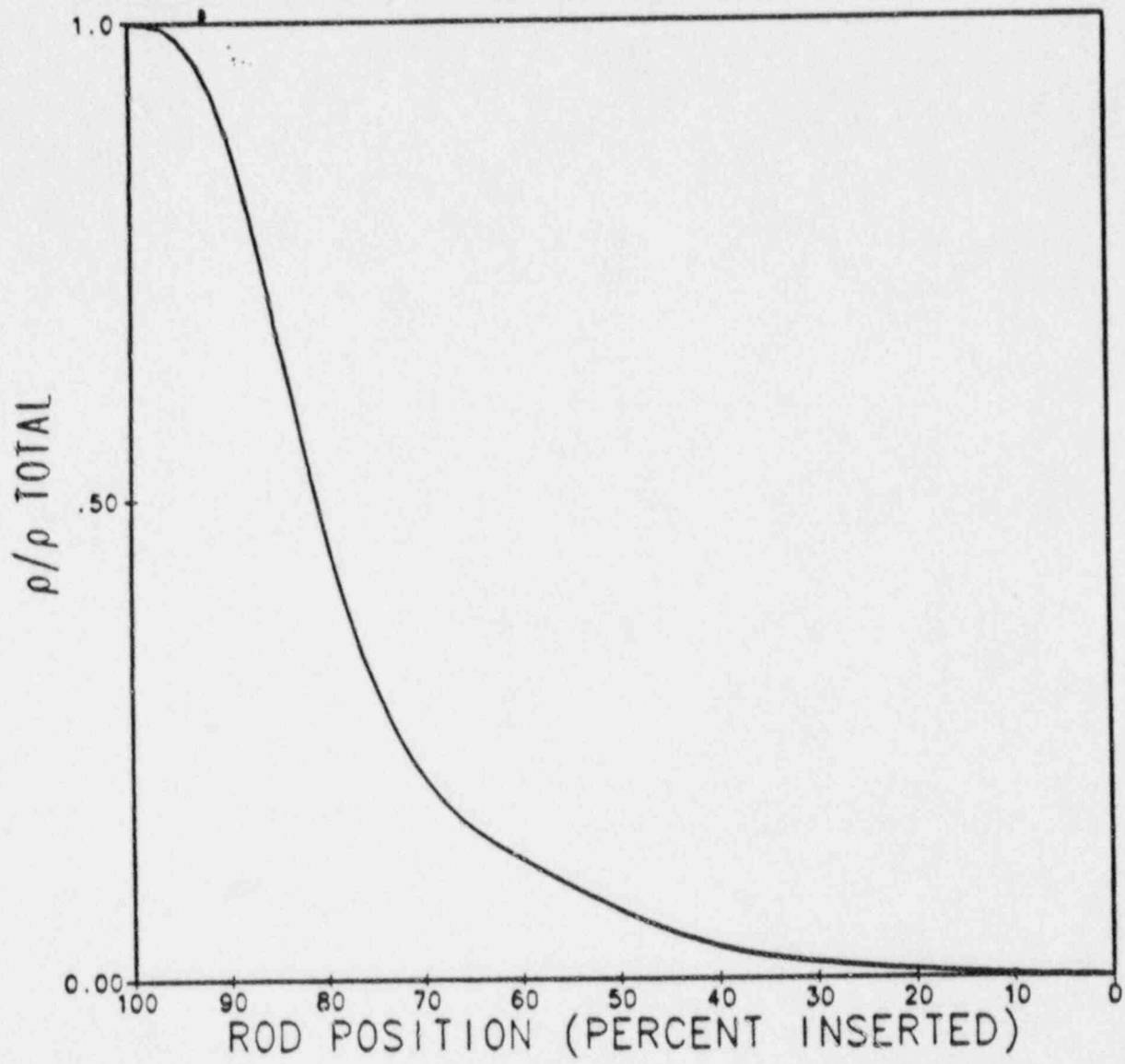
Total Power Defect BOL, EOL  
Cycle 1  
Figure 4.3-35 B



**SOUTH TEXAS PROJECT**  
**UNITS 1 & 2**

Normalized Rod Worth versus Percent Insertion -  
All Rods but One

Figure 4.3-39<sup>A</sup>



**SOUTH TEXAS PROJECT  
UNIT 2**

Normalized Rod Worth versus Percent Insertion -  
All Rods but One

Figure 4.3-30 B



3. Leakage flow from the vessel inlet nozzle directly to the vessel outlet nozzle through the gap between the vessel and the barrel.
4. Flow introduced between the baffle and the barrel for the purpose of cooling these components and which is not considered available for core cooling.
5. Flow in the gaps between the fuel assemblies on the core periphery and the adjacent baffle wall.

The above contributions are evaluated to confirm that the design value of the core bypass flow is met. The design value of core bypass flow is equal to 4.5 percent of the total vessel flow.

Of the total allowance, <sup>for Unit 1,</sup> 2.5 percent is associated with the internals (items 1, 3, 4 and 5 above) and 2.0 percent for the core. Calculations have been performed using drawing tolerances on a worst case basis and accounting for uncertainties in pressure losses. Based on these calculations, the core bypass flow is < 4.5 percent.

Flow model test results for the flow path through the reactor are discussed in Subsection 4.4.2.7.2.

4.4.4.2.2 Inlet Flow Distributions: Data has been considered from several 1/7 scale hydraulic reactor model tests, References 4.4-23, 4.4-24, and 4.4-62, in arriving at the core inlet flow maldistribution criteria used in the THINC analyses (see Subsection 4.4.4.5.1). THINC-I analyses made, using this data, have indicated that a conservative design basis is to consider 5 percent reduction in the flow to the hot assembly, Reference 4.4-63. The same design basis of 5 percent reduction to the hot assembly inlet is used in THINC IV analyses.

The experimental error estimated in the inlet velocity distribution has been considered as outlined in Reference 4.4-18 where the sensitivity of changes in inlet velocity distributions to hot channel thermal performance is shown to be small. Studies [4.4-18] made with the improved THINC model (THINC-IV) show that it is adequate to use the 5 percent reduction in inlet flow to the hot assembly for a loop out of service based on the experimental data in References 4.4-23 and 4.4-24.

The effect of the total flow rate on the inlet velocity distribution was studied in the experiments of Reference 4.4-23. As was expected, on the basis of the theoretical analysis, no significant variation could be found in inlet velocity distribution with reduced flow rate.

4.4.4.2.3 Empirical Friction Factor Correlations: Two empirical friction factor correlations are used in the THINC-IV computer code (described in Subsection 4.4.4.5.1).

The friction factor in the axial direction, parallel to the fuel rod axis, is evaluated using the Novendstern-Sandberg correlation [4.4-64]. This correlation consists of the following:

SPT PSAR

TABLE 4.4-1

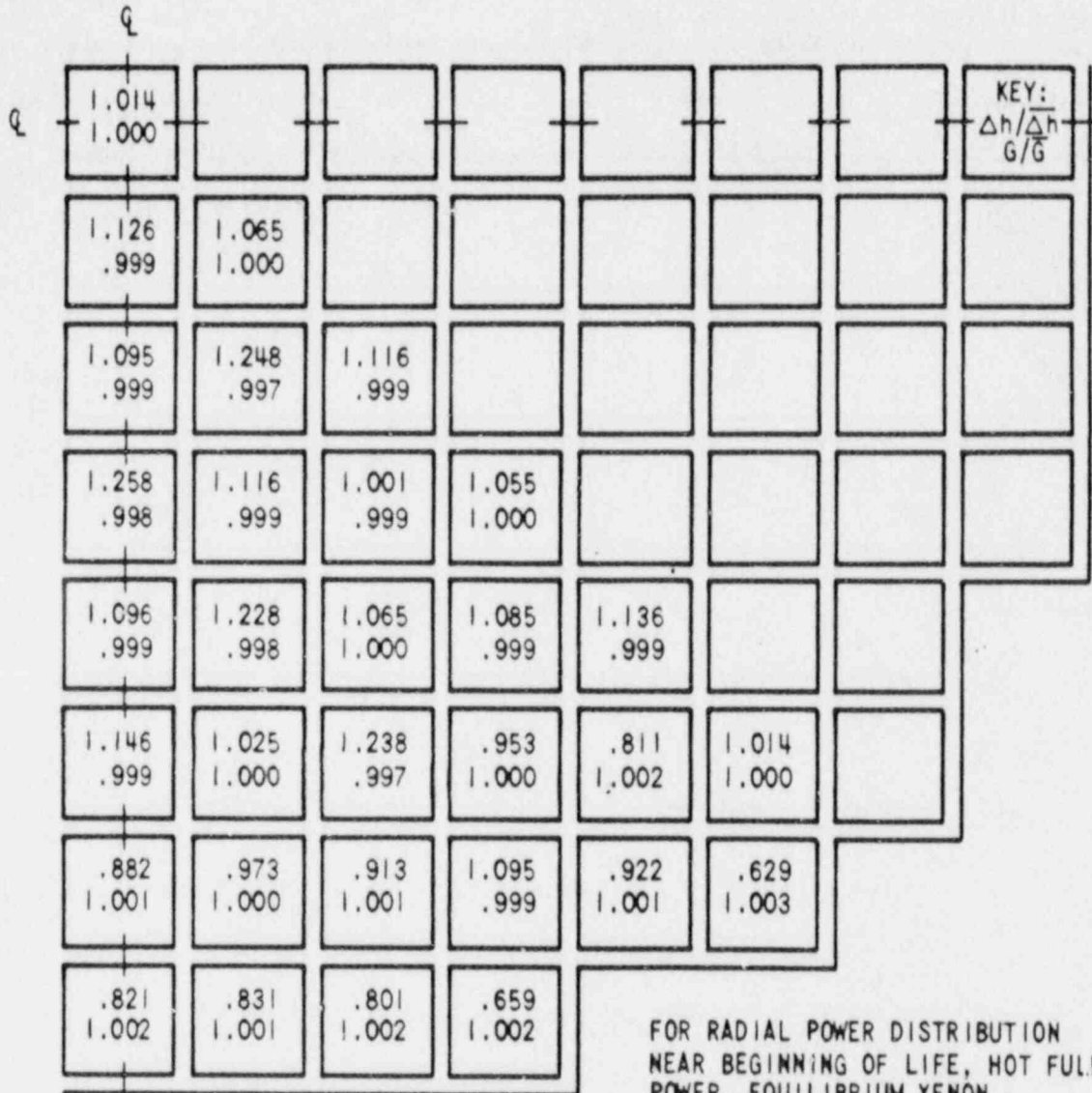
THERMAL AND HYDRAULIC COMPARISON TABLE

<u>Design Parameters</u>	<u>W. B. McGuire Units 1 and 2</u>	<u>South Texas Unit 1</u>	<u>South Texas Unit 2</u>	
Reactor Core Heat Output, MWt	3,411	3,800	3,800	
Reactor Core Heat Output, $10^6$ Btu/hr	11,641	12,969	12,969	
Heat Generated in Fuel, %	97.4	97.4	97.4	
System Pressure, Nominal, psia	2,250	2,250	2,250	
System Pressure, Minimum Steady State, psia	2,220	2,220	2,220	
Minimum DNBR at Nominal Conditions				
Typical Flow Channel	2.08	2.16	2.16	
Thimble (Cold Wall) Flow Channel	1.74	1.77	1.77	1
Minimum DNBR for Design Transients	≥1.30	≥1.30	≥1.30	
DNB Correlation	"R" (W-3 with Modified Spacer Factor)	"R" (W-3 with Modified Spacer Factor)	"R" (W-3 with Modified Spacer Factor)	
<u>Coolant Flow</u>				
Total Thermal Flow Rate, $10^6$ lb <sub>m</sub> /hr	140.3	139.6	141.3	4
Effective Flow Rate for Heat Transfer, $10^6$ lb <sub>m</sub> /hr	134.0	133.2	135.0	1
Effective Flow Area for Heat Transfer, ft <sup>2</sup>	51.1	51.1	51.1	
Average Velocity Along Fuel Rods, ft/sec	16.7	16.7	16.7	
Average Mass Velocity, $10^6$ lb <sub>m</sub> /hr-ft <sup>2</sup>	2.62	2.61	2.64	2

TABLE 4.4-1 (Continued)

THERMAL AND HYDRAULIC COMPARISON TABLE

<u>Design Parameters</u>	<u>W. B. McGuire Units 1 and 2</u>	<u>South Texas Units 1 and 2</u>	<u>South Texas Unit 2</u>
<u>Coolant Temperature</u>			
Nominal Inlet, °F	558.1	560.0	560.4
Average Rise in Vessel, °F	60.2	66.1	65.2
Average Rise in Core, °F	62.7	68.8	67.9
Average in Core, °F (Based on Avg. Enthalpy)	592.1	596.6	576.5
Average in Vessel, °F	588.2	593.0	573.0
<u>Heat Transfer</u>			
Active Heat Transfer, Surface Area, Ft <sup>2</sup>	59,700	69,700	69,700
Average Heat Flux, Btu/hr-ft <sup>2</sup>	189,800	181,200	181,200
Maximum Heat Flux for Normal Operation, Btu/hr-ft <sup>2</sup>	440,300 <sup>(a1)</sup>	453,100 <sup>(a2)</sup>	453,100 <sup>(a2)</sup>
Average Linear Power, kW/ft	5.44	5.20	5.20
Peak Linear Power for Normal Operation, kW/ft	12.6 <sup>(a1)</sup>	13.0 <sup>(a2)</sup>	13.0 <sup>(a2)</sup>
Peak Linear Power Resulting from Overpower Transients/Operators Errors (assuming a maximum overpower of 118%), kW/ft <sup>(b)</sup>	18.0	18.0	18.0
Peak Linear Power for Prevention of Centerline Melt, kW/ft <sup>(c)</sup>	> 18.0	> 18.0	> 18.0
Power Density, kW per liter of core <sup>(d)</sup>	104.5	98.8	98.8
Specific Power, kW per kg Uranium <sup>(d)</sup>	38.4	36.6	36.6



FOR RADIAL POWER DISTRIBUTION  
 NEAR BEGINNING OF LIFE, HOT FULL  
 POWER, EQUILIBRIUM XENON  
 CALCULATED  $F_{\Delta H}^N = 1.37$

- Definitions:
- $\Delta h$  = Enthalpy Rise
  - $\bar{\Delta h}$  = Average Enthalpy Rise
  - $G$  = Mass Flow Rate
  - $\bar{G}$  = Average Mass Flow Rate

**SOUTH TEXAS PROJECT**  
**UNITS 1 & 2**

Normalized Radial Flow and Enthalpy Distribution  
 at Elevation of 1/3 of Core Height  
 Figure 4.4-5<sup>A</sup>

1.005			KEY:				
0.999			$\frac{\Delta h}{\bar{\Delta h}}$				
			$\frac{G}{\bar{G}}$				
1.013	1.004						
1.000	0.999						
1.005	1.013	1.001					
0.999	1.000	0.999					
1.018	1.005	1.007	1.080				
1.000	0.999	1.000	0.999				
1.112	1.019	1.005	0.972	1.233			
0.999	1.000	0.999	1.000	0.999			
1.078	1.005	1.011	1.104	0.988	1.111		
0.999	0.999	1.000	0.999	1.000	0.999		
1.059	0.978	1.059	1.078	0.917	0.942		
0.999	1.000	1.000	0.999	1.000	1.002		
0.992	0.992	0.944	0.936				
1.001	1.001	1.001	1.003				

DEFINITIONS:

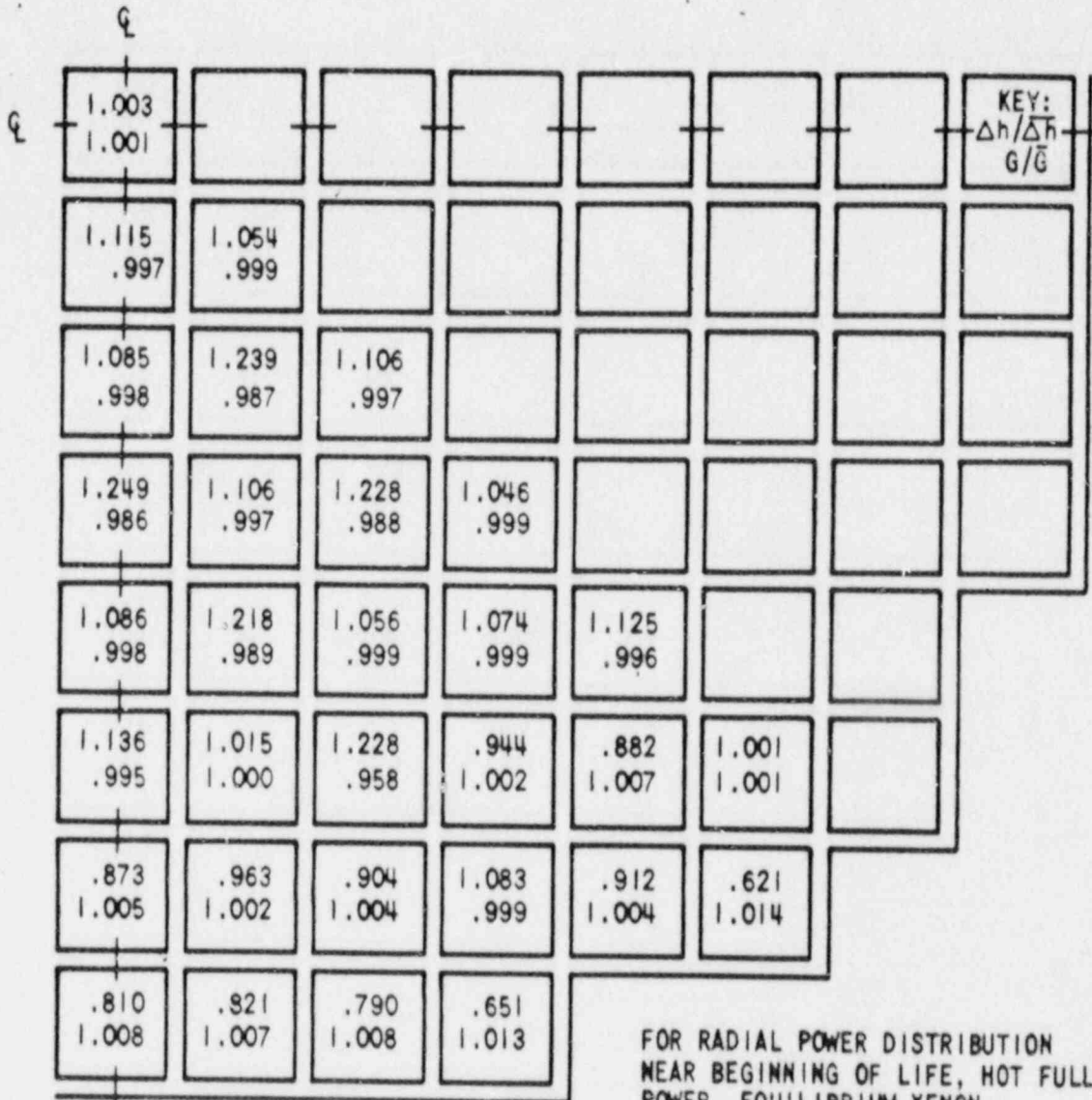
- $\Delta h$  = Enthalpy Rise
- $\bar{\Delta h}$  = Average Enthalpy Rise
- $G$  = Mass Flow Rate
- $\bar{G}$  = Average Mass Flow Rate

FOR RADIAL POWER DISTRIBUTION NEAR BEGINNING  
OF LIFE, NET FULL POWER, EQUILIBRIUM Xenon  
CALCULATED  $F-\Delta H = 1.944$

SOUTH TEXAS PROJECT  
UNIT 2

Normalized Radial Flow and Enthalpy Distribution  
at Elevation of 1/3 of Core Height

Figure 4.4-5 B



FOR RADIAL POWER DISTRIBUTION  
 NEAR BEGINNING OF LIFE, HOT FULL  
 POWER, EQUILIBRIUM XENON  
 CALCULATED  $F_{\Delta H}^N = 1.37$

**SOUTH TEXAS PROJECT**  
**UNITS 1 & 2**

Normalized Radial Flow and Enthalpy Distribution  
 at Elevation of 2/3 of Core Height

Figure 4.4-6<sup>A</sup>



1.006			KEY:				
0.995			$\frac{\Delta H}{\bar{\Delta h}}$				
			$\frac{G}{\bar{G}}$				
1.013	1.005						
1.002	0.995						
1.006	1.012	1.002					
0.995	1.002	0.995					
1.018	1.006	1.007	1.081				
1.002	0.995	1.002	0.997				
1.114	1.020	1.085	0.873	1.229			
0.993	1.001	0.996	1.003	0.980			
1.080	1.087	1.012	1.108	0.987	1.113		
0.998	0.994	1.001	0.953	1.002	0.992		
1.080	0.979	1.083	1.080	0.916	0.942		
0.993	1.003	0.998	0.996	1.004	1.014		
0.882	0.881	0.844	0.836				
1.005	1.008	1.008	1.014				

DEFINITIONS:

$\Delta h$  = Enthalpy Rise

$\bar{\Delta h}$  = Average Enthalpy Rise

$G$  = Mass Flow Rate

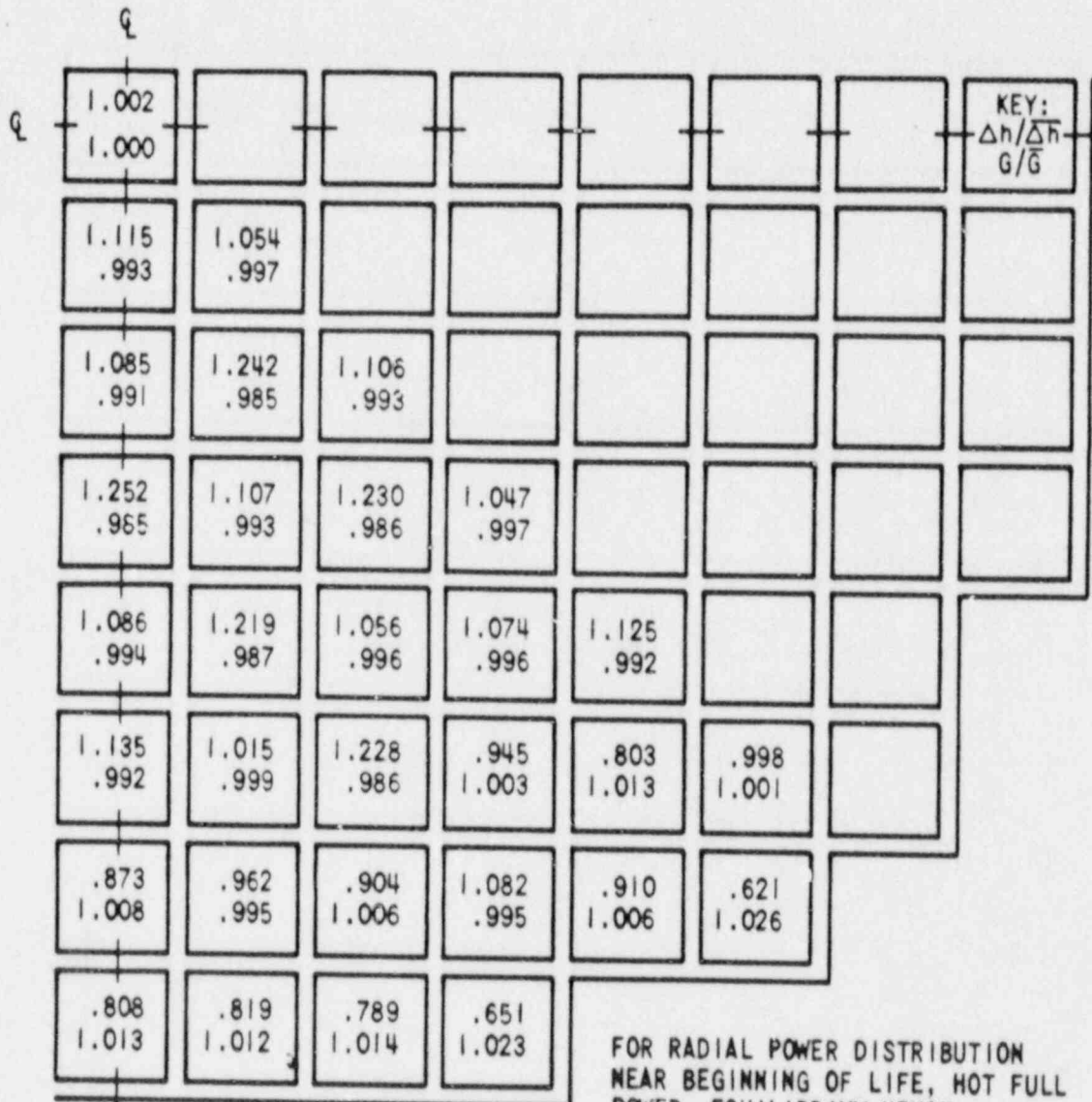
$\bar{G}$  = Average Mass Flow Rate

FOR RADIAL POWER DISTRIBUTION NEAR BEGINNING  
OF LIFE, NOT FULL POWER, EQUILIBRIUM Xenon  
CALCULATED  $F-\Delta H = 1.844$

SOUTH TEXAS PROJECT  
UNIT 2

Normalized Radial Flow and Enthalpy Distribution  
at Elevation of 2/3 of Core Height

Figure 4.4-8 B



FOR RADIAL POWER DISTRIBUTION  
 NEAR BEGINNING OF LIFE, HOT FULL  
 POWER, EQUILIBRIUM XENON  
 CALCULATED  $F_{\Delta H}^N = 1.37$

**SOUTH TEXAS PROJECT**  
**UNITS 1 & 2**  
 Normalized Radial Flow and Enthalpy  
 Distribution at Core Exit Elevation  
 Figure 4.4-7<sup>A</sup>

1.007 0.993			KEY: $\frac{\Delta h}{\bar{G}}$ $\frac{\bar{\Delta h}}{\bar{G}}$				
1.012 0.999	1.008 0.993						
1.007 0.993	1.012 0.999	1.003 0.993					
1.018 0.999	1.007 0.993	1.007 1.000	1.021 0.994				
1.114 0.991	1.020 0.998	1.008 0.994	0.974 1.002	1.239 0.982			
1.001 0.994	1.007 0.992	1.012 0.999	1.108 0.992	0.988 1.000	1.100 0.992		
1.080 0.995	0.978 1.002	1.051 0.995	1.078 0.994	0.918 1.007	0.847 1.028		
0.882 1.009	0.880 1.012	0.845 1.012	0.841 1.028				

DEFINITIONS:

- $\Delta h$  = Enthalpy Rise
- $\bar{\Delta h}$  = Average Enthalpy Rise
- $G$  = Mass Flow Rate
- $\bar{G}$  = Average Mass Flow Rate

FOR RADIAL POWER DISTRIBUTION NEAR BEGINNING  
OF LIFE, NOT FULL POWER, EQUILIBRIUM Xenon  
CALCULATED P- $\Delta H$  = 9.944

**SOUTH TEXAS PROJECT**  
**UNIT 2**

Normalized Radial Flow and Enthalpy  
Distribution at Core Exit Elevation  
Figure 4.47 B

TABLE 15.0-3

NOMINAL VALUES OF PERTINENT PLANT PARAMETERS  
UTILIZED IN THE ACCIDENT ANALYSES<sup>a</sup>

Thermal output of NSSS (Mwt)		See Table 15.0-2	
Core inlet temperature (*F)		560.0 <sup>b</sup>	
Vessel average temperature (*F)		593.0	18
Reactor Coolant System pressure (psia)		2250	
Reactor coolant flow per loop (gpm)	94,100	<del>95,400</del> <sup>b</sup>	18   60
Steam flow from NSSS (lb/hr)		16,960,000	18
Steam pressure at steam generator outlet (psia)		1100	
Maximum steam moisture content (%)		0.25	
Assumed feedwater temperature at steam generator inlet (*F)		440	
Average core heat flux (Btu/hr-ft <sup>2</sup> )		181200	

<sup>a</sup> Steady state errors discussed in Section 15.0.3 are added to these values to obtain initial conditions for transient analyses.

<sup>b</sup> ~~Loop flow of 94,100 gpm was used in all other analysis except the locked rotor rods-in-DNB analysis, which is the most limiting case.~~

→ See revised footnote "b" 15.0-19

Insert to Table 15.0-3

b An inlet temperature of 560.4°F and a loop flow of 95,400 gpm have been used in the following analyses for Unit 1 and Unit 2.

- Turbine Trip (FSAR Section 15.2.3)
- Reactor Coolant Pump Shaft Seizure (Locked Rotor) (FSAR Section 15.3.3)  
(both hot spot and rods-in-DNB analyses)
- Uncontrolled Rod Cluster Control Assembly Bank Withdrawal at Power (FSAR Section 15.4.2)
- Chemical and Volume Control System Malfunction that Results in a Decrease in Boron Concentration in the Reactor Coolant (FSAR Section 15.4.6) (Boron Dilution in Mode 1)
- Inadvertent Opening of a Pressurizer Safety or Relief Valve (FSAR Section 15.6.1)

An inlet temperature of 560.4°F and a loop flow of 95,400 gpm have been used in the following analyses for Unit 2 only.

- Inadvertent Opening of a Steam Generator Relief or Safety Valve Causing a Depressurization of the Main Steam System (FSAR Section 15.1.4)
- Spectrum of Steam System Piping Failures Inside and Outside Containment (FSAR Section 15.1.5)
  
- Partial Loss of Forced Reactor Coolant Flow (FSAR Section 15.3.1)
- Complete Loss of Forced Reactor Coolant Flow (FSAR Section 15.3.2)
  
- Spectrum of Rod Cluster Control Assembly Ejection Accidents (FSAR Section 15.4.8)

STP FSAR

TABLE 15.0-4

TRIP POINTS AND TIME DELAYS TO TRIP

ASSUMED IN ACCIDENT ANALYSES

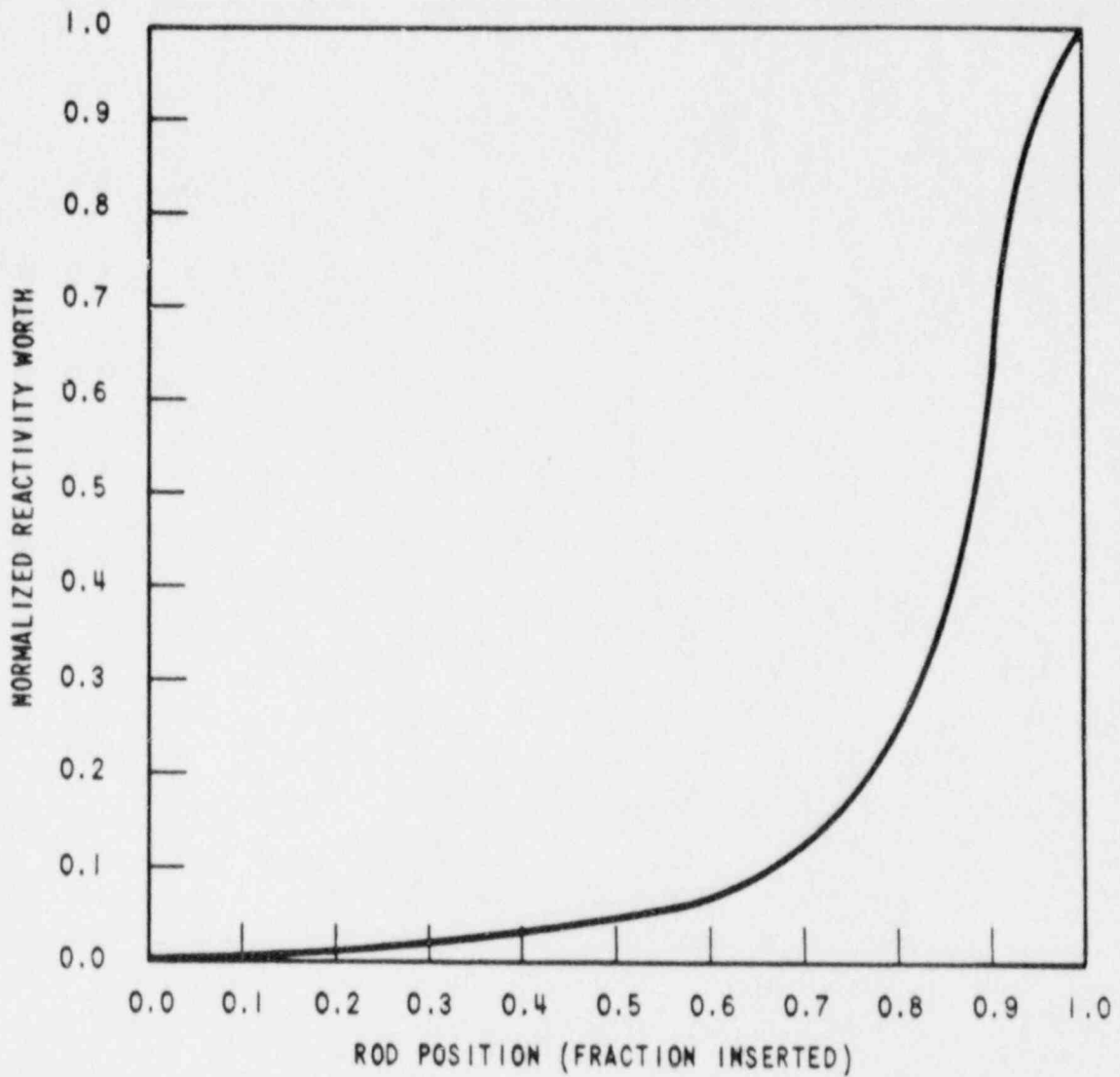
<u>Trip Function</u>	<u>Limiting Trip Point Assumed In Analysis</u>	<u>Time Delays (Seconds)</u>
Power range high neutron flux, high setting	118%	0.5
Power range high neutron flux, low setting	35%	0.5
Neutron Flux Reactor Trip Interlock, P-8 reset for 3 loop operation (coincident with low reactor coolant flow)	85%	1.0
Overtemperature ΔT	Variable see Figure 15.0-1	<del>6.5</del> <sup>a</sup> 8.0
Overpower ΔT	Variable see Figure 15.0-1	<del>6.5</del> <sup>a</sup> 8.0
High pressurizer pressure	<del>2405</del> <sup>2420</sup> psig	2.0
Low pressurizer pressure	1845 psig	2.0
Low reactor coolant flow (from loop flow detectors)	87% loop flow	1.0
Undervoltage trip	68% nominal	1.5
Turbine trip	Not applicable	2.0
Low-low steam generator water level	18% of narrow range level span	2.0

43  
60  
57

<sup>a</sup> Total time delay (including RTD and thermowell time response, trip circuit and channel electronics delay) from the time the temperature difference in the coolant loops exceeds the trip setpoint until the rods are free to fall.

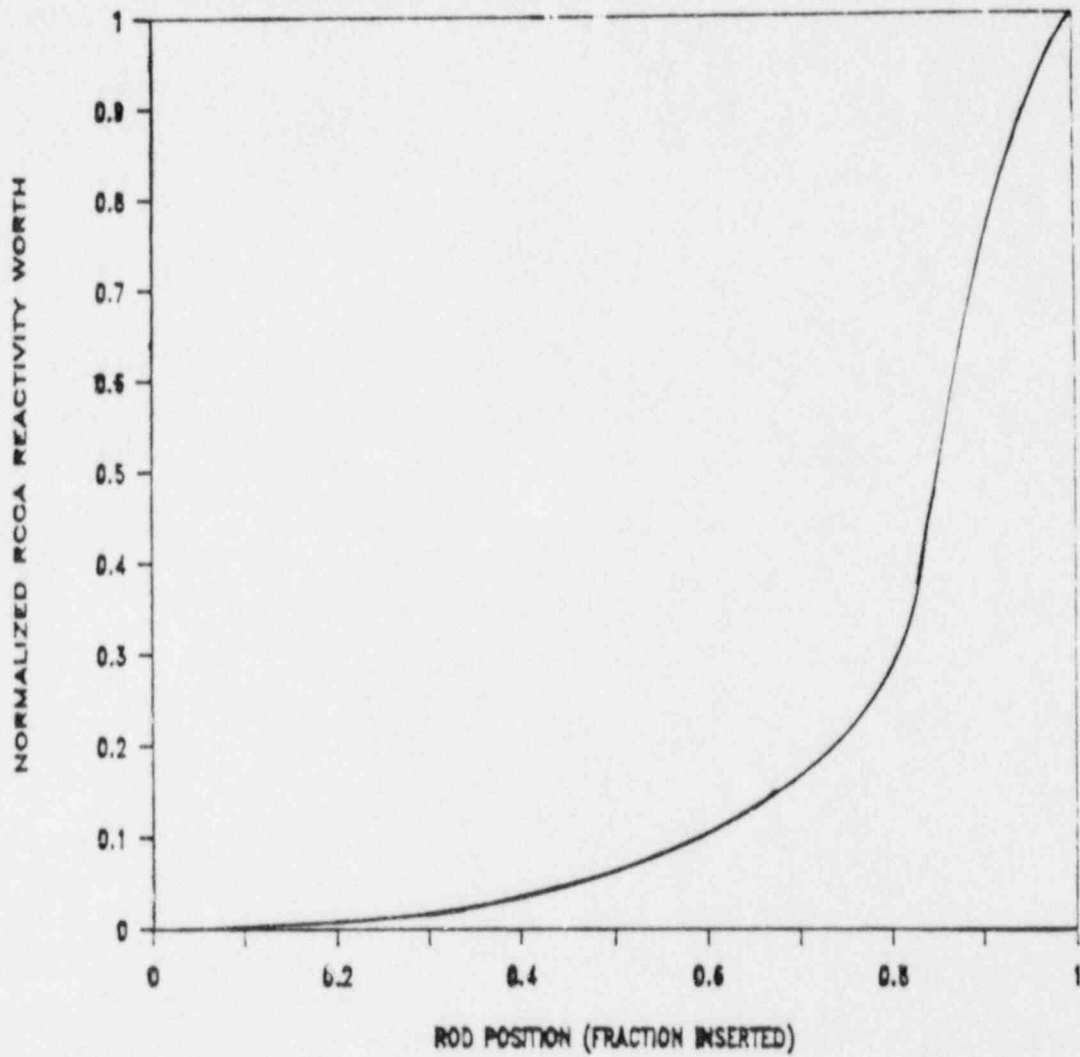
57



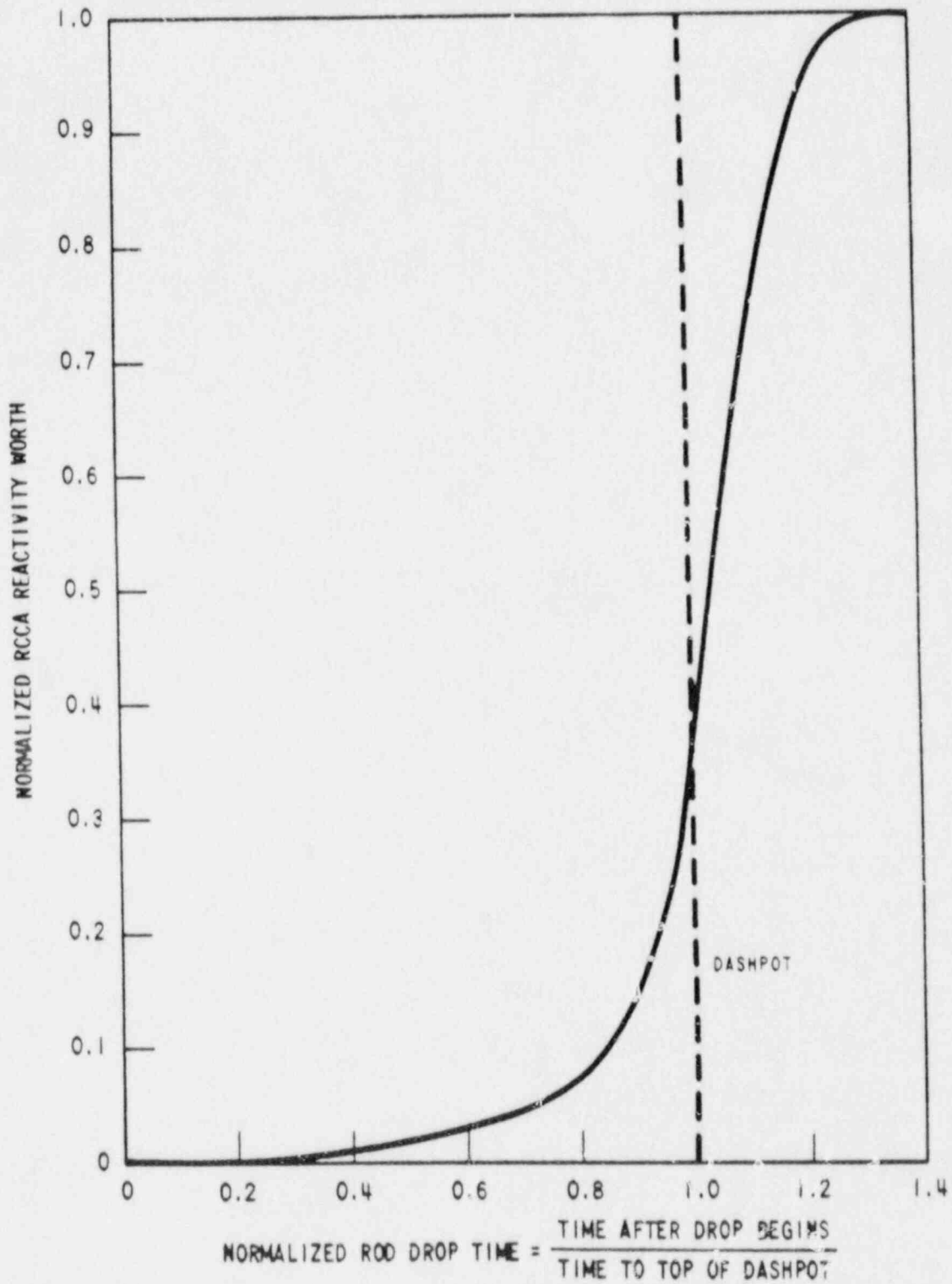


**SOUTH TEXAS PROJECT  
UNIT 1**

Normalized Rod Worth Versus Fraction Inserted  
Figure 15.0-4 A



**SOUTH TEXAS PROJECT**  
**UNIT 2**  
Normalized Rod Worth Versus Fraction Inserted  
Figure 15.0-4 B

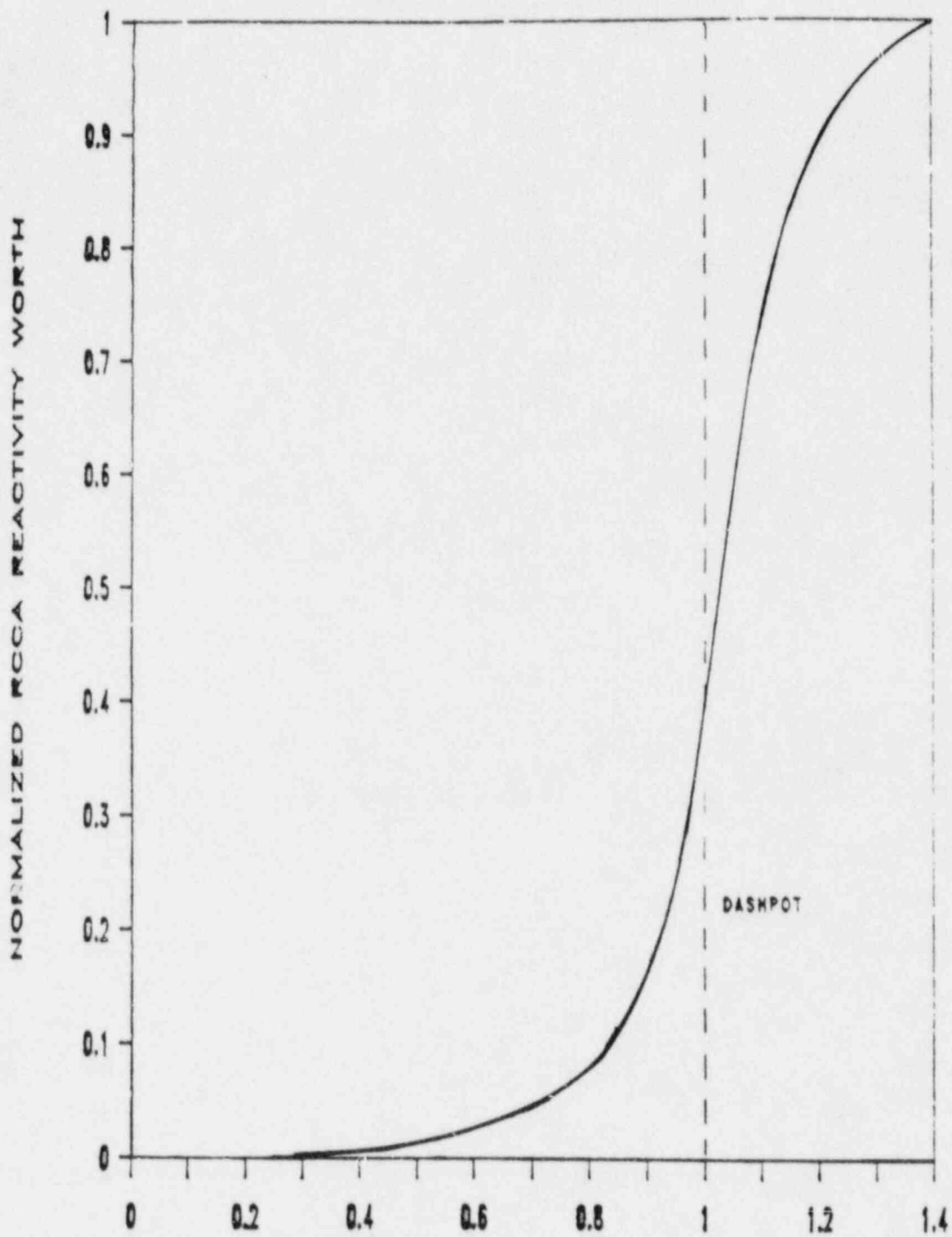


Amendment 18, 5/1/81

## SOUTH TEXAS PROJECT UNIT 1

Figure 15.0-5. A

Normalized RCCA Bank Reactivity Worth  
versus Normalized Drop Time



**SOUTH TEXAS PROJECT  
UNIT 2**

Figure 15.0-5. B  
Normalized RCCA Bank Reactivity Worth  
versus Normalized Drop Time

for Unit 1 and  
1200 psi for Unit 2

2. A negative moderator coefficient corresponding to the end-of-life rodded core with the most reactive rod cluster control assembly in the fully withdrawn position. The variation of the coefficient with temperature and pressure is included. The  $k_{eff}$  versus temperature at 1000 psi corresponding to the negative moderator temperature coefficient used is shown in Figure 15.1-11. The effect of power generation in the core on overall reactivity with the most reactive RCCA in the fully withdrawn position is shown on Figure 15.1-14 for nominal reactor coolant flow.

57

The core properties associated with the sector nearest the affected steam generator and those associated with the remaining sector were conservatively combined to obtain average core properties for reactivity feedback calculations. Further, it was conservatively assumed that the core power distribution was uniform. These two conditions cause underprediction of the reactivity feedback in the high power region near the stuck rod. To verify the conservatism of this method, the reactivity, as well as the power distribution, was checked for the limiting conditions for the cases analyzed. This core analysis considered the Doppler reactivity from the high fuel temperature near the stuck RCCA, moderator feedback from the high water enthalpy near the stuck RCCA, power redistribution and non-uniform core inlet temperature effects. For cases in which steam generation occurs in the high flux regions of the core, the effect of void formation was also included. It was determined that the reactivity employed in the kinetics analysis was always larger than the reactivity calculated, including the above local effects for the conditions. These results verify conservatism (i.e., underprediction of negative reactivity feedback from power generation).

8

3. Minimum capability for injection of high concentration boric acid solution corresponding to the most restrictive single failure in the safety injection system. Low concentration boric acid must be swept from the safety injection lines downstream of the isolation valves prior to the delivery of high concentration boric acid (2,500 ppm) to the reactor coolant loops. This effect has been allowed for in the analysis.

2  
3

4. The case studied is a steam flow of 292 pounds per second at 1300 psia from one steam generator with offsite power available. This is the maximum capacity of any single steam dump, relief, or safety valve. Initial hot shutdown conditions at time zero are assumed since this represents the most conservative initial condition.

2

Should the reactor be just critical or operating at power at the time of a steam release, the reactor will be tripped by the normal overpower protection when power level reaches a trip point. Following a trip at power, the RCS contains more stored energy than at no-load, and there is appreciable energy stored in the fuel. Thus, the additional stored energy is removed via the cooldown caused by the steam release before the no-load conditions of RCS temperature and shutdown margin assumed in the analyses are reached. After the additional stored energy has been removed, the cooldown and reactivity insertions proceed in the same manner as in the analysis which assumes no-load condition at time zero. However, since the initial steam generator water inventory is greatest at no-load, the magnitude and duration of the RCS cooldown are less for steam release occurring at power.

43

STF FSAR

temperature coefficient, the cooldown results in an insertion of positive reactivity. If the most reactive RCCA is assumed stuck in its fully withdrawn position after reactor trip, there is an increased possibility that the core will become critical and return to power. The core is ultimately shut down by the boric acid delivered by the Safety Injection System. | 3

The analysis of a main steam line rupture is performed to demonstrate that the following criterion is satisfied:

Assuming a stuck RCCA, with or without offsite power, and assuming a single failure in the SIS, the core remains in place and intact. | 3

Although DNB and possible clad perforation following a steam pipe rupture are not necessarily unacceptable, the analysis, in fact, shows that no DNB occurs for any rupture assuming the most reactive assembly stuck in its fully withdrawn position.

A major steam line rupture is classified as an ANS Condition IV event (see Section 15.0.1).

The major rupture of a steam line is the most limiting cooldown transient and, thus, is analyzed at zero power with no decay heat. Decay heat would retard the cooldown thereby reducing the return to power. A detailed analysis of this transient with the most limiting break size, a double-ended rupture, is presented here.

The following functions provide the necessary protection for a steam line rupture:

1. Safety injection actuation from either: | 2
    - a. Two out of four low pressurizer pressure signals, or | 57
    - b. Excessive cooldown protection (two out of three low compensated steamline pressure from any SG or two out of three low-low compensated T-cold in any loop). X
  2. The overpower reactor trips (neutron flux and  $\Delta T$ ) and the reactor trip occurring in conjunction with receipt of the SI signal. | 44
  3. Redundant isolation of the main feedwater lines: sustained high feedwater flow would cause additional cooldown. Therefore, in addition to the safety injection signal, an excessive cooldown protection signal will rapidly close all feedwater control valves and feedwater isolation valves, as well as trip the main feedwater pumps. | 43
  4. Closure of the fast-acting <sup>S</sup> Main <sup>I</sup> Steam <sup>V</sup> Isolation <sup>V</sup> Valves (MSIVs) (designed to close in less than 5 seconds) from either a | 43
    - a. High-2 containment pressure signal, | 57
    - b. Low steamline pressure or low-low T-cold signal (two out of three in any loop) above the P-11 setpoint, or
- Lower case letters, same as pg 15.1-9*



- c. High negative steamline pressure rate signal (two out of three in any loop) below the P-11 setpoint. | 57

Fast-acting isolation valves are provided in each steam line that will fully close within 10 seconds of a large break in the steam line. For breaks downstream of the isolation valves, closure of all valves would completely terminate the blowdown. A description of steam line isolation is included in Chapter 10. | 43

Design criteria and methods of protection of safety-related equipment from the dynamic effects of postulated piping ruptures are provided in Section 3.6.

A block diagram summarizing various protection sequences for safety actions required to mitigate the consequences of this event is provided in Figure 15.0-9. | 43

#### 15.1.5.2 Analysis of Effects and Consequences.

##### Method of Analysis

The analysis of the steam pipe rupture has been performed to determine:

1. The core heat flux and RCS temperature and pressure resulting from the cooldown following the steam line break. The LOFTRAN code (Ref. 15.1-1) has been used.
2. The thermal and hydraulic behavior of the core following a steam line break. A detailed thermal and hydraulic digital computer code, THINC, has been used to determine if DNB occurs for the core conditions computed in Item 1 above.

The methodology employed is consistent with that used in the steam line rupture topical report (Ref 15.1-4) *which concludes that the hot zero power steamline break analysis is sufficiently conservative as a licensing basis event to demonstrate compliance with 10CFR 100.* | 32  
The following conditions were assumed to exist at the time of a main steam line break accident:

1. End-of-life shutdown margin at no-load, equilibrium xenon conditions, and with the most reactive RCCA stuck in its fully withdrawn position. Operation of the control rod banks during core burnup is restricted in such a way that addition of positive reactivity in a steam line break accident will not lead to a more adverse condition than the case analyzed. | 2
2. A negative moderator coefficient corresponding to the end-of-life rodded core with the most reactive RCCA in the fully withdrawn position. The variation of the coefficient with temperature and pressure has been included. The  $k_{eff}$  versus temperature at 1000 psi corresponding to the negative moderator temperature coefficient used is shown on Figure 15.1-11. The effect of power generation in the core on overall reactivity with the most reactive RCCA in the fully withdrawn position is shown on Figure 15.1-14 at nominal reactor coolant flow. | 2 | 3

For Unit 1 and  
1200 psi for Unit 2

- b. Case (a) with loss of offsite power simultaneous with the steam line break and initiation of the safety injection signal. Loss of offsite power results in reactor coolant pump coastdown. | 32
6. Power peaking factors corresponding to one stuck RCCA and nonuniform core inlet coolant temperatures are determined at end of core life. The coldest core inlet temperatures are assumed to occur in the sector with the stuck rod. The power peaking factors account for the effect of the local void in the region of the stuck control assembly during the return to power phase following the steam line break. This void in conjunction with the large negative moderator coefficient partially offsets the effect of the stuck assembly. The power peaking factors depend upon the core power, temperature, pressure, and flow, and, thus, are different for each case studied. | 2

The core parameters used for each of the two cases correspond to values determined from the respective transient analysis.

Both the cases assume initial hot shutdown conditions at time zero since this represents the most pessimistic initial condition. Should the reactor be just critical or operating at power at the time of a steam line break, the reactor will be tripped by the normal overpower protection system when power level reaches a trip point. Following a trip at power, the RCS contains more stored energy than at no-load, the average coolant temperature is higher than at no-load and there is appreciable energy stored in the fuel. Thus, the additional stored energy is removed via the cooldown caused by a steam line break before the no-load conditions of RCS temperature and shutdown margin assumed in the analyses are reached. After the additional stored energy has been removed, the cooldown and reactivity insertions proceed in the same manner as in the analysis which assumes no-load condition at time zero. | 57

7. In computing the steam flow during a steam line break, the Moody Curve (Ref. 15.1-3) for  $f(L/D) = 0$  is used.
8. Perfect moisture separation in the steam generator is assumed.

### Results

15 The calculated sequence of events for all cases analyzed is shown in Table 15.1-1.

The results presented are a conservative indication of the events which would occur assuming a steam line rupture since it is postulated that all of the conditions described above occur simultaneously.

### Core Power and Reactor Coolant System Transient

 | 2

Figures 15.1-15 through 15.1-17 show the RCS transient and core heat flux following a main steam line rupture (complete severance of a pipe) at initial no-load condition (case a). Offsite power is assumed available such that full reactor coolant flow exists. The transient shown assumes an uncontrolled

steam release from only one steam generator. Should the core be critical at near zero power when the rupture occurs, the initiation of safety injection by low steam line pressure will trip the reactor. Steam release from more than one steam generator will be prevented by automatic closure of the fast-acting isolation valves in the steam lines via the low steam line pressure signal. Even with the failure of one valve, release is limited to no more than 10 seconds from the other steam generators while the one generator blows down. The steam line stop valves are designed to be fully closed in less than 5 seconds from receipt of a closure signal.

As shown in Figure 15.1-17, the core attains criticality with the RCCAs inserted (with the design shutdown assuming one stuck RCCA) shortly before boron solution at 2,500 ppm enters the RCS. A peak core power less than the nominal full power value is attained.

The calculation assumes the boric acid is mixed with and diluted by the water flowing in the RCS prior to entering the reactor core. The concentration after mixing depends upon the relative flow rates in the RCS and in the SIS. The variation of mass flow rate in the RCS due to water density changes is included in the calculation as is the variation of flow rate in the SIS due to changes in the reactor coolant system pressure. The SIS flow calculation includes the line losses in the system as well as the pump head curve.

Figures 15.1-18 through 15.1-20 show the response of the salient parameters for case b which corresponds to the case discussed above with additional loss of offsite power at the time the safety injection signal is generated. The safety injection delay time includes 10 seconds to start the standby Diesel generator and in 12 seconds the pump is assumed to be at full speed. Criticality is achieved later and the core power increase is slower than in the similar case with offsite power available. The ability of the emptying steam generator to extract heat from the RCS is reduced by the decreased flow in the RCS. For the <sup>DNB</sup> DNB evaluation, a power and power shape analysis consistent with the fluid conditions was used. The peak power remains well below the nominal full power value.

It should be noted that following a steam line break only one steam generator blows down completely. Thus, the remaining steam generators are still available for dissipation of decay heat after the initial transient is over. In the case of loss of offsite power, this heat is removed to the atmosphere via the steam line safety valves.

#### Margin to Critical Heat Flux

A DNB analysis was performed for both of these cases. It was found that the DNB design basis as stated in Section 4.4 was met for all cases.

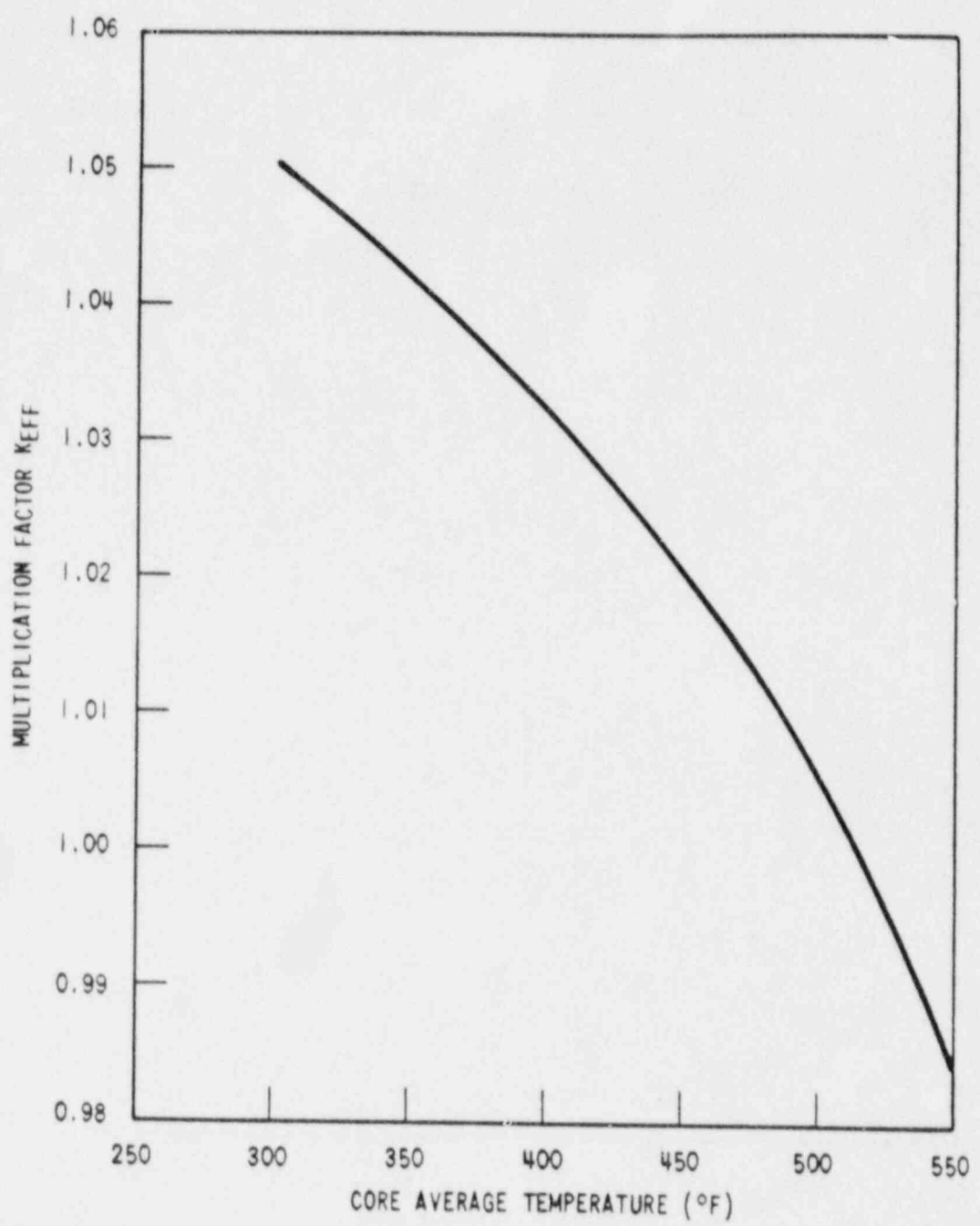
15.1.5.3 Radiological Consequences. The postulated accidents involving release of steam from the secondary system do not result in a release of radioactivity unless there is leakage from the RCS to the secondary system in the steam generators (SG's). A conservative analysis of the potential offsite doses resulting from a steamline break outside Containment upstream of the main steam isolation valve (MSIV) is presented using the Technical Specification limit secondary coolant concentrations. Parameters used in the analysis are listed in Table 15.1-2.

STP FSAR

TABLE 15.1-1 (Continued)

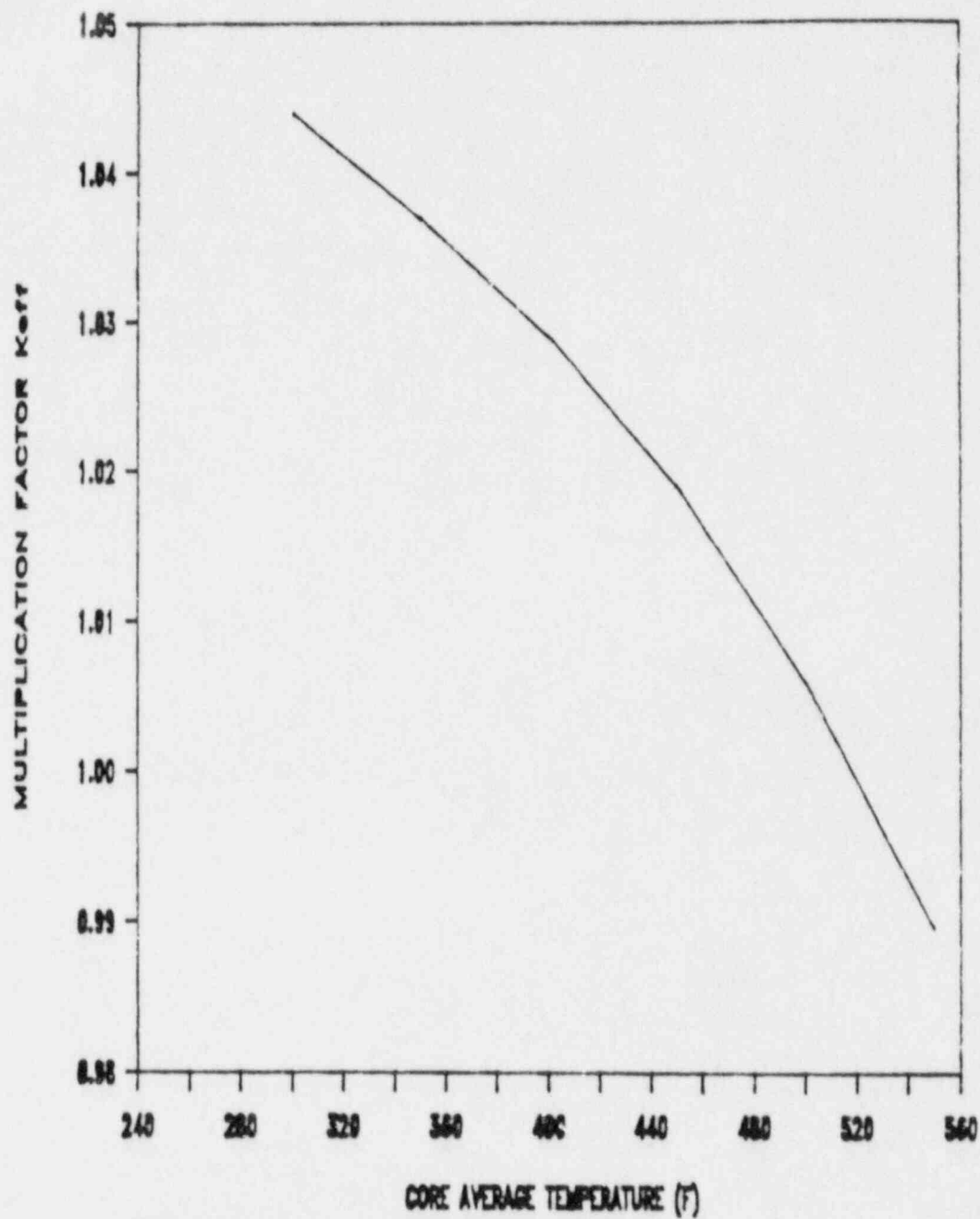
TIME SEQUENCE OF EVENTS FOR INCIDENTS WHICH CAUSE  
AN INCREASE IN HEAT REMOVAL BY THE SECONDARY SYSTEM

<u>Accident</u>	<u>Event</u>	<u>Time (sec)</u>	
		<u>Unit 1</u>	<u>Unit 2</u>
3. Automatic Reactor Control (Minimum moderator feedback)	10% step load increase	0.0	0.0
	Equilibrium conditions reached (approximate time only)	100	100
4. Automatic Reactor Control (Maximum moderator feedback)	10% step load increase	0.0	0.0
	Equilibrium conditions reached (approximate time only)	150	150
Accidental Depressurization of the Main Steam System	Inadvertent opening of one main steam safety or relief valve	0.0	0.0
	Pressurizer empties	181	249
	2,500 ppm boron reaches core	290	378
Steam System Piping Failure	1. Case a (Plant initially at no load, with off-site power)		
	Steam line ruptures	0	0
	Pressurizer empties	18.2	16.4
	Criticality attained	20.7	25.6
	2,500 ppm boron reaches core	111	100
2. Case b (Same as Case a except for loss of offsite power)			
Steam line ruptures	0	0	
Pressurizer empties	21.2	19.0	
Criticality attained	28.7	30.2	
2,500 ppm boron reaches core	193	182	



**SOUTH TEXAS PROJECT  
UNIT 1**

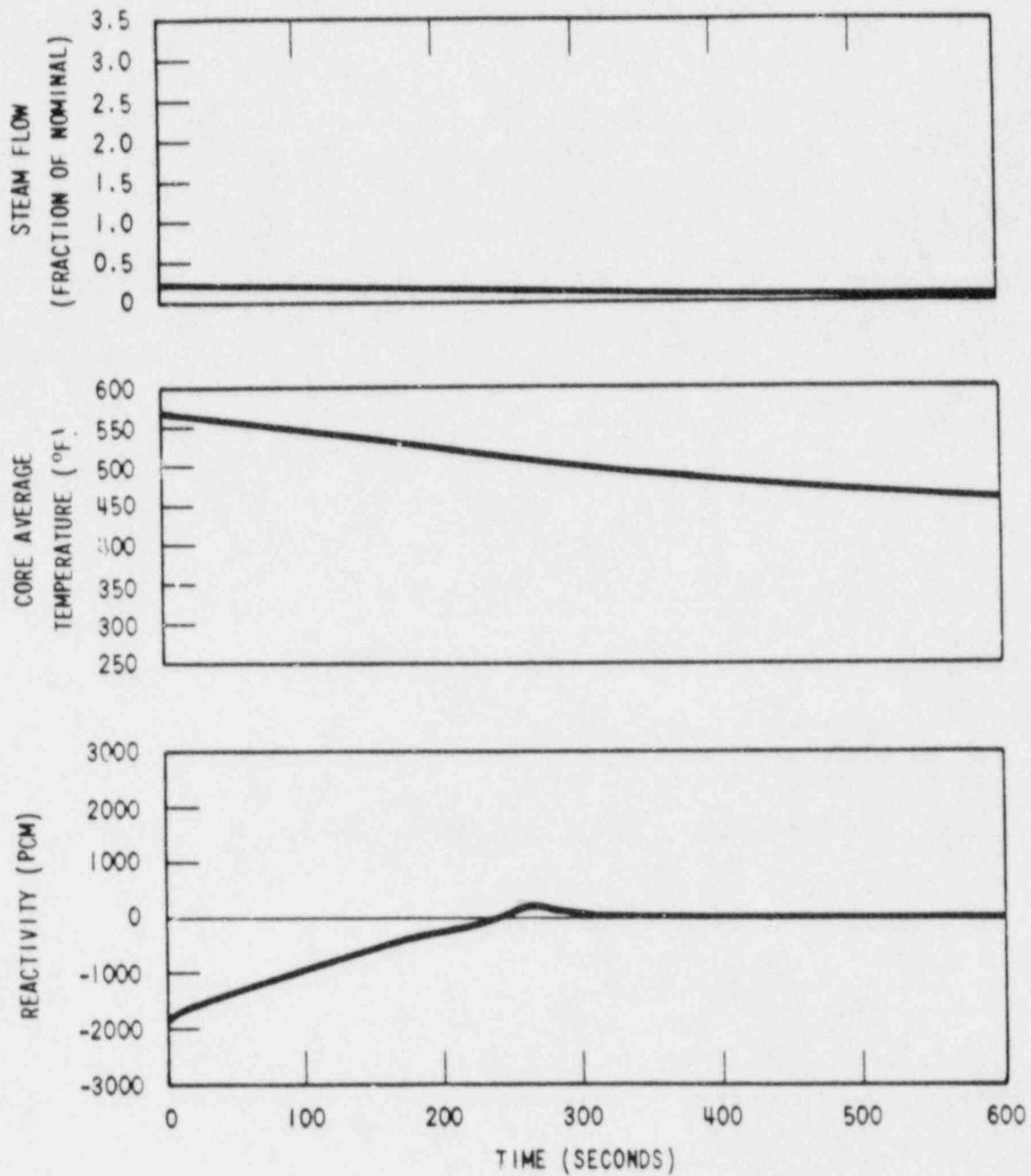
$K_{eff}$  Versus Core  
Average Temperature  
Figure 15.1-11 A



**SOUTH TEXAS PROJECT  
UNIT . 2**

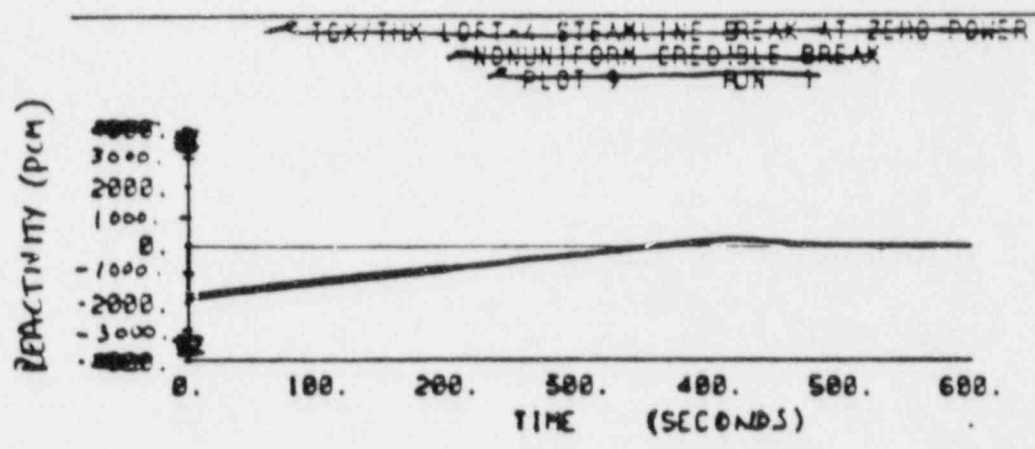
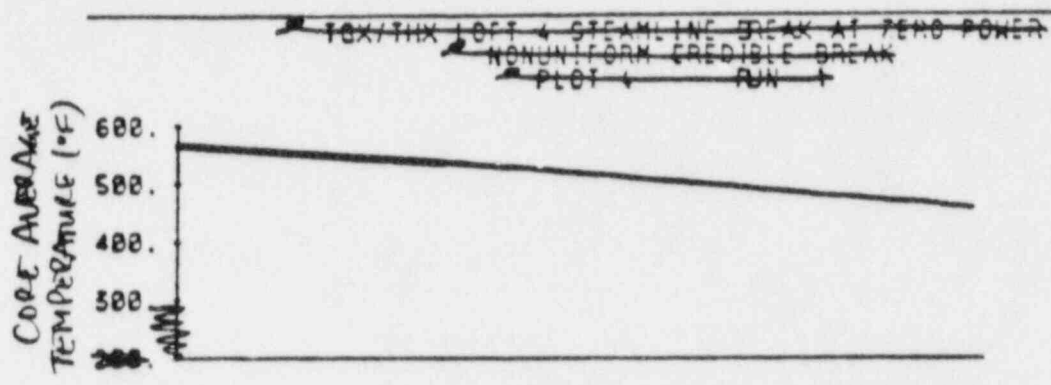
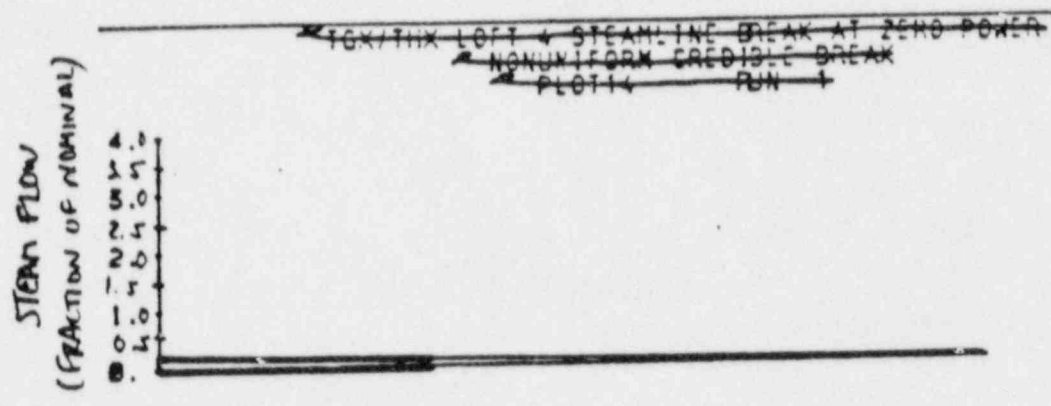
$K_{eff}$  Versus Core  
Average Temperature  
Figure 15.1-11 B





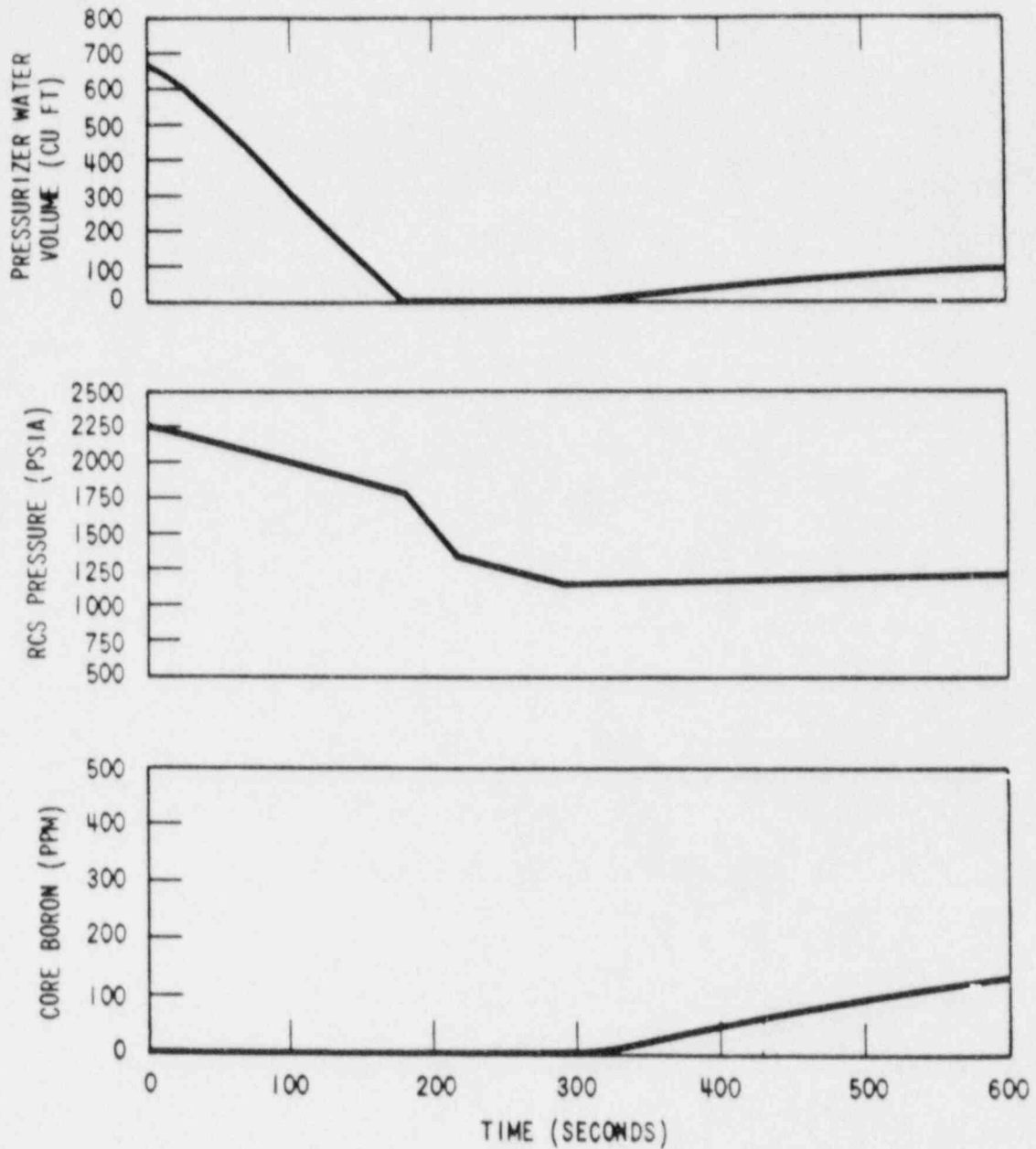
**SOUTH TEXAS PROJECT  
UNIT 1**

Figure 15.1-12. A *Reactor*  
Failure of a Steam Generator Safety or Dump Valve, Steam Flow versus Time, Average Temperature versus Time, Reactivity versus Time



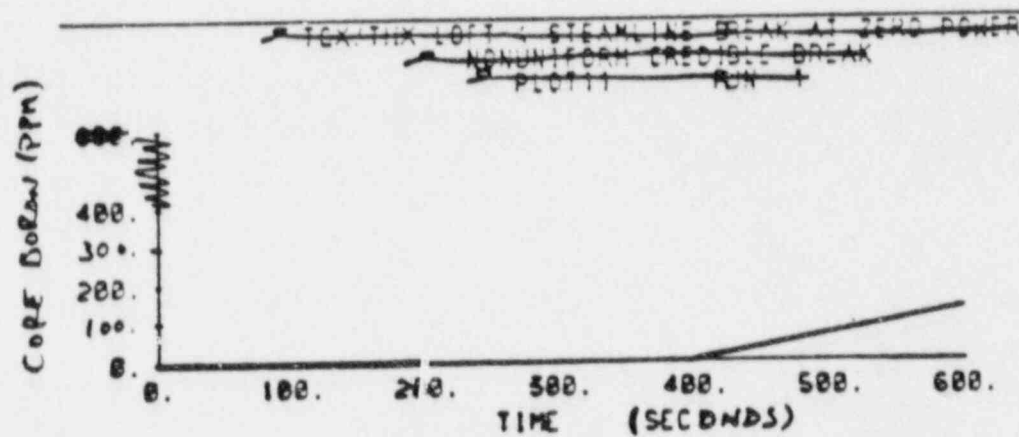
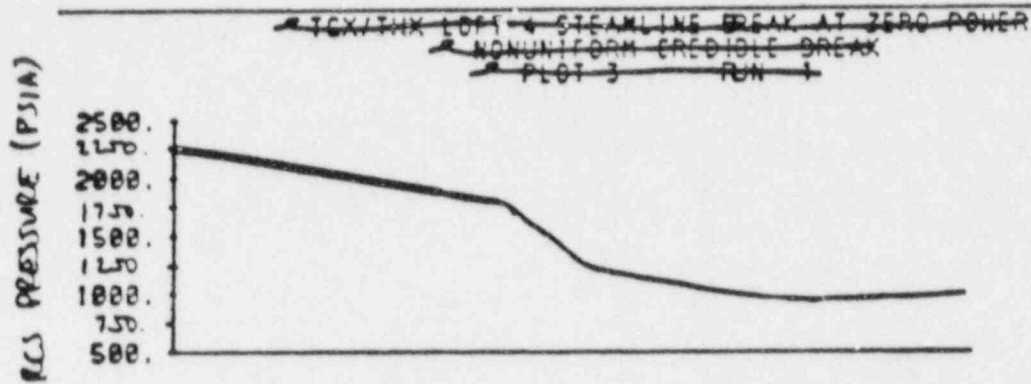
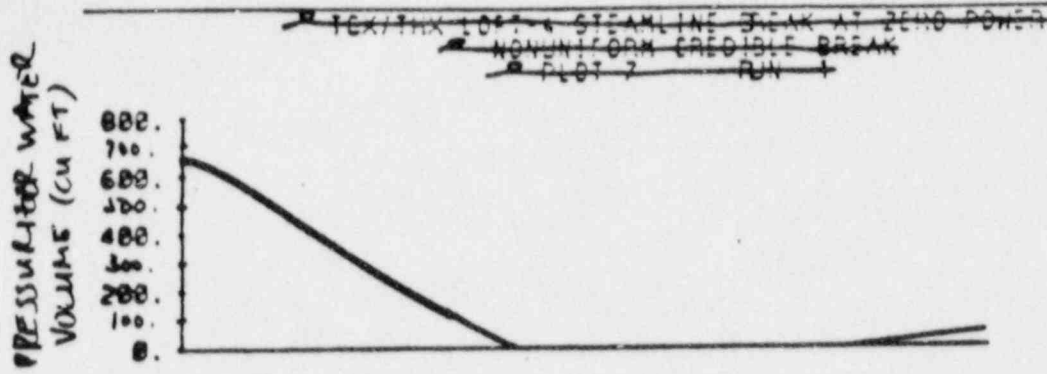
**SOUTH TEXAS PROJECT  
UNIT: 2**

Figure 15.1-12 <sup>B</sup> Relief  
 Failure of a Steam Generator Safety or Dump  
 Valve, Steam Flow versus Time, Average  
 Temperature versus Time, Reactivity versus  
 Time



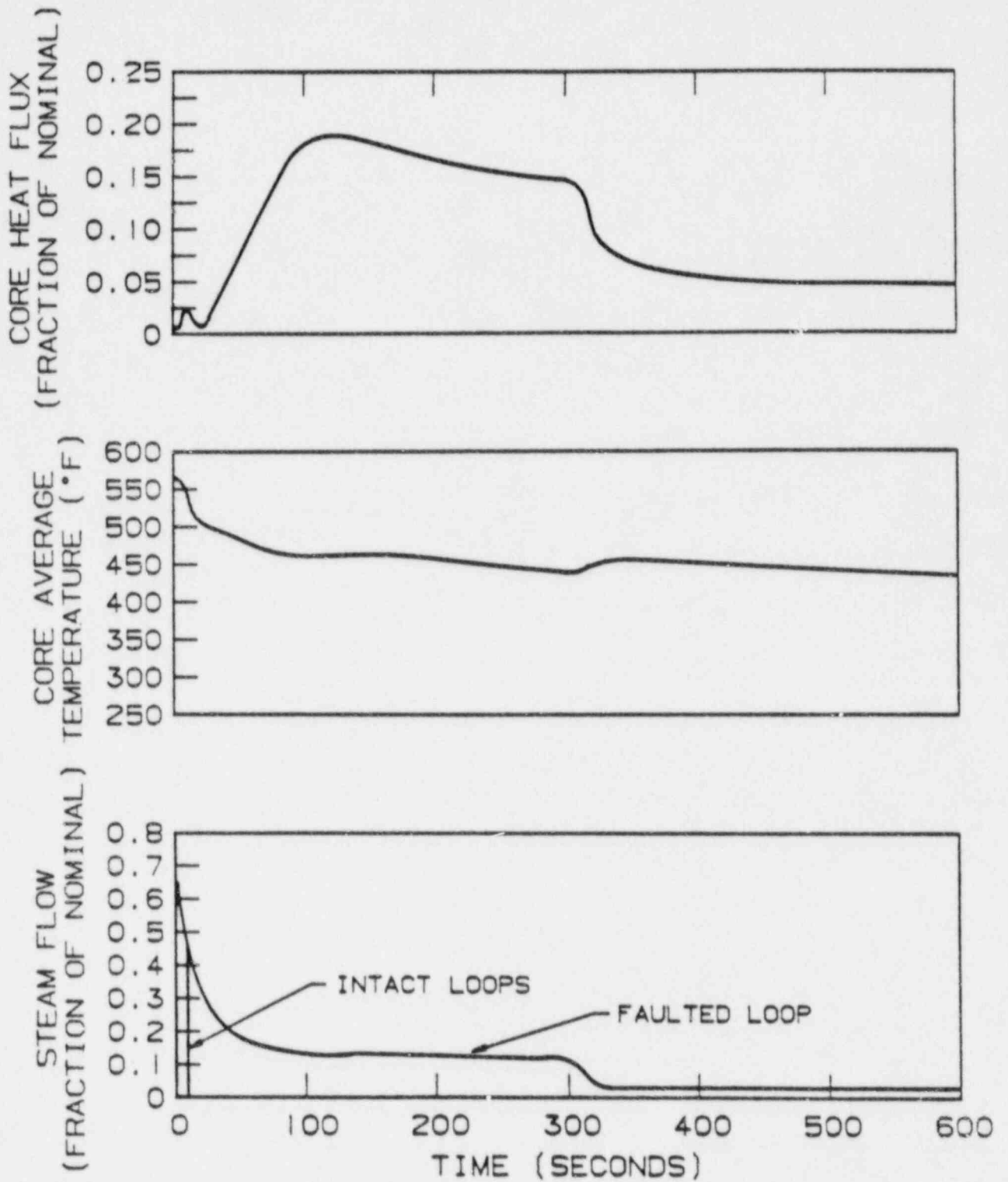
## SOUTH TEXAS PROJECT UNIT 1

Figure 15.1-13. A *Rel-F*  
 Failure of a Steam Generator Safety or Dump  
 Valve, RCS Pressure versus Time, Pressurizer  
 Water Volume versus Time, Boron Concentra-  
 tion versus Time



**SOUTH TEXAS PROJECT  
UNIT 2**

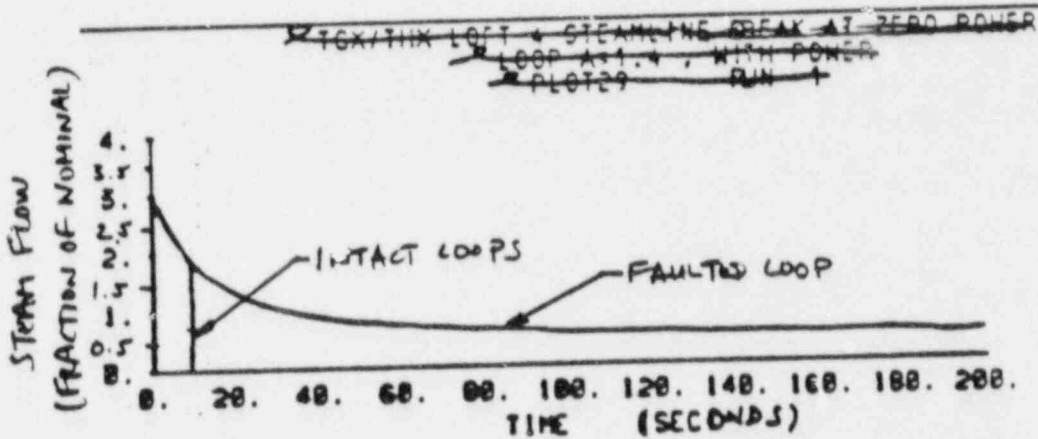
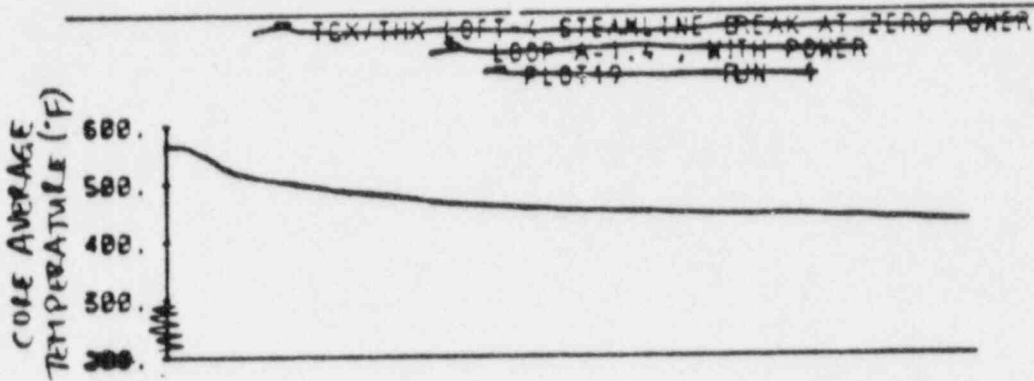
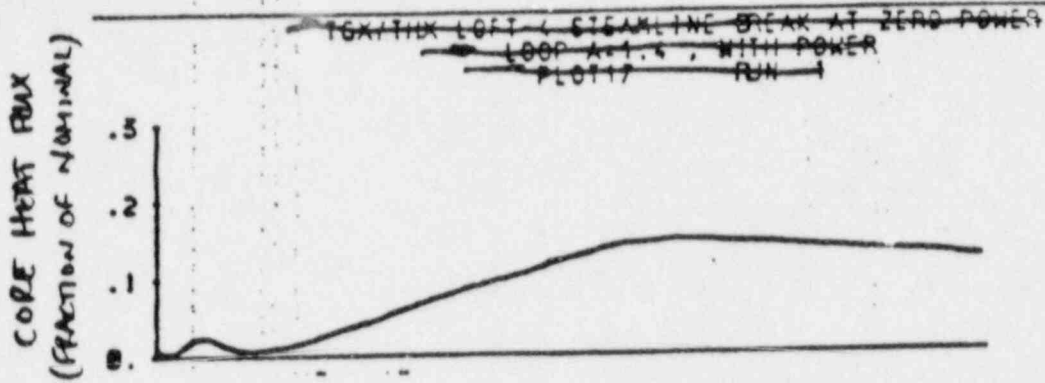
Figure 15.1-13. *B Relief*  
 Failure of a Steam Generator Safety or Dump Valve, RCS Pressure versus Time, Pressurizer Water Volume versus Time, Boron Concentration versus Time



**SOUTH TEXAS PROJECT  
UNIT 1**

1.4 FT<sup>2</sup> STEAM LINE RUPTURE, OFFSITE  
POWER AVAILABLE, HEAT FLUX VS TIME,  
AVERAGE TEMP. VS TIME, STEAM FLOW PER  
LOOP VS TIME

Figure 15.1-15 A



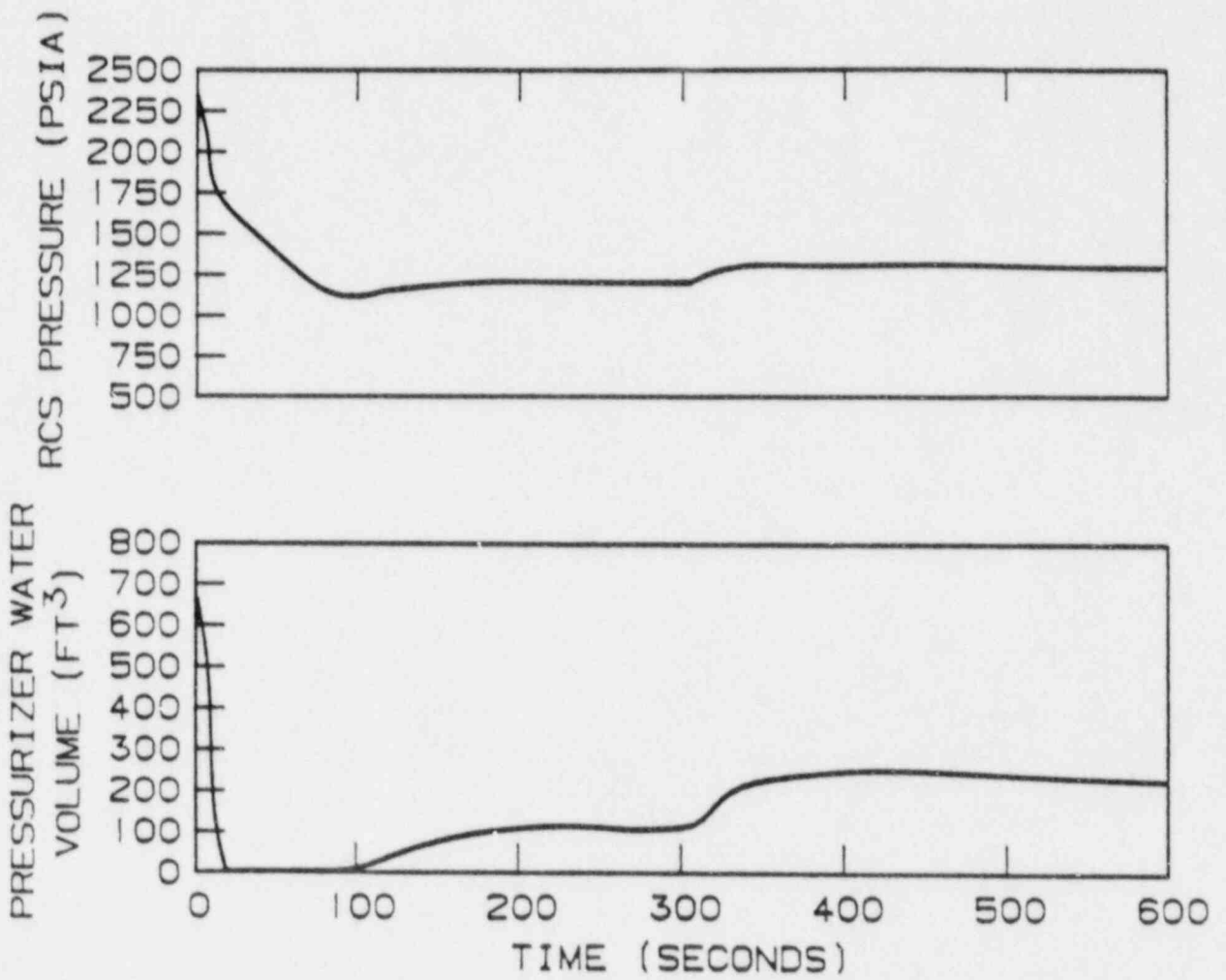
**SOUTH TEXAS PROJECT  
UNIT 2**

1.4 FT<sup>2</sup> STEAM LINE RUPTURE, OFFSITE  
POWER AVAILABLE, HEAT FLUX VS TIME,  
AVERAGE TEMP. VS TIME, STEAM FLOW  
VS TIME PLANT

Figure 15.1-15 B

Amendment 57

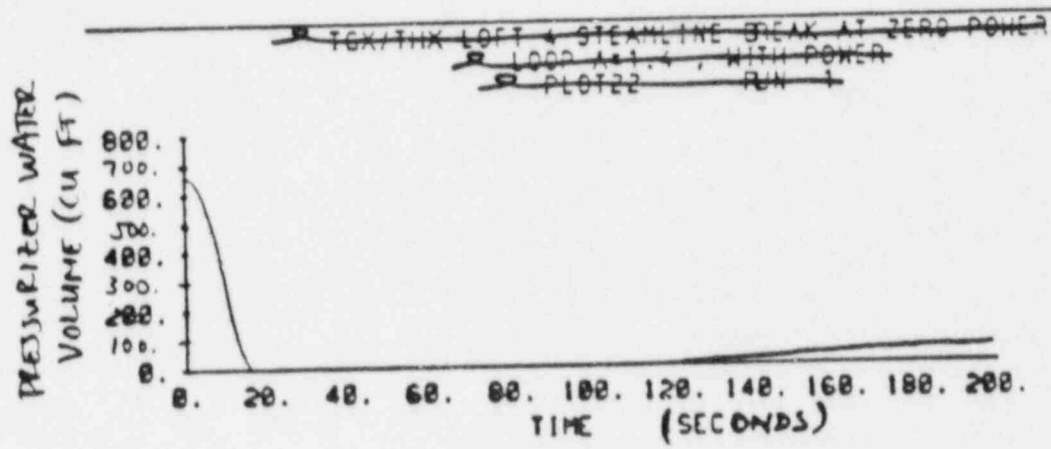
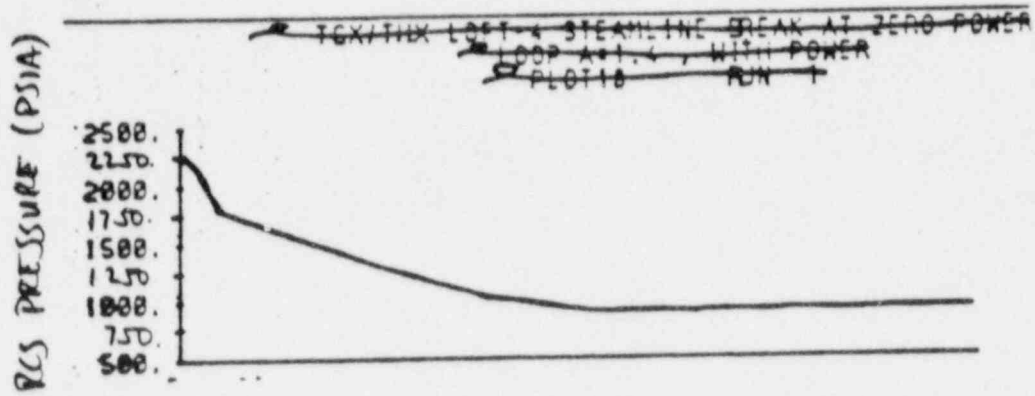




**SOUTH TEXAS PROJECT  
UNIT 1**

1.4FT<sup>2</sup> STEAM LINE RUPTURE, OFFSITE  
POWER AVAILABLE, RCS PRESSURE VS  
TIME, PRESSURIZER WATER VOLUME VS  
TIME

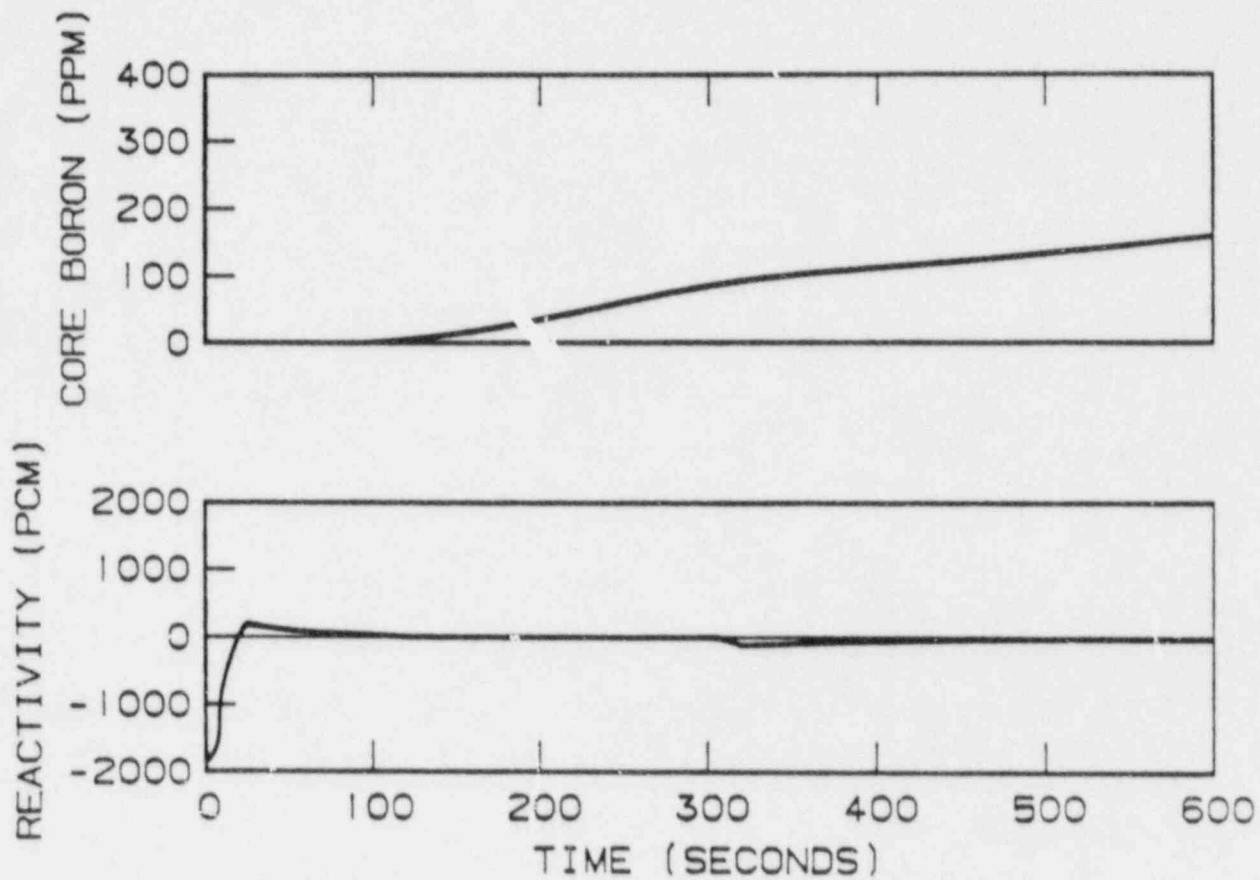
Figure 15.1-16 A



**SOUTH TEXAS PROJECT**  
**UNIT 2**

1.4FT<sup>2</sup> STEAM LINE RUPTURE, OFFSITE  
 POWER AVAILABLE, RCS PRESSURE VS  
 TIME, PRESSURIZER WATER VOLUME VS  
 TIME

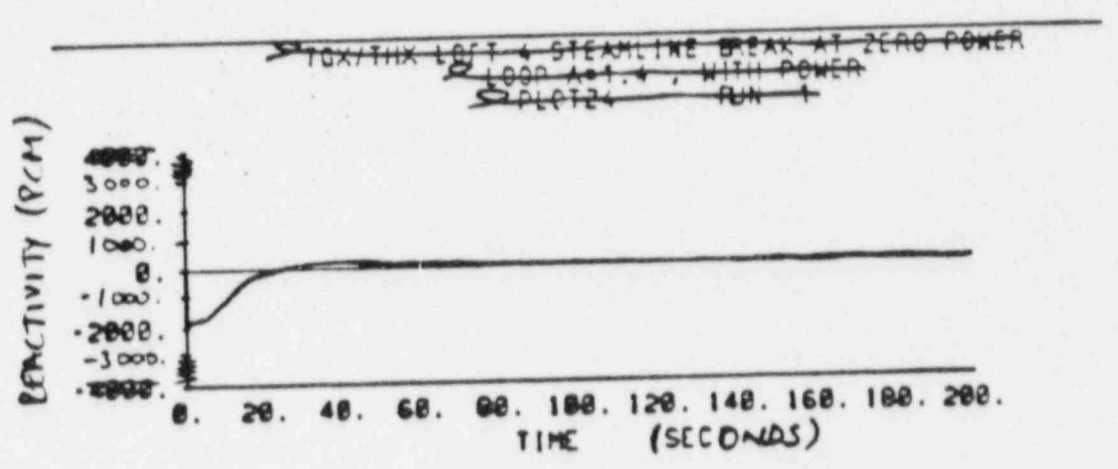
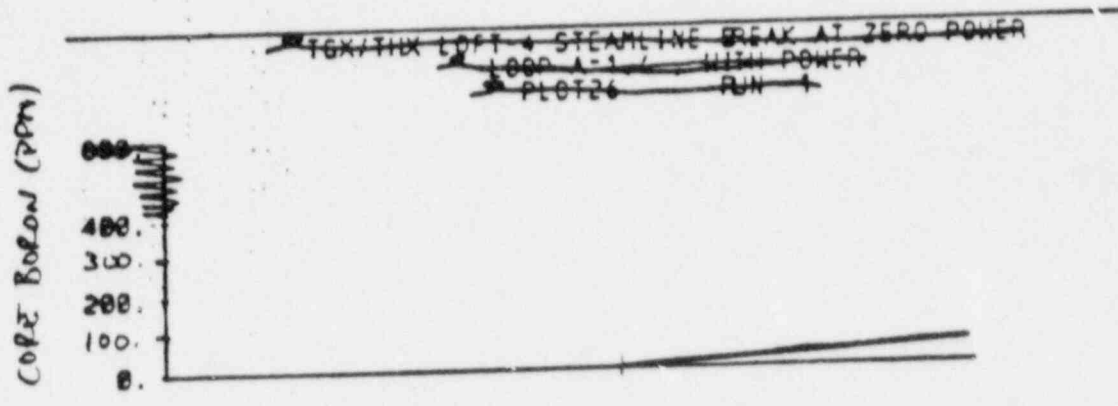
Figure 15.1-16 B



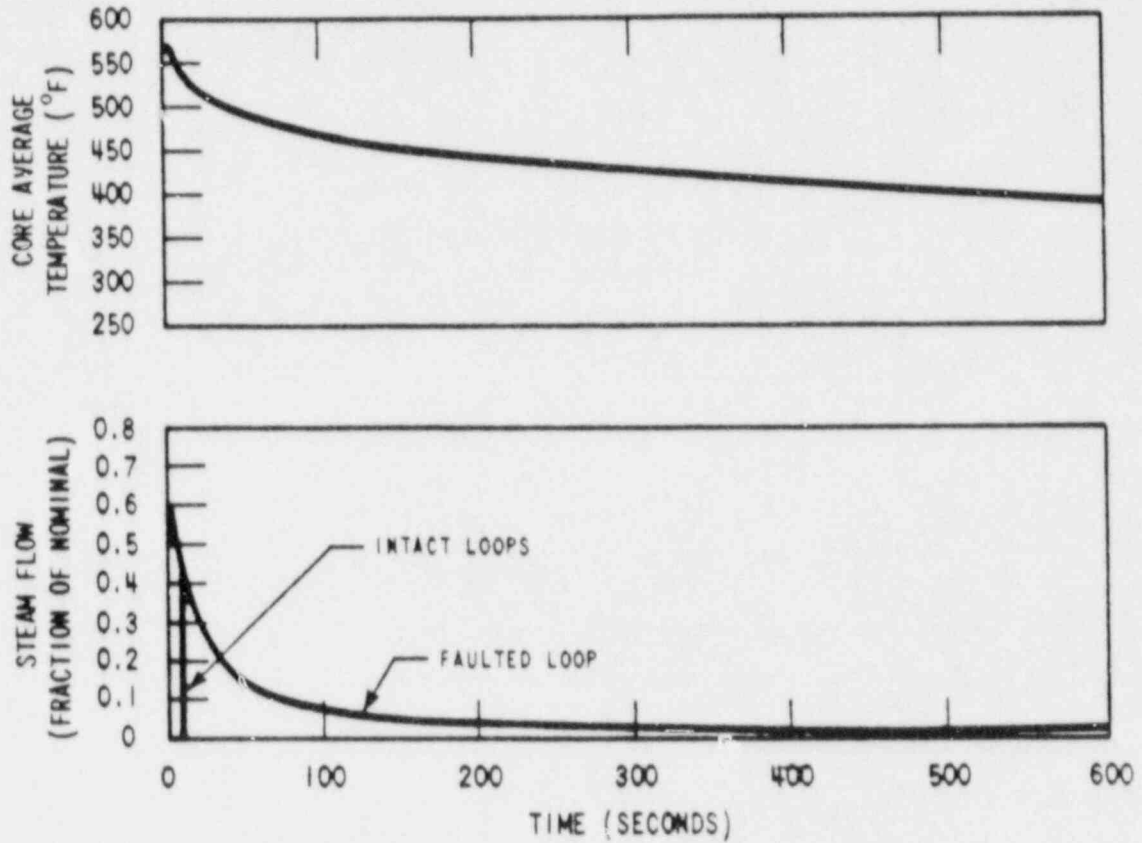
**SOUTH TEXAS PROJECT  
UNIT 1**

1.4FT<sup>2</sup> STEAM LINE RUPTURE, OFFSITE  
POWER AVAILABLE, BORON CONCENTRA-  
TION VS TIME, REACTIVITY VS TIME

Figure 15.1-17 A

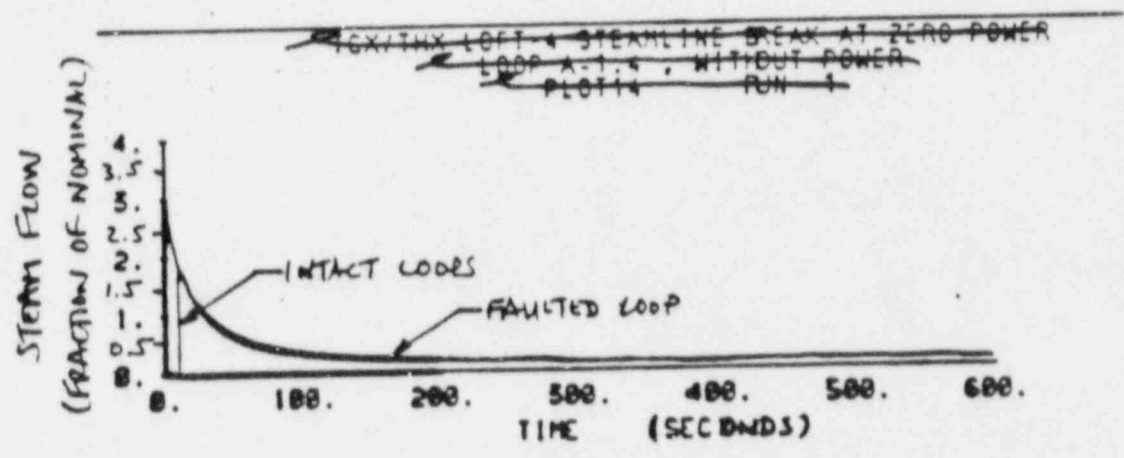
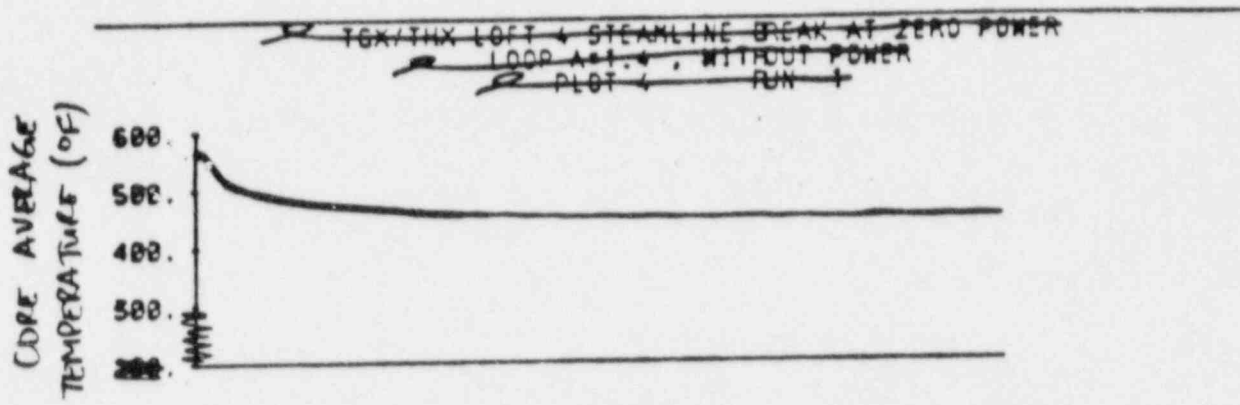


<b>SOUTH TEXAS PROJECT UNIT 2</b>
1.4FT <sup>2</sup> STEAM LINE RUPTURE, OFFSITE POWER AVAILABLE, BORON CONCENTRA- TION VS TIME, REACTIVITY VS TIME
Figure 15.1-17 <b>B</b> <span style="float: right;"><del>Amendment 57</del></span>



## SOUTH TEXAS PROJECT UNIT 1

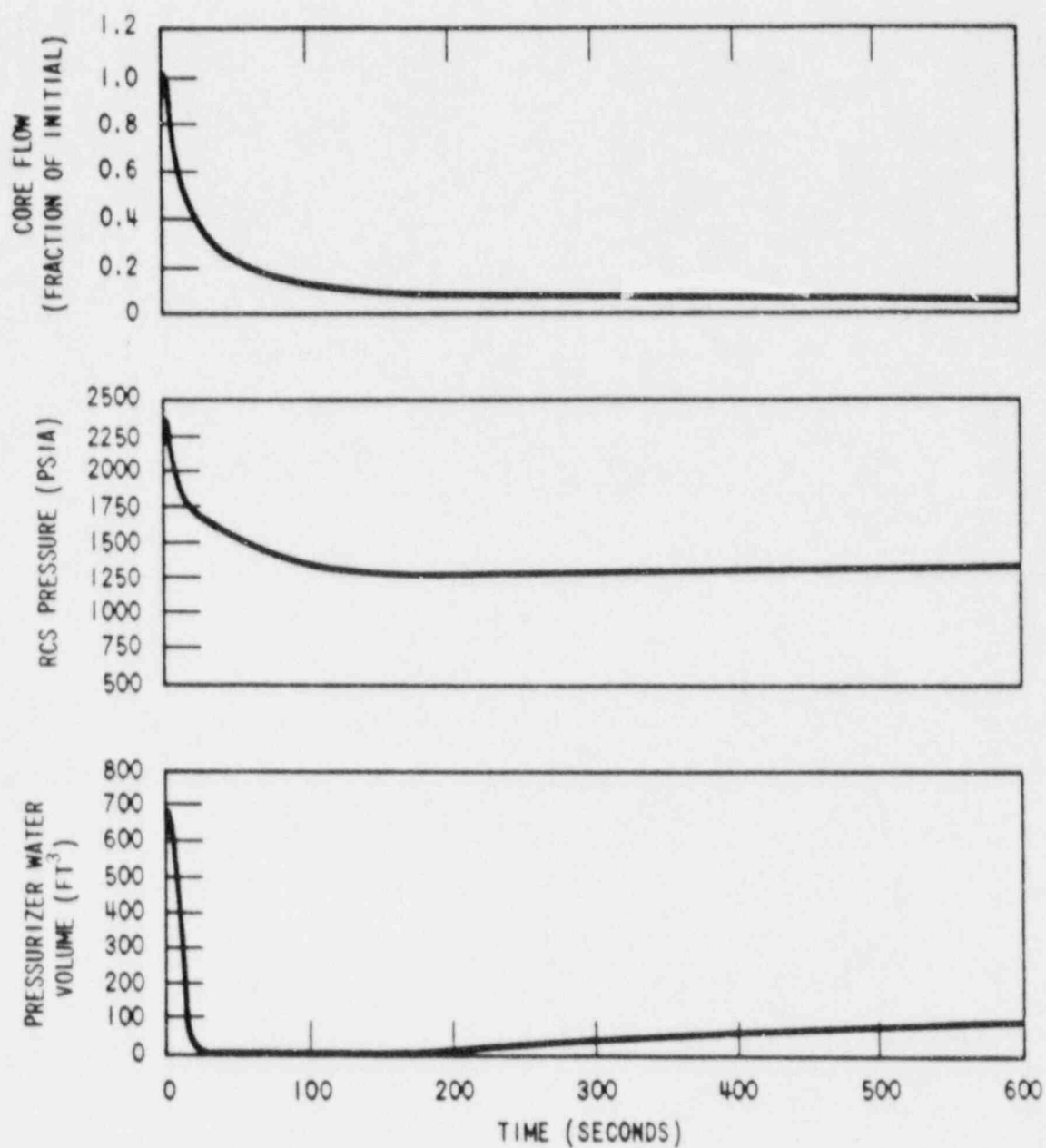
Figure 15.1-18. A  
1.4 Ft<sup>2</sup> Steam Line Rupture, Offsite Power Not Available, Average Temperature versus Time, Steam Flow per Loop versus Time



**SOUTH TEXAS PROJECT  
UNIT . . . 2**

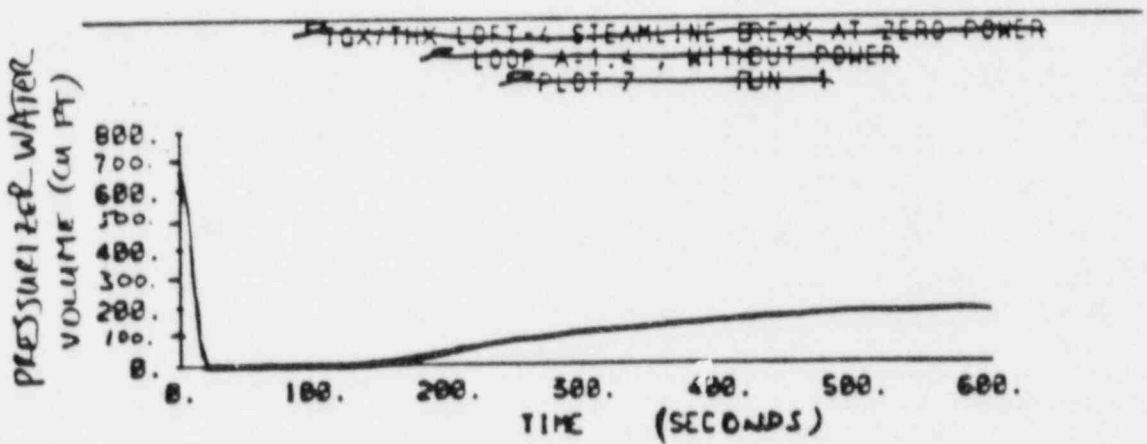
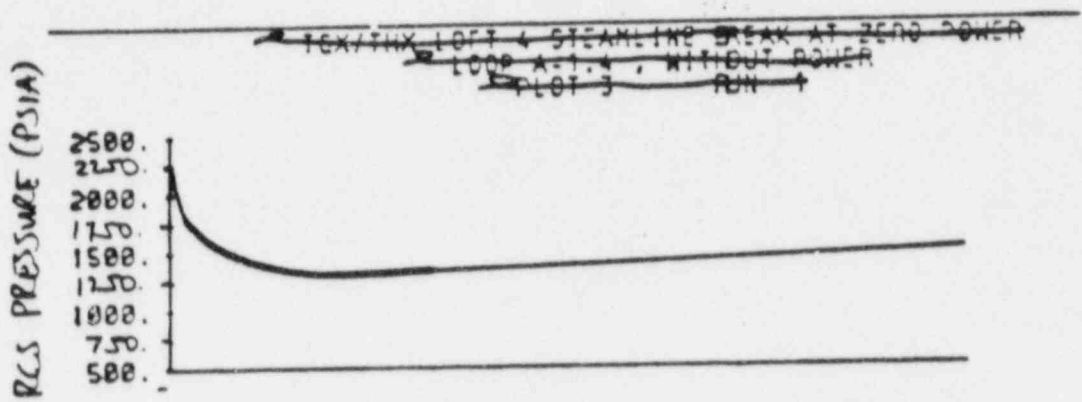
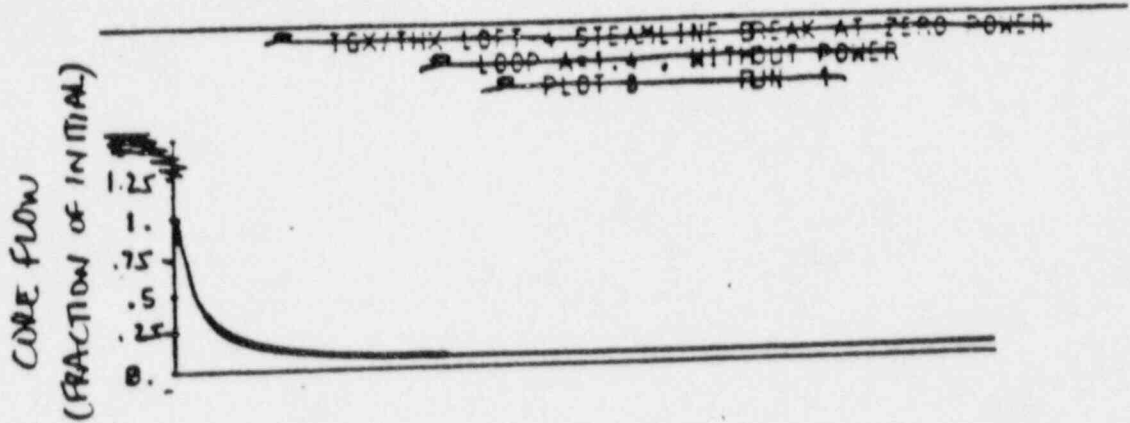
Figure 15.1-18 B  
1.4 Ft<sup>2</sup> Steam Line Rupture, Offsite Power Not Available, Average Temperature versus Time, Steam Flow ~~versus~~ versus Time Plant





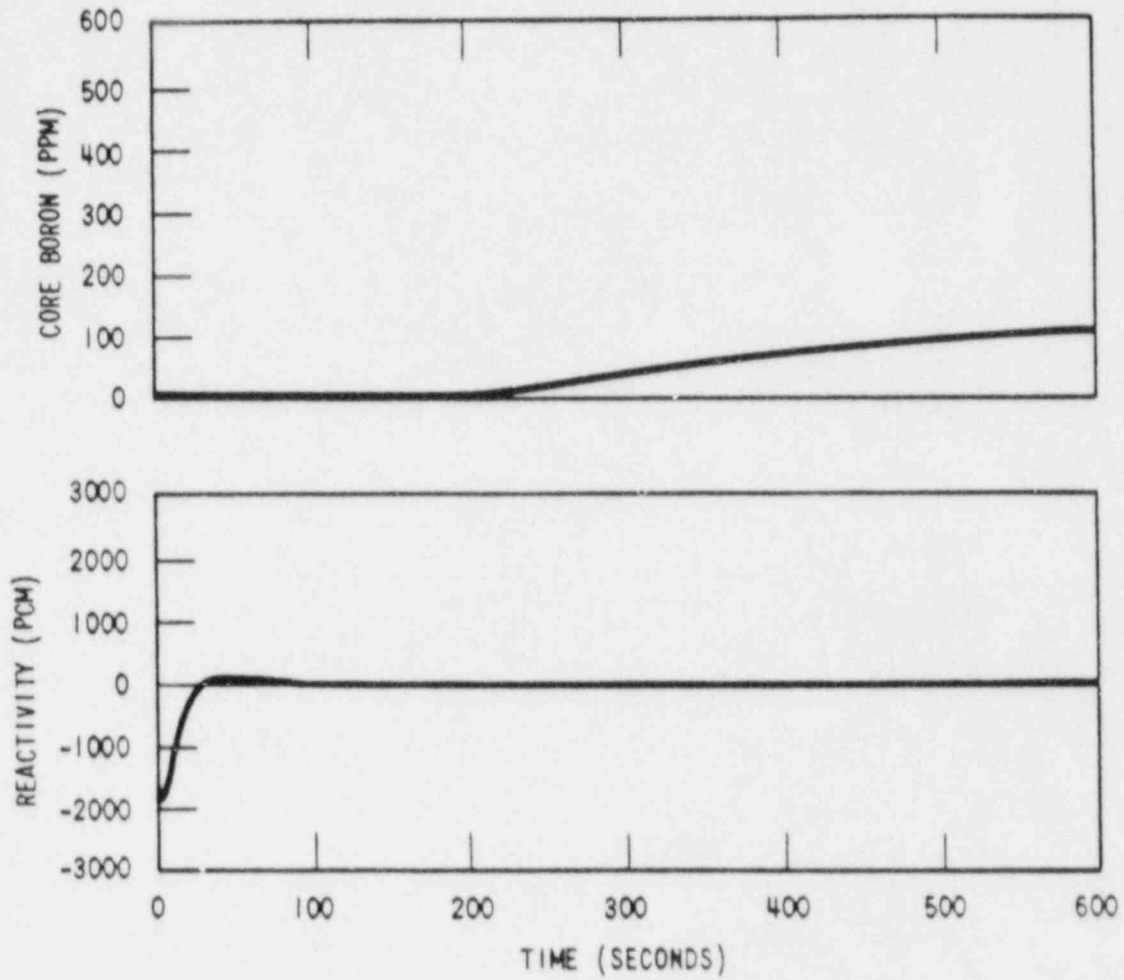
## SOUTH TEXAS PROJECT UNIT 1

Figure 15.1-19.A  
1.4 Ft<sup>2</sup> Steam Line Rupture, Offsite Power Not  
Available, Core Flow versus Time, RCS Pressure  
versus Time, Pressurizer Water Volume versus Time



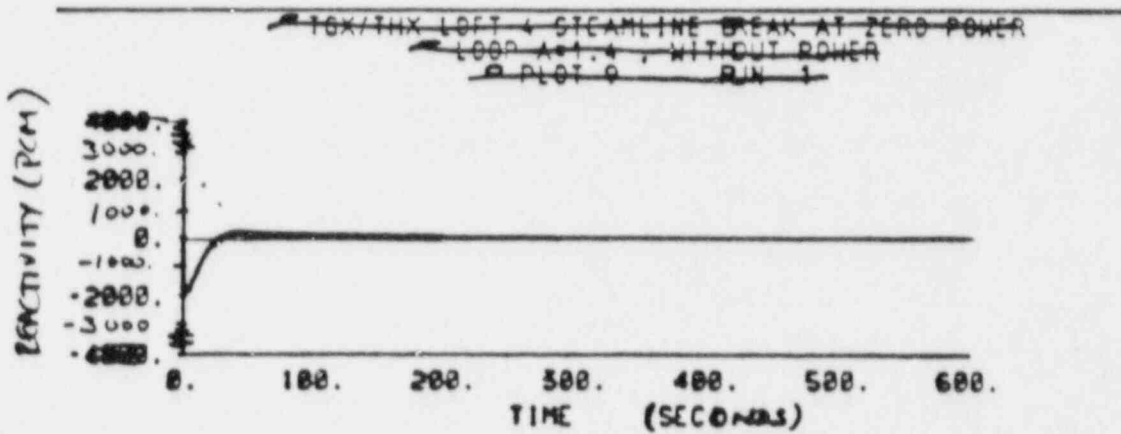
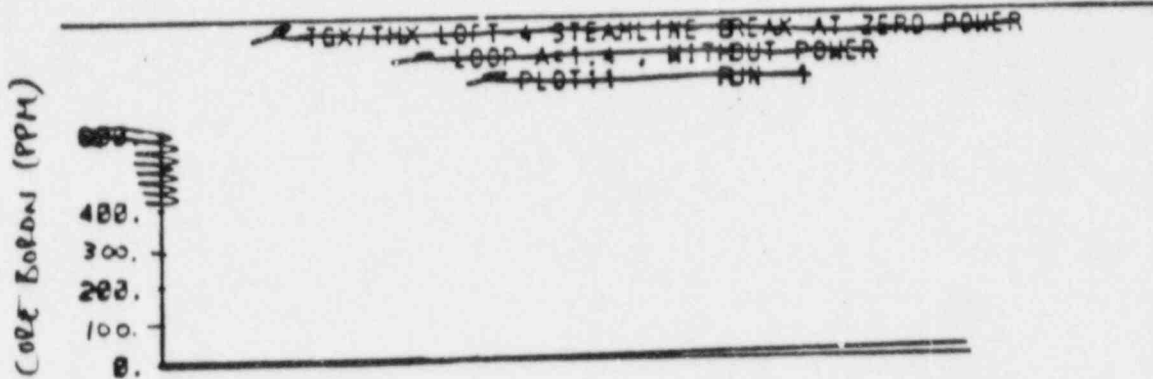
**SOUTH TEXAS PROJECT**  
**UNIT 2**

Figure 15.1-19 B  
 1.4 Ft<sup>2</sup> Steam Line Rupture, Offsite Power Not Available, Core Flow versus Time, RCS Pressure versus Time, Pressurizer Water Volume versus Time



## SOUTH TEXAS PROJECT UNIT 1

Figure 15.1-20.A  
1.4 Ft<sup>2</sup> Steam Line Rupture, Offsite Power Not  
Available, Boron Concentration versus Time,  
Reactivity versus Time



**SOUTH TEXAS PROJECT  
UNIT 2**

Figure 15.1-20 B  
1.4 Ft<sup>2</sup> Steam Line Rupture, Offsite Power Not Available, Boron Concentration versus Time, Reactivity versus Time

15.3.1.2 Analysis of Effects and Consequences.Method of Analysis

The case analyzed is the loss of one pump with four loops in operation.

This transient is analyzed by three digital computer codes. First the LOFTRAN code (Reference 15.3-1) is used to calculate the loop and core flow during the transient, the time of reactor trip based on the calculated flows, the nuclear power transient, and the primary system pressure and temperature transients. The FACTRAN code (Reference 15.3-2) is then used to calculate the heat flux transient based on the nuclear power and flow from LOFTRAN. Finally, the THINC code (Section 4.4) is used to calculate the DNBR during the transient based on the heat flux from FACTRAN and flow from LOFTRAN. The departure from nucleate boiling ratio (DNBR) transients presented represent the minimum of the typical or thimble cell.

Initial Conditions

Plant characteristics and initial conditions are discussed in Section 15.0.3. Initial operating conditions assumed for this event are the most adverse with respect to the margin to DNB; i.e., maximum steady state power level, minimum steady state pressure, and maximum steady state coolant average temperature. The pressure uncertainty used in this analysis is 34 psi, and the coolant average temperature uncertainty is 4.7°F.

Reactivity Coefficients

The most negative Doppler-only power coefficient is used (see Figure 15.0-2). This is the equivalent of a total integrated Doppler reactivity from 0 to 100 percent of 0.016 percent  $\Delta k$ .

The least negative moderator temperature coefficient (see Figure 15.0-6) is assumed since this results in the maximum core power during the initial part of the transient when the minimum DNBR is reached.

Flow Coastdown

The flow coastdown analysis is based on a momentum balance around each reactor coolant loop and across the reactor core. This momentum balance is combined with the continuity equation, a pump momentum balance and the pump characteristics and is based on high estimates of system pressure losses.

Plant systems and equipment which are available to mitigate the effects of the accident are discussed in Section 15.0.8 and listed in Table 15.0-6. No single active failure in any of these systems or equipment will adversely affect the consequences of the accident.

For Unit 1,

undervoltage or underfrequency. A one variation between this analysis and that of the previous section is that the RCCA insertion time to dashpot entry is 2.58 seconds. This is a conservative insertion time under the reduced flow conditions that exist when the RCCAs are inserted for this transient.

### Results

Figures 15.3-9 through 15.3-12 show the transient response for the loss of power to all reactor coolant pumps with four loops in operation. The reactor is again assumed to be tripped on undervoltage signal. Figure 15.3-12 shows the DNBR to be always greater than 1.30.

Since DNB does not occur, the ability of the primary coolant to remove heat from the fuel rod is not greatly reduced. Thus, the average fuel and clad temperatures do not increase significantly above their respective initial values.

The calculated sequence of events is shown in Table 15.3-1. The reactor coolant pumps will continue to coastdown, and natural circulation flow will eventually be established, as demonstrated in Section 15.2.6. With the reactor tripped, a stable plant condition will be attained. Normal plant shutdown may then proceed.

15.3.2.3 Radiological Consequences. A complete loss of reactor coolant flow from full load results in a reactor and turbine trip. Assuming, in addition, that the condenser is not available, atmospheric steam dump would be required. The quantity of steam released would be the same as for a loss of offsite power.

There are only minimal radiological consequences associated with this event. Therefore, this event is not limiting. Since fuel damage is not postulated, the radiological consequences resulting from atmospheric steam dump are less severe than the steam line break, discussed in Section 15.1.5.

15.3.2.4 Conclusions. The analysis performed has demonstrated that for the complete loss of forced reactor coolant flow, the DNBR does not decrease below 1.30 at any time during the transient. Thus, the DNB design basis as described in Section 4.4 is met.

### 15.3.3 Reactor Coolant Pump Shaft Seizure (Locked Rotor)

15.3.3.1 Identification of Causes and Accident Description. The accident postulated is an instantaneous seizure of a reactor coolant pump rotor such as is discussed in Section 5.4. Flow through the affected reactor coolant loop is rapidly reduced, leading to an initiation of a reactor trip on a low reactor coolant flow signal.

Following initiation of the reactor trip, heat stored in the fuel rods continues to be transferred to the coolant causing the coolant to expand. At the same time, heat transfer to the shell side of the steam generators is reduced, first because the reduced flow results in a decreased tube side film coefficient and then because the reactor coolant in the tubes cools down while the shell side temperature increases (turbine steam flow is reduced to zero upon turbine trip). The rapid expansion of the coolant in the reactor core, combined with reduced heat transfer in the steam generators causes an insurge



into the pressurizer and a pressure increase throughout the RCS. The insurge into the pressurizer compresses the steam volume, actuates the automatic spray system, opens the power-operated relief valves, and opens the pressurizer safety valves, in that sequence. The two power-operated relief valves are designed for reliable operation and would be expected to function properly during the accident. However, for conservatism, their pressure reducing effect as well as the pressure reducing effect of the spray is not included in the analysis.

This event is classified as an ANS Condition IV incident (a limiting fault) as defined in Section 15.0.1.

### 15.3.3.2 Analysis of Effects and Consequences.

#### Method of Analysis

Three digital computer codes are used to analyze this transient. The LOFTRAN code (Reference 15.3-1) is used to calculate the resulting loop and core flow transients following the pump seizure, the time of reactor trip based on the loop flow transients, the nuclear power following reactor trip, and to determine the peak pressure. The thermal behavior of the fuel located at the core hot spot is investigated using the FACTRAN code (Reference 15.3-2), using the core flow and the nuclear power calculated by LOFTRAN. The FACTRAN code includes the use of a film boiling heat transfer coefficient. The FACTRAN code is also used to calculate the heat flux transient based on the nuclear power and flow from LOFTRAN. Finally, the THINC code (Section 4.4) is used to calculate the DNBR distribution in the core during the transient based on the heat flux from FACTRAN and flow from LOFTRAN. The DNBR distribution is used to calculate the number of rods in DNB.

Two cases are analyzed:

1. Four loops operating, one locked rotor
2. Four loops operating, one locked rotor, loss of power to the other reactor coolant pumps

At the beginning of the postulated locked rotor accident, i.e., at the time the shaft in one of the reactor coolant pumps is assumed to seize, the plant is assumed to be in operation under the most adverse steady state operating condition (i.e., maximum steady state power level, maximum steady state pressure, and maximum steady state coolant average temperature). Plant characteristics and initial conditions are further discussed in Section 15.0.3. The pressure uncertainty used in these analyses is 34 psi and the coolant average temperature uncertainty is 4.7°F.

For the case without offsite power available, power is lost to the unaffected pumps 2 seconds after reactor trip. (Note: Grid stability analyses show that the grid will remain stable and that offsite power will not be lost because of a unit trip from 100-percent power. The 2 second delay is a conservative assumption based on grid stability analyses.)

When the peak pressure is evaluated, the initial pressure is conservatively estimated as 34 psi above nominal pressure (2250 psia) to allow for errors in

for Unit 1, and 46  
psi above nominal pressure  
for Unit 2  
(2250 psia) Amendment 55

the pressurizer pressure measurement and control channels. To obtain the maximum pressure in the primary side, conservatively high loop pressure drops are added to the calculated pressurizer pressure. The pressure responses shown on Figure 15.3-18 are the responses at the point in the RCS having the maximum pressure.

| 18

| 54

#### Evaluation of the Pressure Transient

After pump seizure, the neutron flux is rapidly reduced by control rod insertion. Rod motion begins one second after the flow in the affected loop reaches 87 percent of nominal flow. No credit is taken for the pressure reducing effect of the pressurizer power-operated relief valves, pressurizer spray, steam dump or controlled feedwater flow after reactor trip. Although these are expected to occur and would result in a lower peak pressure, an additional degree of conservatism is provided by ignoring their effects.

The pressurizer safety valves are full open at 2575 psia and their capacity for steam relief is as described in Section 5.4.

#### Evaluation of DNB in the Core During the Accident

For this accident, DNB is assumed to occur in the core, and therefore, an evaluation of the consequences with respect to fuel rod thermal transients is performed. Results obtained from analysis of this "hot spot" condition represent the upper limit with respect to clad temperature and zirconium water reaction.

In the <sup>Unit 1</sup> evaluation, rod power at the hot spot is assumed to be 2.50 times the average rod power (i.e.,  $F = 2.50$ ) at the initial core power level. In the Unit 2 evaluation, rod power at the hot spot is assumed to be 2.65 times the average rod power (i.e.,  $F_g = 2.65$ ) at the initial core power level.

#### Film Boiling Coefficient

The film boiling coefficient is calculated in the FACTRAN code using the Bishop-Sandberg-Tong film boiling correlation. The fluid properties are evaluated at film temperature (average between wall and bulk temperatures). The program calculates the film coefficient at every time step based upon the actual heat transfer conditions at the time. The neutron flux, system pressure, bulk density and mass flow rate as a function of time are used as program input.

For this analysis, the initial values of the pressure and the bulk density are used throughout the transient since they are the most conservative with respect to clad temperature response. For conservatism, DNB was assumed to start at the beginning of the accident.

#### Fuel Clad Gap Coefficient

The magnitude and time dependence of the heat transfer coefficient between fuel and clad (gap coefficient) has pronounced influence on the thermal results. The larger the value of the gap coefficient, the more heat is transferred between pellet and clad. Based on investigations on the effect of the gap coefficient upon the maximum clad temperature during the transient, the gap coefficient was assumed to increase from a steady state value consistent with initial fuel temperature to 10,000 Btu/hr-ft<sup>2</sup>-°F at the initiation of the

transient. Thus the large amount of energy stored in the fuel because of the small initial value is released to the clad at the initiation of the transient.

#### Zirconium Steam Reaction

The zirconium steam reaction can become significant above 1800°F (clad temperature). The Baker-Just parabolic rate equation shown below is used to define the rate of the zirconium steam reaction.

$$\frac{d(w^2)}{dt} = \cancel{33} \times 10^6 \exp \frac{-(45,500)}{1.986T}$$

33.3

where:

- w = amount reacted, mg/cm<sup>2</sup>  
 t = time, sec  
 T = temperature, °K

The reaction heat is 1510 cal/gm.

The effect of zirconium steam reaction is included in the calculation of the "hot spot" clad temperature transient.

Plant systems and equipment which are available to mitigate the effects of the accident are discussed in Section 15.0.8 and listed in Table 15.0-6. No single active failure in any of these systems or equipment will adversely affect the consequences of the accident.

#### Results

##### Locked Rotor with Four Loops Operating

The transient results for this case are shown on Figures 15.3-17 through 15.3-20. The results of these calculations are also summarized in Table 15.3-2a. The peak RCS pressure reached during the transient is less than that which would cause stresses to exceed the faulted condition stress limits. Also, the peak clad surface temperature is considerably less than 2700°F. It should be noted that the clad temperature was conservatively calculated assuming that DNB occurs at the initiation of the transient. The number of rods in DNB was conservatively calculated as 7 percent of the total rods in the Unit 1 core and 10 percent of the total rods in the Unit 2 core.

##### Locked Rotor with Four Loops Operating, Loss of Power to the Remaining Pumps

The transient results for this case are shown on Figures 15.3-17 through 15.3-20. The results of these calculations are also summarized in Table 15.3-2b. The peak RCS pressure reached during the transient is less than that which would cause stresses to exceed the faulted condition stress limits. Also, the peak clad surface temperature is considerably less than 2700°F. Both the peak RCS pressure and the peak clad surface temperature for this case are similar to the 4 loop transient with power available as discussed above. The total percentage of fuel cladding damaged is the same as the with-power case, thus the conclusions of Section 15.3.3.3 are applicable to both events.

The calculated sequence of events for the two cases analyzed is shown in Table 15.3-1. Figure 15.3-17 shows that with offsite power available, the core flow reaches a new equilibrium value by 10 seconds. With the reactor tripped, a stable plant condition will eventually be attained.

15.3.3.3 Radiological Consequences. The postulated accidents involving release of steam from the secondary system do not result in a release of radioactivity unless there is leakage from the Reactor Coolant System (RCS) to the secondary system in the steam generators (SGs). A conservative analysis of the potential offsite doses resulting from a reactor coolant pump shaft seizure accident is presented using the Technical Specification limit secondary coolant concentrations. Parameters used in the analysis are listed in Table 15.3-3.

The conservative assumptions and parameters used to calculate the activity released and offsite doses for a pump shaft seizure accident are the following:

1. Prior to the accident, the primary coolant concentrations are assumed to be equal to the technical specification limit for full power operation following an iodine spike (I-131 equivalent of 60  $\mu\text{Ci/g}$ ). These concentrations are presented in Table 15.A-4.
2. Prior to the accident, the secondary coolant specific activity is equal to the technical specification limit of 0.10  $\mu\text{Ci/gm}$  dose equivalent I-131. This dose equivalent specific activity is presented in Table 15.A-5.
3. ~~TEN~~ <sup>TEN</sup> percent of the total core fuel cladding is damaged, which results in the release to the reactor coolant of ~~seven~~ <sup>TEN</sup> percent of the total gap inventory of the core. This activity is assumed uniformly mixed in the primary coolant. *A SECOND ANALYSIS WITH A RELEASE TO THE REACTOR COOLANT OF FIFTEEN PERCENT OF THE TOTAL GAP INVENTORY OF THE CORE IS INCLUDED TO BOUND THE RELEASE.*
4. The primary-to-secondary leakage of 1 gal/min (Technical Specification limit) is assumed to continue for 8 hrs following the accident.
5. Offsite power is lost; MS condensers are not available for steam dump.
6. Eight hours after the accident, the Residual Heat Removal System (RHRS) starts operation to cool down the plant. No further steam or activity is released to the environment.
7. The iodine partition factor in the SGs is equal to 0.01.

The steam releases and meteorological parameters are given in Table 15.3-3.

The thyroid, gamma and beta doses for the reactor coolant pump shaft seizure accident are given in Table 15.3-4 for the Exclusion Zone Boundary (EZB) of 1430 meters and the Low Population Zone (LPZ) of 4800 meters.

15.3.3.4 Conclusions. Since the peak RCS pressure reached during any of the transients is less than that which would cause stresses to exceed the faulted condition stress limits, the integrity of the primary coolant system is not endangered.

STP FSAR

REFERENCES

SECTION 15.3

- 15.3-1 Burnett, T. W. T., et al, "LOFTRAN Code Description," WCAP-7907-P-A (Proprietary), WCAP-7907-A, (Non-Proprietary), April 1984. | 54
- 15.3-2 Hargrove, H. G., "FACTRAN, a Fortran IV Code for Thermal Transients in a UO<sub>2</sub> Fuel Rod," WCAP-7908, June 1972. | 43
- 15.3-3 ~~Burnett, T. W., "Reactor Protection System Diversity in Westinghouse Pressurized Water Reactors," WCAP-7306, April, 1969.~~ *wrong ref.*

*Baldwin, M.S., et al, "An Evaluation of Loss of Flow Accidents Caused by Power System Frequency Transients in Westinghouse PWRs," WCAP-8424, Revision 1, May 1975.*



STP FSAR

TABLE 15.3-1

TIME SEQUENCE OF EVENTS FOR INCIDENTS WHICH RESULT  
IN A DECREASE IN A REACTOR COOLANT SYSTEM FLOW

<u>Accident</u>	<u>Event</u>	<u>Time (sec)</u>		
		<u>UNIT 1</u>	<u>UNIT 2</u>	
Partial Loss of Forced Reactor Coolant Flow				
Four loops operating, one pump coasting down	Coastdown begins <del>low</del>	0	0	43
	<i>Low</i> reactor coolant flow trip	1.30	1.31	18
	rods begin to drop	2.30	2.31	
	minimum DNBR occurs	3.40	3.80	
	<del>S</del>			
Complete Loss of Forced Reactor Coolant Flow				
		<u>Four Loop</u>		
	All operating pumps lose power and begin coasting down	0	0	54
	Reactor coolant pump undervoltage trip point reached	0	0	
	Rods begin to drop	1.5	1.5	
	Minimum DNBR occurs	3.3	3.5	
Reactor Coolant Pump Shaft Seizure (Locked Rotor) (With offsite power)				
	Rotor on one pump locks	0	0	
	Low reactor coolant flow setpoint reached	0.07	0.07	



STP FSAR

TABLE 15.3-1 (Continued)

TIME SEQUENCE OF EVENTS FOR INCIDENTS WHICH RESULT  
IN A DECREASE IN A REACTOR COOLANT SYSTEM FLOW

<u>Accident</u>	<u>Event</u>	<u>Time (sec)</u>		
		<u>Four Loop</u>		
		<u>Operation</u>		
		<u>Unit 1</u>	<u>Unit 2</u>	
	Rods begin to drop	1.07	1.07	18
	Maximum RCS pressure occurs	3.3	3.2	56
	Maximum clad temperature occurs	3.7	3.6	18
Reactor Coolant Pump Shaft Seizure (Locked Rotor) (Without offsite power)	Rotor on one pump locks	0	0	54
	Low reactor coolant flow setpoint	0.07	0.07	
	Rods begin to drop	1.07	1.07	
	RCPs lose power, coastdown begins	3.07	3.07	
	Maximum RCS pressure occurs	3.3	3.2	
	Maximum clad temperature occurs	3.9	3.9	

TABLE 15.3-2a

SUMMARY OF RESULTS FOR LOCKED ROTOR TRANSIENTS

(With offsite power)

	4 Loops Operating Initially	UNIT 2
	<u>UNIT 1</u>	
Maximum Reactor Coolant System Pressure (psia)	2589	2615
Maximum Clad Temperature at Core Hot Spot (*F)	1675	1713
Zr-H <sub>2</sub> O reaction at Core Hot Spot (% by weight)	.169	0.2

54

STP FSAR

TABLE 15.3-2b

SUMMARY OF RESULTS FOR LOCKED ROTOR TRANSIENTS

(Without offsite power)

	<u>4 Loops Operating Initially</u>	
	<u>UNIT 1</u>	<u>UNIT 2</u>
Maximum Reactor Coolant System Pressure (psia)	2589	2616
Maximum Clad Temperature at Core Hot Spot (°F)	1680	1717
Zr-H <sub>2</sub> O reaction at Core Hot Spot (% by weight)	.188	0.3

54

TABLE 15.3-3

PARAMETERS USED IN RC PUMP SHAFT SEIZURE ACCIDENT ANALYSIS

<u>Parameters</u>	
Core thermal power, MWt	3,900
SG tube leak rate prior to accident and initial 8 hrs following accident	1.0 gm
GWPS operating prior to accident	No
Offsite power	Lost
Fuel defects	1.0%
Primary coolant concentrations	Table 15.A-4
Secondary coolant concentrations	Table 15.A-5
Failed fuel (following accident)	7% (Unit 1), 10% (Unit 2) <del>7.0%</del> of fuel rods in core
Activity released to reactor coolant from failed fuel and available for release	10% of total gap inventory of noble gases and iodines
Iodine partition factor in SG's during accident	0.01
Steam release from four SGs, lb	614,000* (0-2 hr) 1,264,000 (2-8 hr)
Meteorology	5 percentile Table 15.B-1
Dose model	Appendix 15.B

43

\*Condensers assumed unavailable for steam dump.

\*\* A bounding analysis has also been performed assuming 15% failed fuel and gap inventory

TABLE 15.3-4

DOSES RESULTING FROM RC PUMP SHAFT SEIZURE ACCIDENT

TEN % TOTAL GAP INVENTORY

Exclusion Zone Boundary  
1430 m, 0-2 hrs

Low Population Zone  
4800 m, Duration

thyroid dose, Rems

1.04 ~~7.3 X 10<sup>-1</sup>~~

1.53 ~~7.3 X 10<sup>-1</sup>~~

whole-body gamma dose, Rems

3.8 ~~3.8 X 10<sup>-2</sup>~~

2.2 ~~3.8 X 10<sup>-2</sup>~~

skin beta dose, Rems

2.1 ~~2.1 X 10<sup>-2</sup>~~

1.3 X 10<sup>-2</sup>

FIFTEEN % TOTAL GAP INVENTORY

thyroid dose, Rems

1.56<sup>-2</sup>

2.28<sup>-2</sup>

Whole-body gamma dose, Rems

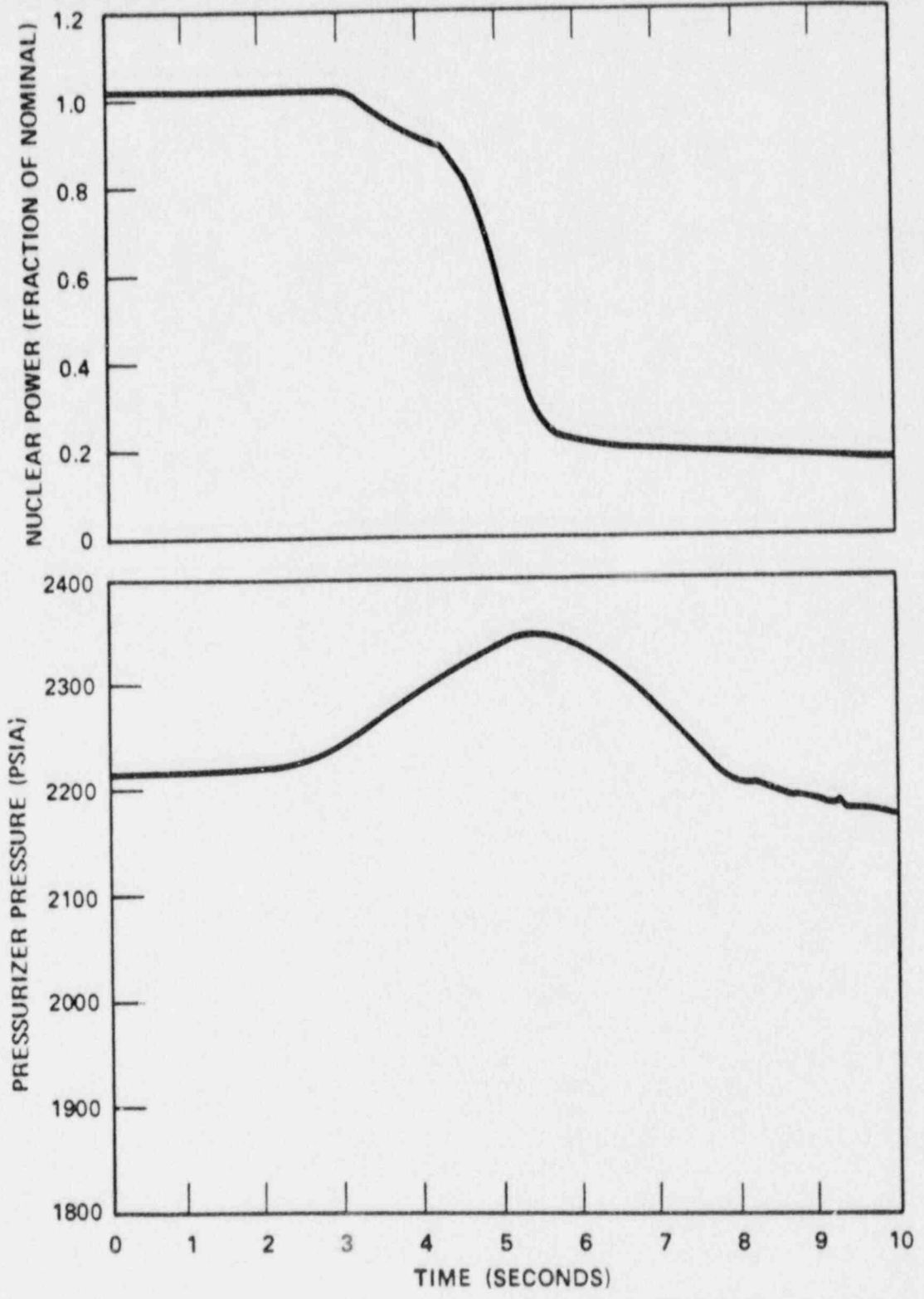
5.7 X 10<sup>-2</sup>

3.4 X 10<sup>-2</sup>

skin beta dose, Rems

3.1 X 10<sup>-2</sup>

1.9 X 10<sup>-2</sup>



**SOUTH TEXAS PROJECT  
UNIT 1**

NUCLEAR POWER TRANSIENT AND  
PRESSURIZER PRESSURE TRANSIENT FOR  
PARTIAL LOSS OF FLOW, FOUR LOOPS IN  
OPERATION, ONE PUMP COASTING DOWN

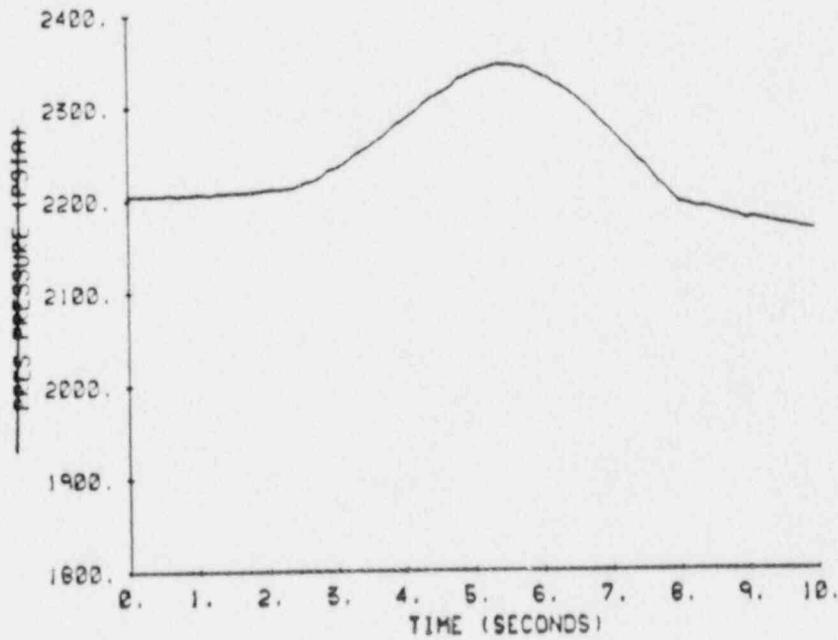
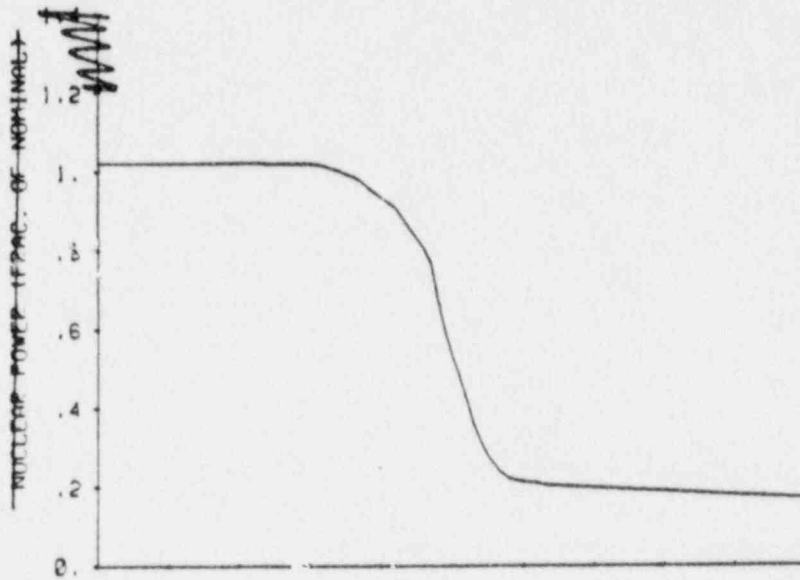
Figure 15.3-2 A



~~THE REDESIGN 1/4 LOSS OF FLOW TRIP~~

~~THE 1/4 LOSS OF FLOW~~

~~PLOT 1 RUN 1~~

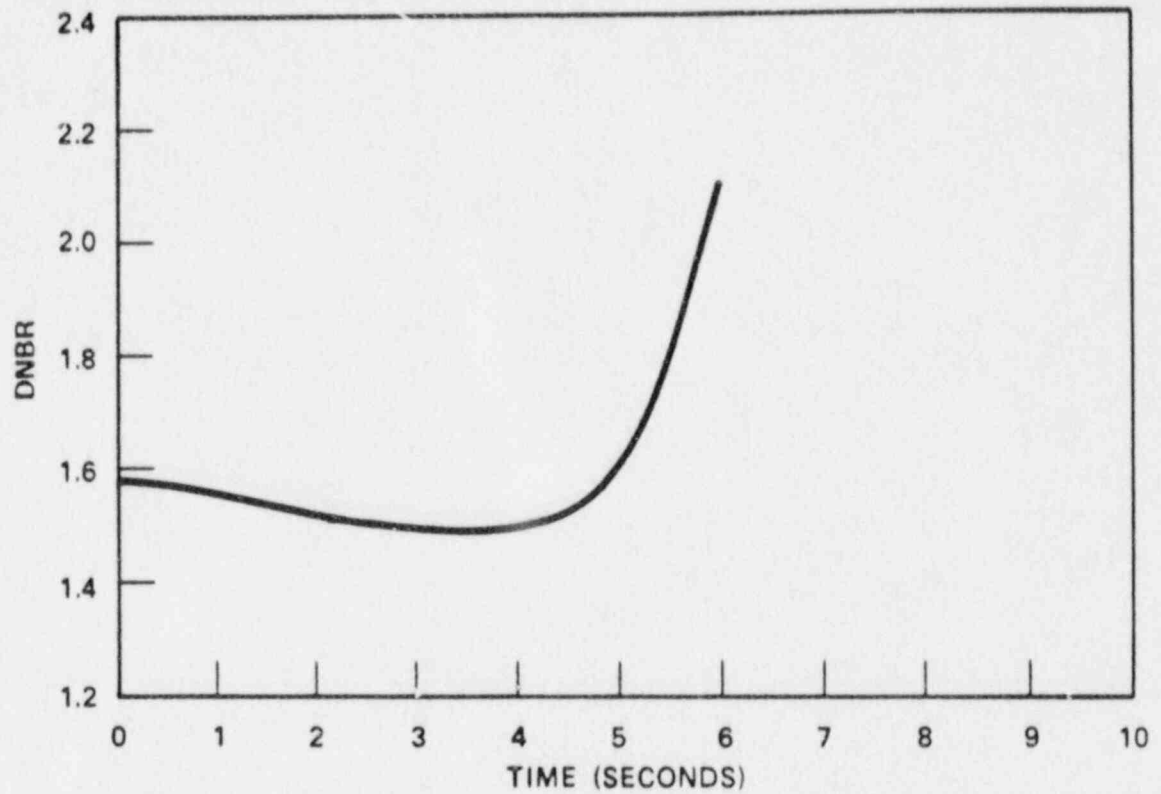


**SOUTH TEXAS PROJECT  
UNIT 2**

NUCLEAR POWER TRANSIENT AND  
PRESSURIZER PRESSURE TRANSIENT FOR  
PARTIAL LOSS OF FLOW, FOUR LOOPS IN  
OPERATION, ONE PUMP COASTING DOWN

Figure 15.3-2 B

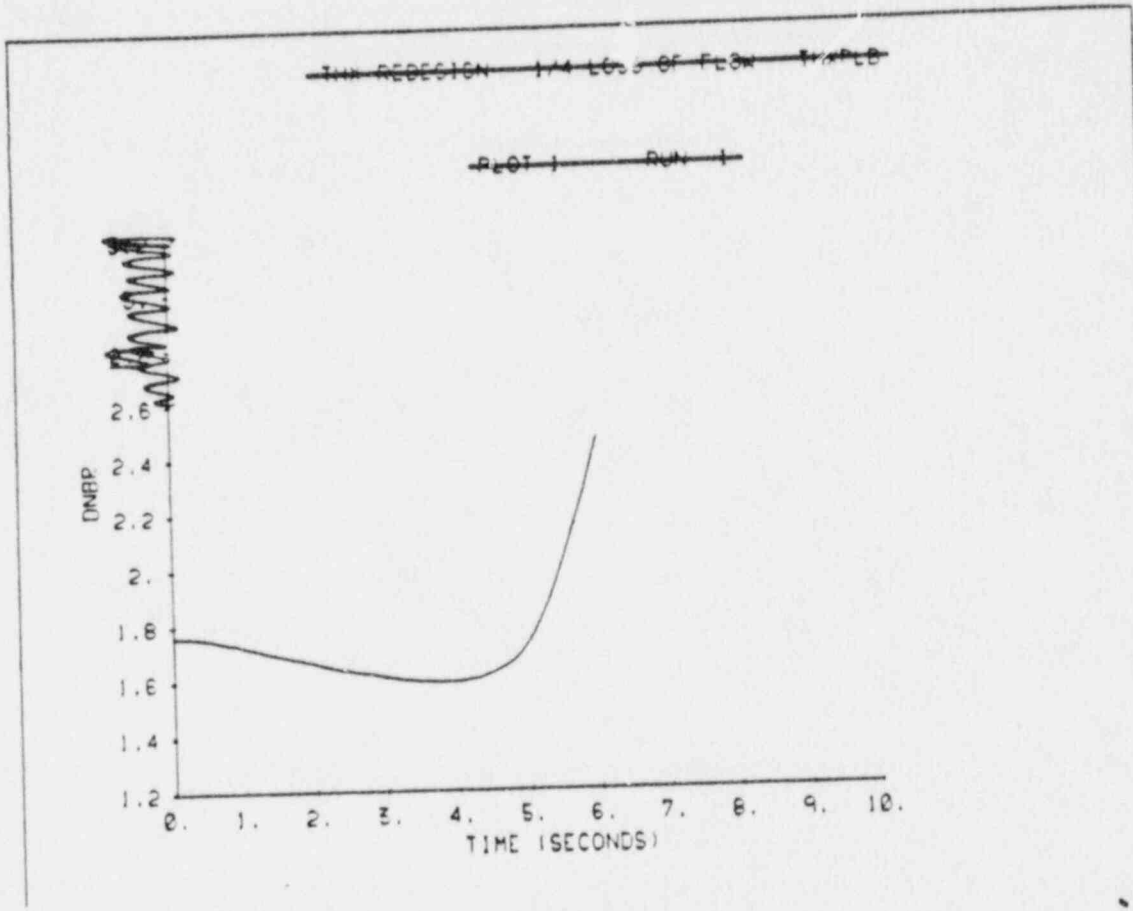
~~Amendment~~



**SOUTH TEXAS PROJECT  
UNIT 1**

DNBR VERSUS TIME FOR PARTIAL LOSS  
OF FLOW, FOUR LOOPS IN OPERATION,  
ONE PUMP COASTING DOWN

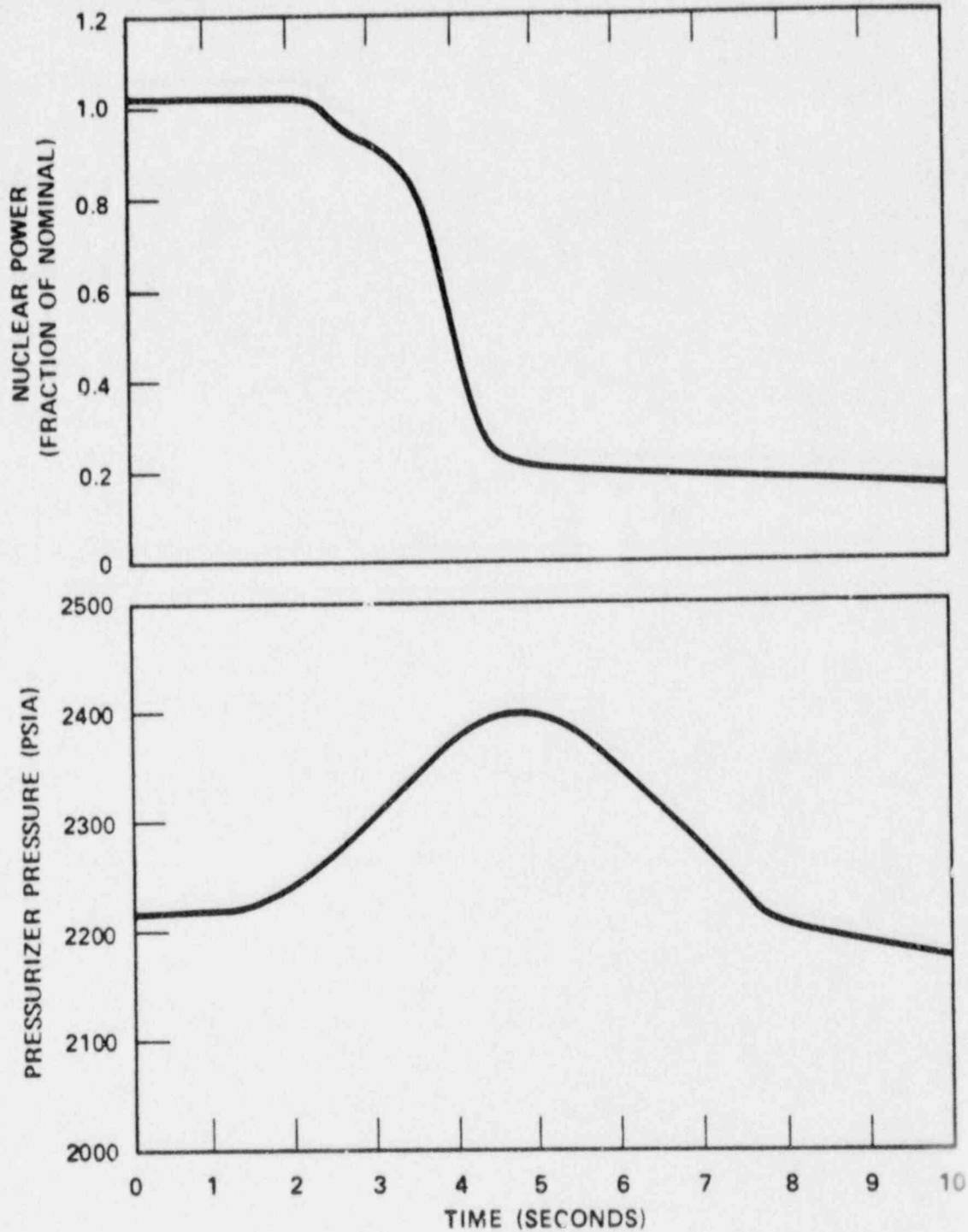
Figure 15.3-4 A



**SOUTH TEXAS PROJECT  
UNIT 2**

DNBR VERSUS TIME FOR PARTIAL LOSS  
OF FLOW, FOUR LOOPS IN OPERATION,  
ONE PUMP COASTING DOWN

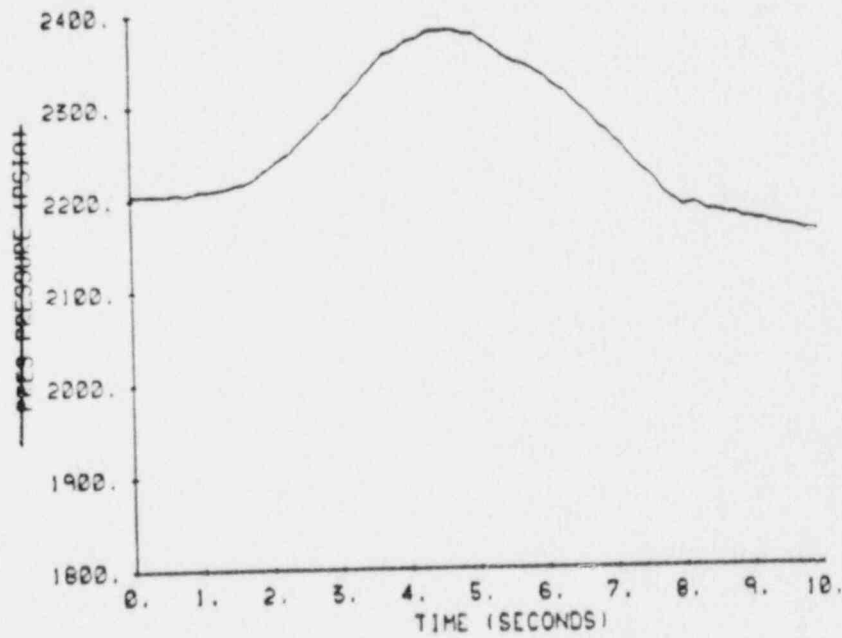
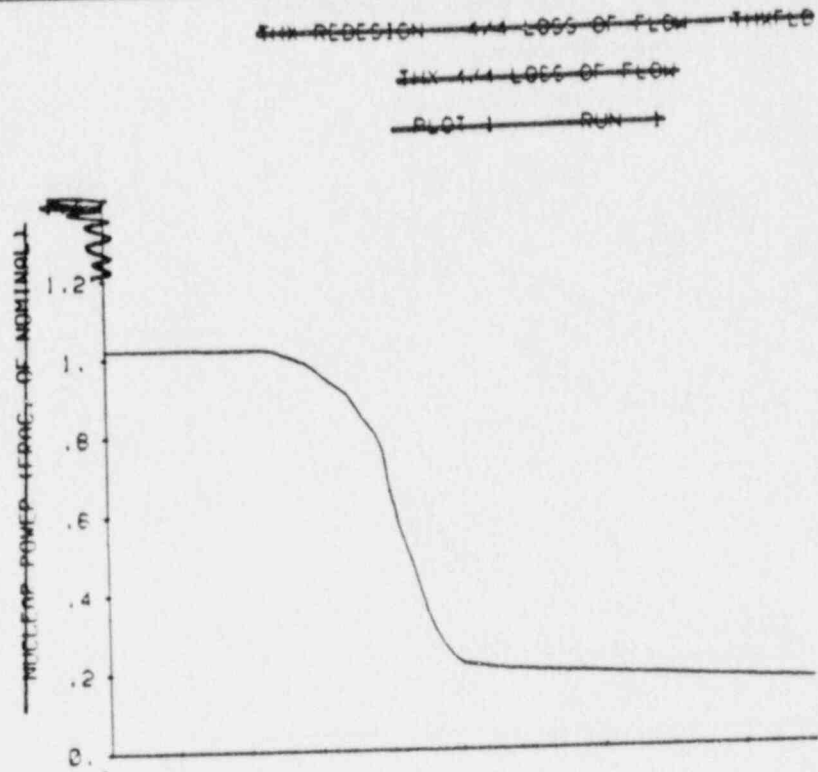
Figure 15.3-4 **B** ~~XXXXXXXXXX~~



**SOUTH TEXAS PROJECT  
UNIT 1**

NUCLEAR POWER TRANSIENT AND  
PRESSURIZER PRESSURE TRANSIENT FOR  
FOUR LOOPS IN OPERATION, FOUR PUMPS  
COASTING DOWN, COMPLETE LOSS OF  
FLOW

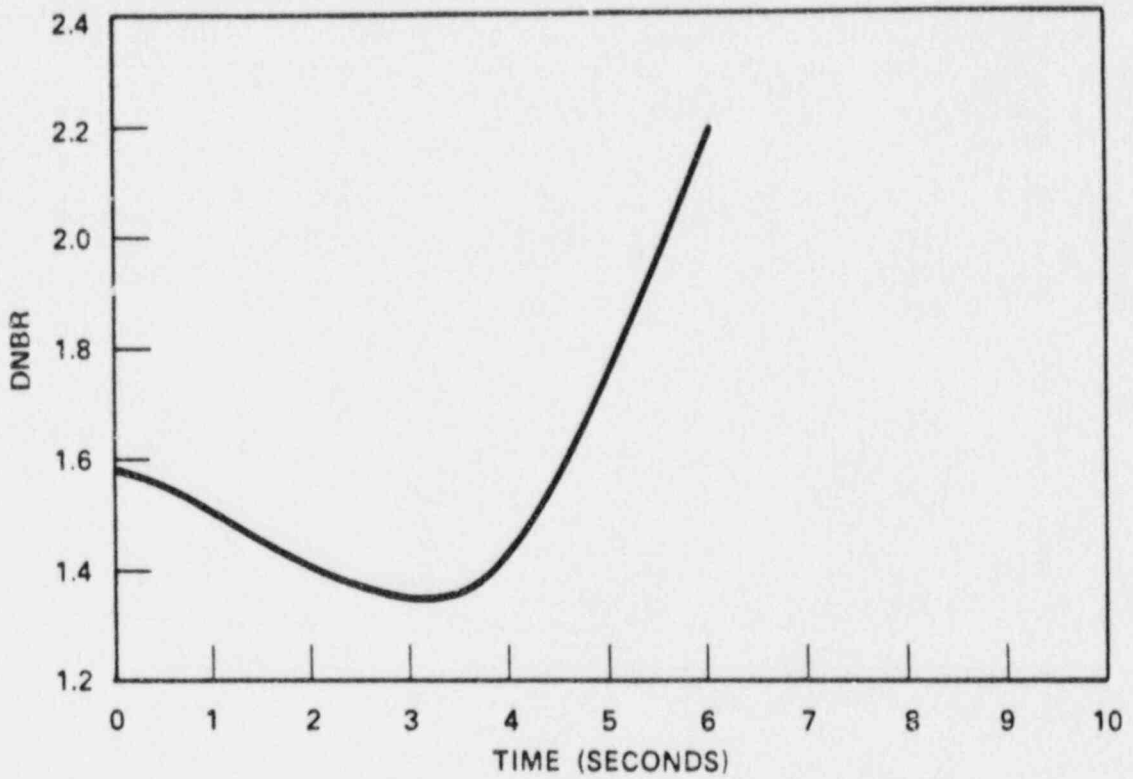
Figure 15.3-10 A



**SOUTH TEXAS PROJECT**  
**UNIT 2**

NUCLEAR POWER TRANSIENT AND  
PRESSURIZER PRESSURE TRANSIENT FOR  
FOUR LOOPS IN OPERATION, FOUR PUMPS  
COASTING DOWN, COMPLETE LOSS OF  
FLOW

Figure 15.3-10 B

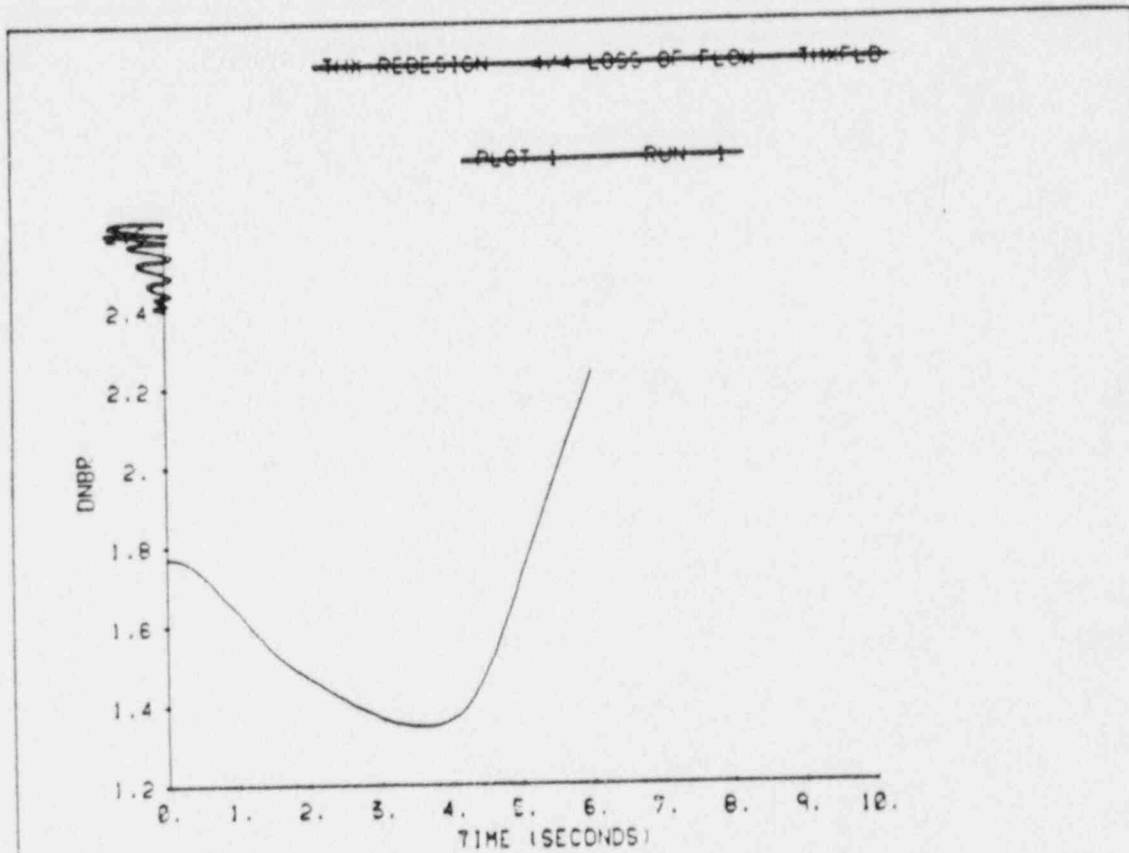


**SOUTH TEXAS PROJECT  
UNIT 1**

DNBR VERSUS TIME FOR FOUR LOOPS IN  
OPERATION, FOUR PUMPS COASTING  
DOWN, COMPLETE LOSS OF FLOW

Figure 15.3-12 A

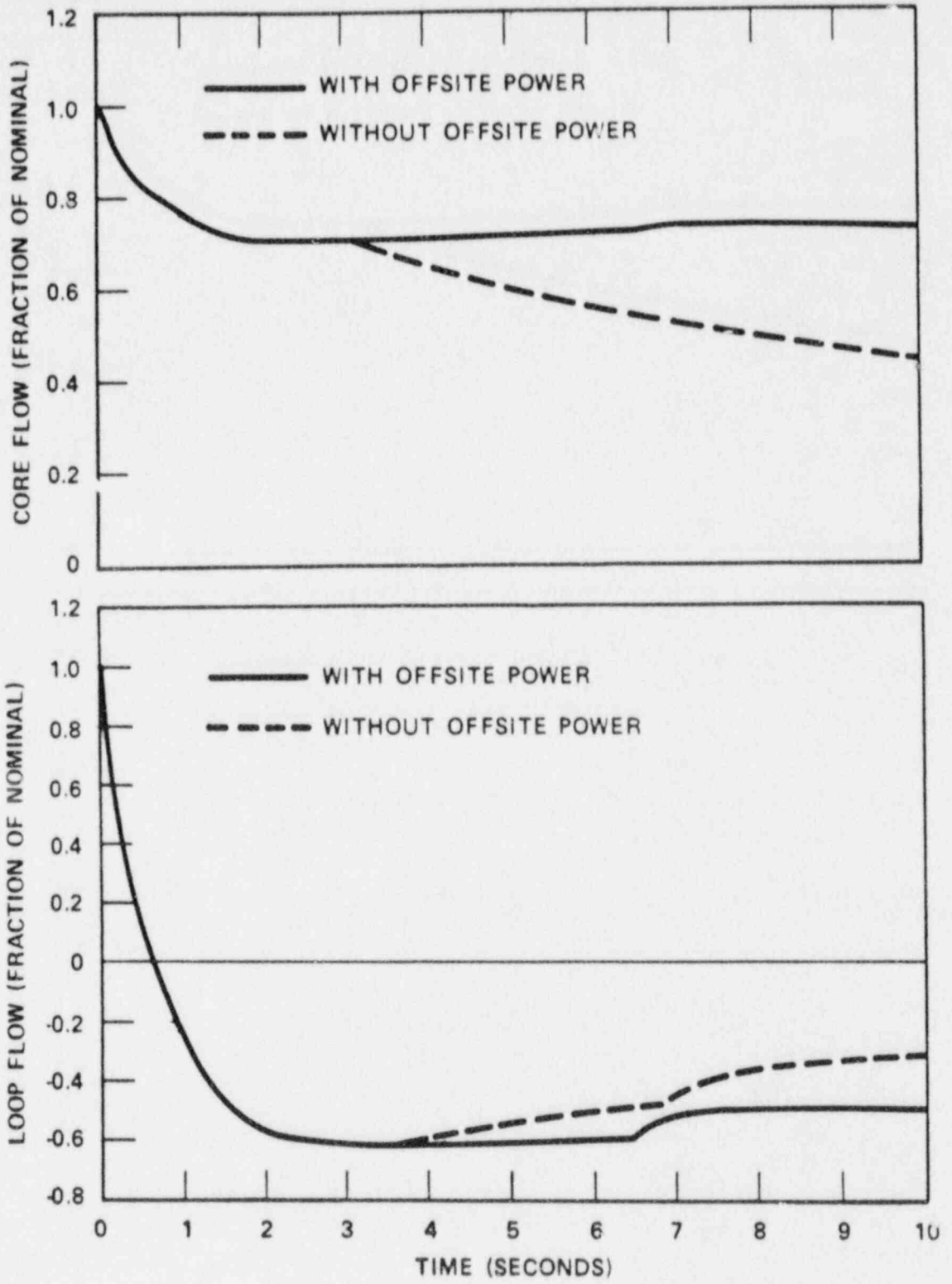




**SOUTH TEXAS PROJECT  
UNIT 2**

DNBR VERSUS TIME FOR FOUR LOOPS IN  
OPERATION, FOUR PUMPS COASTING  
DOWN, COMPLETE LOSS OF FLOW

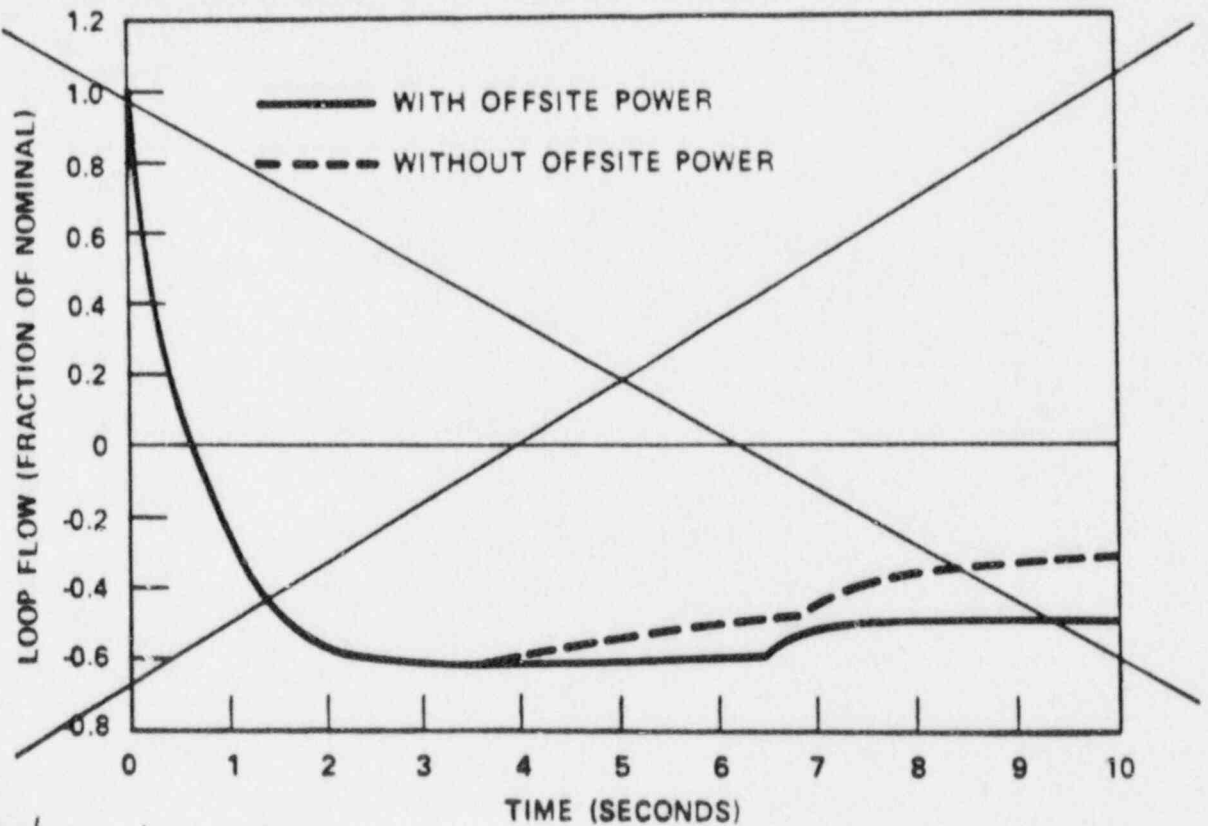
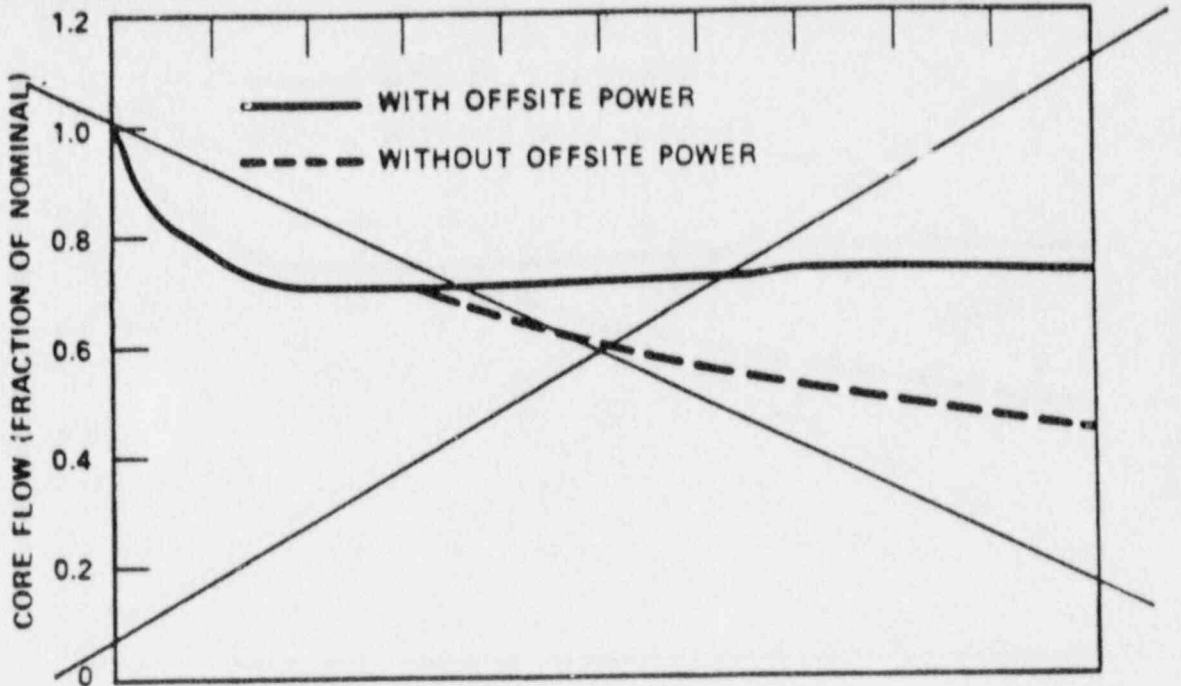
Figure 15.3-12 B ~~XXXXXXXXXX~~



**SOUTH TEXAS PROJECT  
UNIT: 1**

FLOW TRANSIENTS FOR FOUR  
LOOPS IN OPERATION,  
ONE LOCKED ROTOR

Figure 15.3-17A

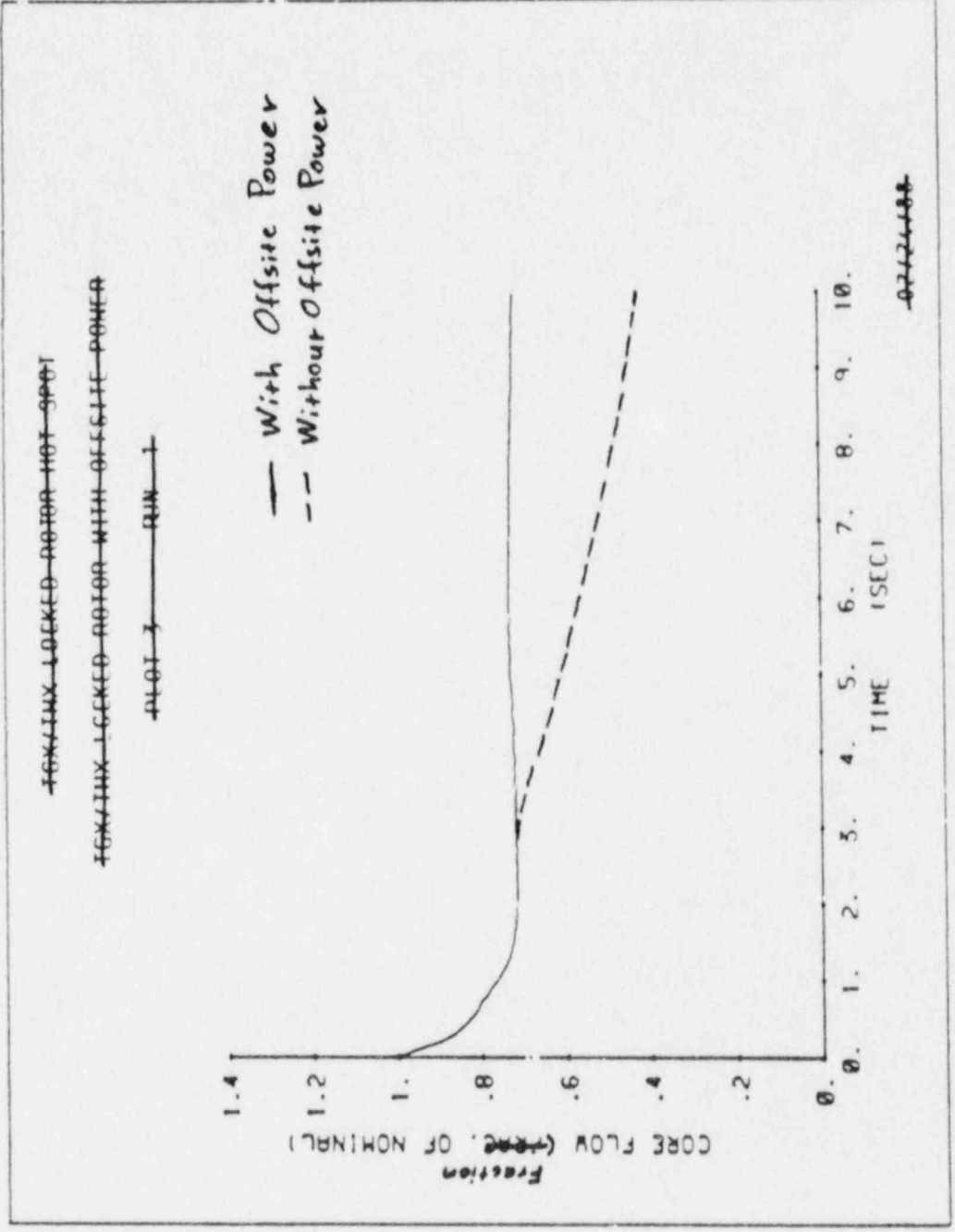


Replace above figures  
with following two figures

**SOUTH TEXAS PROJECT  
UNIT 2**

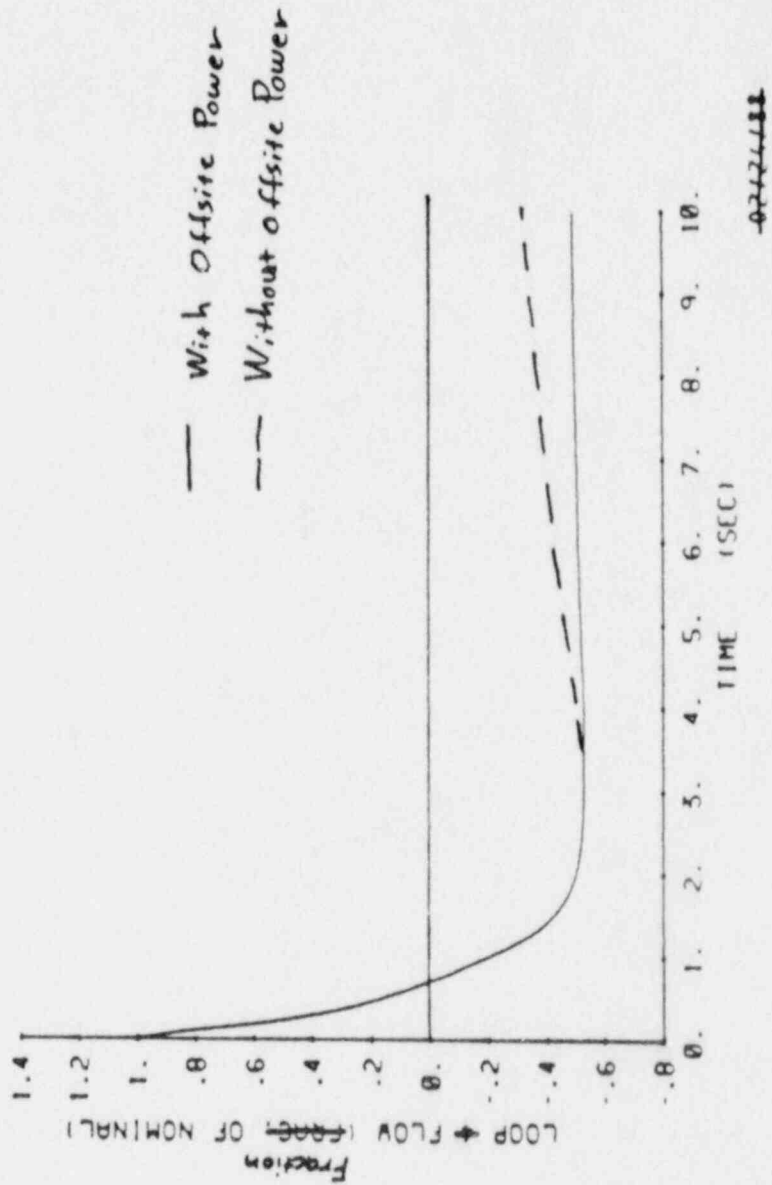
FLOW TRANSIENTS FOR FOUR  
LOOPS IN OPERATION,  
ONE LOCKED ROTOR

Figure 15.3-17 B

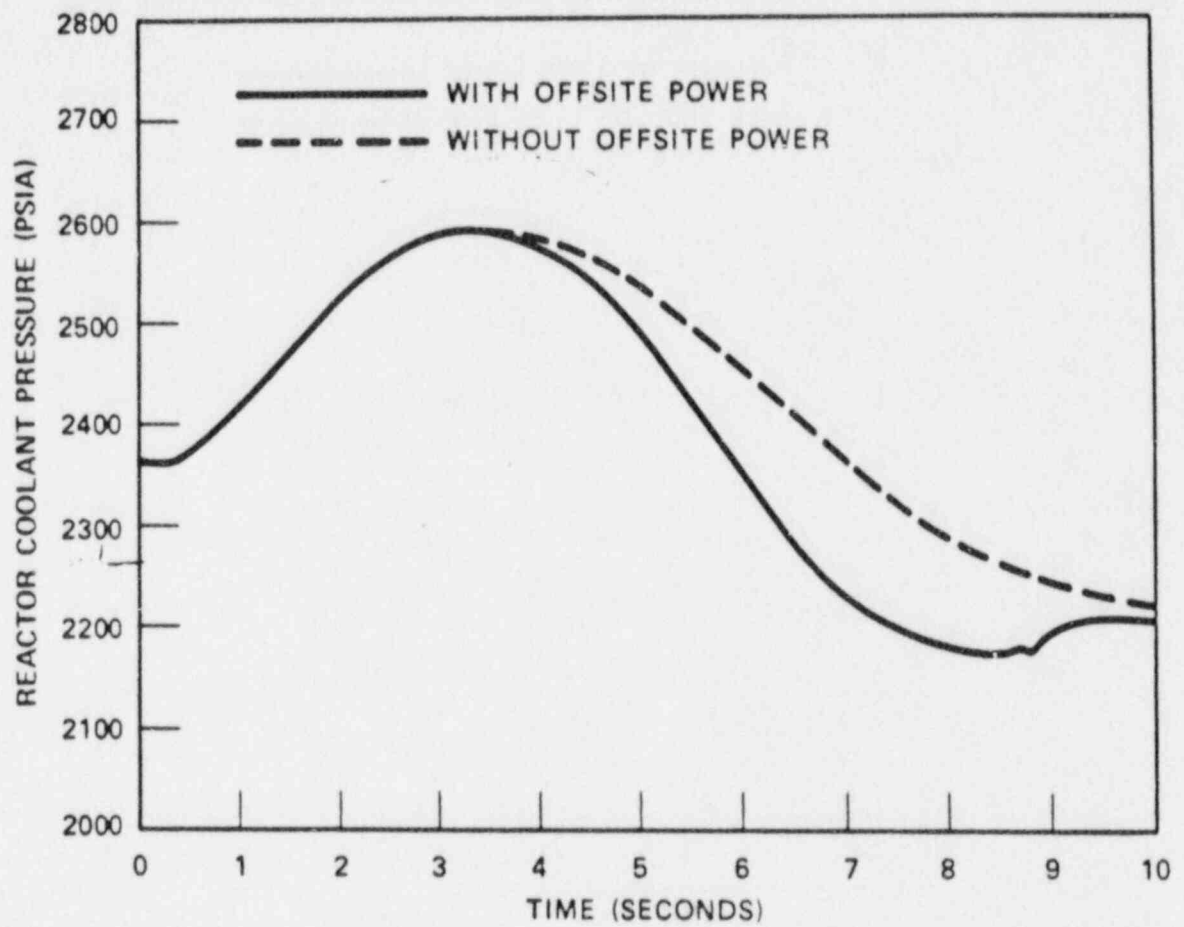


STP FSAR Figure 15.3-17B (1 of 2)

~~FIGURE 15.3-17B (2 of 2)~~  
~~LOCKED ROTOR WITH OFFSITE POWER~~  
~~PLOT 7 RUN 1~~



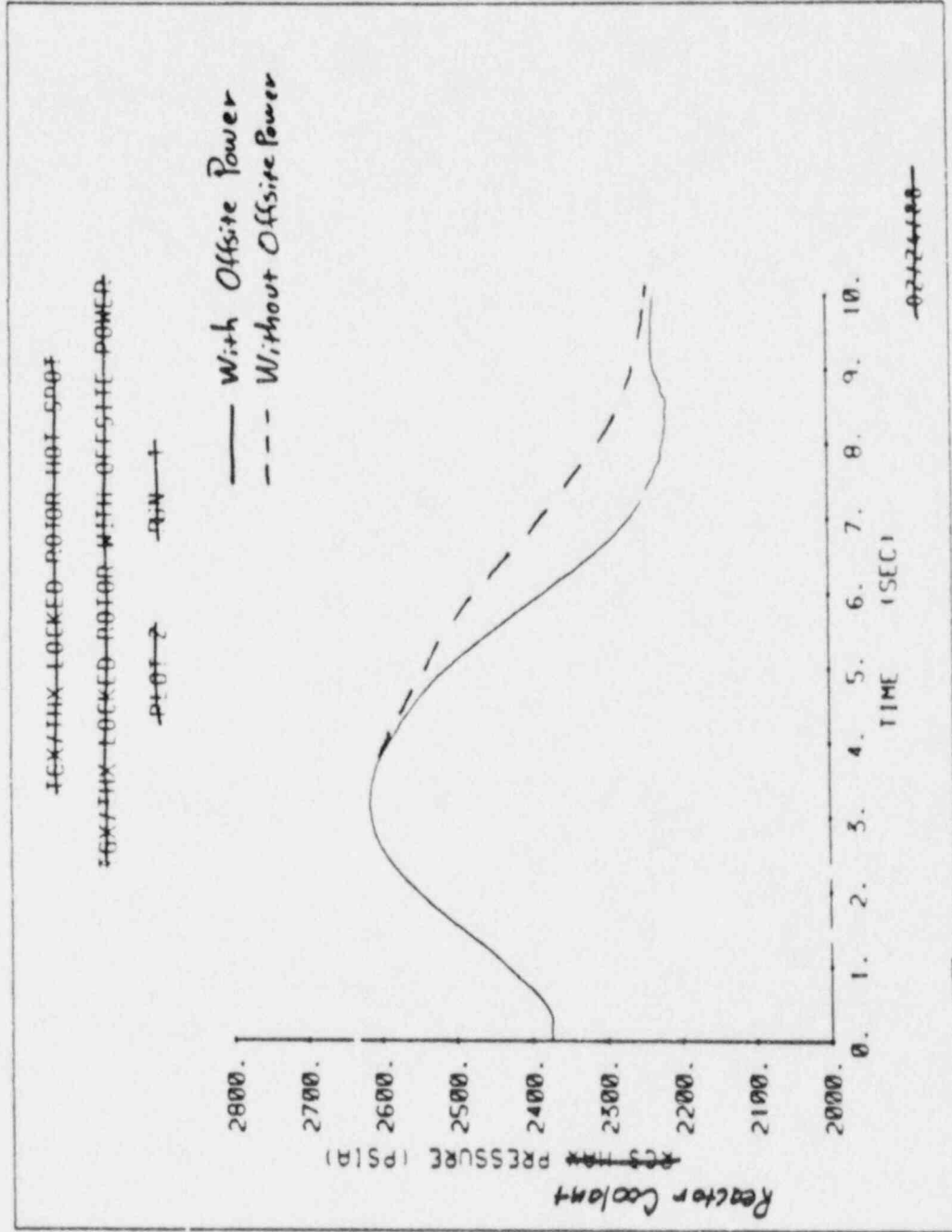
STP FSAR Figure 15.3-17B(2 of 2)



**SOUTH TEXAS PROJECT  
UNIT 1**

REACTOR COOLANT SYSTEM PRESSURE  
TRANSIENT FOR FOUR LOOPS IN  
OPERATION, ON LOCKED ROTOR

Figure 15.3-18 A



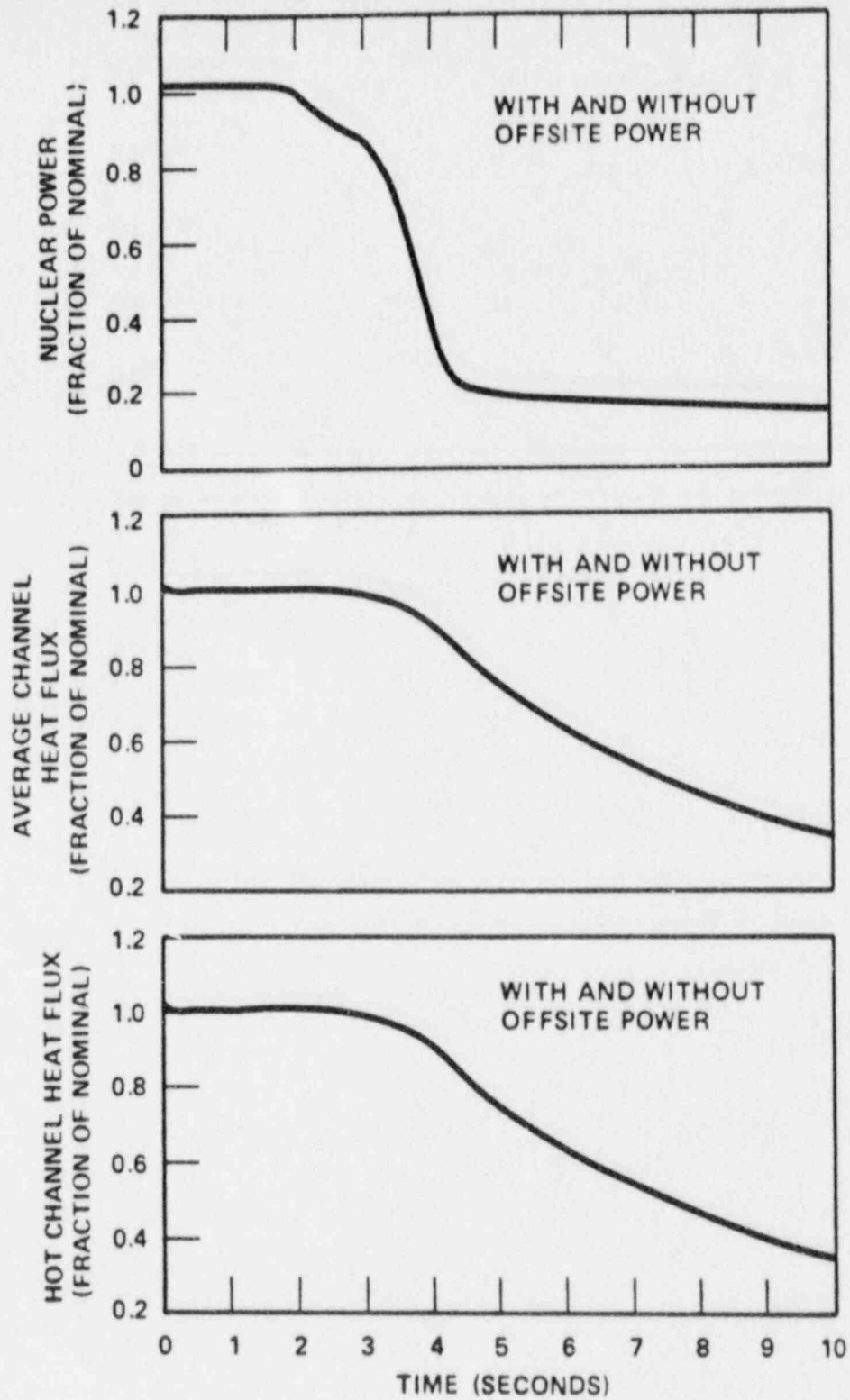
STP FSAR Figure 15.3-18

**SOUTH TEXAS PROJECT**  
**UNIT 2**

REACTOR COOLANT SYSTEM PRESSURE  
TRANSIENT FOR FOUR LOOPS IN  
OPERATION, ON LOCKED ROTOR

Figure 15.3-18 **B** ~~Amendment 54~~

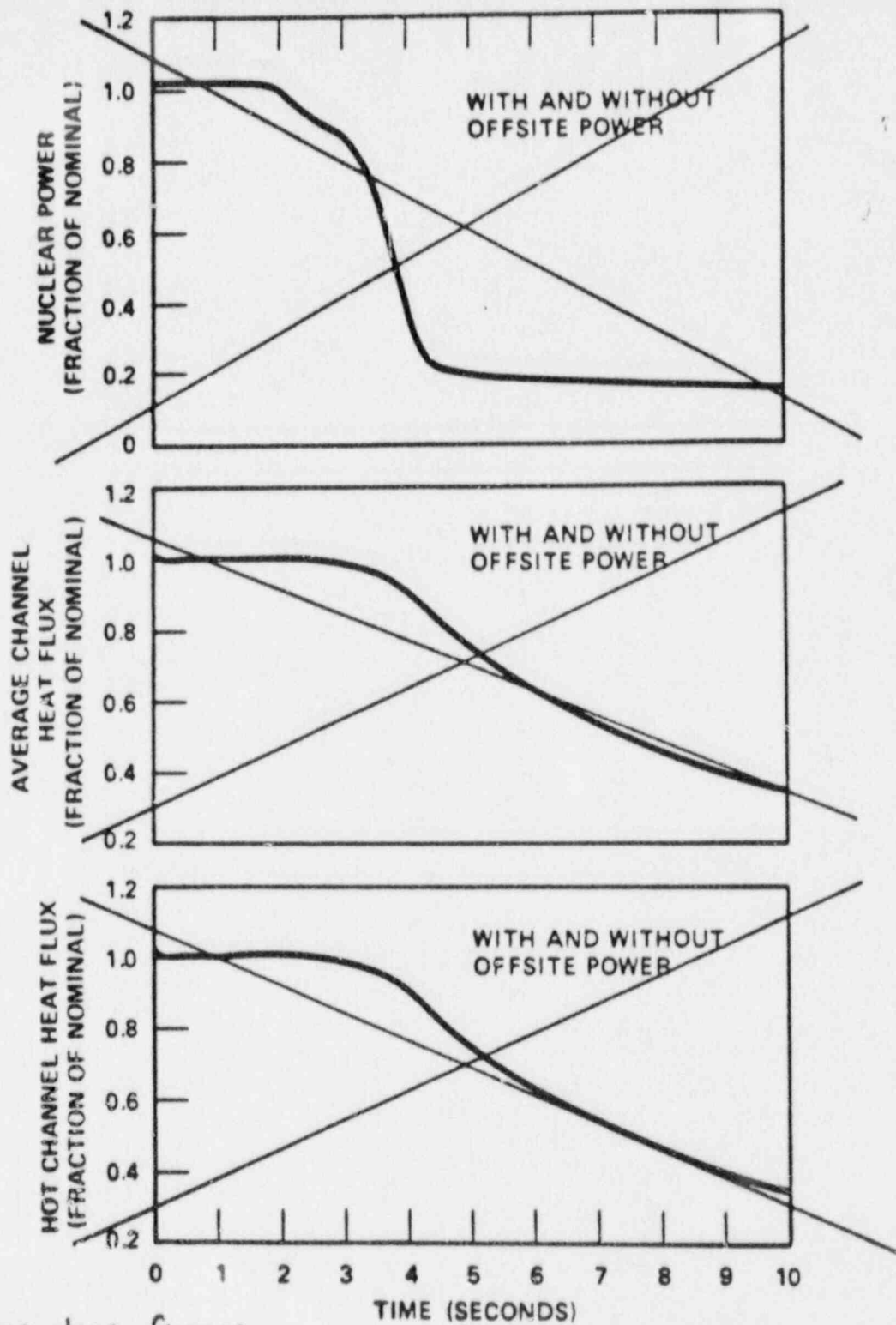




**SOUTH TEXAS PROJECT  
UNIT 1**

NUCLEAR POWER TRANSIENT, AVERAGE  
& HOT CHANNEL HEAT FLUX TRANSIENTS  
FOR FOUR LOOPS IN OPERATION, ONE  
LOCKED ROTOR

Figure 15.3-19 A

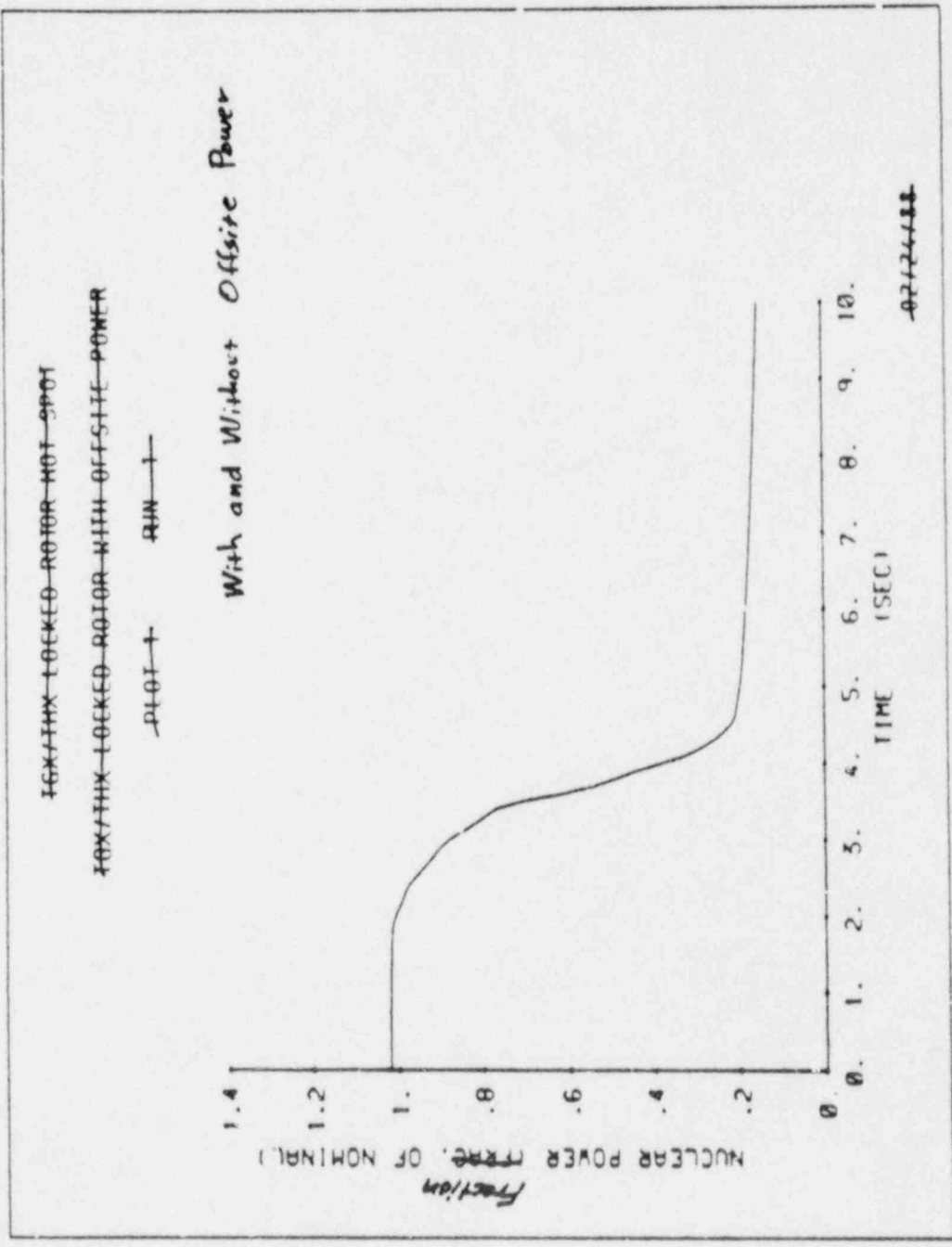


Replace above figures  
with following three figures

**SOUTH TEXAS PROJECT  
UNIT 2**

NUCLEAR POWER TRANSIENT, AVERAGE  
& HOT CHANNEL HEAT FLUX TRANSIENTS  
FOR FOUR LOOPS IN OPERATION, ONE  
LOCKED ROTOR

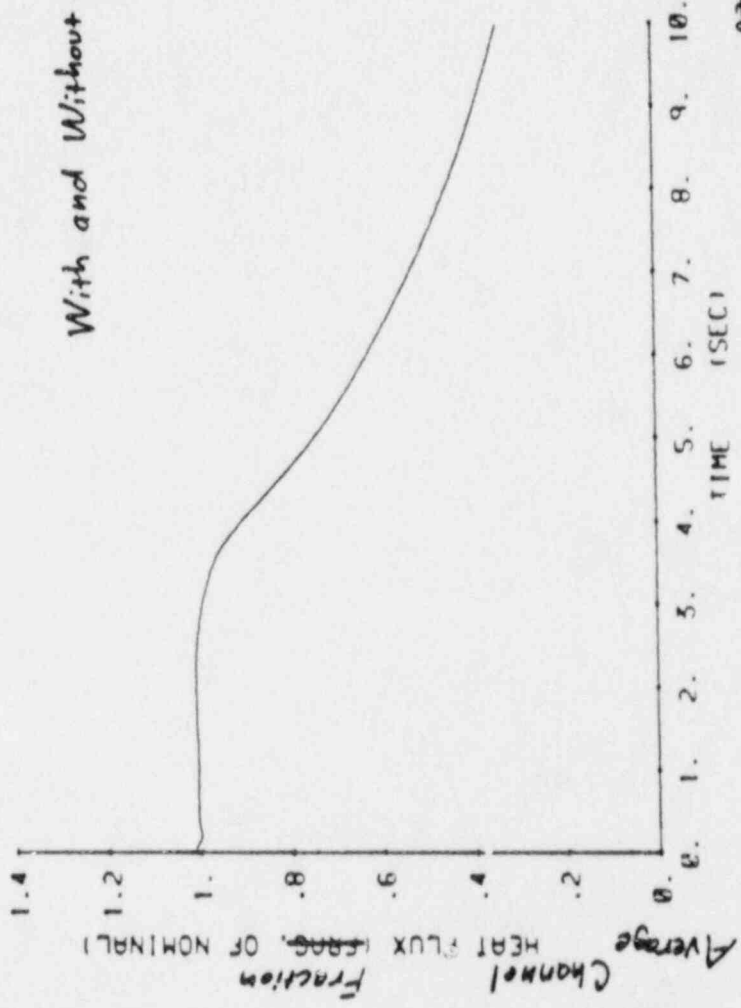
Figure 15.3-19 **B**



Step FSAR Figure 15.3-19 B (1 of 3)

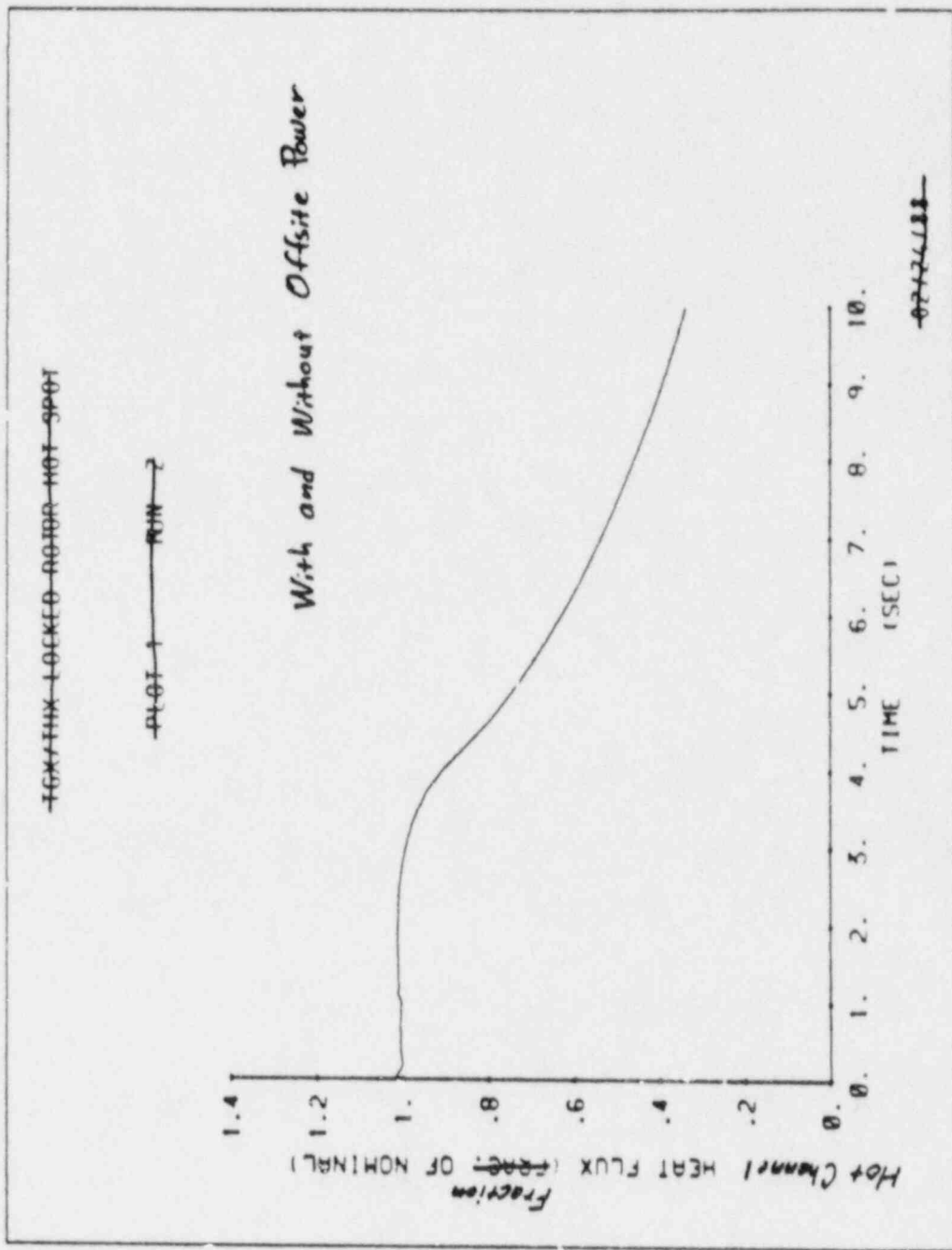
~~TOP/THX LOCKED ROTOR HOLD GRAB~~

~~PLT~~ ~~THX~~



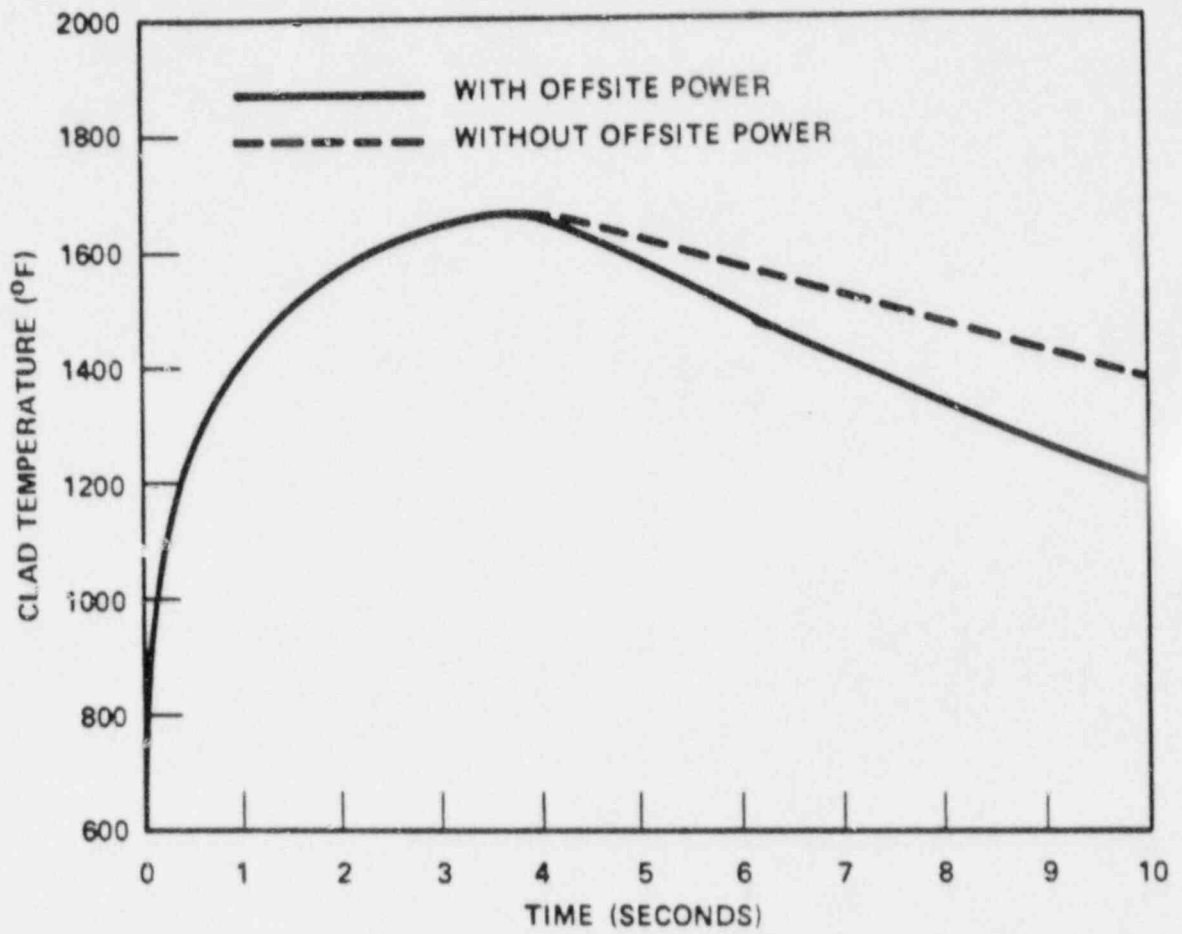
~~02224100~~

STP FSAR Figure 15.3-19 B (2 of 3)



STP FSAR

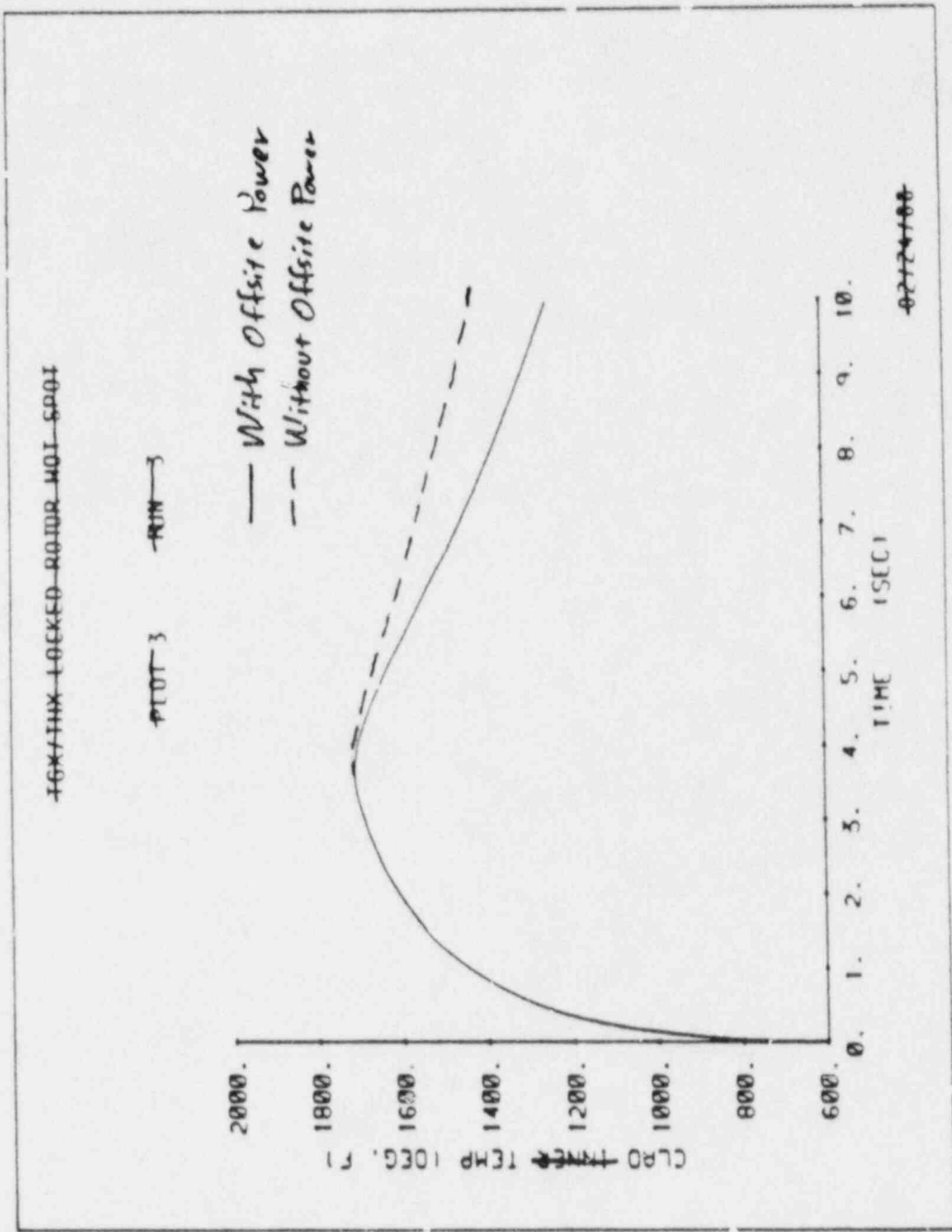
Figure 15.3-19 B (3 of 3)



**SOUTH TEXAS PROJECT  
UNIT 1**

MAXIMUM CLAD TEMPERATURE AT HOT SPOT  
FOR FOUR LOOPS IN OPERATION,  
ONE LOCKED ROTOR

Figure 15.3-20 A



STP FSAR

Figure 15.3-20

**SOUTH TEXAS PROJECT**

**UNIT 2**

---

MAXIMUM CLAD TEMPERATURE AT HOT SPOT  
FOR FOUR LOOPS IN OPERATION,  
ONE LOCKED ROTOR

Figure 15.3-20 B



Plant characteristics and initial conditions are discussed in Section 15.0.3. In order to obtain conservative results for an uncontrolled rod withdrawal at power accident, the following assumptions are made:

1. Initial conditions of maximum <sup>for Unit 1 and +5.0°F uncertainty for Unit 2</sup> core power and reactor coolant average temperature (+4.7°F uncertainty) and minimum reactor coolant pressure (~~-34 psi uncertainty~~) <sup>for Unit 1 and -46 psi uncertainty for Unit 2</sup> resulting in the minimum initial margin to DNB. 57
2. Reactivity Coefficients - Two cases are analyzed.
  - a. Minimum Reactivity Feedback: A least negative moderator temperature coefficient of reactivity and a least negative Doppler-only power coefficient of reactivity (See Fig. 15.0-2) are assumed corresponding to the beginning of core life.
  - b. Maximum Reactivity Feedback: A conservatively large negative moderator temperature coefficient and a most negative Doppler-only power coefficient are assumed.
3. The reactor trip on high neutron flux is assumed to be actuated at a conservative value of 118 percent of nominal full power. The  $\Delta T$  trips include all adverse instrumentation and setpoint errors, while the delays for the trip signal actuation are assumed at their maximum values.
4. The RCCA trip insertion characteristic is based on the assumption that the highest worth assembly is stuck in its fully withdrawn position.
5. The maximum positive reactivity insertion rate is greater than that for the simultaneous withdrawal of the combinations of the two control banks having the maximum combined worth at maximum speed.
6. The effect of RCCA movement on the axial core power distribution is accounted for by causing a decrease in overtemperature  $\Delta T$  setpoint proportional to a decrease in margin to DNB.

A block diagram summarizing various protection sequences for safety actions required to mitigate the consequences of this event is provided in Figure 15.0-15. 2  
Q211.  
6

Plant systems and equipment which are available to mitigate the effects of the accident are discussed in Section 15.0.8 and listed in Table 15.0-6. No single active failure in any of these systems or equipment will adversely affect the consequences of the accident. A discussion of anticipated transients without trip (ATWT) considerations is presented in Reference 15.4-4.

### Results

Figures 15.4-4 through 15.4-6 show the transient response for a rapid RCCA withdrawal incident starting from full power. Reactor trip on high neutron flux occurs shortly after the start of the accident. Since this is rapid with respect to the thermal time constants of the plant, small changes in  $T_{avg}$  and pressure result and margin to DNB is maintained.

The transient response for a slow RCCA withdrawal from full power is shown on Figures 15.4-7 through 15.4-9. Reactor trip on overtemperature  $\Delta T$  occurs after a longer period. Again, the minimum DNBR is greater than 1.30. |18

Figure 15.4-10 shows the minimum DNBR as a function of reactivity insertion rate from initial full power operation for minimum and maximum reactivity feedback. It can be seen that two reactor trip channels provide protection over the whole range of reactivity insertion rates. These are the high neutron flux and overtemperature  $\Delta T$  channels. The minimum DNBR is always greater than 1.30. |18

Figures 15.4-11 and 15.4-12 show the minimum DNBR as a function of reactivity insertion rate for RCCA withdrawal incidents starting at 60 and 10 percent power respectively. The results are similar to the 100 percent power case, except as the initial power is decreased, the range over which the overtemperature  $\Delta T$  trip is effective is increased. In neither case does the DNBR fall below 1.30. |18

The shape of the curves of minimum DNBR versus reactivity insertion rate in the referenced figures is due both to reactor core and coolant system transient response and to protection system action in initiating a reactor trip.

Referring to the minimum feedback case in Figure 15.4-11, for example, it is noted that:

1. For high reactivity<sup>3</sup> insertion rates (i.e., between approximately  $\lambda \times 10^{-4}$   $\Delta k/\text{sec}$  and  $1.0 \times 10^3$   $\Delta k/\text{sec}$ ) reactor trip is initiated by the high neutron flux trip. The neutron flux level in the core rises rapidly for these insertion rates while core heat flux and coolant system temperature lag behind due to the thermal capacity of the fuel and coolant system fluid. Thus, the reactor is tripped prior to significant increase in heat flux or water temperature with resultant high minimum DNBRs during the transient. As reactivity insertion rate decreases, core heat flux and coolant temperatures can remain more nearly in equilibrium with the neutron flux; minimum DNBR during the transient thus decreases with decreasing insertion rate.
2. The overtemperature  $\Delta T$  reactor trip circuit initiates a reactor trip when measured coolant loop  $\Delta T$  exceeds a setpoint based on measured RCS average temperature and pressure. This trip circuit is described in detail in Chapter 7; however, it is important in this context to note that the average temperature contribution to the circuit is lead-lag compensated in order to decrease the effect of the thermal capacity of the RCS in response to power increases.
3. With further decrease in reactivity insertion rate, the overtemperature  $\Delta T$  and high neutron flux trips become equally<sup>4</sup> effective in terminating the transient (e.g., at approximately  $\lambda \times 10^3$   $\Delta k/\text{sec}$  reactivity insertion rate).<sup>3</sup>

For reactivity insertion rates between approximately  $\lambda \times 10^{-4}$   $\Delta k/\text{sec}$  and approximately  $5 \times 10^{-5}$   $\Delta k/\text{sec}$  the effectiveness of the overtemperature  $\Delta T$  trip increases (in terms of increased minimum DNBR) due to the fact that with lower insertion rates the power increase rate is slower, the rate of

rise of average coolant temperature is slower and the system lags and delays become less significant.

4. For reactivity insertion rates less than approximately  $5 \times 10^{-5} \Delta k/\text{sec}$ , the rise in the reactor coolant temperature is sufficiently high so that the steam generator safety valve setpoint is reached prior to trip. Opening of these valves, which act as an additional heat load of the RCS, sharply decreases the rate of rise of RCS average temperature. This decrease in rate of rise of the average coolant system temperature during the transient is accentuated by the lead-lag compensation causing the overtemperature  $\Delta T$  trip setpoint to be reached later with resulting lower minimum DNBRs.

For transients initiated from higher power levels (for example, see Figure 15.4-10) this effect, described in Item 4 above, which results in the sharp peak in minimum DNBR at approximately  $5 \times 10^{-5} \Delta k/\text{sec}$ , does not occur since the steam generator safety valves are never actuated prior to trip.

Since the RCCA withdrawal at power incident is an overpower transient, the fuel temperatures rise during the transient until after reactor trip occurs. For high reactivity insertion rates, the overpower transient is fast with respect to the fuel rod thermal time constant, and the core heat flux lags behind the neutron flux response. Due to this lag, the peak core heat flux does not exceed 118 percent of its nominal value (i.e., the high neutron flux trip setpoint assumed in the analysis). Taking into account the effect of the RCCA withdrawal on the axial core power distribution, the peak fuel temperature will still remain below the fuel melting temperature.

For slow reactivity insertion rates, the core heat flux remains more nearly in equilibrium with the neutron flux. The overpower transient is terminated by the overtemperature  $\Delta T$  reactor trip before a DNB condition is reached. The peak heat flux again is maintained below 118 percent of its nominal value. Taking into account the effect of the RCCA withdrawal on the axial core power distribution, the peak fuel temperature will remain below the fuel melting temperature.

Since DNB does not occur at any time during the RCCA withdrawal at power transient, the ability of the primary coolant to remove heat from the fuel rod is not reduced. Thus, the fuel cladding temperature does not rise significantly above its initial value during the transient.

The calculated sequence of events for this accident is shown in Table 15.4-1. With the reactor tripped, the plant eventually returns to a stable condition. The plant may subsequently be cooled down further by following normal plant shutdown procedures.

**15.4.2.3 Radiological Consequences.** There are only minimal radiological consequences associated with an uncontrolled RCCA bank withdrawal at power event. The reactor trip causes a turbine trip and heat is removed from the secondary system through the steam generator power-operated relief valves (PORVs) or safety valves. Since no fuel damage is postulated to occur, the radiological consequences associated with atmospheric steam release from this event are less severe than the steam line break event analyzed in Section 15.1.5.3.

15.4.2.4 Conclusions. The high neutron flux and overtemperature  $\Delta T$  trip channels provide adequate protection over the entire range of possible reactivity insertion rates (i.e., the minimum value of DNBR is always larger than 1.30). Thus, the DNB design basis as described in Section 4.4 is met.

15.4.3 Rod Cluster Control Assembly Misoperation

15.4.3.1 Identification of Causes and Accident Description. RCCA misoperation accidents include:

1. One or more dropped RCCAs within the same group;
2. A dropped RCCA bank;
3. Statically misaligned RCCA;
4. Withdrawal of a single RCCA.

Each RCCA has a position indicator channel which displays the position of the assembly. The displays of assembly positions are grouped for the operator's convenience. Fully inserted assemblies are further indicated by a rod at bottom signal, which actuates a local alarm and a control room annunciator. Group demand position is also indicated.

RCCAs are always moved in preselected banks, and the banks are always moved in the same preselected sequence. Each bank of RCCAs is divided into two groups. The rods comprising a group operate in parallel through multiplexing thyristors. The two groups in a bank move sequentially such that the first group is always within one step of the second group in the bank. A definite schedule of actuation or deactuation of the stationary gripper, movable gripper, and lift coils of a mechanism is required to withdraw the RCCA attached to the mechanism. Since the stationary gripper, movable gripper, and lift coils associated with the four RCCAs of a rod group are driven in parallel, any single failure which would cause rod withdrawal would affect a minimum of one group. Mechanical failures are in the direction of insertion or immobility.

The dropped RCCA, dropped RCCA bank, and statically misaligned RCCA events are classified as American Nuclear Society (ANS) Condition II incidents (incidents of moderate frequency) as defined in Section 15.0.1. However, the single RCCA withdrawal incident is classified as an ANS Condition III event, as discussed below.

No single electrical or mechanical failure in the rod control system could cause the accidental withdrawal of a single RCCA from the inserted bank at full power operation. The operator could withdraw a single RCCA in the control bank since this feature is necessary in order to retrieve an assembly should one be accidentally dropped. The event analyzed must result from multiple wiring failures (probability for single random failure is on the order of  $10^{-4}$ /year; refer to Section 7.7.2.2) or multiple serious operator errors and subsequent and repeated operator disregard of event indication. The probability of such a combination of conditions is very low. The consequences, however, may include slight fuel damage. Thus, consistent with



The insertion limits in the Technical Specifications may vary from time to time depending on a number of limiting criteria. It is preferable, therefore, to analyze the misaligned RCCA case at full power for a position of the control bank as deeply inserted as the criteria on minimum DNBR and power peaking factor will allow. The full power insertion limits on control bank D must then be chosen to be above that position and will usually be dictated by other criteria. Detailed results will vary from cycle to cycle depending on fuel arrangements.

For this RCCA misalignment with bank D inserted to its full power insertion limit and one RCCA fully withdrawn, DNBR does not fall below the limit value. This case is analyzed assuming the initial reactor power, pressure and RCS temperature are at their nominal values (as given in Table 15.0-2) including a +2 percent power uncertainty, a -34 psia pressure uncertainty and a +4.7°F temperature uncertainty, but with the increased radial peaking factor associated with the misaligned RCCA. 53 57

DNB calculations have not been performed specifically for RCCAs missing from other banks; however, power shape calculations have been performed, as required, for the RCCA ejection analysis. Inspection of the power shapes shows that the DNB and peak kW/ft situation is less severe than the bank D case discussed above assuming insertion limits on the other banks equivalent to a bank D full-in insertion limit. 53

For RCCA misalignments with one RCCA fully inserted, the DNBR does not fall below the limit value. This case is analyzed assuming the initial reactor power, pressure and RCS temperature are at their nominal values (as given in Table 15.0-2) including a +2 percent power uncertainty, a -34 psia pressure uncertainty, and a +4.7°F temperature uncertainty, but with the increased radial peaking factor associated with the misaligned RCCA. 53 57

DNB does not occur for the RCCA misalignment incident and thus the ability of the primary coolant to remove heat from the fuel rod is not reduced.

for Unit 1 and a -46 psia pressure uncertainty for Unit 2

for Unit 1 and a 5.0 °F temperature uncertainty for Unit 2

For this reason, a rod insertion limit is defined as a function of power level. Operation with the RCCAs above this limit guarantees adequate shutdown capability and acceptable power distribution. The position of all RCCAs is continuously indicated in the control room. An alarm will occur if a bank of RCCAs approaches its insertion limit or if one RCCA deviates from its bank. Operating instructions require boration at low level alarm. <sup>5</sup>

#### Reactor Protection

The reactor protection in the event of a rod ejection accident has been described in Reference 15.4-7. The protection for this accident is provided by high neutron flux trip (high and low setting) and high positive rate of neutron flux trip. These protection functions are described in detail in Section 7.2. |43

#### Effects on Adjacent Housings

Disregarding the remote possibility of the occurrence of a complete RCCA mechanism housing failure, investigations have shown that failure of a housing due to either longitudinal or circumferential cracking would not cause damage to adjacent housings. The CRDM is described in Section 3.9.4. |43

#### Effects of Rod Travel Housing Longitudinal Failures

If a longitudinal failure of the rod travel housing should occur, the region of the position indicator assembly opposite the break would be stressed by the reactor coolant pressure of 2,250 psia. The most probable leakage path would be provided by the radial deformation of the position indicator coil assembly, resulting in the growth of axial flow passages between the rod travel housing and the hollow tube along which the coil assemblies are mounted.

If failure of the position indicator coil assembly should occur, the resulting free radial jet from the failed housing could cause it to bend and contact adjacent rod housings. If the adjacent housings were on the periphery, they might bend outward from their bases. The housing material is quite ductile; plastic hinging without cracking would be expected. Housings adjacent to a failed housing, in locations other than the periphery, would not be bent because of the rigidity of multiple adjacent housings.

#### Effect of Rod Travel Housing Circumferential Failures

If circumferential failure of a rod travel housing should occur, the broken-off section of the housing would be ejected vertically because the driving force is vertical and the position indicator coil assembly and the drive shaft would tend to guide the broken-off piece upwards during its travel. Travel is limited by the missile shield, thereby limiting the projectile acceleration. When the projectile reached the missile shield it would partially penetrate the shield and dissipate its kinetic energy. The water jet from the break would continue to push the broken off piece against the missile shield.

If the broken-off piece of the rod travel housing were short enough to clear the break when fully ejected, it would rebound after impact with the missile

Trip Reactivity Insertion

The trip reactivity insertion assumed is given in Table 15.4-3 and includes the effect of one stuck RCCA adjacent to the ejected rod. These values are reduced by the ejected rod reactivity. The shutdown reactivity was simulated by dropping a rod of the required worth into the core. The start of rod motion occurred 0.5 seconds after the high neutron flux trip point is reached. This delay is assumed to consist of 0.2 seconds for the instrument channel to produce a signal, 0.15 seconds for the trip breaker to open and 0.15 seconds for the coil to release the rods. A curve of trip rod insertion versus time was used which assumed that insertion to the dashpot does not occur until 2.8 seconds after the start of fall. The choice of such a conservative insertion rate means that there is over one second after the trip point is reached before significant shutdown reactivity is inserted into the core. This conservatism is particularly important for hot full power accidents.

The minimum design shutdown margin available for this plant at hot zero power (HZP) may be reached only at end of life in the equilibrium cycle. This value includes an allowance for the worst stuck rod, adverse xenon distribution, conservative Doppler and moderator defects, and an allowance for calculational uncertainties. Physics calculations have shown that the effect of two stuck RCCAs (one of which is the worst ejected rod) is to reduce the shutdown by about an additional one percent  $\Delta k$ . Therefore, following a reactor trip resulting from an RCCA ejection accident, the reactor will be subcritical when the core returns to HZP.

Reactor Protection

As discussed in Section 15.4.8.1.1, reactor protection for a rod ejection is provided by high neutron flux trip (high and low setting) and high positive neutron flux rate trip. These protection functions are part of the Reactor Trip System (RTS). No single failure of the RTS will negate the protection functions required for the rod ejection accident, or adversely affect the consequences of the accident.

| 43  
| 57

Results

Cases are presented for both beginning and end of life at zero and full power.

1. Beginning of Cycle, Full Power

Control bank D was assumed to be inserted to its insertion limit. The worst ejected rod worth and hot channel factor were conservatively calculated to be 0.20 percent  $\Delta k$  and 7.10 respectively. The peak hot spot clad average temperature was 2,219°F. The peak hot spot fuel center temperature reached melting, conservatively assumed at 4,900°F. However, melting was restricted to less than ten percent of the pellet.

| 18

for Unit 1 and 2,292°F for Unit 2.

2. Beginning of Cycle, Zero Power

For this condition, control bank D was assumed to be fully inserted and banks B and C were at their insertion limits. The worst ejected rod is located in control bank D and has a worth of 0.86 percent  $\Delta k$  and a hot channel factor of 13.0. The peak hot spot clad average temperature reached 2,001°F the fuel center temperature was 3,476°F.

| 18

for Unit 1 and 2,606°F for Unit 2

for Unit 1 and 4,213°F for Unit 2  
Amendment 57



3. End of Cycle, Full Power

Control bank D was assumed to be inserted to its insertion limit. The ejected rod worth and hot channel factors were conservatively calculated to be 0.20 percent  $\Delta k$  and 7.10, respectively. This resulted in a peak clad average temperature of 2,096°F. The peak hot spot fuel center temperature reached melting at 4,800°F. However, melting was restricted to less than ten percent of the pellet.

| 18

for Unit 1 and 2,092°F for Unit 2.

4. End of Cycle, Zero Power

The ejected rod worth and hot channel factor for this case were obtained assuming control bank D to be fully inserted and banks B and C at their insertion limits. The results were 1.0 percent  $\Delta k$  and 20.00% respectively. The peak clad average and fuel center temperatures were 2,422°F and 4,154°F. The Doppler weighting factor for this case is significantly higher than for the other cases due to the very large transient hot channel factor.

| 18

for Unit 1 and 1.0 percent  $\Delta k$  and 23.00 for Unit 2.

for Unit 1 and 2,651°F and 4,012°F for Unit 2.

A summary of the cases presented above is given in Table 15.4-3. The nuclear power and hot spot fuel and clad temperature transients for the worst cases (beginning of life full power and end of life zero power) are presented on Figures 15.4-26 through 15.4-29.

The calculated sequence of events for the worst case rod ejection accidents, as shown on Figures 15.4-26 through 15.4-29, is presented in Table 15.4-1. For all cases, reactor trip occurs very early in the transient, after which the nuclear power excursion is terminated. The reactor will remain subcritical following reactor trip.

The ejection of a RCCA constitutes a break in the RCS, located in the reactor pressure vessel head. The effects and consequences of loss-of-coolant accidents are discussed in Section 15.6.5. Following the RCCA ejection, the operator would follow the same emergency instructions as for any other loss-of-coolant accident to recover from the event.

Fission Product Release

It is assumed that fission products are released from the gaps of all rods entering DNB. In all cases considered, less than 10 percent of the rods entered DNB based on a detailed three-dimensional THINC analysis (Ref. 15.4-10). Although limited fuel melting at the hot spot was predicted for the full power cases, it is highly unlikely that melting will occur since the analysis conservatively assumed that the hot spots before and after ejection were coincident.

Pressure Surge

A detailed calculation of the pressure surge for an ejection worth of one dollar at beginning of life, hot full power, indicates that the peak pressure does not exceed that which would cause stress to exceed the faulted condition stress limits (Ref. 15.4-10). Since the severity of the present analysis does not exceed the "worst case" analysis, the accident for this plant will not result in an excessive pressure rise or further damage to the RCS.

STP FSAR

Table 15.4-1

TIME SEQUENCE OF EVENTS FOR INCIDENTS WHICH CAUSE REACTIVITY  
AND POWER DISTRIBUTION ANOMALIES

<u>Accident</u>	<u>Event</u>	<u>Time (sec.)</u>	
		<u>Unit 1</u>	<u>Unit 2</u>
Uncontrolled Rod Cluster Control Assembly Bank Withdrawal from a Subcritical or Low Power Startup Condition	Initiation of uncontrolled rod withdrawal from 10 <sup>-9</sup> of nominal power	0.0	0.0
	Power range high neutron flux low setpoint reached	13.7	13.7
	Peak nuclear power occurs	13.8	13.8
	Rods begin to fall into core	14.2	14.2
	Minimum DNBR occurs	15.6	15.6
	Peak average clad temperature occurs	15.6	15.6
	Peak heat flux occurs	15.6	15.6
	Peak average fuel temperature occurs	15.8	15.8
Uncontrolled RCCA Bank Withdrawal at Power	1. Case A		
	Initiation of uncontrolled RCCA withdrawal at a high reactivity insertion rate (70 pcm/sec)	0	0
	Power range high neutron flux high trip point reached	1.7	1.7
	Rods begin to fall into core	2.2	2.2
	Minimum DNBR occurs	3.2	3.4

STP FSAR

Table 15.4-1 (Continued)

TIME SEQUENCE OF EVENTS FOR INCIDENTS WHICH CAUSE REACTIVITY  
AND POWER DISTRIBUTION ANOMALIES

<u>Accident</u>	<u>Event</u>	<u>Time (sec.)</u>	
		<u>Unit 1</u>	<u>Unit 2</u>
2. Case B	Initiation of uncontrolled RCCA withdrawal at a small reactivity insertion rate (5 pcm/sec)	0	0
	Overtemperature $\Delta T$ reactor trip signal initiated	12.6 <del>11.8</del>	11.8
	Rods begin to fall into core	14.1 <del>13.3</del>	13.3
	Minimum DNBR occurs	14.6 <del>15.9</del>	13.9
	Startup of an Inactive Reactor Coolant Loop	0	0
	Power reached P-8 interlock setpoint, coincident with low reactor coolant flow	10.2	10.2
	Rods begin to drop	11.2	11.2
	Minimum DNBR occurs	12.0	12.0
Uncontrolled Boron Dilution			
1.	Dilution during startup	0	0
	Shutdown margin lost (if dilution continues after trip)	-1200	~1200

STP FSAR

Table 15.4-1 (Continued)

TIME SEQUENCE OF EVENTS FOR INCIDENTS WHICH CAUSE REACTIVITY  
AND POWER DISTRIBUTION ANOMALIES

<u>Accident</u>	<u>Event</u>	<u>Time (sec.)</u>		
		<u>UNIT 1</u>	<u>UNIT 2</u>	
2 Dilution during full power operation	a. Automatic reactor control	Operator receives low-low rod insertion limit alarm due to dilution	0	0
		Shutdown margin lost	-1620	~ 1620
	b. Manual reactor control	Reactor trip on overtemperature $\Delta T$ due to dilution	0	0
		Shutdown margin lost (if dilution continues after trip)	-1020	~ 1020
	Rod Cluster Control Assembly Ejection			
	1. Beginning of Life, Full Power	Initiation of rod ejection	0.0	0.0
Power range high neutron flux setpoint reached		0.06	0.05	
Peak nuclear power occurs		0.13	0.13	
Rods begin to fall into core		0.56	0.55	
Peak <del>core</del> <sup>fuel average</sup> temperature occurs		2.59	2.53	
Peak <del>fuel</del> <sup>clad</sup> temperature occurs		2.59	2.56	
Peak heat flux occurs		2.59	2.57	
2. End of Life, Zero Power		Initiation of rod ejection	0.0	0.0
	Power range high neutron flux low setpoint reached	0.14	0.14	

STP FSAR

Table 15.4-1 (Continued)

TIME SEQUENCE OF EVENTS FOR INCIDENTS WHICH CAUSE REACTIVITY  
AND POWER DISTRIBUTION ANOMALIES

<u>Accident</u>	<u>Event</u>	<u>Time (sec.)</u>	
		<u>Unit 1</u>	<u>Unit 2</u>
	Peak nuclear power occurs	0.17	0.17
	Rods begin to fall into core	0.64	0.64
	clad temperature		
	Peak <del>heat flux</del> occurs	1.46	1.26
	heat flux		
	Peak <del>clad temperature</del> occurs	1.46	1.32
	average		
	Peak fuel temperature occurs	1.97	1.83

TABLE 15.4-3 A

UNIT 1 PARAMETERS USED IN THE ANALYSIS OF THE ROD CLUSTER  
CONTROL ASSEMBLY EJECTION ACCIDENT

	<u>Beginning</u> <u>of cycle</u>	<u>Beginning</u> <u>of cycle</u>	<u>End</u> <u>of cycle</u>	<u>End</u> <u>of cycle</u>
Power level, %	102	0	102	0
Ejected rod worth, %ΔK	0.20	0.86	0.20	1.0
Delayed neutron fraction, %	0.55	0.55	0.44	0.44
Feedback reactivity weighting	1.60	2.50	1.30	4.5
Trip reactivity, %ΔK	5.0	2.0	4.0	2.0
F <sub>q</sub> before rod ejection	2.50	—	2.50	—
F <sub>q</sub> after rod ejection	7.10	13.0	7.10	20.00
Number of operational pumps	4	2	4	2
Max. fuel pellet average temperature, °F	4090	2856	3900	3453
Max. fuel center temperature, °F	4900	3476	4800	4154
Max. clad average temperature, °F	2219	2001	2096	2422
Max. fuel stored energy, cal/gm	179	117	169	146

18

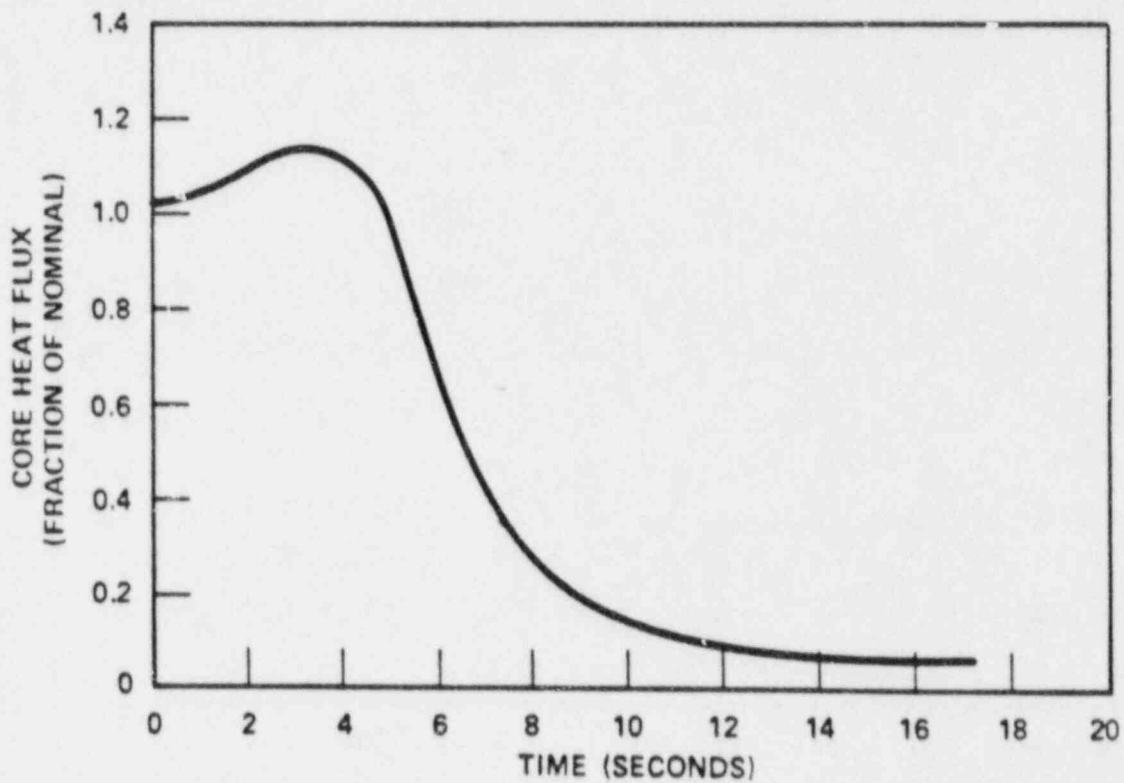
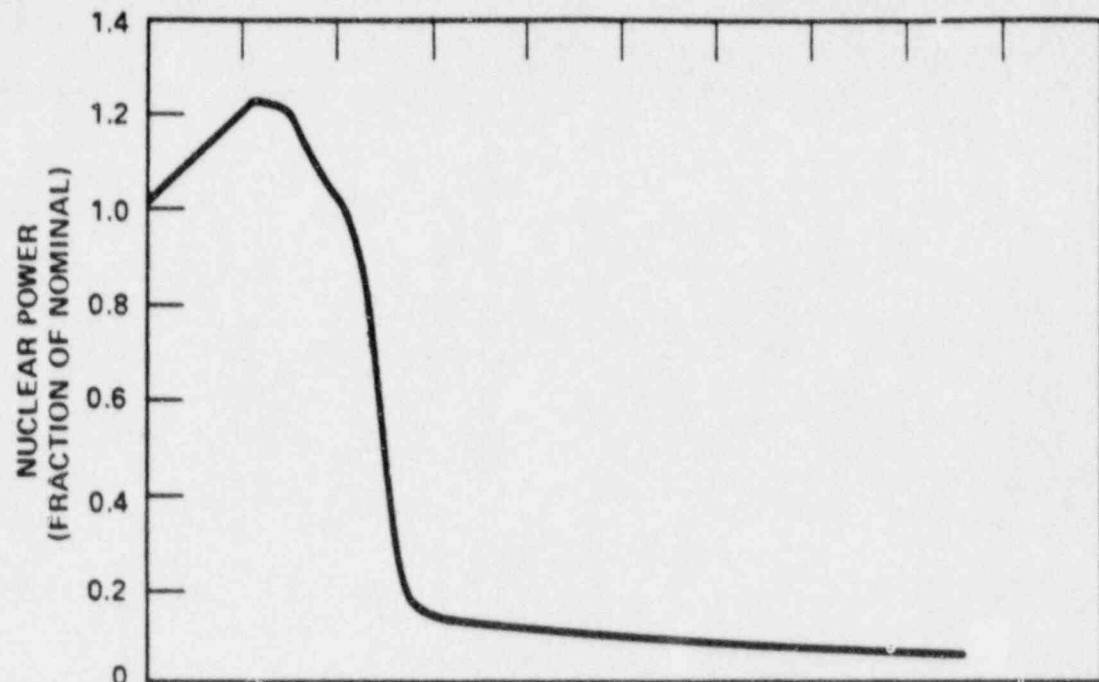


TABLE 15.4-3 B

Unit 2 PARAMETERS USED IN THE ANALYSIS OF THE ROD CLUSTER  
CONTROL ASSEMBLY EJECTION ACCIDENT

	<u>Beginning</u> <u>of cycle</u>	<u>Beginning</u> <u>of cycle</u>	<u>End</u> <u>of cycle</u>	<u>End</u> <u>of cycle</u>
Power level, %	102	0	102	0
Ejected rod worth, %ΔK	0.20	0.86	0.20	1.0
Delayed neutron fraction, %	0.55	0.55	0.44	0.44
Feedback reactivity weighting	1.30 <del>2.60</del>	2.23 <del>2.50</del>	1.30	<del>3.55</del>
Trip reactivity, %ΔK	4.0 <del>3.0</del>	2.0	4.0	2.0
F <sub>q</sub> before rod ejection	2.65 <del>2.50</del>	-	2.65 <del>2.50</del>	-
F <sub>q</sub> after rod ejection	7.10	13.0	7.10	<del>23.00</del>
Number of operational pumps	4	2	4	2
Max. fuel pellet average temperature, °F	4176 <del>3900</del>	3611 <del>3500</del>	3809 <del>3900</del>	<del>3537</del>
Max. fuel center temperature, °F	4900	4213 <del>3900</del>	4800	<del>4712</del>
Max. clad average temperature, °F	2292 <del>2200</del>	2606 <del>2500</del>	2092 <del>2000</del>	<del>2651</del>
Max. fuel stored energy, cal/gm	<del>184</del> 184	<del>154</del> 154	<del>165</del> 165	<del>151</del> 151
Percent fuel melt	<10	0	<10	0

18

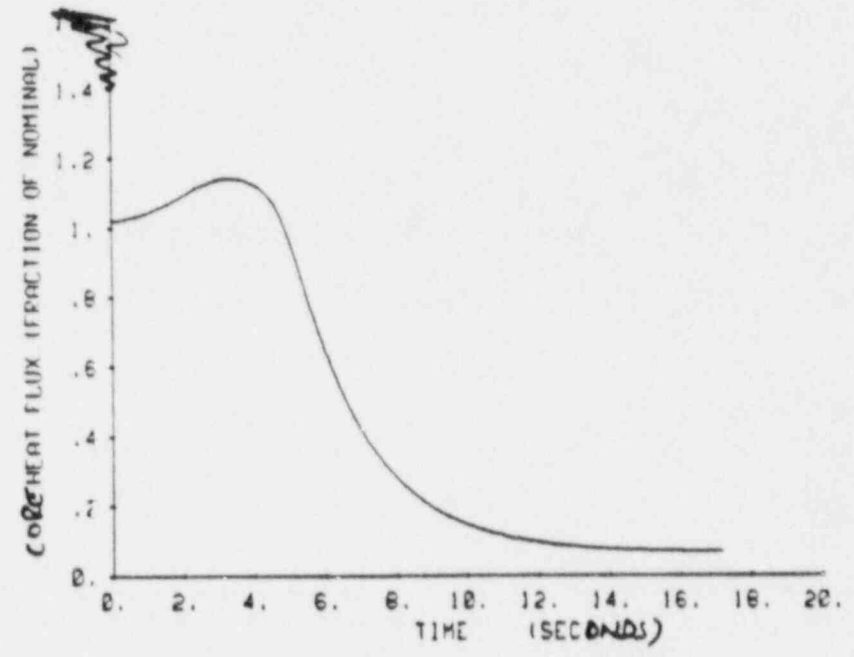
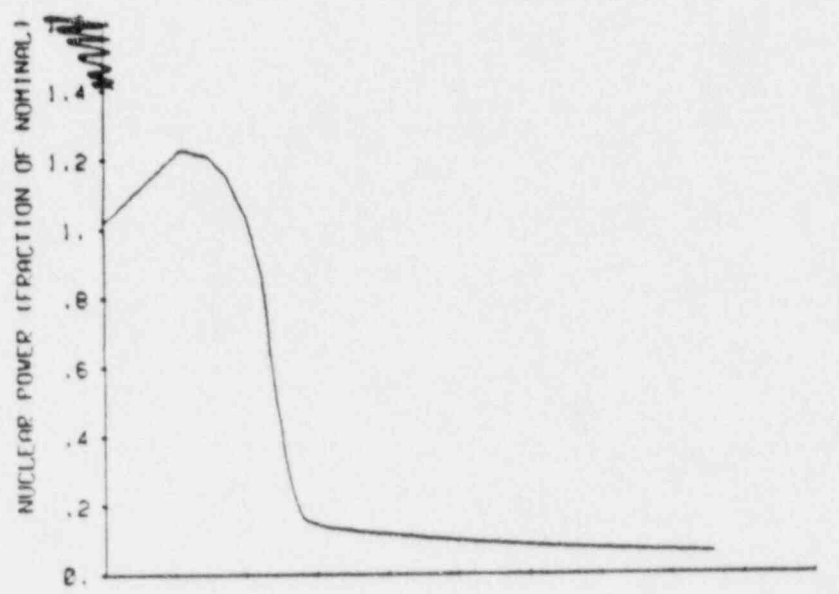


**SOUTH TEXAS PROJECT  
UNIT 1**

NUCLEAR POWER TRANSIENT & CORE  
HEAT FLUX TRANSIENT FOR  
UNCONTROLLED ROD WITHDRAWAL FROM  
FULL POWER WITH MINIMUM FEEDBACK  
AND 70 pcm/sec WITHDRAWAL RATE

Figure 15.4-4 A

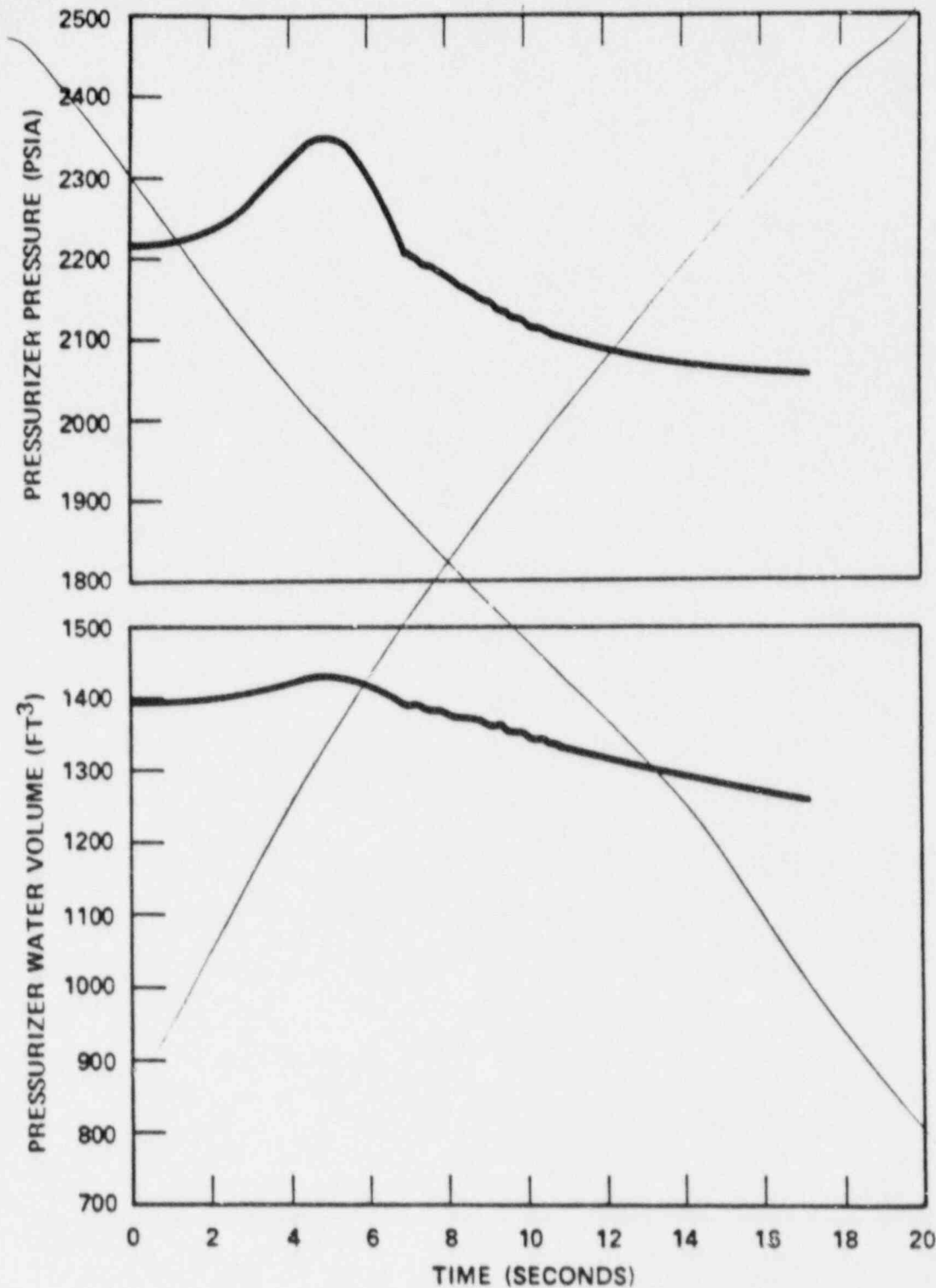
~~TCX/TIX ROD FOR REVISED TRIP REACTIVITY~~  
~~100 PC POWER, MIN FEEDBACK, RATE=70 PCM/SEC~~  
~~PLOT 1 RUN 2~~



**SOUTH TEXAS PROJECT**  
**UNIT 2**

NUCLEAR POWER TRANSIENT & CORE  
 HEAT FLUX TRANSIENT FOR  
 UNCONTROLLED ROD WITHDRAWAL FROM  
 FULL POWER WITH MINIMUM FEEDBACK  
 AND 70 pcm/sec WITHDRAWAL RATE

Figure 15.4-4 B ~~Amended 67~~

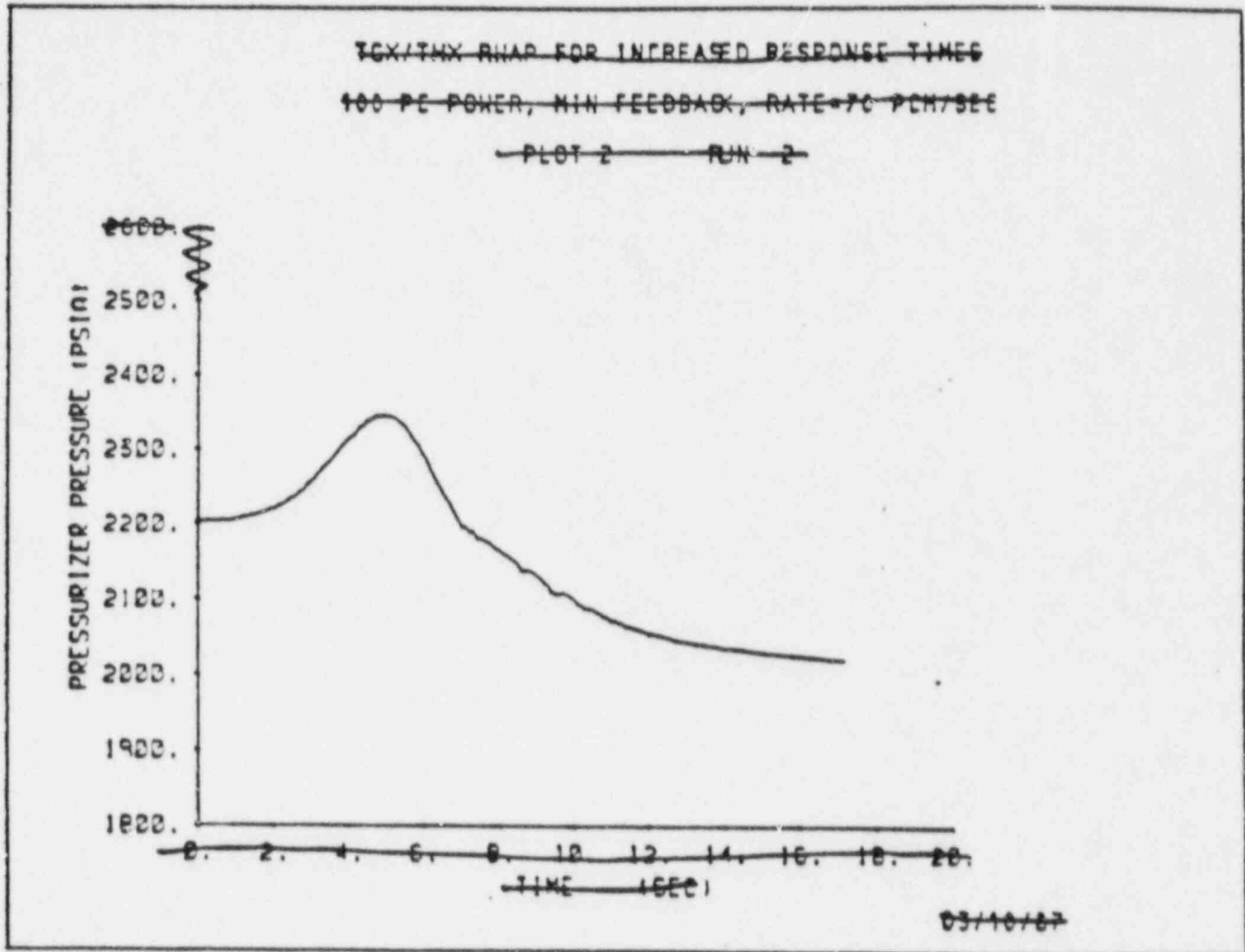


Replace with  
following 2 pages

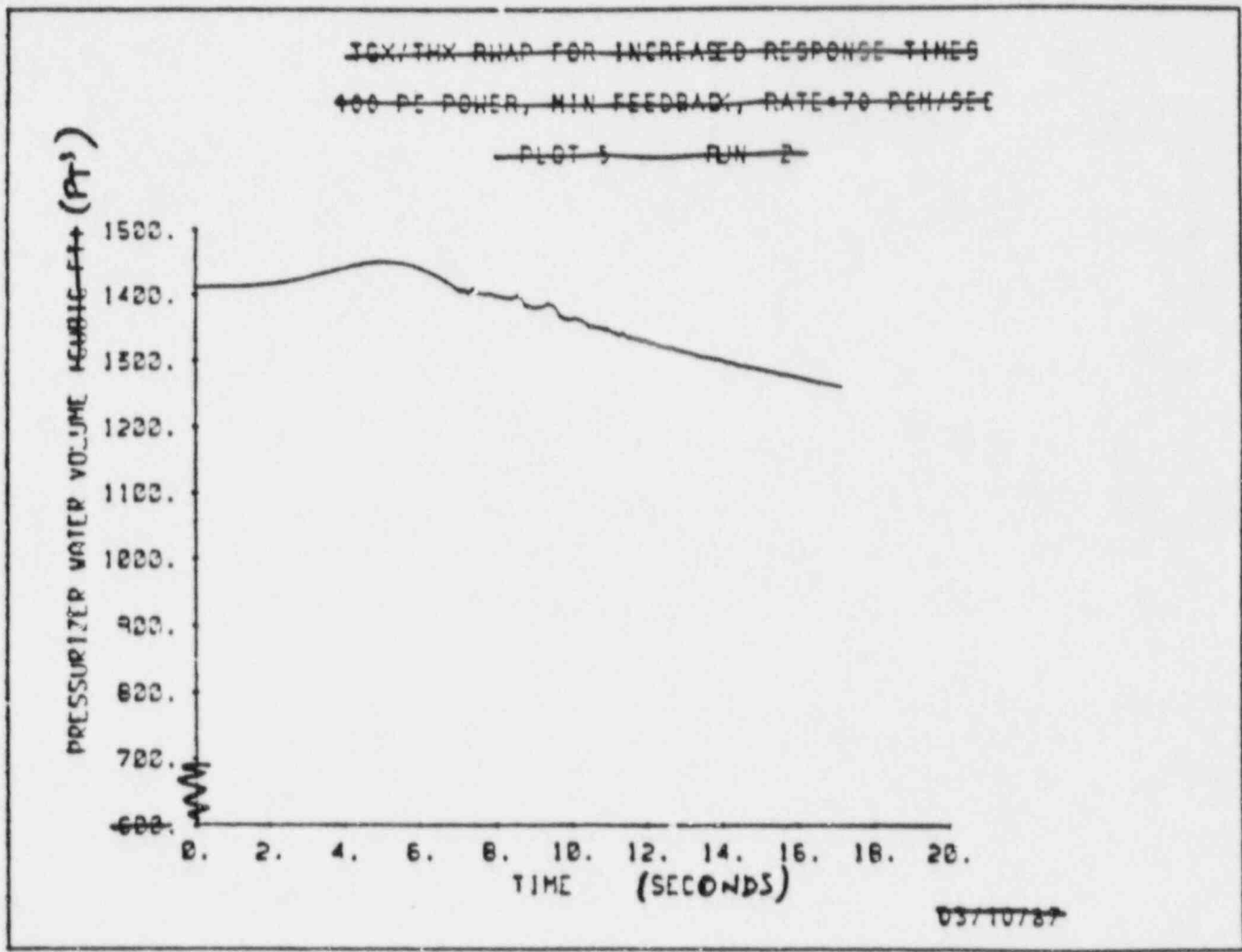
**SOUTH TEXAS PROJECT  
UNIT 1**

PRESSURIZER PRESS. & WATER VOLUME  
TRANSIENTS FOR UNCONTROLLED  
ROD WITHDRAWAL FROM FULL POWER  
WITH MINIMUM FEEDBACK AND  
70 pcm/sec WITHDRAWAL RATE

Figure 15.4-5 A

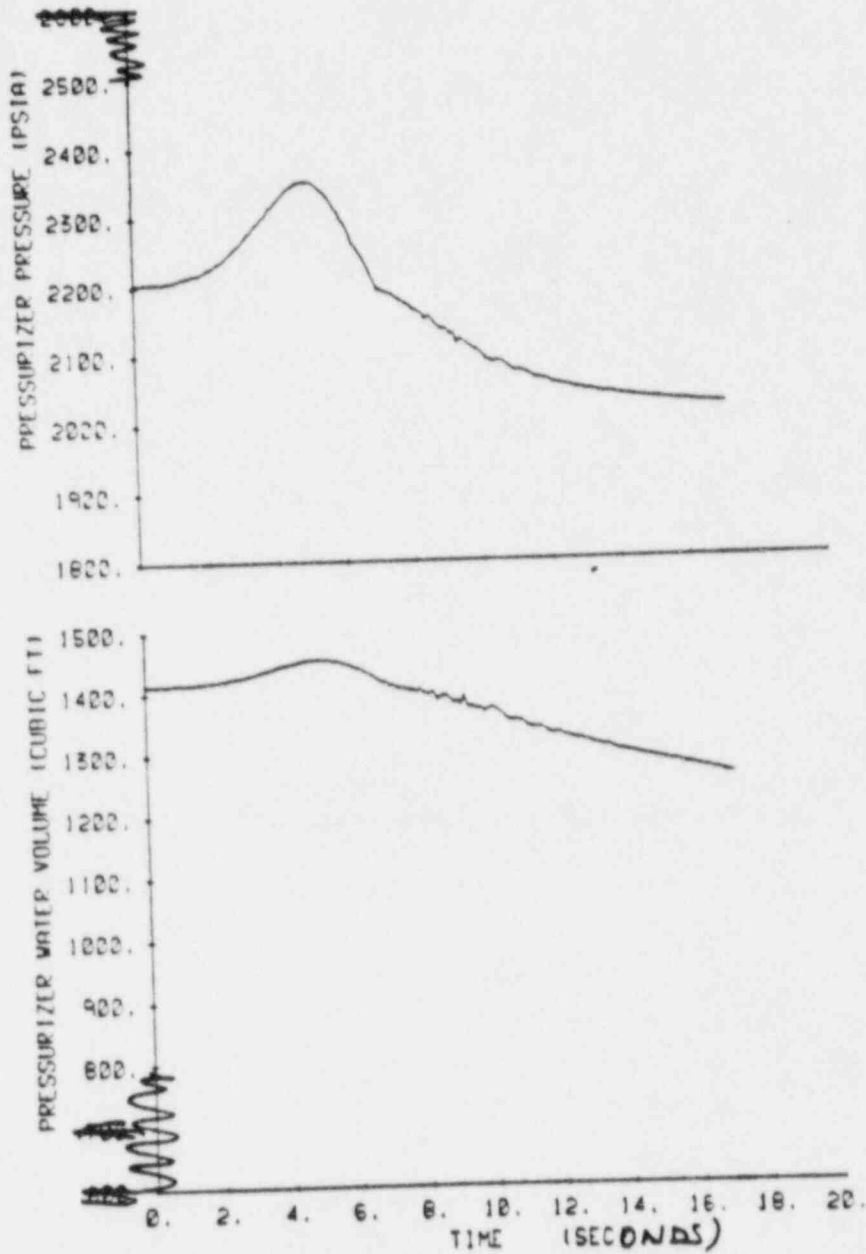


Replacement Figure 15.4-5 A (top curve)



Replacement Figure 15.4-5A (bottom curve)

~~TO THE RAMP FOR REVISED TRIP REACTIVITY~~  
~~100 PC POWER, MIN FEEDBACK, RATE 70 PCM/SEC~~  
~~— PLOT 2 — RUN 2~~

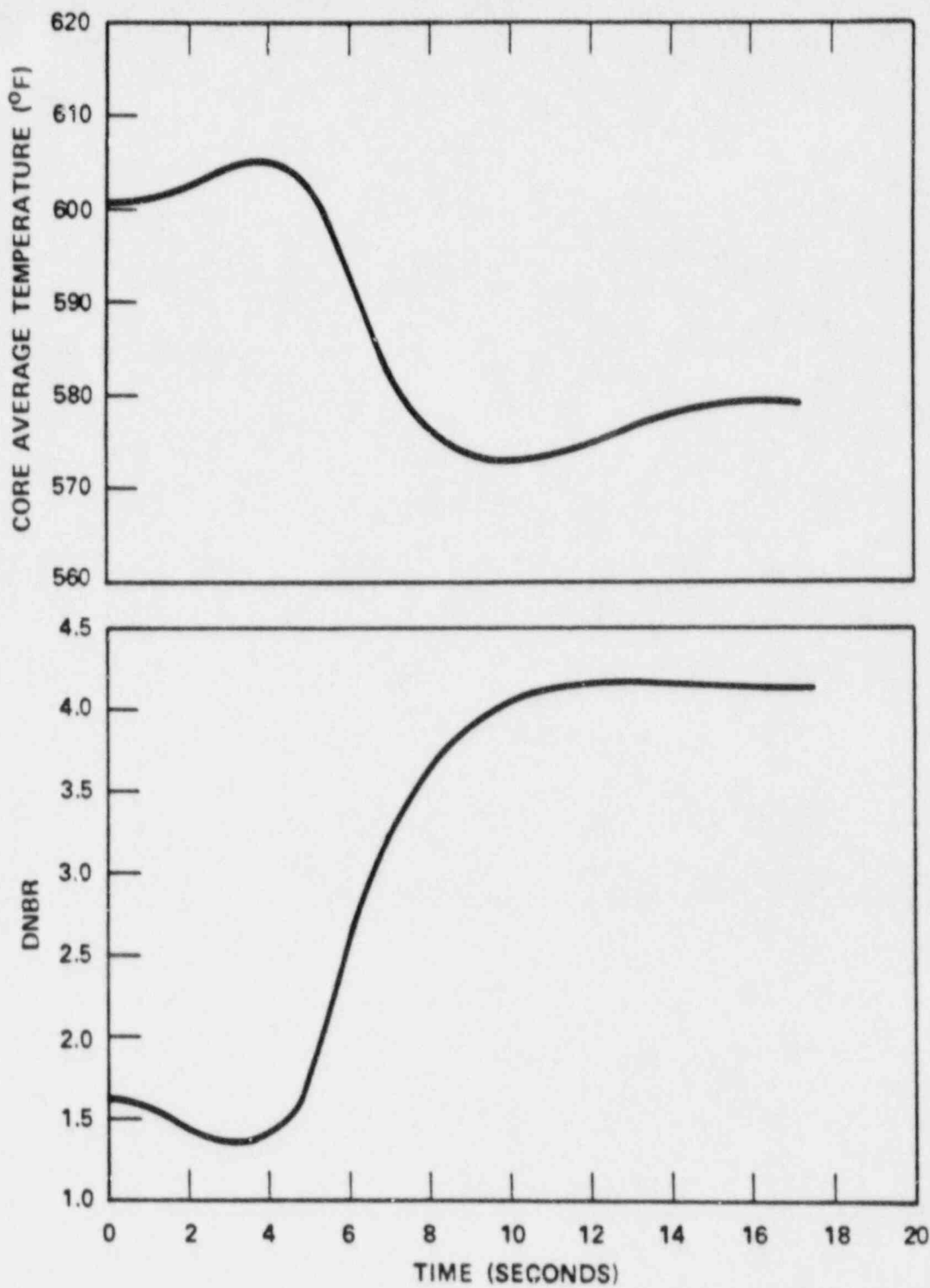


**SOUTH TEXAS PROJECT  
 UNIT 2**

PRESSURIZER PRESS. & WATER VOLUME  
 TRANSIENTS FOR UNCONTROLLED  
 ROD WITHDRAWAL FROM FULL POWER  
 WITH MINIMUM FEEDBACK AND  
 70 pcm/sec WITHDRAWAL RATE

Figure 15.4-5 B *Amendment 87*



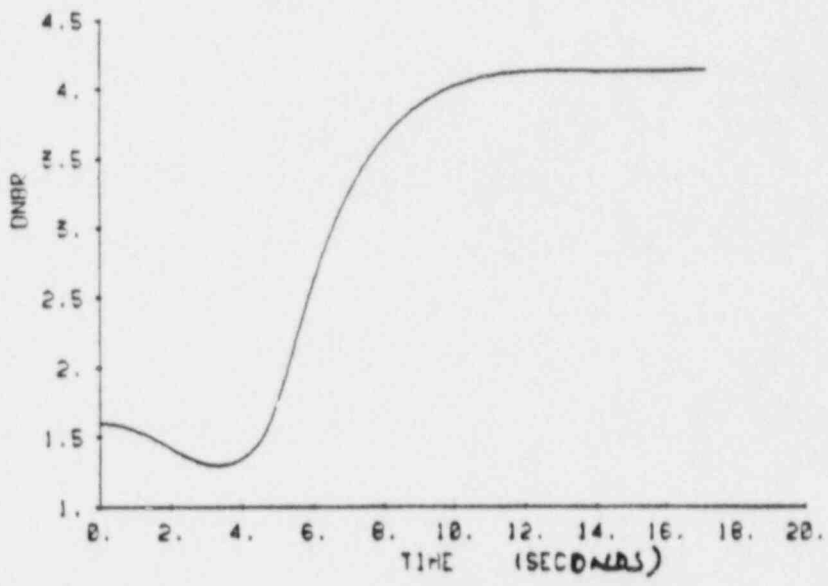
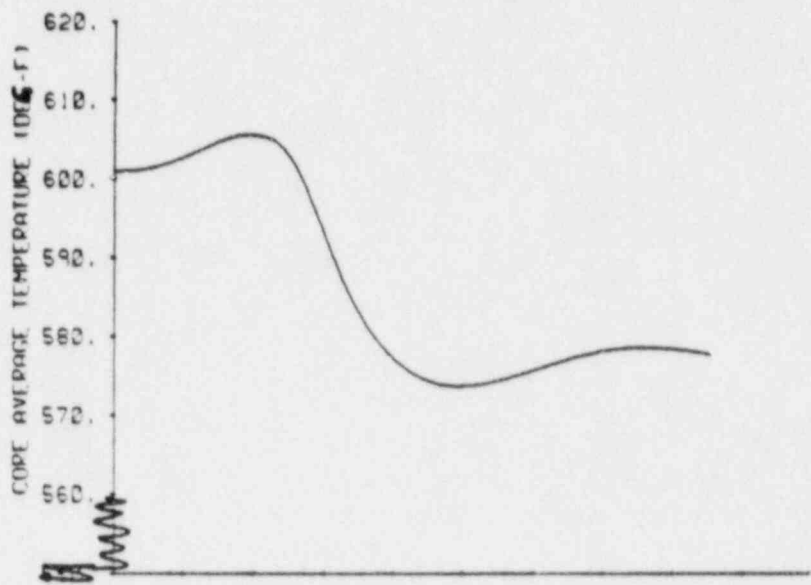


**SOUTH TEXAS PROJECT  
UNIT 1**

CORE AVG. TEMP. TRANSIENT AND DNBR  
vs TIME FOR UNCONTROLLED ROD WITH-  
DRAWAL FROM: FULL POWER WITH MIN-  
IMUM FEEDBACK AND 70 pcm/sec  
WITHDRAWAL RATE

Figure 15.4-6 A

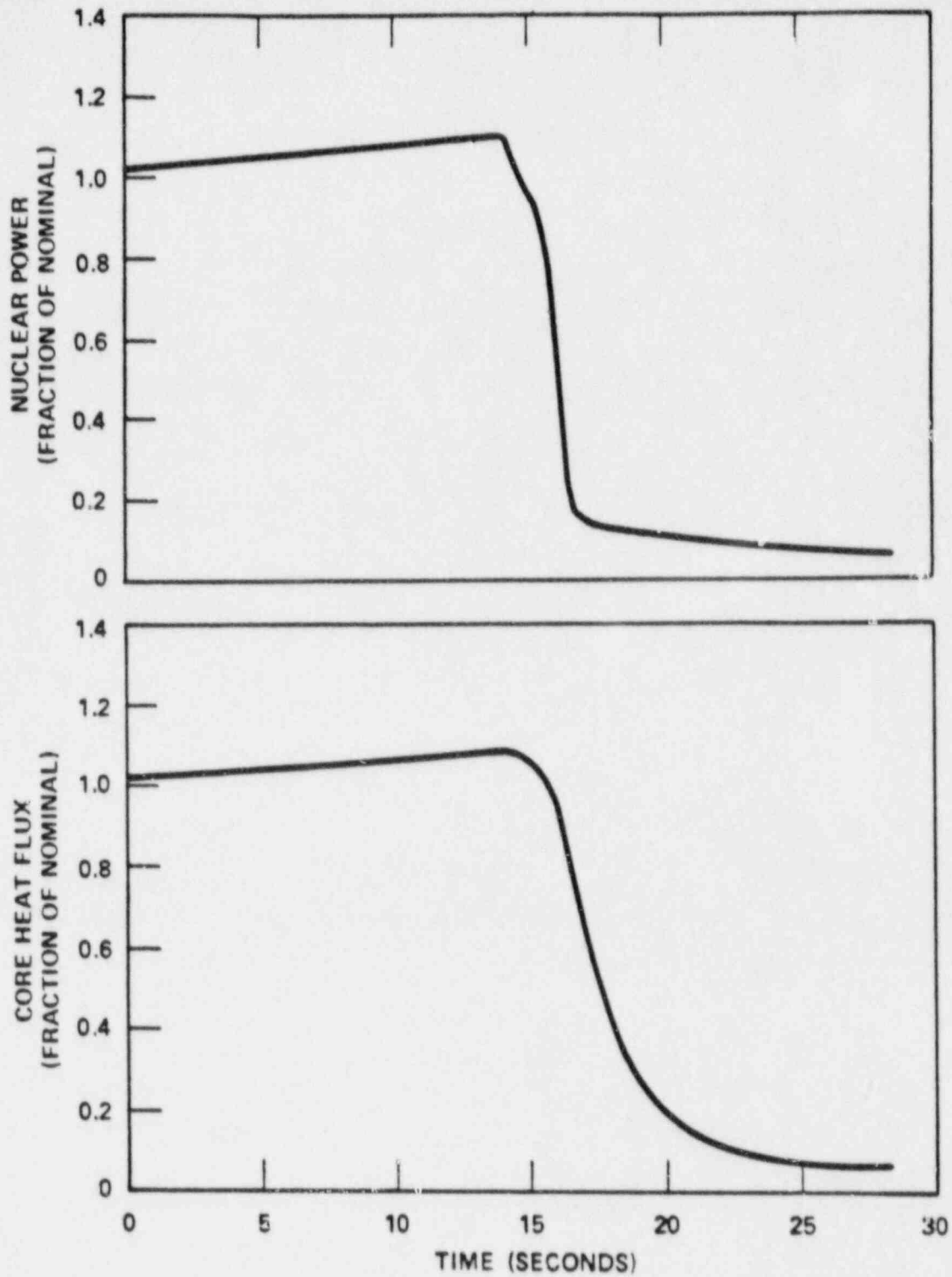
~~TCX/THX RUMP FOR REVISED TRIP REACTIVITY~~  
~~100 PC POWER, MIN FEEDBACK, RATE 70 PCM/SEC~~  
~~PLOT 3 RUN 2~~



**SOUTH TEXAS PROJECT  
 UNIT 2**

CORE AVG. TEMP. TRANSIENT AND DNBR  
 vs TIME FOR UNCONTROLLED ROD WITH-  
 DRAWAL FROM FULL POWER WITH MIN-  
 IMUM FEEDBACK AND 70 pcm/sec  
 WITHDRAWAL RATE

Figure 15.4-6 B

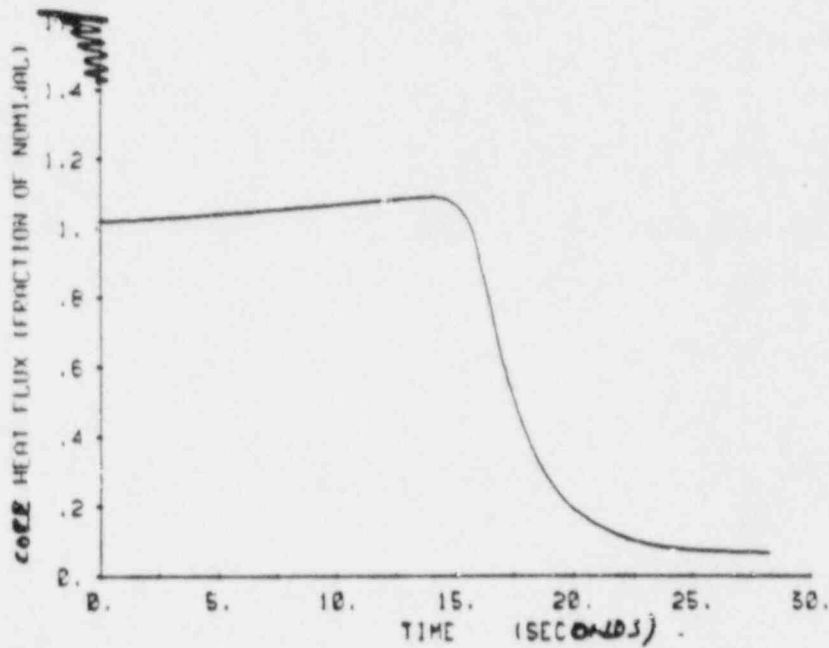
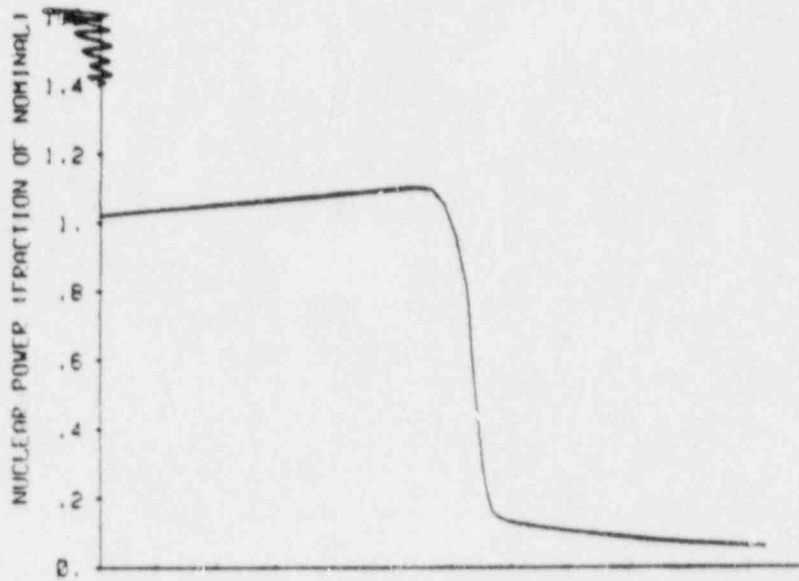


**SOUTH TEXAS PROJECT  
UNIT 1**

NUCLEAR POWER TRANSIENT & CORE  
HEAT FLUX TRANSIENT FOR UNCON-  
TROLLED ROD WITHDRAWAL FROM  
FULL POWER WITH MINIMUM FEEDBACK  
AND 5 pcm/sec WITHDRAWAL RATE

Figure 15.4-7 A

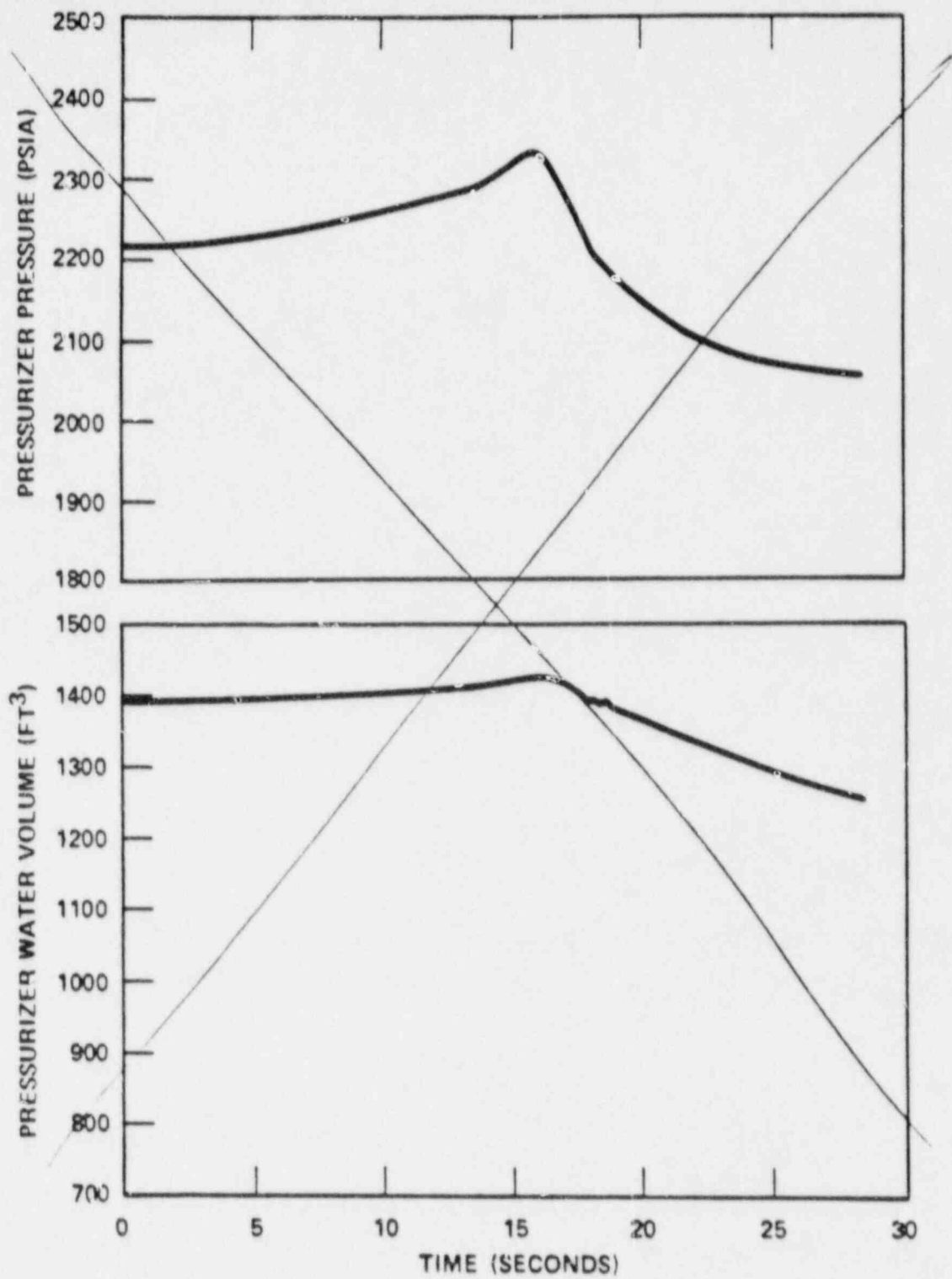
~~EXCITING ROD FOR REVISED TRIP REACTIVITY~~  
~~100 PER POWER, MIN FEEDBACK, RATE = 5 pcm/SEC~~  
~~PLOT 1 RUN 1~~



**SOUTH TEXAS PROJECT  
UNIT 2**

NUCLEAR POWER TRANSIENT & CORE  
HEAT FLUX TRANSIENT FOR UNCON-  
TROLLED ROD WITHDRAWAL FROM  
FULL POWER WITH MINIMUM FEEDBACK  
AND 5 pcm/sec WITHDRAWAL RATE

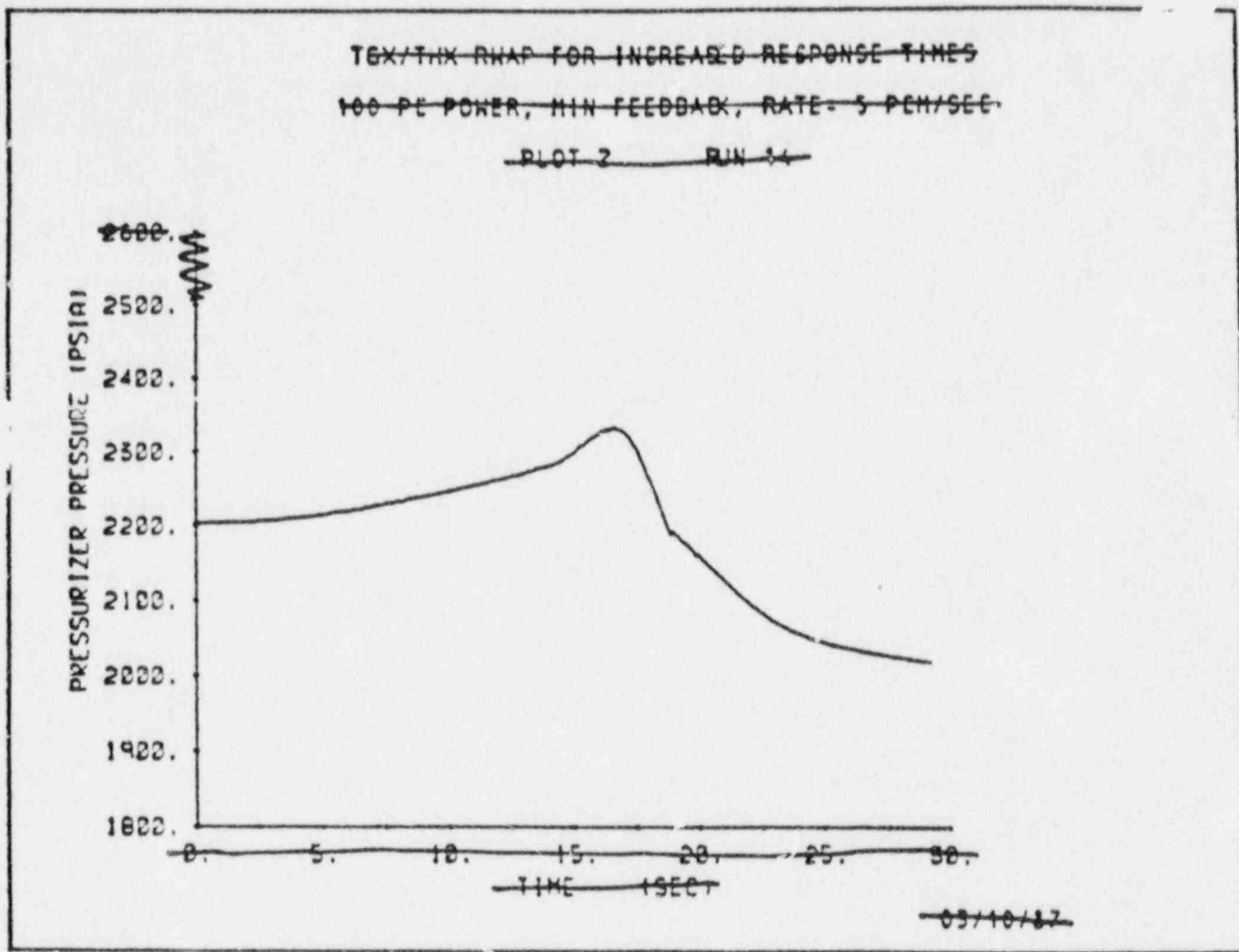
Figure 15.4-7 B



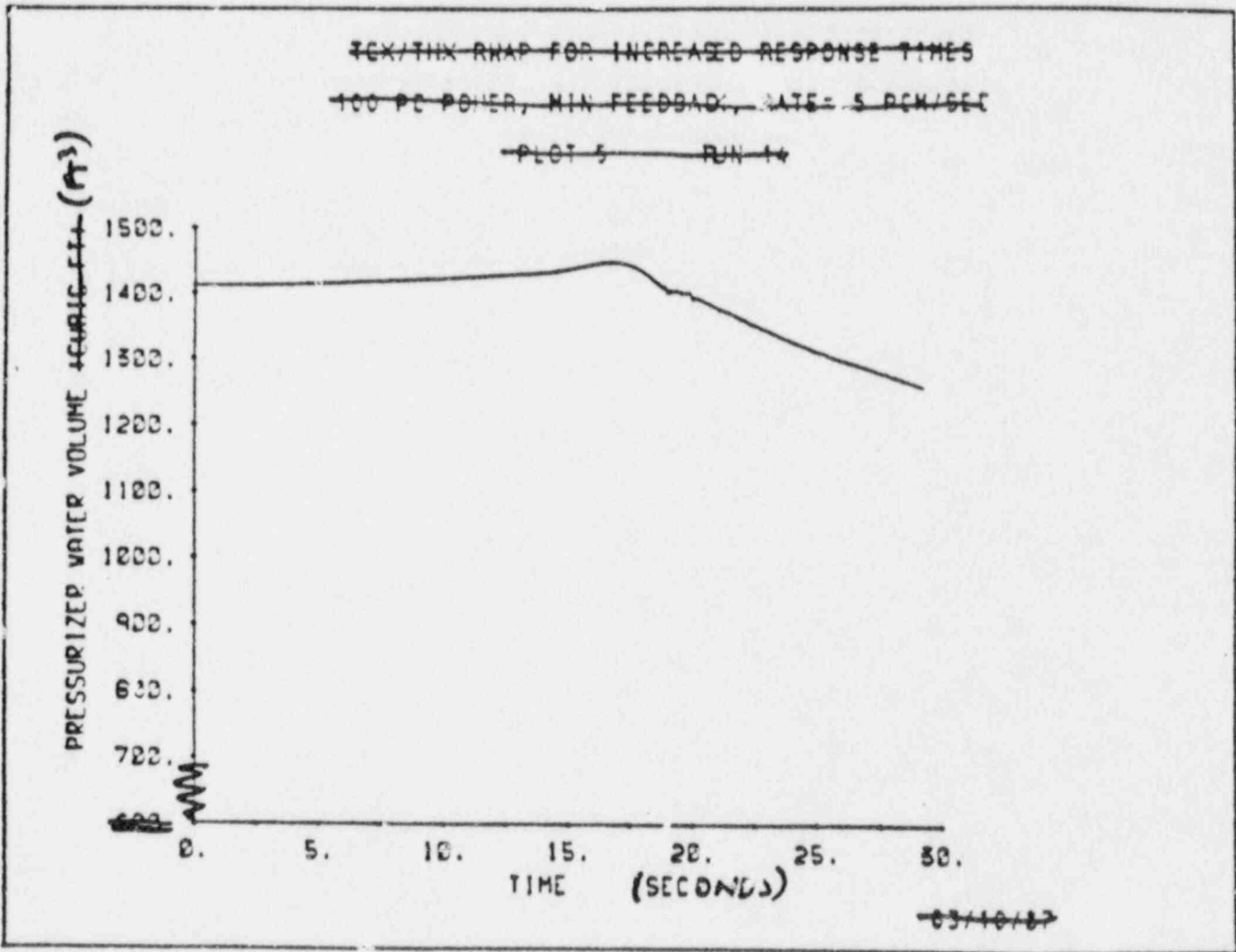
*Replace with  
Following 2 pages*

**SOUTH TEXAS PROJECT  
UNIT 1**

PRESSURIZER PRESSURE & WATER  
VOLUME TRANSIENTS FOR  
UNCONTROLLED ROD WITHDRAWAL  
FROM FULL POWER WITH MINIMUM  
FEEDBACK & 5pcm/sec WITHDRAWAL RATE  
Figure 15.4-8 A



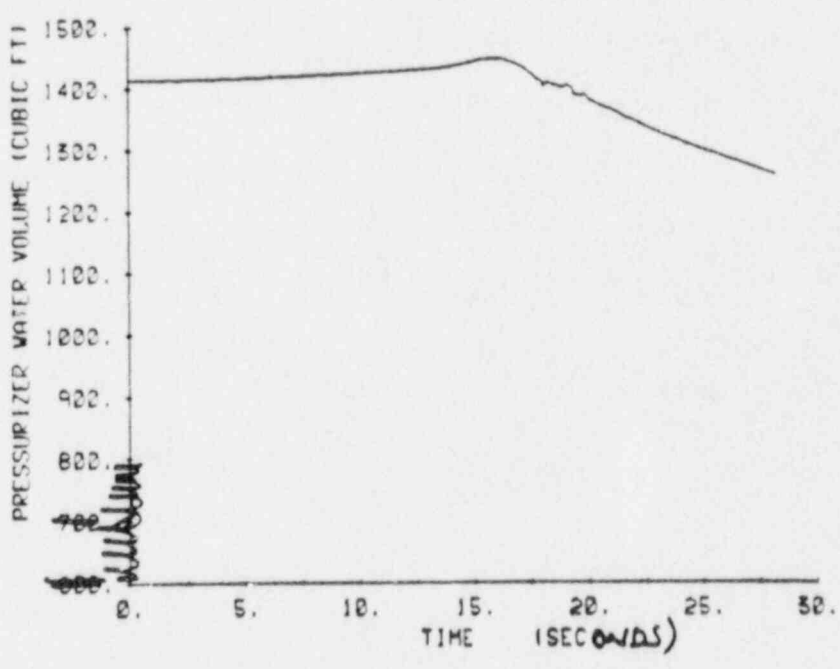
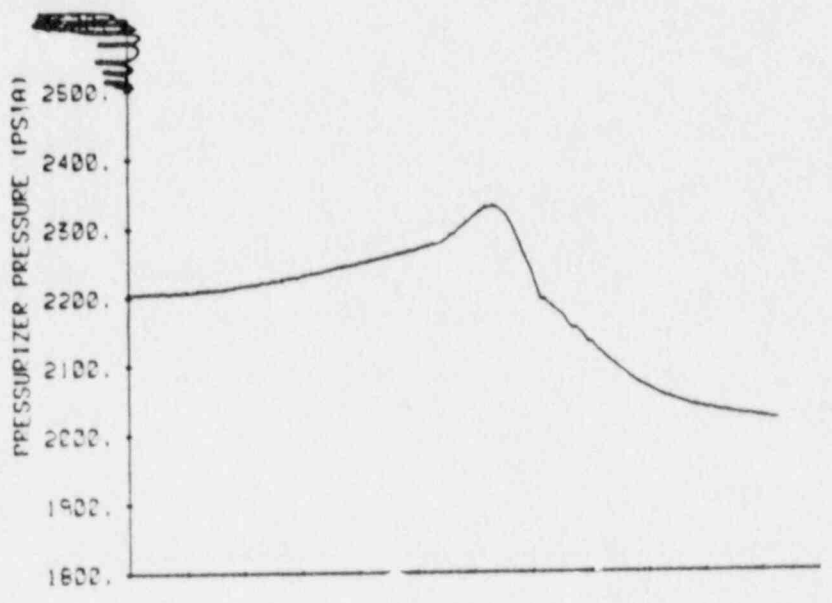
Replacement Figure 15.4-8 A (top curve)



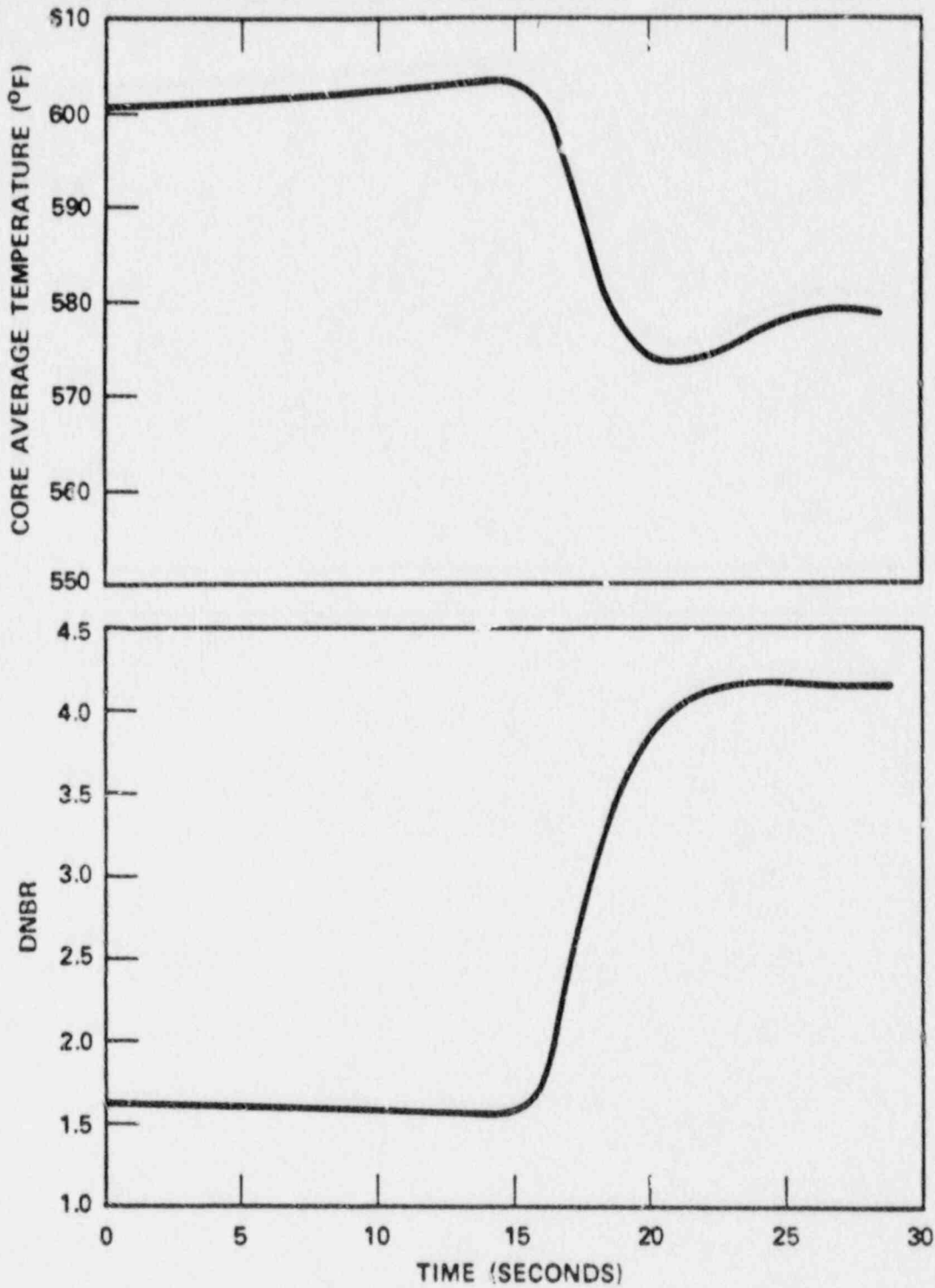
Replacement Figure 15.4-8A (bottom curve)



~~10% TRIP DUMP FOR REVISED TRIP SENSITIVITY~~  
~~100 PC POWER, MIN FEEDBACK RATE = 5 PCM/SEC~~  
~~PLOT 2 RUN 14~~



**SOUTH TEXAS PROJECT**  
**UNIT 2**  
 PRESSURIZER PRESSURE & WATER  
 VOLUME TRANSIENTS FOR  
 UNCONTROLLED ROD WITHDRAWAL  
 FROM FULL POWER WITH MINIMUM  
 FEEDBACK & 5pcm/sec WITHDRAWAL RATE  
 Figure 15.4-8 B

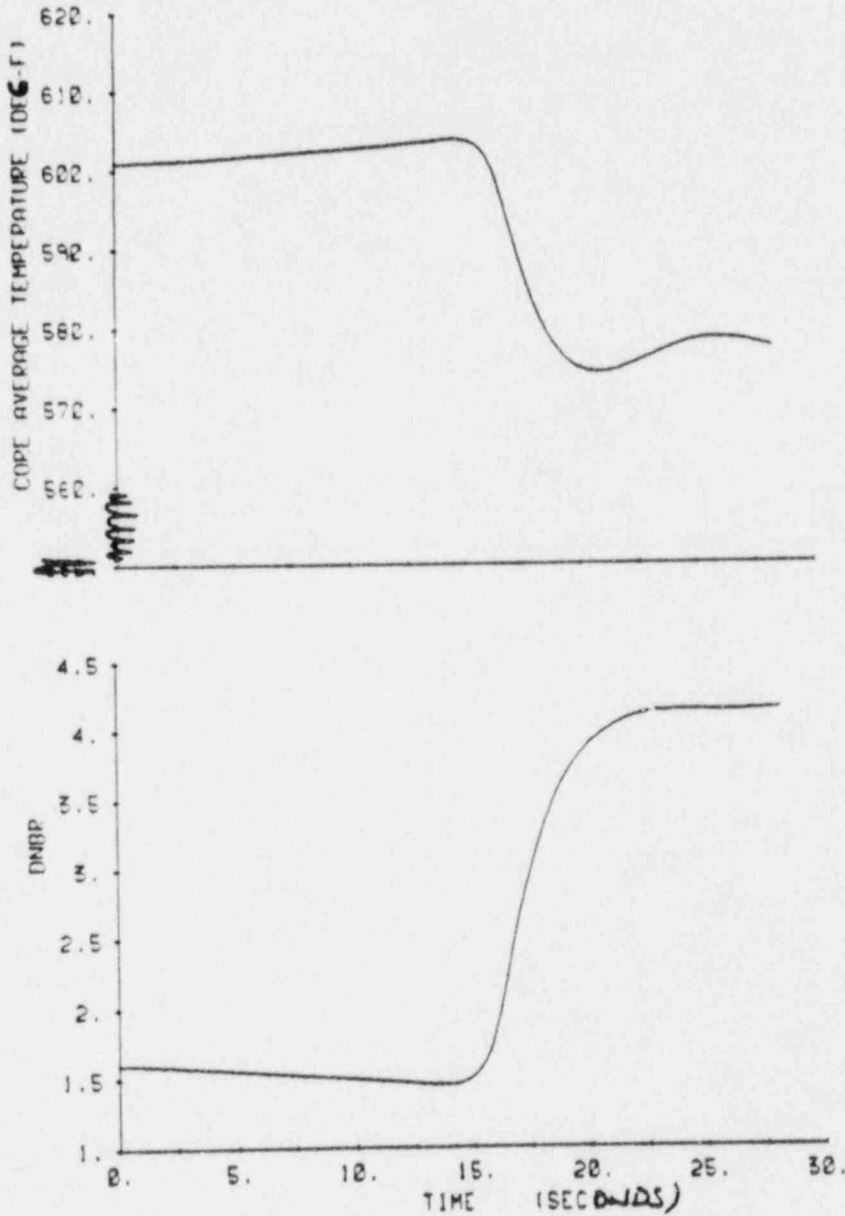


**SOUTH TEXAS PROJECT  
UNIT 1**

CORE AVERAGE TEMP. & DNBR vs TIME  
FOR UNCONTROLLED ROD WITHDRAWAL  
FROM FULL POWER WITH MINIMUM  
FEEDBACK & 5 pcm/sec WITHDRAWAL  
RATE

Figure 15.4-9 A

~~FOR THE RUN FOR REVISED TAD REACTIVITY~~  
~~100 PC POWER, MIN FEEDBACK, RATE = 5 pcm/SEC~~  
 PLOT 3 RUN 14

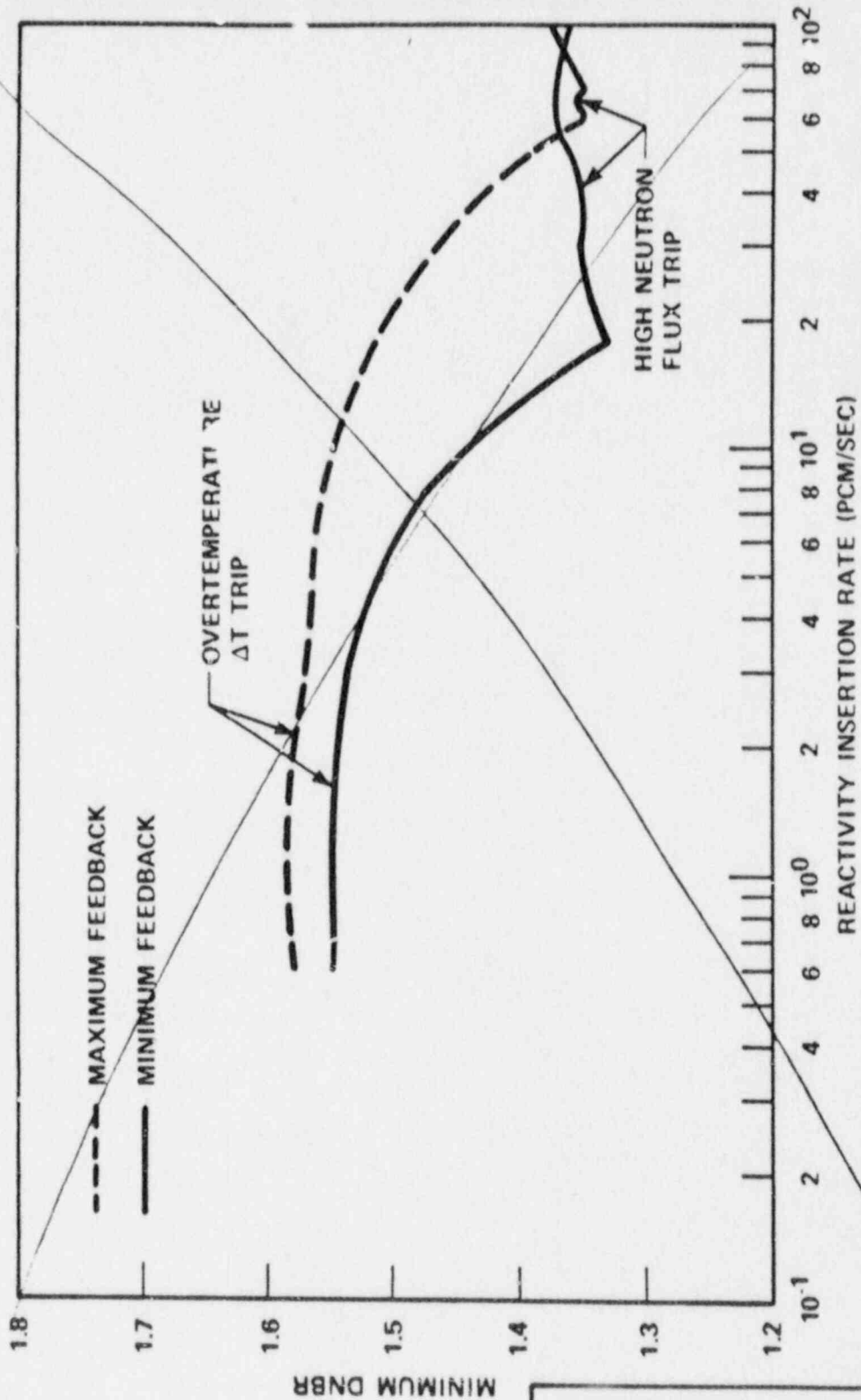


**SOUTH TEXAS PROJECT  
 UNIT 2**

CORE AVERAGE TEMP. & DNBR vs TIME  
 FOR UNCONTROLLED ROD WITHDRAWAL  
 FROM FULL POWER WITH MINIMUM  
 FEEDBACK & 5 pcm/sec WITHDRAWAL  
 RATE

Figure 15.4-9 B

~~CONFIDENTIAL~~

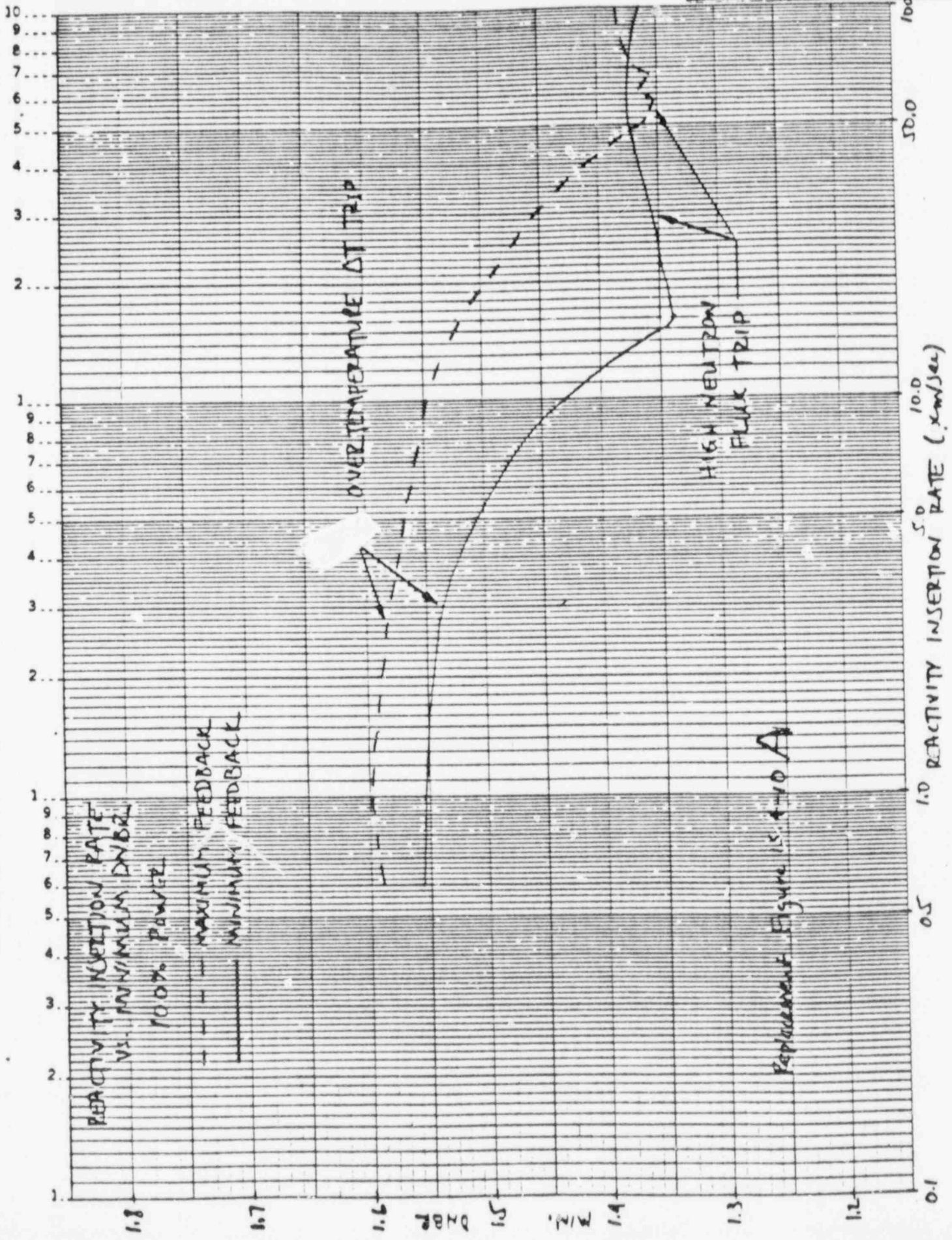


Replace with  
following page

**SOUTH TEXAS PROJECT  
UNIT 1**

**ROD WITHDRAWAL AT POWER  
(100% POWER)**

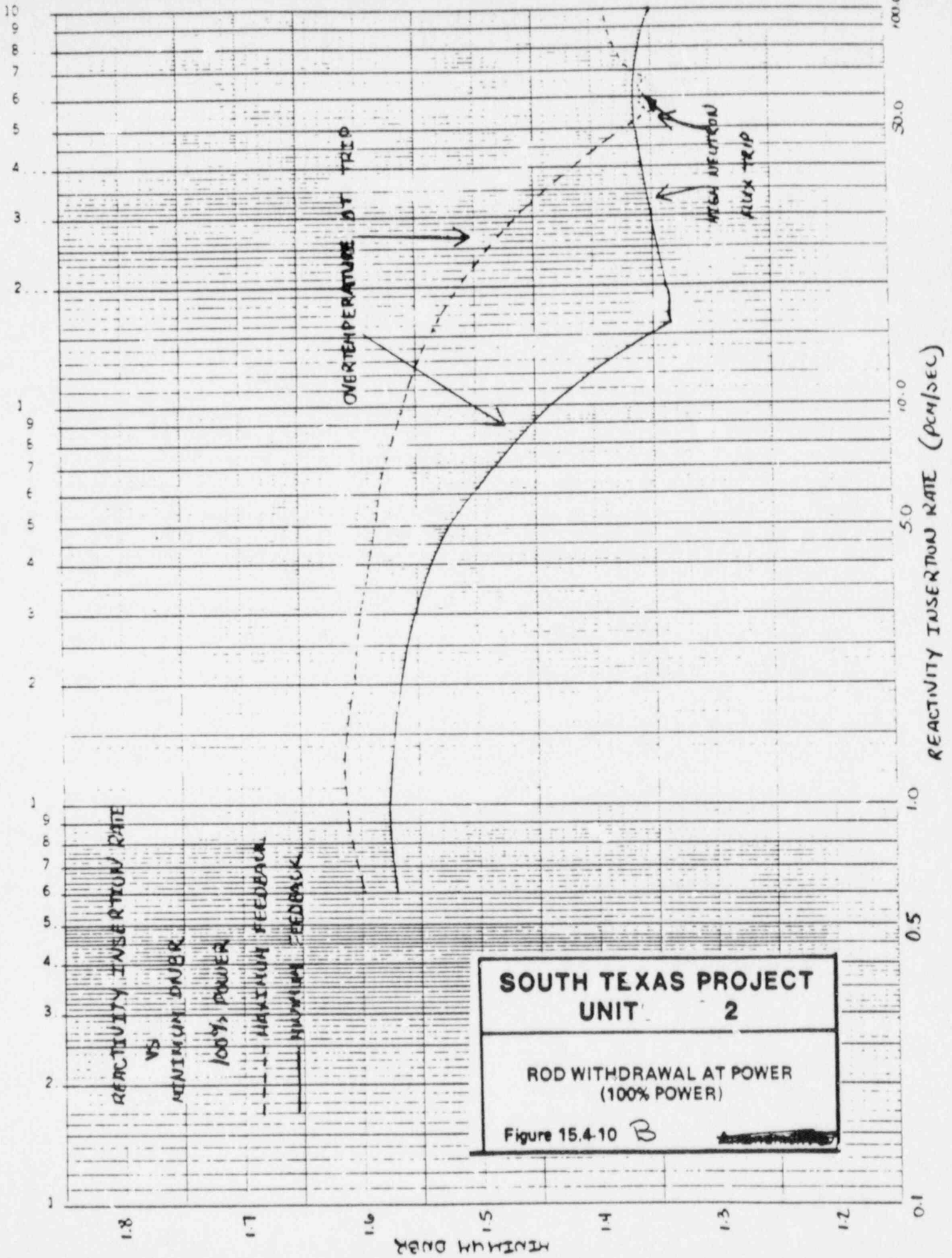
Figure 15.4-10 A

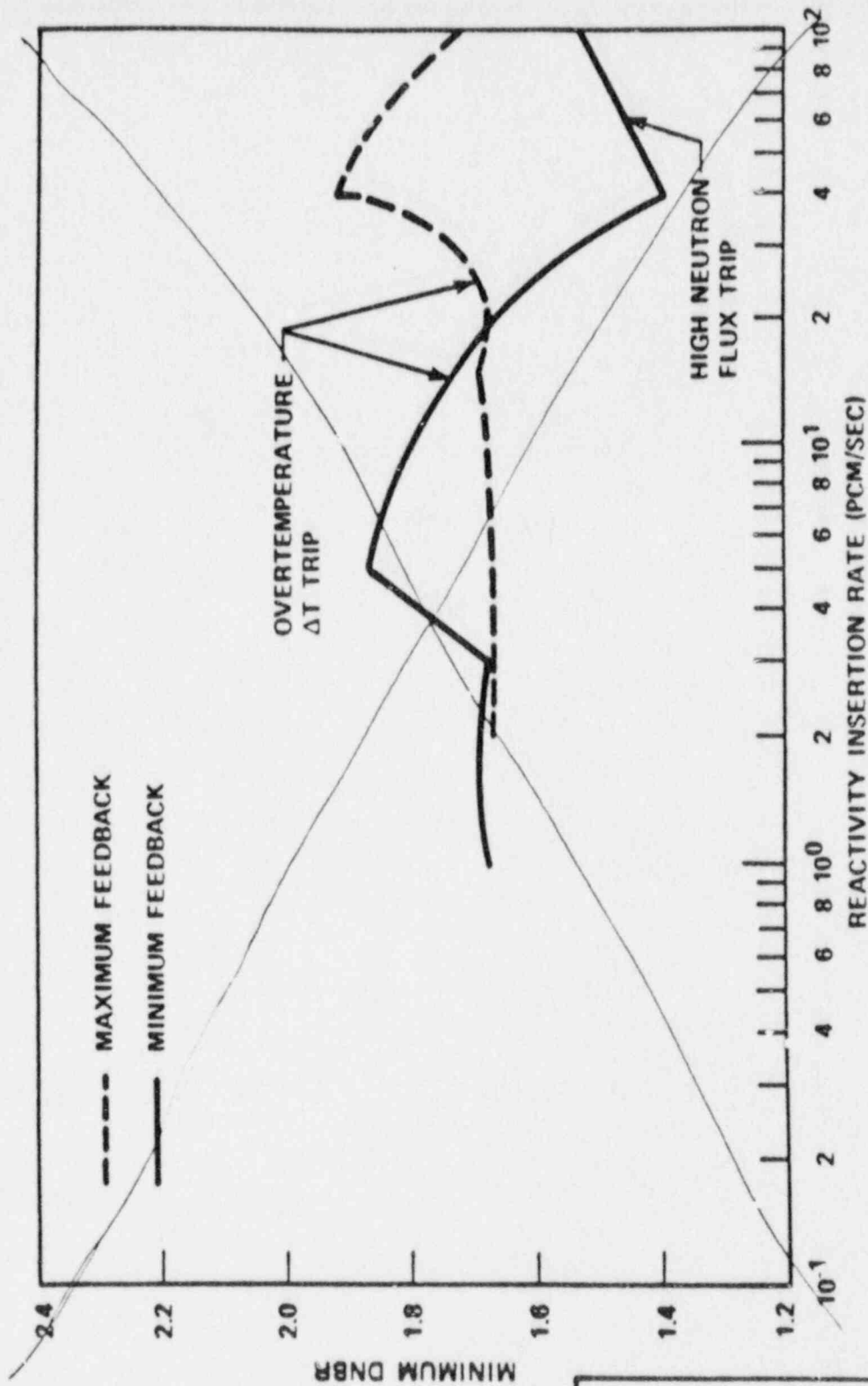


Replacement Figure 15.4-10 A

Figure 15.4-10 A





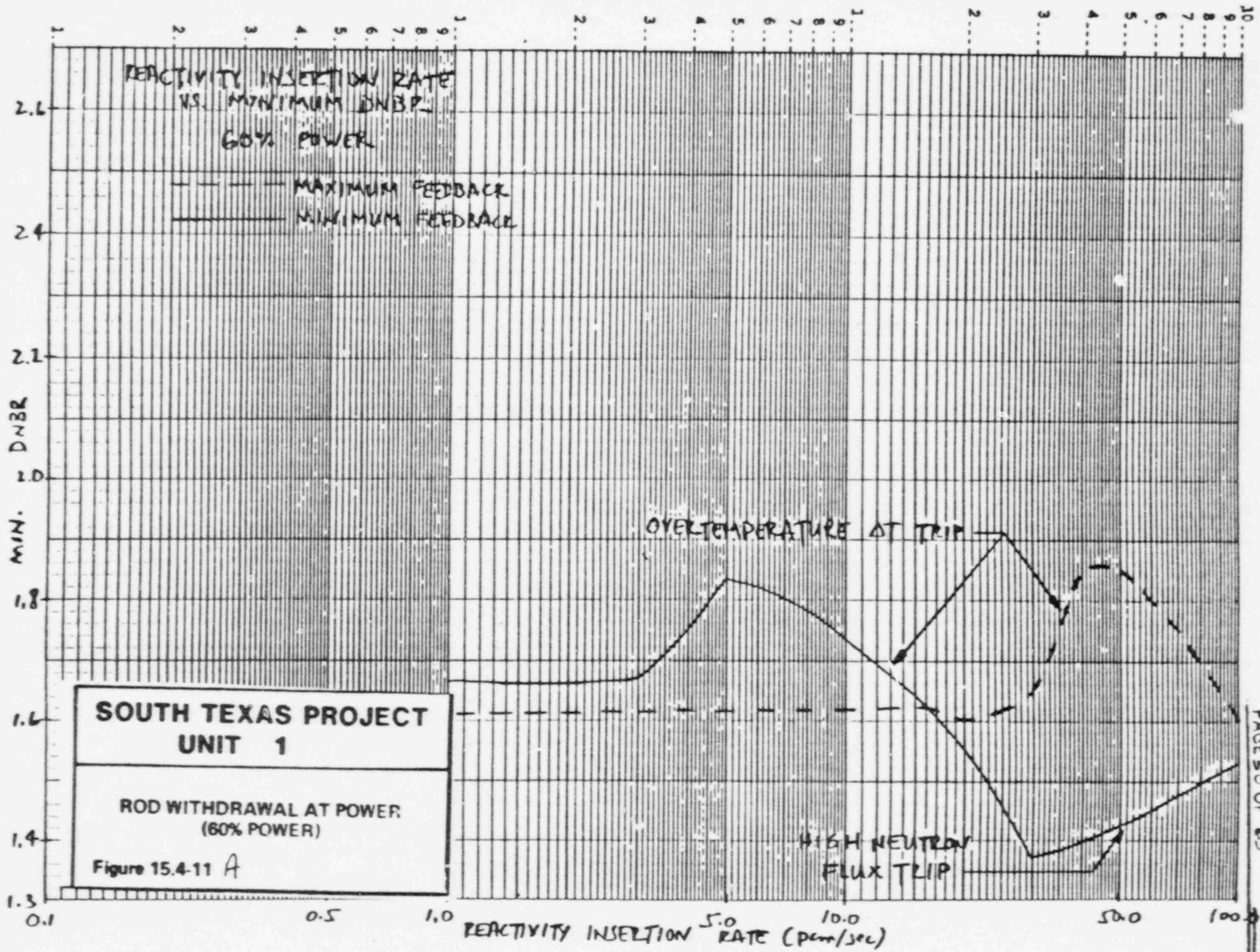


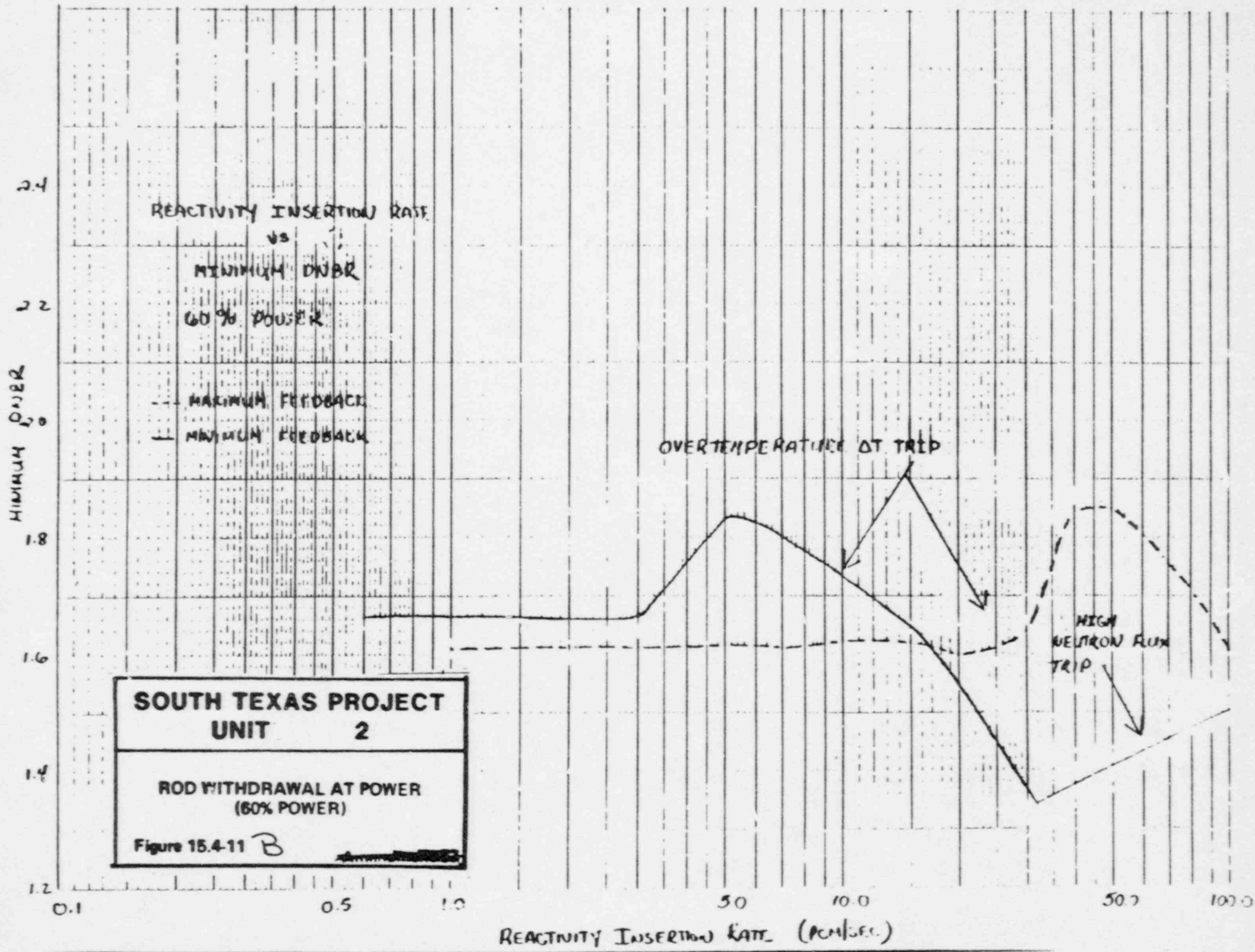
**SOUTH TEXAS PROJECT  
UNIT 1**

ROD WITHDRAWAL AT POWER  
(60% POWER)

Figure 15.4-11 A



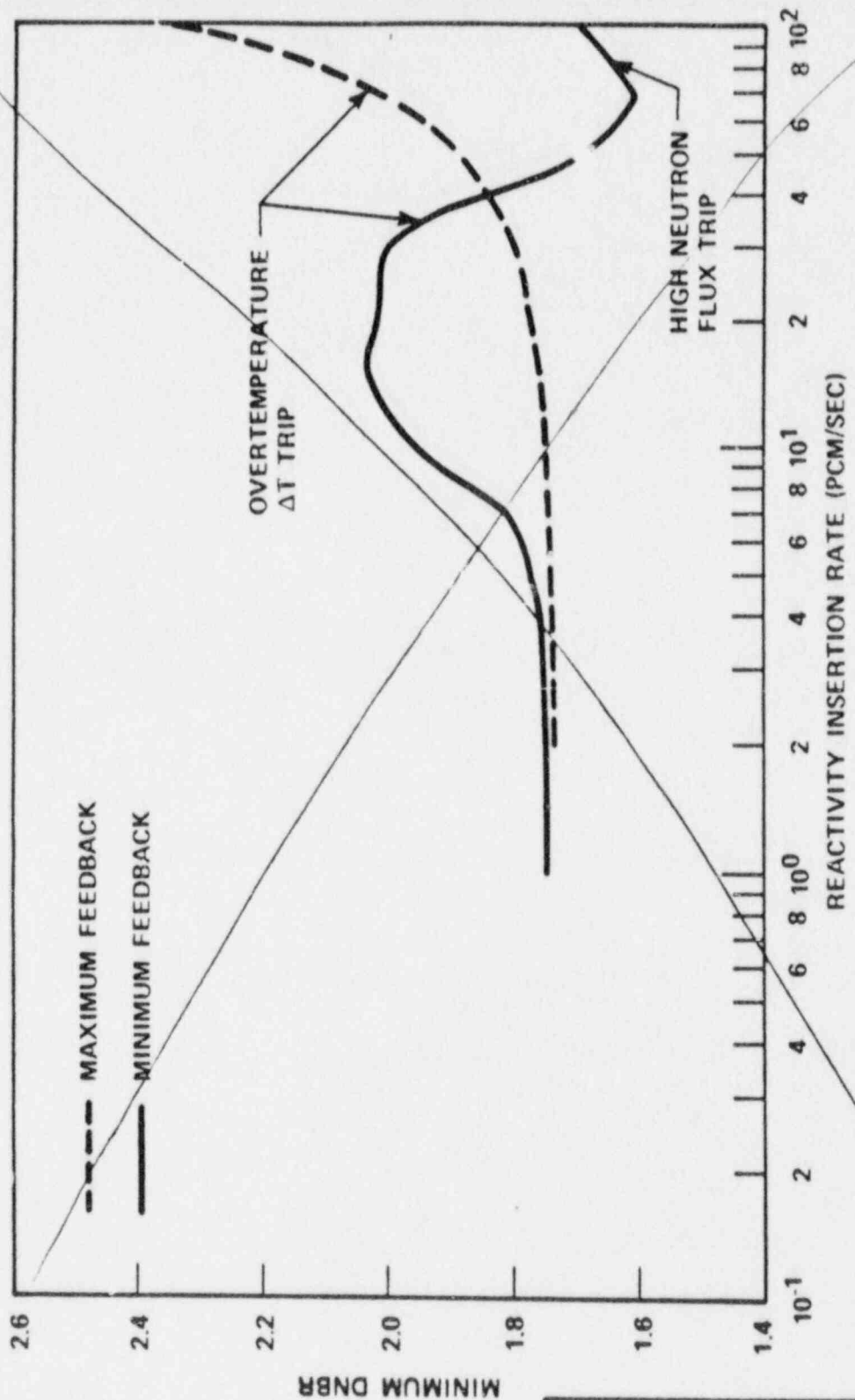




**SOUTH TEXAS PROJECT  
UNIT 2**

ROD WITHDRAWAL AT POWER  
(60% POWER)

Figure 15.4-11 B



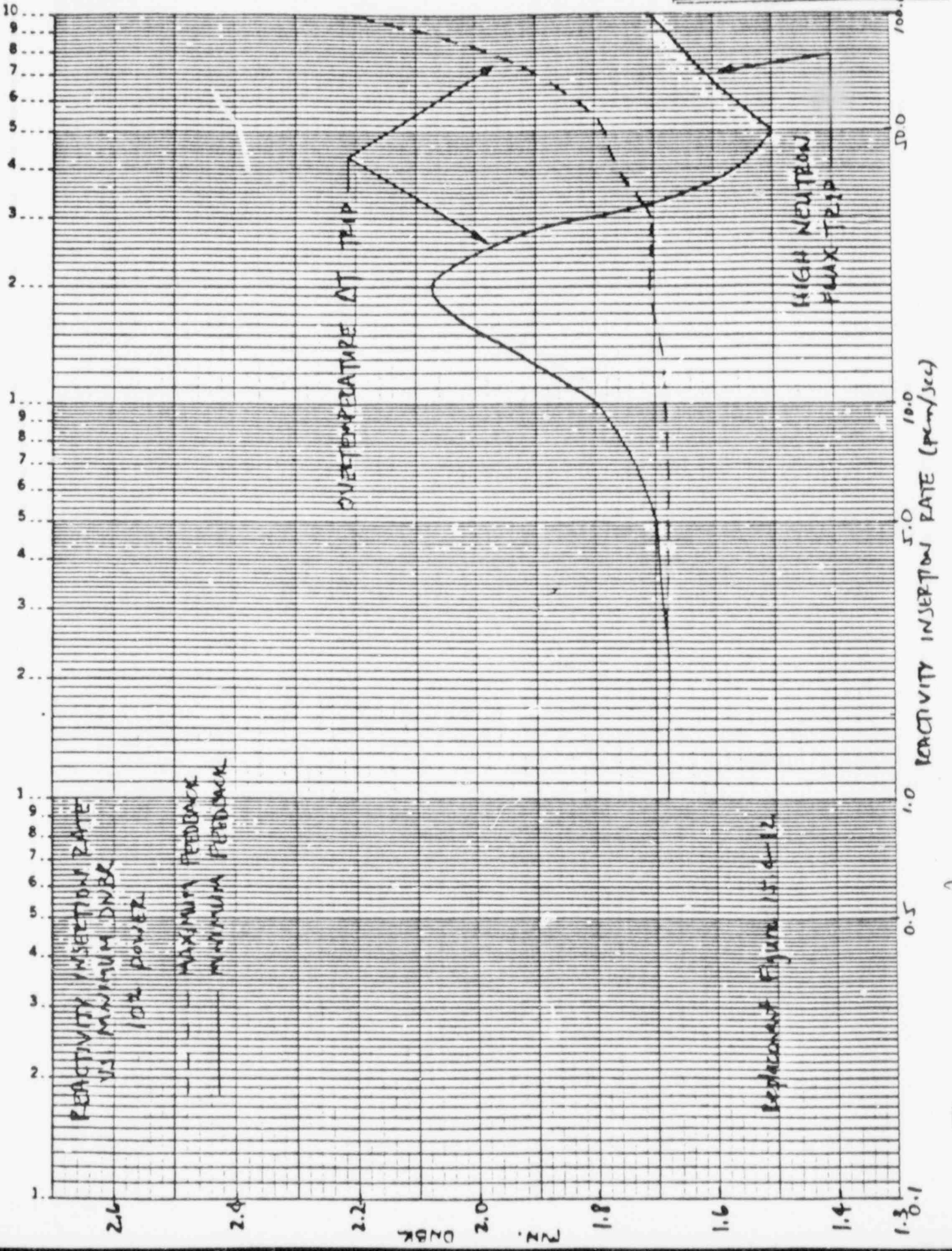
*Replace with following page*

**SOUTH TEXAS PROJECT  
UNIT 1**

ROD WITHDRAWAL AT POWER  
(10% POWER)

Figure 15.4-12 A



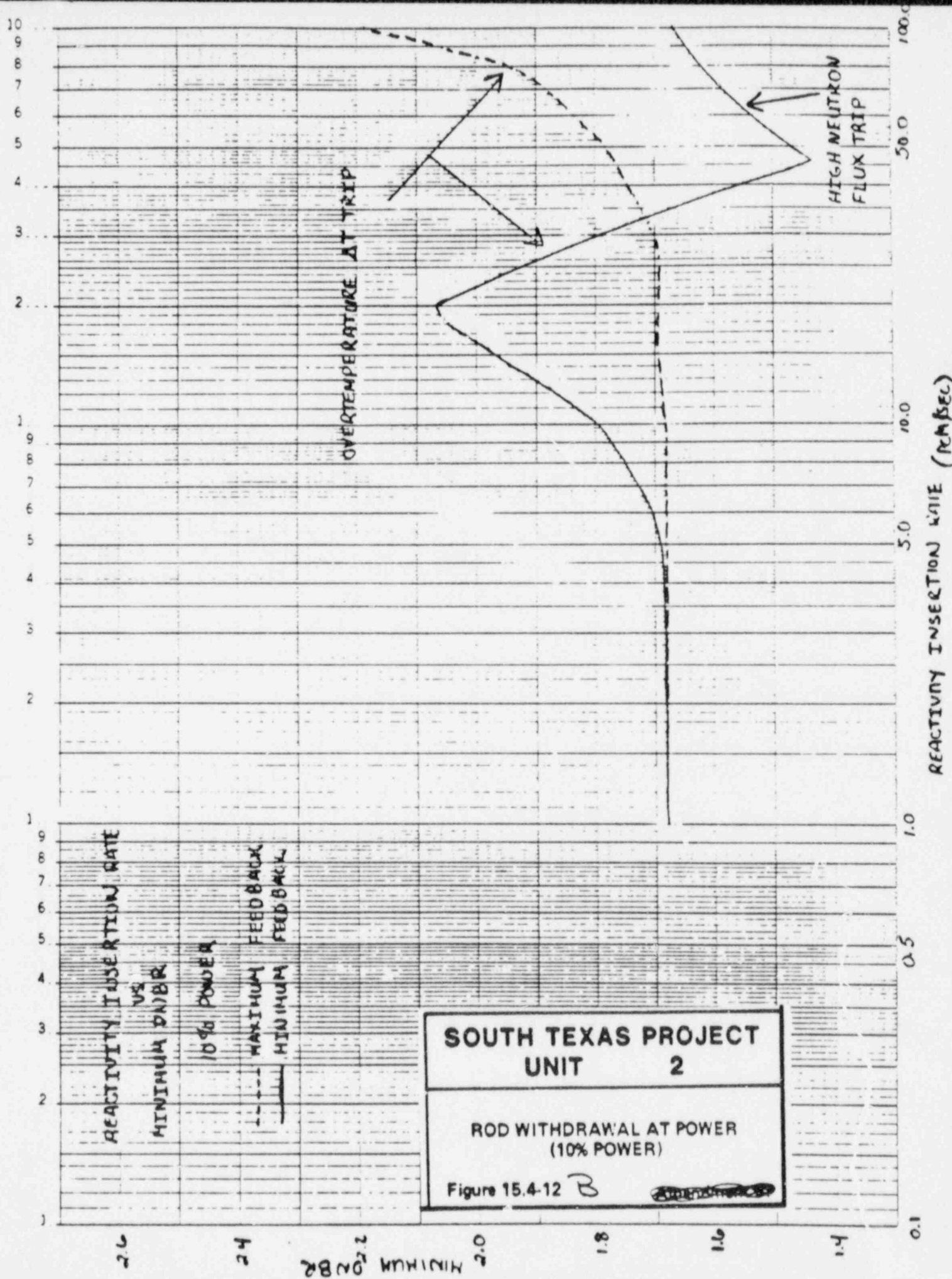


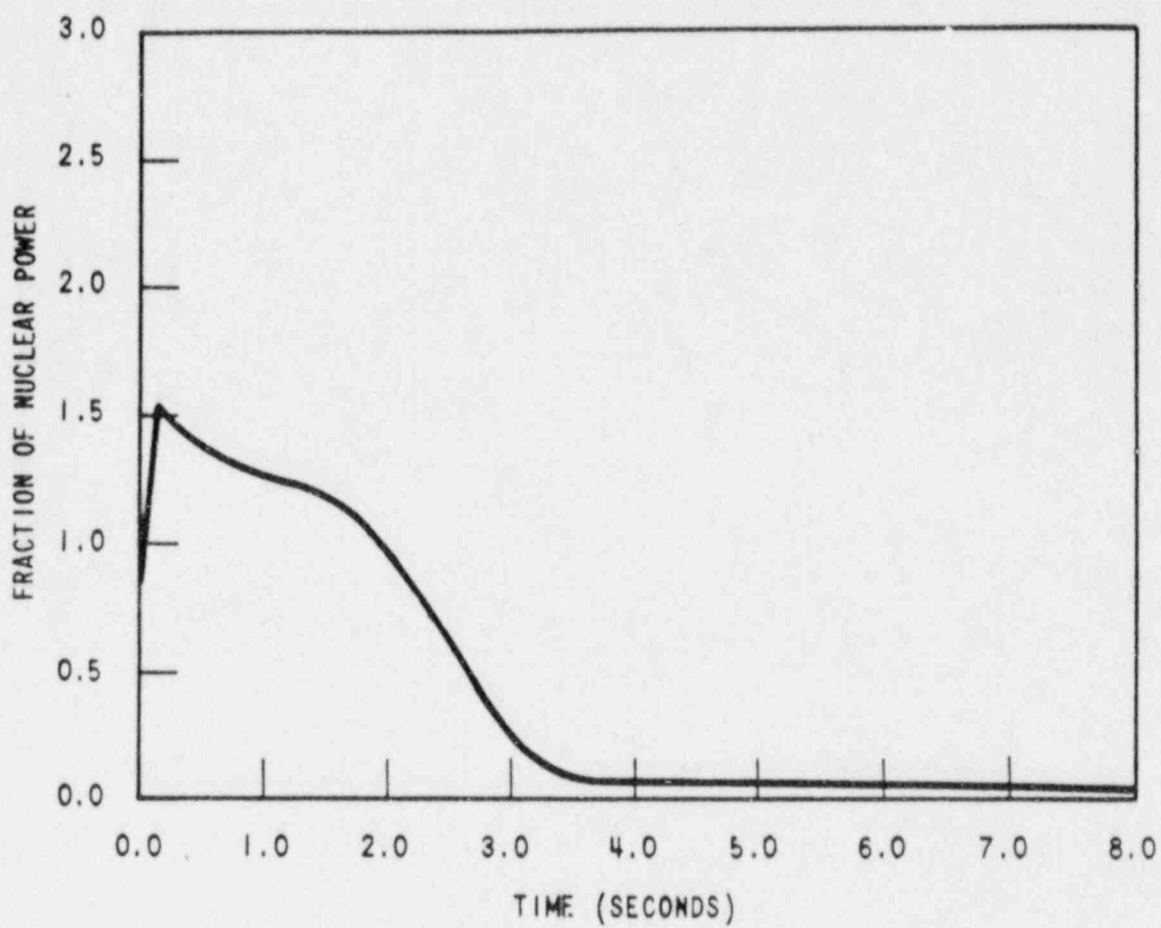
Replacement Figure 15.4-12

Figure 15.4-12A

40 2490

ST. L. NEUFEL & ESTER CO. MEMPHIS, TN

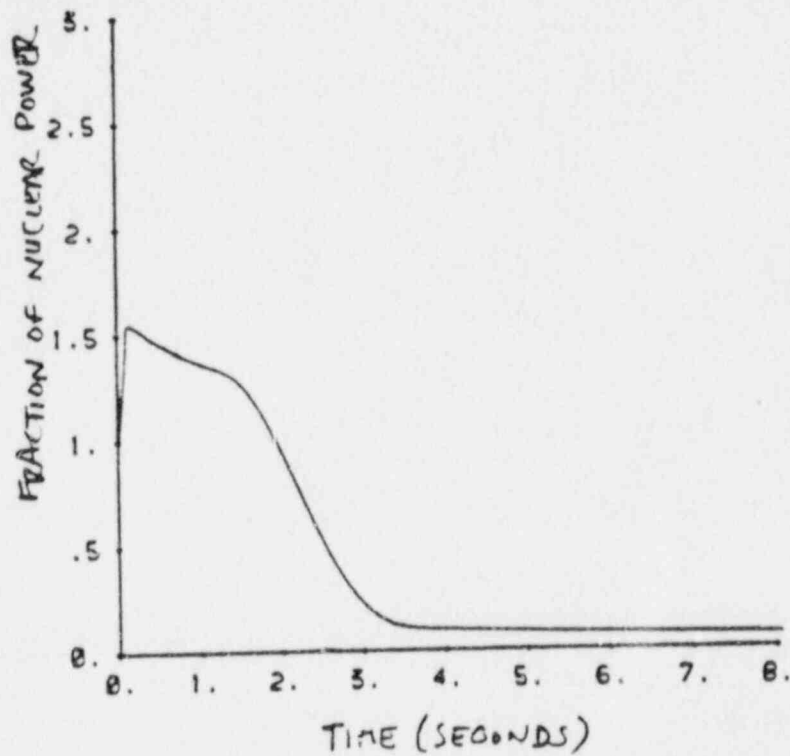




**SOUTH TEXAS PROJECT  
UNIT 1**

Nuclear Power Transient, BOL HFP  
Rod Ejection Accident

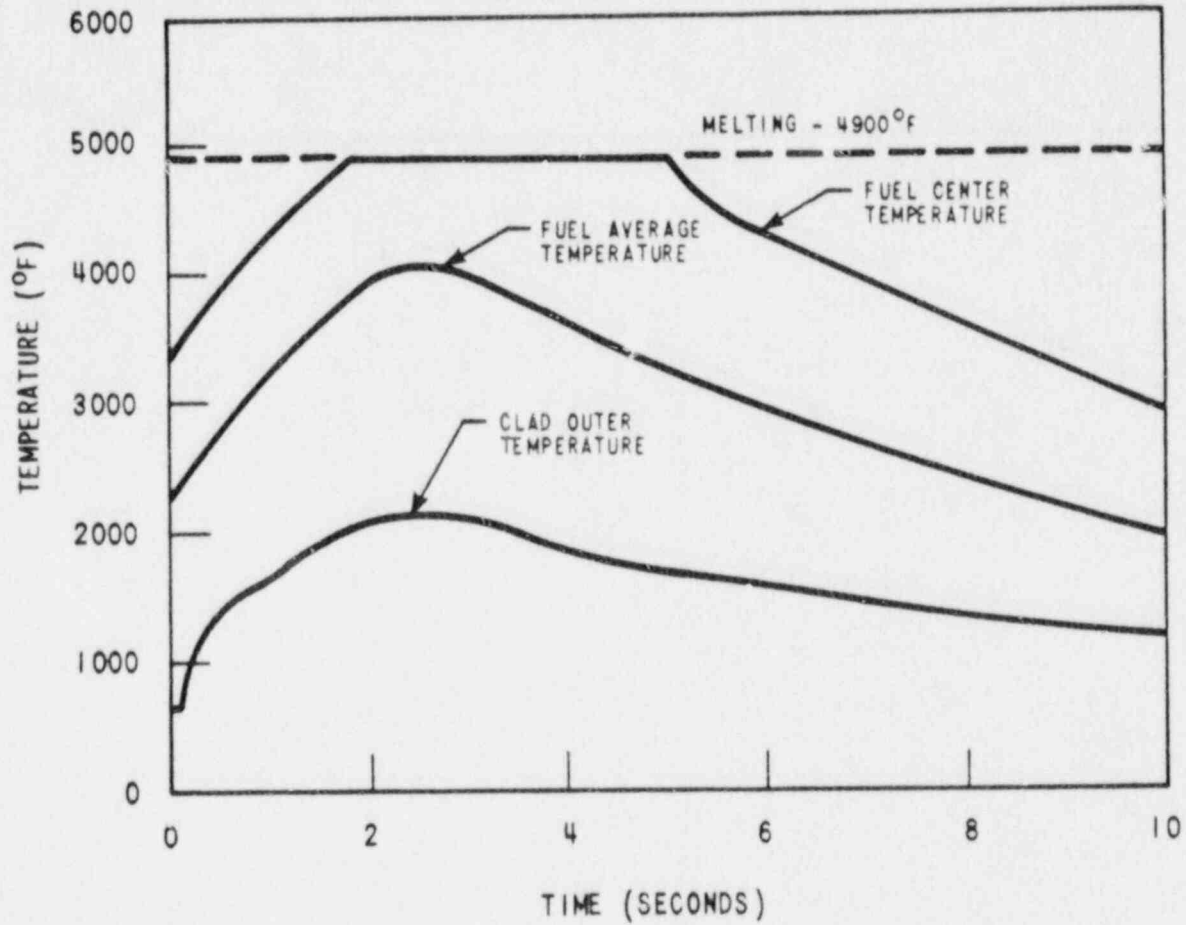
Figure 15.4-26 A



<p><b>SOUTH TEXAS PROJECT</b>  <b>UNIT 2</b></p>
<p>Nuclear Power Transient, BDL HFP          Rod Ejection Accident</p>
<p>Figure 15.4-26 <b>B</b></p>

~~Nuclear Power Transient~~  
 (BDL HFP)

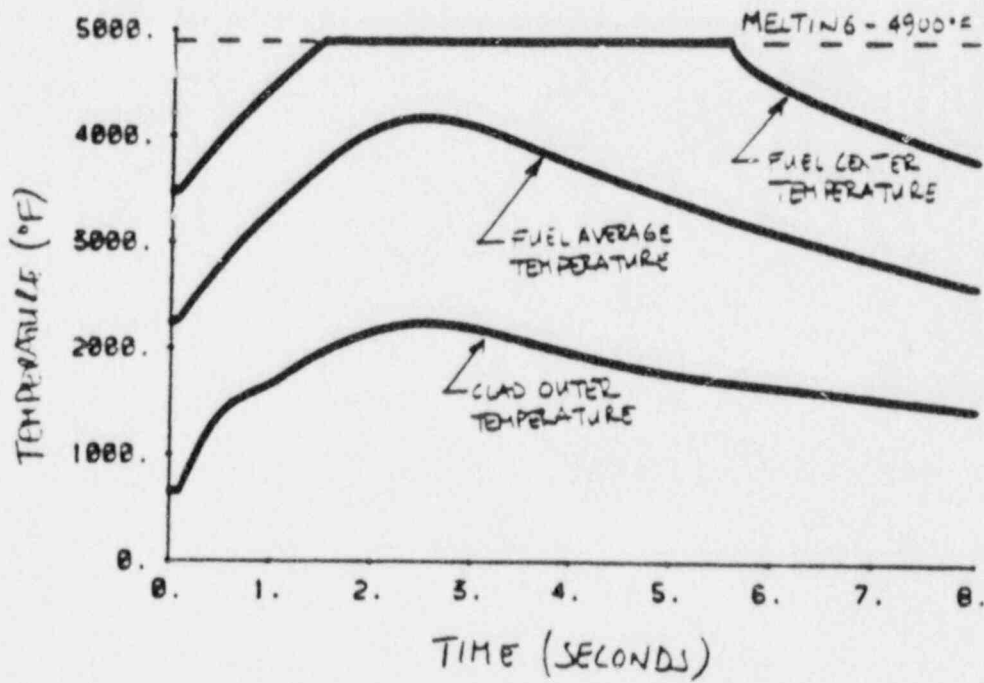




## SOUTH TEXAS PROJECT UNIT 1

Hot Spot Fuel and Clad Temperature Versus  
Time, BOL HFP Rod Ejection Accident

Figure 15.4-27 A



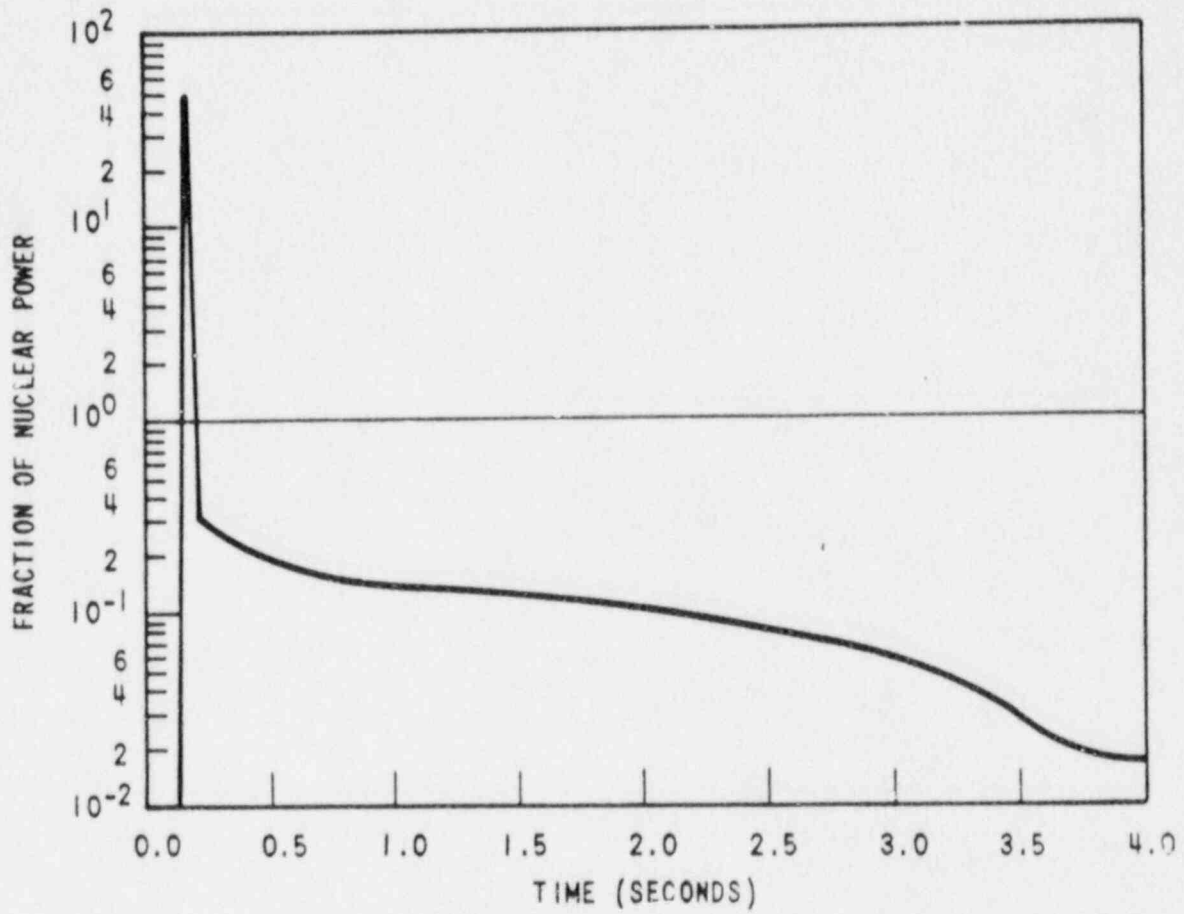
**SOUTH TEXAS PROJECT**  
**UNIT . 2**

---

Hot Spot Fuel and Clad Temperature Versus  
Time, BOL HFP Rod Ejection Accident

Figure 15.4-27 **B**

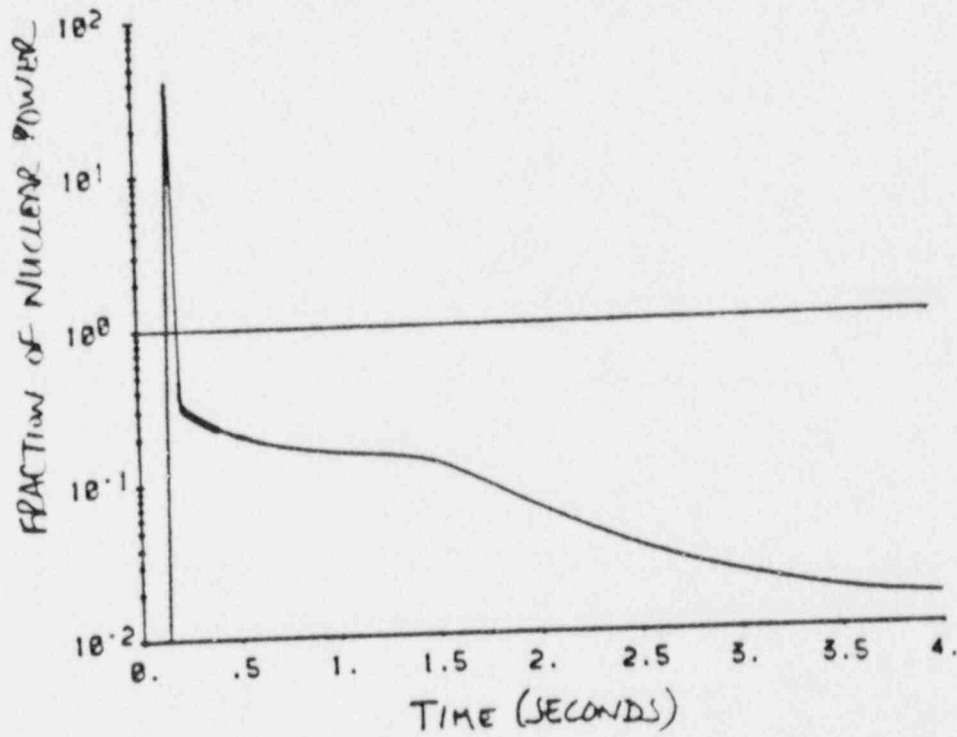
~~Spot Fuel and Clad  
Temperature (BOL HFP)~~



**SOUTH TEXAS PROJECT  
UNIT 1**

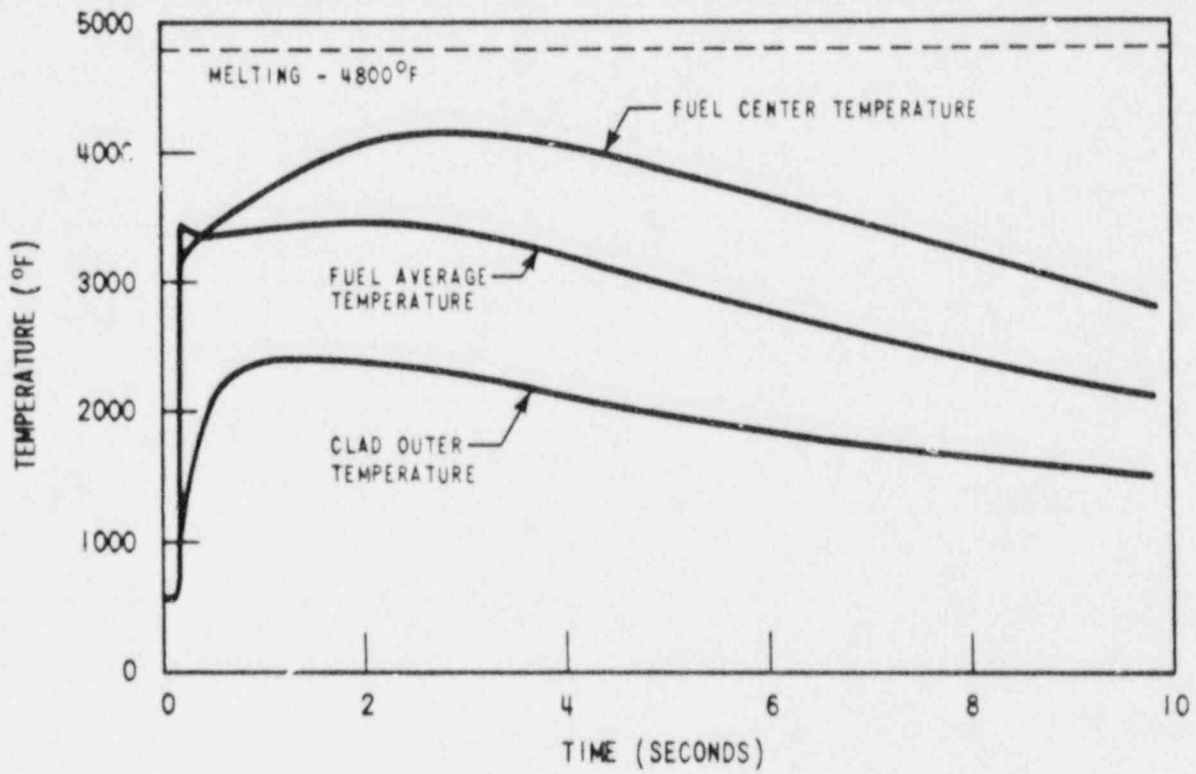
Nuclear Power Transient, EOL HZP  
Rod Ejection Accident

Figure 15.4-28 A



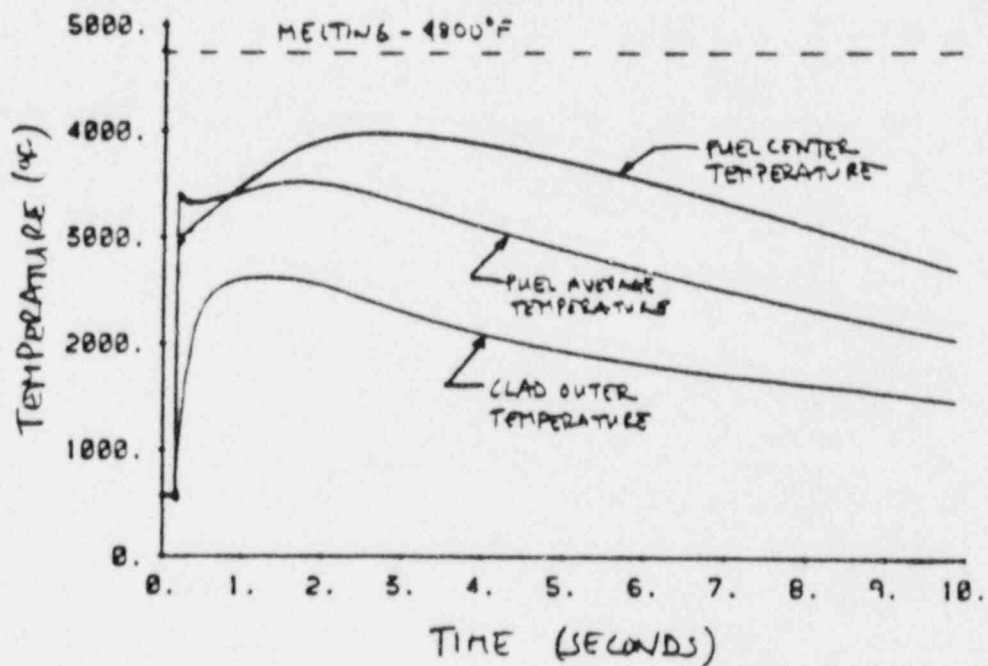
SOUTH TEXAS PROJECT  
 UNIT 2  
 Nuclear Power Transient, EOL HZP  
 Rod Ejection Accident  
 Figure 15.4-28 B

~~Nuclear Power Transient~~  
~~(EOL HZP)~~



## SOUTH TEXAS PROJECT UNIT 1

Figure 15.4-29, A  
Hot Spot Fuel and Clad Temperature versus Time  
EOL HZP Rod Ejection Accident



**SOUTH TEXAS PROJECT  
UNIT 2**

Figure 15.4-29. B  
Hot Spot Fuel and Clad Temperature versus Time  
EOL HZP Rod Ejection Accident

~~Spot Fuel and Clad  
Temperature (EOL HZP)~~



Question 440.47N

General Design Criterion 17 states "...The safety function for each (onsite or offsite electric power) system (assuming the other system is not functioning) shall be to provide sufficient capacity and capability to assure that (1) specified acceptable fuel design limits (SAFDLs) and design conditions of the reactor coolant pressure boundary are not exceeded as a result of anticipated operational occurrences (AOOs) and (2) the core is cooled and containment integrity and other vital functions are maintained in the event of postulated accidents (PAs)."

Please demonstrate that for all AOOs and PAs analyzed in Chapter 15 these limits are still met assuming loss of offsite power (LOOP). For those AOO and PA analyses which do not assume LOOP, demonstrate the conservatism of this assumption. Justify any delay time assumed between turbine trip and LOOP occurrence. Consider the effect of the assumed delay time on the conservatism of the Chapter 15 AOO and PA analyses, particularly for the "complete loss of RCS flow" and "locked rotor" analyses (See also Question 440.65).

Response

Upon loss of offsite power (LOOP), the following pumps lose power: the reactor coolant pumps (RCPs), circulating water pump and the condensate pumps. As a result of losing power to the RCPs, the reactor would trip on the RCP undervoltage signal and follow the transient scenario described in Section 15.3.2, Complete Loss of Forced Reactor Coolant Flow. Even though this event is a Condition III event, it is analyzed to show that the minimum departure from nucleate boiling ratio (DNBR) is greater than the limiting value. The results reported in the FSAR show that this is indeed the case.

All of the Condition II events are analyzed assuming offsite power is available with the exception of the Loss of Nonemergency AC Power to the Station Auxiliaries. This event is the Loss of Normal Feedwater transient without offsite power.

For the purposes of the analyses, the staff has previously stated it is acceptable to assume that LOOP results from turbine trip, and that any delay that is expected to occur between turbine trip, and LOOP due to frequency decay time can be assumed. Grid stability analyses have shown that the grid will remain stable and that offsite power will not be lost because of a unit trip from 100 percent power. A two second delay for LOOP is a conservative assumption based on grid stability analyses.

Response (Continued)

As shown in Table Q440.47N-1, the minimum DNBR and rod motion for most of the Condition II events occur in less than two seconds after reactor trip. Should a LOOP occur two seconds after reactor trip, the RCPs would coast down at the same rate as the complete loss of flow analysis (Section 15.3.2). Since the coastdown is occurring after the time of minimum DNBR and the reactor power is decreasing rapidly due to rod motion, the minimum DNBR is not adversely affected. For the cases where the minimum DNBR occurs after the conservatively assumed two second delay, it is easy to show that should a loss of offsite power occur two seconds after reactor trip, the results would be bounded by the complete loss of flow. For example, in case b) of the uncontrolled rod cluster control assembly (RCCA) withdrawal at power analysis, the minimum DNBR occurs ~~2.5 seconds after reactor trip~~ and rod motion ~~2.5 seconds after reactor trip~~. Should a LOOP occur at the time of rod motion the nuclear power would decrease rapidly due to the rod motion, while the flow would be approximately 98 percent of thermal design flow. These core conditions are less severe than those of the complete loss of flow at the time of minimum DNBR. Thus, the uncontrolled RCCA withdrawal at power event with LOOP is bounded by the complete loss of flow event. A similar argument can be made for the inadvertent opening of a pressurizer safety or relief valve event.

All of the design basis events are analyzed with and without offsite power available.

2.0 seconds after reactor trip for Unit 1  
and 2.1 seconds after reactor trip for Unit 2

for both Units.

For Unit 1, and  
97 percent of  
thermal design flow  
for Unit 2

STP FSAR

TABLE Q440.47N-1

FSAR Section	Accident	Time of Reactor Trip	Time of Rod Motion	Time of minimum DNBR	Comments
15.1.1	Feedwater malfunctions that result in a decrease in feedwater temperature				Bounded by results of Sec. 15.1.3
15.1.2	Feedwater malfunctions that result in an increase in feedwater flow	137		27	
15.1.3	Excessive increase in secondary steam flow				No reactor trip
15.1.4	Inadvertant opening of a steam generator relief or safety valve				Bounded by results of Sec. 15.1.5
15.1.5	Steam system piping failure				Analysis done with and without offsite power available
15.2.1	Steam pressure regulator malfunction or failure that results in decreasing steam flow				Not applicable to South Texas
15.2.2	Loss of electrical load				Bounded by results of Sec. 15.2.3
15.2.3	Turbine trip				
	1)	6.1 <del>5.9</del>	2.9	8.1 (a)	
	2)	7.1 <del>5.8</del>	2.8	7.1 (a)	
	3)	4.6 <del>4.4</del>	6.4	6.6 (a)	
	4)	4.6 <del>4.4</del>	6.4	6.6 (a)	
		4.6		5.6 (a)	
15.2.4	Inadvertent closure of main steam isolation valves				Bounded by results of Sec. 15.2.3
15.2.5	Loss of condenser trip vacuum and other events resulting in a turbine trip				Bounded by results of Sec. 15.2.3

STP FSAR

TABLE Q440.47-1N (Continued)

FSAR Section	Accident	Time of Reactor Trip	Time of Rod Motion	Time of minimum DNBR	Comments
15.2.6	Loss of nonemergency ac power to the plant auxiliaries				This is a LOOP
15.2.7	Loss of normal feed-water flow				Sec. 15.2.6 is case with LOOP
15.2.8	Feedwater system pipe break				Done with and without LOOP
15.3	Decrease in reactor coolant system flowrate				Bounded by Complete Loss of Flow
15.4.1	Uncontrolled RCCS withdrawal from a subcritical or low power startup condition	10.2	10.7	12.0	
15.4.2	Uncontrolled RCCA withdrawal at power a) b)	<del>10.2</del>	<del>10.7</del>	<del>12.0</del>	
15.4.3	RCCA misalignment	Unit 1 Unit 2 1.7 1.7 12.6 11.8	Unit 1 Unit 2 2.2 2.2 14.1 13.3	Unit 1 Unit 2 3.2 3.4 14.6 13.9	DNB design basis will be met. FSAR being updated to incorporate negative flux rate trip methodology per CAP-10297-P-A
15.4.4	Startup of an inactive reactor coolant loop at an incorrect temperature	10.2	11.2	12.0	
15.4.5	Failure of a BWR flow controller				Not applicable to South Texas

STP FSAR

TABLE Q440.47N-1 (Continued)

FSAR Section	Accident	Time of Reactor Trip	Time of Rod Motion	Time of minimum DNBR	Comments
15.4.6	CVCS malfunctions that results in a decrease in the boron concentration in the reactor coolant				At-power case bounded by Sec. 15.4.2
15.4.7	Inadvertent loading and operation of a fuel assembly in an improper position				Static analysis
15.4.8	Spectrum of RCCA ejection accidents 1) BOL HFP 2) EOL HZP	0.05 0.14	0.55 0.64	NA NA	
15.5.1	Inadvertent operation of the ECCS during power operation				Not applicable to South Texas due to low ECCS shutoff head of 1600 psia
15.5.2	CVCS malfunctions that increase reactor coolant inventory 1) 2) 3) 4)	349 278 462 363	351 280 464 365	NA NA NA NA	
15.6.1	Inadvertent opening of a pressurizer safety or relief valve	<del>18.8</del> 8.5	<del>20.8</del> 10.0	<del>21.0</del> 10.6	



Note:  
 (a) The minimum DNBR increases throughout the transient.  
 NA - Not Applicable.

Question 211.51

For Chapter 15 accident events, provide the number of fuel rods calculated to be in DNB.

Response

For Condition II events, it is demonstrated that DNBR remains greater than the limiting value; thus, the number of rods calculated to be in DNB corresponds to the criteria set forth in Section 4.4.1.

For large and small LOCA's, uncovering of the core results in DNE for all rods. For the steamline break events (Section 15.1.5), the feedwater line break events (Section 15.2.8), and the complete loss of forced reactor coolant flow events (Section 15.3.2), the DNBR does not fall below the limiting value as indicated in the appropriate sections of Chapter 15. Therefore, the criteria for rods in DNB presented in Chapter 4 applies to these events also. | 43

As stated in Section 15.4.3, the number of fuel rods with DNBR less than the limiting value for the single RCCA withdrawal event is less than 5% of the rods in the core. For an improper fuel loading event, undetected errors will cause sufficiently small perturbations to be acceptable within calculational uncertainties, as stated in Section 15.4.7; thus, the effect due to improper loading on rods in DNB for transient event will be negligible.

The RCCA ejection analysis presented in Section 15.4.8 conservatively assumes that 10% of the rods in the core go into DNB and fail. For the locked rotor event presented in Section 15.3.3, the maximum number of fuel rods in DNB is conservatively calculated to be less than 7.0% of the rods in the core. <sup>(A)</sup>As stated in Section 15.3.4, the consequences of an reactor cooling pump shaft break will be less severe than those for a locked rotor event. | 43

Evaluation of the steam generator tube rupture indicates that no clad damage would be expected in this transient. The RCS depressurization due to flow out of the tube rupture presents the possibility of obtaining a low DNBR. However, the depressurization in a tube rupture is much less severe than the depressurization transient analyzed in Section 15.6.1. In this accident, it was determined that the DNBR is always greater than the limiting value, and thus no clad damage is expected. From this, it is concluded that no clad damage is expected in the steam generator tube rupture accident. For all other events discussed in Chapter 15, DNBR remains above the limiting value. | 43

(A) for Unit 2 and less than 10% of the rods in the core for Unit 2.



Question 211.79

Section 15.3.3.3 contains conflicting statements as to whether or not fuel failure occurs. Clarify this discrepancy and, if fuel failure is not assumed for some conditions, provide a justification, with bases, since DNB is assumed to occur.

Response

The locked rotor transient for South Texas presented in Section 15.3.3 of the FSAR is performed in several different parts.

Part 1 Calculation of Peak Fuel Clad Temperature

To maximize the fuel clad temperatures, DNB is assumed to occur at the start of the transient. The analysis showed the peak clad temperature is approximately 1800°F, well below the limit value of 2700°F. Thus, no clad failures are calculated to occur.

Part 2 The Number of Rods in DNB

The number of fuel rods calculated to experience DNB was 7 percent. A rod experiencing DNB does not necessarily mean it fails.

*for Unit 1 and 10 percent for Unit 2.*

Part 3 Dose Release

For the purpose of calculating dose releases it was conservatively assumed that fuel experiencing DNB fails, even though the peak clad temperature was not high enough to cause fuel failure. The South Texas dose release evaluation for a locked rotor conservatively assumed 7 percent of the fuel failed.

*10 and 15*

*(see Table 15.3-4 for the results)*